

FLORIDA STATE UNIVERSITY
FAMU-FSU COLLEGE OF ENGINEERING

PERFORMANCE OF AASHTO
GIRDER BRIDGES UNDER BLAST LOADING

By

A.K.M. ANWARUL ISLAM

A Dissertation submitted to the
Department of Civil Engineering
in partial fulfillment of the
requirements for the degree of
Doctor of Philosophy

Degree Awarded:
Summer Semester, 2005

The members of the Committee approve the Dissertation of A.K.M. Anwarul Islam defended on May 4, 2005.

Nur Yazdani
Professor Directing Dissertation

Robert Braswell
Outside Committee Member

Jerry Wekezer
Committee Member

Andrew Dzurik
Committee Member

Approved:

Kamal Tawfiq, Chair, Department of Civil & Environmental Engineering.

Ching-Jen Chen, Dean, FAMU-FSU College of Engineering.

The Office of Graduate Studies has verified and approved the above named committee members.

DEDICATED

to

My Mother
Razia Sultana
and
My Father
Abdul Awal Mallik

To whom I owe my life and knowledge

and

My Wife
Tamanna Chowdhury
To whom I owe my time

ACKNOWLEDGEMENT

An exclusive gratitude is extended to Professor Nur Yazdani for giving me the opportunity to perform this research, for his tireless editing efforts, and unique suggestions and advice. Thanks very much to Professors Jerry Wekezer, Andrew Dzurik and Robert Braswell for their time and participation on this committee. Their valuable suggestions and guidance made this research possible for me. Their academic courses, which I took to fulfill the course requirements, helped me prepare to conduct this research and write this dissertation. Special thanks go to Professor Kamal Tawfiq for his valuable advice and suggestions.

Appreciation goes to Mr. Don Harrell and Mr. Jerry O'steen of Post, Buckley, Schuh and Jernigan, Inc. for their technical lessons, advice and suggestions. Their long-term support helped me perform this research.

This research would not have been possible without the tremendous inspiration from my father Abdul Awal Mallik. I have been seeing him always dreaming of his children pursuing the Doctor of Philosophy degree since elementary school. His thoughts and blessings encouraged me to continue this doctoral research. I sincerely express my gratitude to my father for all of my achievements, including Doctor of Philosophy degree, throughout these years.

Finally, I am extremely grateful to my wife Tamanna Chowdhury, and my sons Bisshoy Anwar and Ikra Anwar for their continued support through the entire period of pursuing the Doctor of Philosophy degree. They sacrificed a major portion of their time by giving me the opportunity to complete this research.

TABLE OF CONTENTS

LIST OF TABLES	viii
LIST OF FIGURES.....	ix
ABSTRACT	xi
1. INTRODUCTION.....	1
1.1 Problem Statement	1
1.2 Types of Bridges in Florida.....	2
1.3 Florida Highway Infrastructure.....	2
1.4 Goals and Objectives.....	3
2. LITERATURE SURVEY	5
2.1 Explosive Attacks.....	5
2.2 Background Review	7
2.3 Bridge Failures	10
2.4 Blast Vulnerability Assessment	12
3. MODELING AND ANALYSIS	13
3.1 Model Bridge Selection.....	13
3.2 Failure Criteria	17
3.2.1 Column Failure.....	19
3.2.2 Pier Cap Failure.....	20
3.2.3 Girder Failure	21
3.2.4 Slab Failure	21
3.3 Model Bridge Design	23
3.3.1 Geometric Parameters	23
3.3.2 Traffic Data	25
3.3.3 Loads and Load Factors	25

3.3.4	Deck Slab Design	27
3.3.5	Prestressed Girder Design	27
3.3.6	Pier Cap Design.....	29
3.3.7	Column Design.....	32
3.4	Model Bridge Capacity	32
3.4.1	Prestressed Girder Capacity	32
3.4.2	Pier Cap Capacity.....	35
3.4.3	Column Capacity.....	36
3.4.4	Assumptions and Limitations.....	37
3.5	Blast Load	37
3.5.1	Equivalent Static Load	39
3.5.2	Comparison of Blast and Seismic Loading.....	45
3.6	STAAD.Pro Software.....	48
3.7	Bridge Model.....	49
3.8	Locations of Blast Load Application	52
3.9	Blast Load Cases	53
3.9.1	Load Case 1	55
3.9.2	Load Case 2.....	58
3.9.3	Load Case 3.....	60
3.9.4	Load Case 4.....	63
3.9.5	Load Case 5.....	65
3.10	Limitations of Analysis	67
4.	MODEL BRIDGE PERFORMANCE	69
4.1	Bridge Performance under Typical Blast Load.....	69
4.1.1	Performance under Case 1 Blast Load	70
4.1.2	Performance under Case 2 Blast Load	71
4.1.3	Performance under Case 3 Blast Load	72
4.1.4	Performance under Case 4 Blast Load	73
4.1.5	Performance under Case 5 Blast Load	74
4.2	Blast Capacity of Bridge Elements	75
4.2.1	AASHTO Girder Capacity	75
4.2.2	Pier Cap Capacity.....	77

4.2.3	Column Capacity.....	78
4.3	Minimum Standoff Distance	80
4.4	Experimental Validation	81
5.	CONCLUSION AND RECOMMENDATIONS.....	83
5.1	Conclusion.....	83
5.2	Recommendations and Future Research Directions.....	84
APPENDIX A.	DECK SLAB DESIGN.....	88
APPENDIX B.	PRESTRESSED GIRDER DESIGN	90
APPENDIX C.	PIER CAP AND COLUMN DESIGN.....	103
APPENDIX D.	MEMBER CAPACITY CALCULATIONS.....	112
D.1	Prestressed Girder Capacity	112
D.2	Pier Cap Capacity.....	114
D.3	Column Capacity.....	115
APPENDIX E.	BLAST DISTRIBUTION	122
E.1	Distribution of Blast Loading.....	122
APPENDIX F.	MODEL ANALYSIS RESULTS.....	128
F.1	Selected Output of Case 1 Blast Load.....	128
F.2	Selected Output of Case 2 Blast Load.....	137
F.3	Selected Output of Case 3 Blast Load.....	146
F.4	Selected Output of Case 4 Blast Load.....	155
F.5	Selected Output of Case 5 Blast Load.....	165
REFERENCES.....		175
BIOGRAPHICAL SKETCH		177

LIST OF TABLES

Table 3.1:	Typical Span Lengths for Different AASHTO Girders	13
Table 3.2:	Equivalent Static Parameters for 500 lb of TNT Explosion.....	42
Table 3.3:	Summary of Seismic and Blast Load Differences	47
Table 3.4:	Material Properties Used.....	51
Table 3.5:	Converted Pressure for 500 lb of TNT Explosion.....	54
Table 3.6:	Various Load Cases.....	55
Table 4.1:	Member Status for Case 1 Blast Load.....	70
Table 4.2:	Member Status for Case 2 Blast Load.....	71
Table 4.3:	Member Status for Case 3 Blast Load.....	72
Table 4.4:	Member Status for Case 4 Blast Load.....	73
Table 4.5:	Member Status for Case 5 Blast Load.....	74
Table 4.6:	Converted Pressure for 1.7 lb of TNT Explosion.....	76
Table 4.7:	Converted Pressure for 14.5 lb of TNT Explosion.....	77
Table 4.8:	Converted Pressure for 5.7 lb of TNT Explosion.....	79
Table 4.9:	Converted Pressure for 13 lb of TNT Explosion.....	79

LIST OF FIGURES

Figure 2.1:	Alfred P. Murrah Federal Building after Explosion.....	6
Figure 2.2:	Oil-Tanker Burned on Interstate 95.	11
Figure 3.1:	Cross-Sections of AASHTO Girders.	14
Figure 3.2:	Perspective View of the Model Bridge.	16
Figure 3.3:	Elevation of the Model Bridge.....	16
Figure 3.4:	Cross Section of the Model Bridge.....	17
Figure 3.5:	Column Damage Due to Explosion under Bridge.....	20
Figure 3.6:	Deck-Girder Failure Due to Explosion over Bridge.	22
Figure 3.7:	Typical Reinforcement Detail in 32 in. Barrier.....	24
Figure 3.8:	Partial Plan – Neoprene Bearing Pad.	25
Figure 3.9:	Typical Rebar Detail in Type III AASHTO Girder.	26
Figure 3.10:	Deck Slab Reinforcement Detail.....	28
Figure 3.11:	Tendon Layout in Prestressed Girder.....	29
Figure 3.12:	Pier Cap Reinforcement Detail.	30
Figure 3.13:	Column Reinforcement Detail.	31
Figure 3.14:	Section Properties of Beam and Slab.	33
Figure 3.15:	Nominal and Ultimate Moment Strength.....	34
Figure 3.16:	Nominal and Ultimate Shear Strength.	35
Figure 3.17:	Column Interaction Diagram.....	36
Figure 3.18:	Variation of Pressure with Distance from Explosion.....	43
Figure 3.19:	Blast Pressure Distribution on Bridge Deck (Elevation).	44
Figure 3.20:	Blast Pressure Distribution on Bridge Deck (Plan).....	45
Figure 3.21:	Comparison of Blast and Seismic Action on Structures.	46
Figure 3.22:	The Bridge Model in STAAD.Pro.	50
Figure 3.23:	Case 1 Load on Model Bridge.....	56

Figure 3.24:	Moment Diagram for Case 1 Load.....	57
Figure 3.25:	Shear Force Diagram for Case 1 Load.....	57
Figure 3.26:	Case 2 Load on Model Bridge.....	59
Figure 3.27:	Moment Diagram for Case 2 Load.....	59
Figure 3.28:	Shear Force Diagram for Case 2 Load.....	60
Figure 3.29:	Case 3 Load on Model Bridge.....	61
Figure 3.30:	Moment Diagram for Case 3 Load.....	61
Figure 3.31:	Shear Force Diagram for Case 3 Load.....	62
Figure 3.32:	Case 4 Load on Model Bridge.....	63
Figure 3.33:	Moment Diagram for Case 4 Load.....	64
Figure 3.34:	Shear Force Diagram for Case 4 Load.....	64
Figure 3.35:	Case 5 Load on Model Bridge.....	66
Figure 3.36:	Moment Diagram for Case 5 Load.....	66
Figure 3.37:	Shear Force Diagram for Case 5 Load.....	67
Figure B.1:	Typical Beam Elevation.....	90
Figure B.2:	Partial Superstructure Section.....	91
Figure B.3:	Composite Dead Load Moments and Shear.....	93
Figure B.4:	Non-Composite Dead Load Moments and Shear.....	93
Figure B.5:	Distributed Live Load Moments and Shear.....	94
Figure B.6:	Compression at Release and Final Tension.....	95
Figure B.7:	Top, Bottom and Allowable Release Stresses.....	97
Figure B.8:	Top, Bottom and Allowable Final Stresses.....	98
Figure B.9:	Camber and Dead Load Deflection.....	100
Figure D.1:	Blast Load for Negative Moment Capacity.....	112
Figure D.2:	Interaction Diagram Slice at Axial Load.....	120

ABSTRACT

The purpose of this research is to assess the performance of an American Association of State Highway and Transportation Officials (AASHTO) girder bridge under blast loading. The AASHTO has specified probability based design methodology and load factors for designing bridge piers against ship impact and vehicular collision. Currently, no specific AASHTO design guideline exists for bridges against blast loading. Structural engineering methods to protect infrastructure systems from terrorist attacks are required.

Bridges are unique in terms of materials used, length, width, skewness, span, loading, traffic conditions, and overall geometry. This research investigated the most common types of concrete bridges on the interstate highways. A 2-span 2-lane bridge with Type III AASHTO girders was used for modeling. Girder spacing was chosen based on the span length and loading conditions. AASHTO Load and Resistance Factor Design (LRFD) methods were used for bridge design. Performance of AASHTO girders, piers and columns under typical blast loading were analyzed and documented for future use in blast resistant design of concrete bridges.

The model bridge failed under typical blast loads applied over and underneath the bridge. The research findings concluded that the AASHTO girders, pier cap and columns could not resist typical blast loads. The amount of blast loads, which the individual members can resist before failure, was determined. The model bridge columns were capable of resisting typical blast loads if the explosion occurs at a minimum standoff distance. From these research findings, necessary measures to protect existing bridges from explosion impact are specified and recommended for bridge modification and design guidelines.

CHAPTER 1

INTRODUCTION

1.1 Problem Statement

Bridges in America need to be protected from blast explosions. For example, more than 6,000 stringer or multi-beam girder bridges exist in the State of Florida, of which 1,727 bridges are on interstate highways (NBI, FHWA 2003). Approximately 90 percent of the prestressed girder bridges in Florida are American Association of State Highway and Transportation Officials (AASHTO) girder bridges, Type III girders being the most common. None of these bridges have been designed to resist impact of explosion. The intent of this research is to investigate performance of AASHTO girder bridges under typical blast loading that will help determine necessary structural design criteria to reduce the probability of catastrophic structural damage, which in turn will lessen human casualties, economic losses and socio-political damage.

The AASHTO has probability based design methodology and load factors to be considered while designing bridge piers against ship impact and vehicular collision. It also has definite criteria to design bridges in different seismic zones with different acceleration coefficients. But it has no specific guidelines to design concrete bridge that will be able to resist typical explosion. In response to this vital need, while blast attacks are of growing concerns, National Cooperative Highway Research Program (NCHRP) has invited project proposals to conduct research in order to develop design and detailing guidelines for blast-resistant highway bridges that can be adopted in the AASHTO manual on bridge design (NCHRP 2004).

1.2 Types of Bridges in Florida

Among various types of bridges, AASHTO girder bridges, suspension bridges, cable-stayed bridges and box girder bridges are the most common. About 90 percent of the bridges in Florida are made of AASHTO girders, with Type III girders being the most common. Because of the complex nature of suspension, cable-stayed or box girder bridges, and less vulnerability of attack as they are well-protected because of their importance, performance of only AASHTO girder bridges, which are the most common in Florida, will be investigated in this research.

Five different types of AASHTO girder are used, such as Type II, Type III, Type IV, Type V and Type VI. Selection of types of girder for a particular bridge depends on various factors including span length, girder spacing, and traffic loading conditions. Other types of AASHTO girders are not as commonly used as Type III girders in Florida.

1.3 Florida Highway Infrastructure

Both Interstate 75 and Interstate 95 carry large volume of traffic to and from the state. Being famous for tourism because of its attractive geological location and fun activities, Florida, the 3rd most populated state in the nation, attracts millions of tourists and short time visitors from the nation as well as from other countries around the world. The interstate and highway system is networked through the state connecting spectacular tourist spots including Disney World, Sea World, Universal Studios, Cape Canaveral, Kennedy Space Center, South Beach, Key West and other beautiful cities. Moreover, because of excellent climatic conditions during winter and summer, people living in the northern part of the country visit and spend time in Florida during vacation and holidays. Considering all these factors, Florida is one of the most important states in the nation that requires special precautionary measures to develop strategies and practices for deterring, disrupting and mitigating potential attacks against the vulnerable bridge structures networked through the highways around the state. After considering the nature of the bridge components in the highway systems, and the lessons learned from natural disasters such as earthquake, the effects of the transportation related problems caused by the World Trade Center (WTC) debris removal as a result of September 11, 2001 (9/11) attacks and

the Interstate 40 bridge collapse in May 26, 2002, after being struck by an empty oil barge near Webber's Falls, Oklahoma, it is easily understandable that the loss of a critical bridge in the highway system can result in millions of dollars of direct reconstruction costs, and even greater socio-economic costs. Finally, revenue from Florida bridge toll facilities might dramatically be affected because of traffic disruption in the event of bridge collapse due to terrorist attacks.

1.4 Goals and Objectives

Bridges are unique in terms of span length, width, skewness, materials used, loading, traffic conditions, and overall geometry. In this research, a 2-span AASHTO girder bridge with two lanes of traffic will be considered for computer modeling and analysis. Span lengths will be chosen based on the maximum capacity of a specific girder type and spacing. The AASHTO Load and Resistance Factor Design (LRFD) method, 2nd Edition, 1999, with Interims through 2003 (AASHTO LRFD 2003), along with Florida Department of Transportation (FDOT) Structures Design Guidelines (SDG 2004), will be followed for bridge design. Design of bridge components will be performed to develop the prototype models for analysis.

The main structural components of a concrete bridge are barriers, deck, beams, pier cap, columns and foundation. In case of an extreme event, each component of a bridge responds in a different way. Due to unpredictable nature of the mode of attack and complex behavior of explosive loads, amount of damage may greatly vary depending on the redundancy of the structure. Most structures are complex even under static loads. So, their responses to dynamic loads, such as blast load, tend to be more complicated that require more sophisticated elastic and inelastic analysis. Blast analysis and design software such as yield line theory based TM 5-1300, developed by US Department of Defense (DOD 1990), is not available to general public but only to contractors who work for the government agencies. A common approach to determine the dynamic responses of a structure to specific loading conditions is to develop a model of the structure and analyze it. To determine the structural performance of the components, the prototype model bridge will be designed and analyzed under typical blast load. Based on the defined failure criteria, the available strengths of the individual bridge components will

be compared with the applied loads to be determined using commercially available structural analysis software STAAD.Pro (REI 2003). In addition to the STAAD.Pro, MathCAD, and FDOT LRFD Prestressed Beam Program (FDOT 2001), FDOT Biaxial Column Program (FDOT 2001) and other free-to-public FDOT software will also be used in the typical bridge design and analysis.

It can be reasonably assumed that a bridge may collapse due to the individual failure of one or more of the main structural components – deck, beam, pier or column. Deck failure may not lead to a total collapse of the structure because of its high redundancy and localized mode of failure, but it can cause the structure to go out of service. FDOT has no specific guidelines on categorizing structures to be completely or partially out of service in case of any structural damage. It is chosen on a case-by-case basis depending on the location, amount and intensity of damage.

Material strengths and section properties of different components of the bridge, as required by traditional design, will be keyed into the STAAD.Pro model bridge. Typical amount of blast loads will be converted into static loads using the ATBlast software developed by the Applied Research Associates, Inc (ARA Inc.). The converted static loads will then be applied on the bridge models at selected locations for each separate event of explosion. After analyzing the model bridge in the STAAD.Pro, response of the respective components will be observed, documented, and analyzed to determine the performance of the bridge.

Performance of the AASHTO girder bridge will be assessed following finite element analysis (FEA) of the bridge model in the STAAD.Pro. FEA is a numerical modeling technique that combines structural geometry and loading information with material properties to predict stresses and strains in a structure. The technique is quite flexible, and has wide applicability and acceptability in the engineering community.

The proposed research will be an important step towards blast-resistant bridge design. It will benefit the state, county and local engineering agencies, and the Department of Homeland Security in securing the bridge structures of the country from terrorist attacks. It will also help assess the amount of damage due to an explosion on an existing structure, and to identify proper methods of emergency works required to put the bridge back in service in the shortest possible time.

CHAPTER 2

LITERATURE SURVEY

2.1 Explosive Attacks

Terrorist attacks in the United States have created concern over the safety and protection of the public. Protecting existing and future infrastructure including bridges, tunnels, public places, shopping malls, halls, recreational facilities, workplace, and other important structures from terrorist activities is the vital issue in homeland security. Bridges are the most common infrastructures in the nation's highway system. As a result of the terrorist threats and attacks, engineers and transportations officials are becoming more active in protecting the bridges from potential blast attacks. Some of the significant explosive attacks, which motivated to conduct this research, are discussed herein.

On September 11, 2001 (9/11), the World Trade Center (WTC) Towers in New York City collapsed because of the largest terrorist attacks in the history of the United States with 2,892 people killed and several hundreds injured in that horrible attack. On the very same day, the Pentagon, a symbol of National Security, was also attacked killing nearly 200 people and injuring many more. The WTC had been a victim of a terrorist attack for the first time on February 26, 1993. Six people were killed in the first attack with many more being injured.

Almost two years after the first WTC bombing, on April 19, 1995, another terrorist explosion shattered portions of the Alfred P. Murrah Federal Building in Oklahoma City, killing 168 people. Figure 2.1 shows the damaged building in the aftermath of the explosion. All these attacks caused thousands of casualties, impacts on society, and billions of dollars worth of removal, reconstruction and repair cost.

Therefore, it has become very important for the country to protect the public and infrastructures from future possible blast attacks.



Figure 2.1: Alfred P. Murrah Federal Building after Explosion.

The WTC attacks have significantly increased public awareness to the need to protect the nation's important and critical infrastructure. Numerous research and demonstration initiatives have been undertaken since 9/11 to find cost-effective and efficient retrofit, security and rapid reconstruction techniques for such buildings. The Department of Homeland Security, Federal Emergency Management Agency and the Department of Defense are taking the primary leads in these efforts. However, the possibility of terrorist attacks on the nation's transportation infrastructure is also significant.

Bridges are very important elements of the highway system in the United States. While building collapse may cause thousands of casualties, bridge collapse may cause significant human casualties as well as social and economic impact on the country by disrupting traffic movements and transportation system as evidenced through the WTC debris removal.

Conventional structures, particularly those above the grade, normally are not designed to resist blast loads. Because the magnitudes of the explosive loads are

significantly higher than the design loads, conventional structures are more susceptible to damage from explosions. Structures above grade, such as bridges, are part and parcel of the highway system. Important bridges on highway system have higher chances of being potential target for terrorist explosions to disrupt traffic movement, to cause human casualties and impact socio-economic condition.

2.2 Background Review

The American Society of Civil Engineers (ASCE) developed a guideline entitled “Design of Blast Resistant Buildings in Petrochemical Facilities” (ASCE 1997). This report provides general guidelines in the structural design of blast resistant petrochemical facilities. Informational coverage is provided for Occupational Safety and Health Administration (OSHA) requirements, design objectives, siting considerations, and load determination with references mentioned for more detailed information. More detailed coverage is provided for types of construction, dynamic material strengths, allowable response criteria, analysis methods, and design procedures. Typical details and ancillary considerations, such as doors and windows, are also included. A "how to" discussion on the upgrade of existing buildings is provided for older facilities which may not meet current needs. Three example calculations are included to illustrate design procedures. In 1992, the OSHA published new requirements for the management of explosive hazards (OSHA 1992). The OSHA Process Safety Management of Highly Hazardous Chemicals regulations (CFR 29, 1910.119) requires operating plants to perform a Process Hazards Analysis (PHA). The focus of these regulations is on toxic, fire and explosion hazards. In many cases, a PHA reveals vulnerabilities because of the location and/or the structural strength of the occupied process plant buildings. This regulation, the recent heightened awareness of terrorist activities, and rising insurance costs have resulted in a drastic increase in the demand for structural consequence evaluations and engineering designs of buildings and structures subject to explosive load. Advances in process and structural engineering now make it possible to design and analyze buildings subject to external blast load from accidental explosions and terrorist bombs with acceptable accuracy.

The National Center for Explosion Resistant Design (NCERD) in the Department of Civil and Environmental Engineering at the University of Missouri-Columbia has been

offering courses on “Explosion Effects and Structural Design for Blast.” The course focuses on the fundamentals of explosion effects, determining blast loads on structures, computing structural response to blast loads, and the design and retrofit of structures to resist blast effects. The emphasis is given on terrorist threats from vehicle bombs, but the fundamental concepts can be applied to other explosive scenarios. Currently available software and publications for blast effects, and design guidance are being discussed and demonstrated. Although much of the design guidance and software is restricted for distribution to government agencies and their contractors, specific information on how to use and obtain the software is being covered in the course. The participant gains an understanding of how to compute blast loads on a structure, how to compute structural response to blast loading, and practical methods for designing and retrofitting structures to resist blast effects.

The design and construction of public buildings to provide life safety in the face of explosions are receiving renewed attention from structural engineers. This highly effective approach of blast resistant design is only feasible where a standoff zone is available and affordable. For many urban settings, the proximity to unregulated traffic brings the terrorist threat to or within the perimeter of the building. For these structures, blast protection has the more modest goal of containing damage in the immediate vicinity of the explosion and the prevention of progressive collapse. In suburban and government facilities, the minimum standoff zone can be easily established. In the urban area, it is relatively harder to attain these standoff distances surrounding the facilities.

Buildings, such as offices, apartments and stores, designed using building codes, do not require blast resistance. Hazard process buildings have building code requirements for special safety considerations. For example, the Uniform Building Codes (UBC 1997) states that, “Walls, floors and roofs, separating a use from an explosion exposure, shall be designed to resist a minimum internal pressure of 100 lb per square foot in addition to other conventional loads.” Some level of blast resistance is required for new federal buildings. Existing federal buildings undergoing expansion also must include blast resistance. In each case, the General Service Administration establishes design requirements. Specific action involves: protecting windows; installing a secure perimeter fence and/or hardening a portion of the building; and determining the likelihood of

progressive collapse and designing against it. There is no comparable, universal guidance in the civilian sector. Neither any Building Code nor the American Concrete Institute guideline for concrete design has addressed the issue of how to perform blast resistant design of building or other structures. Therefore, there are growing concerns among the engineering community for code regulated blast resistant design of concrete structures.

Following the 9/11 attacks, bridge and highway infrastructure engineers face new and largely unexpected challenges relating to the physical security of critical structures against terrorists attacks. Although the 9/11 attacks targeted buildings, threats against bridges, tunnels and other highway infrastructure in various parts of the United States have heightened awareness and concern. Bridge and highway engineers are being tasked to assess the vulnerability of structures and to identify means for reducing this vulnerability. In response to this need, the AASHTO Transportation Security Task Force sponsored the preparation of a guide to assist transportation professionals as they identify critical highway structures and take action to reduce their blast vulnerability. In order to provide guidance to bridge owners and operators, Federal Highway Administrator appointed ten renowned engineers to form the Blue Ribbon Panel (AASHTO BRP 2003) on bridge and tunnel security. The AASHTO Transportation Security Task Force provided support for this initiative. The panel's objective was to apply its collective experience and knowledge about structural design, structural integrity, and new ways of examining how critical bridges and tunnels can be protected against potential terrorist attacks. The panel met four times to identify and clarify issues, develop and evaluate potential solutions, and formulate and refine recommendations for improving bridge and tunnel security. The recommendations presented in the report include recommendations on actions that can be taken either by bridge and tunnel owners and operators or by FHWA, and other state and federal agencies that will result in improved security and reduced vulnerabilities for critical bridges and tunnels. Additionally, to develop and transfer knowledge rapidly within the bridge community to improve structure protection against attack, a series of workshops were conducted in early 2003 under the NCHRP, Project 20-59(2).

Some researchers at the University of Texas at Austin have been conducting parametric research to develop performance-based blast design standards tailored

specifically for bridge substructures. The goal of their research, as collected from Wessex Institute of Technology Press (WIT Press 2004), UK, is to investigate economical, unobtrusive and effective methods to mitigate the risk of terrorist attacks against critical bridges. The potential effects of blast loads on bridge substructures were presented, and the structural design and retrofit solutions to counter these effects were discussed.

2.3 Bridge Failures

Bridge failures across the nation were studied for categorizing failure conditions of a bridge. Some notable failures are as follows:

On March 26, 2004, an oil tanker burned over a bridge on Interstate 95 near exit 26 on southbound lane linking New York and Boston in Bridgeport, Connecticut, damaging major components including the beams and a significant portion of the deck slab, as shown in Fig. 2.2 (Connecticut Post, March 2004). The top portion of the bridge was completely replaced and put in service within 2 weeks of the incident, while maintaining traffic flow through an alternate route during emergency replacement works.

About 3:30 p.m. central time on May 28, 1993, the towboat CHRIS, pushing the empty hopper barge DM 3021, collided with a support pier of the eastern span of the Judge William Seeber Bridge in New Orleans. The Judge William Seeber Bridge, known locally as the Claiborne Avenue Bridge, carries Highway Route 39 over the New Orleans Inner Harbor Navigation Canal, known locally as the Industrial Canal. The impact severed bent 21, causing two approach spans (i.e., 145 ft of bridge deck) and the two-column bent to collapse onto the barge and into the shallow waters of the canal. Two automobiles carrying three people fell with the four-lane bridge deck, resulting in one death and serious injuries to the other two people. As a result of the accident, the canal was closed to navigation traffic for 2 days, and the bridge was closed to vehicle traffic for 2 months to complete repair works (National Transportation Safety Board, NTSB, Report No. HAR-94/03, 1994).

On May 19, 1993, at 1:35 a.m. central time, while traveling south on Interstate 65 near Evergreen, Alabama, a tractor with bulk-cement-tank semi-trailer left the paved road, traveled along the embankment, overran a guardrail, and collided with a supporting bridge column of the County Road 22 overpass. Two spans of the overpass collapsed

onto the semi-trailer and the southbound lanes of Interstate 65, sending a cloud of cement dust into the air. An automobile and a tractor-semi-trailer, also southbound, then collided with the collapsed bridge spans. The cement-tank truck driver sustained serious injuries; the drivers of the other two vehicles were killed. Contributing to the severity of the accident was the collapse of the bridge. After the semi-trailer collided with and demolished the north column, the failure resulted due to a combination of the nonredundant bridge design, the close proximity of the column bent to the road, and the lack of protection for the column bent from high-speed heavy-vehicle collision (NTSB, Report No. HAR-94/02, 1994).



Figure 2.2: Oil-Tanker Burned on Interstate 95.
(AP, Connecticut Post, March 2004)

About 9:25 p.m. on February 23, 1975, an automobile struck a vital structural member of the Yadkin River Bridge near Siloam, North Carolina. The collision occurred in heavy fog. Following the impact, the bridge collapsed, and both the automobile and the bridge fell into the river. Six more vehicles vaulted into the collapse zone within a 17-minute period. Four persons were killed and 16 others were injured as a result of that accident (NTSB Report No. HAR-76/03, 1976).

2.4 Blast Vulnerability Assessment

Not much work has been done on the blast vulnerability of bridge structures. Naturally, the bridges are less protected as compared to other structures such as high-rise buildings, federal and state offices, and other important structures. The national highway system has been carefully networked with almost 600,000 bridges around the country (NBI 2003). As traffic flow continues over the interstate and state highways 24 hours a day, it is a common perception that the bridges are protected to some extent by the moving traffic. However, there are growing concerns evolving nowadays because of the terrorist attacks on the American facilities at home and abroad. The government has adopted utmost security measures for protecting important bridges in the United States, such as the Golden Gate Suspension Bridge in San Francisco, Sunshine Skyway Cable-Stayed Bridge in Tampa, and the Brooklyn Suspension Bridge in New York City, in response to the terrorist threats of attacking these bridge structures. On the other hand, regular interstate and highway bridges are not being paid enough attention to secure them against terrorist attack. Therefore, these bridges are more vulnerable to attack, which may cause casualty as well as social and economic losses, and disrupt traffic movement affecting the transportation system and network around the country.

CHAPTER 3

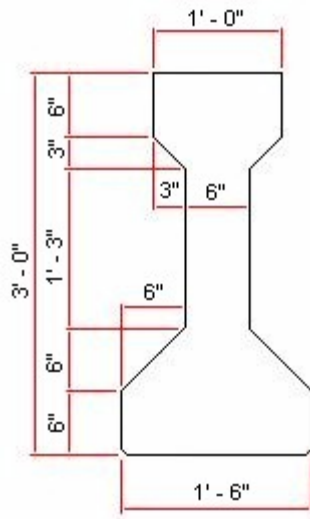
MODELING AND ANALYSIS

3.1 Model Bridge Selection

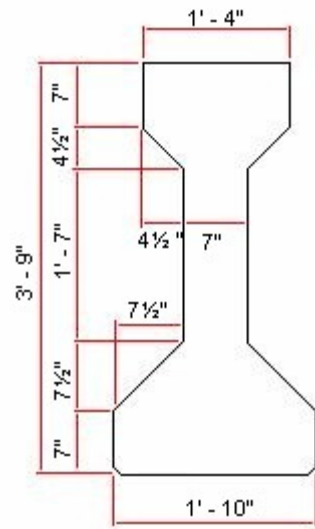
For simplicity and being the most common among the interstate bridges, a Type III AASHTO girder bridge of span length 80 ft with appropriate girder spacing was selected for this research. Span lengths for Type III AASHTO girder bridges in Florida typically vary from 50 to 80 ft. The corresponding range of span lengths for each type of AASHTO girder is presented in Table 3.1. Figure 3.1 illustrates cross-sectional dimensions of typical Type II, III and IV AASHTO girders. For the model bridge, 80 ft span length was chosen to represent the most common span length for Type III AASHTO girders. Width of the bridge was selected based on Average Annual Daily Traffic (AADT), design speed and other relevant requirements. The most common type of barrier used in the interstate bridges is 32 in. high and 1 ft 6 in. wide. The model bridge for this research was assumed to be of two 12 ft lanes, one 10 ft shoulder and another 6 ft shoulder, and two 1 ft 6 in. wide barriers producing an overall bridge width of 43 ft. Seven Type III AASHTO girders with center-to-center spacing of 6 ft were used in the model bridge.

Table 3.1: Typical Span Lengths for Different AASHTO Girders

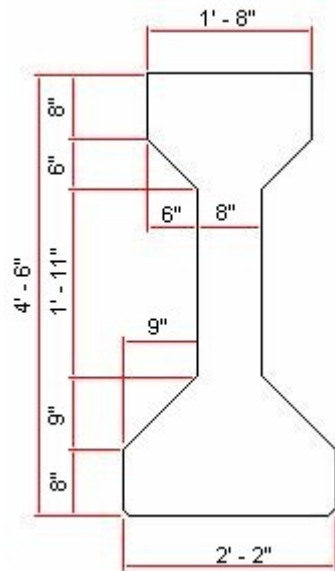
ASSHTO Girder	Depth	Span Length
Type II	3'-0"	40 to 60 ft
Type III	3'-9"	50 to 80 ft
Type IV	4'-6"	70 to 120 ft
Type V	5'-3"	110 to 140 ft
Type VI	6'-0"	130 to 160 ft



Type II AASHTO Girder



Type III AASHTO Girder



Type IV AASHTO Girder

Figure 3.1: Cross-Sections of AASHTO Girders.

Environmental conditions such as, the presence of chloride, sulfate, and pH value of soil also play important roles in the design of bridge components. FDOT classifies environmental conditions in three broad categories – slightly aggressive, moderately aggressive and extremely aggressive based on the amount of chloride and sulfate presence, and the pH value of the soil. This classification applies to substructure (pier, column and foundation) and superstructure (slab, girder and barrier) element design. For this research, moderately aggressive environment was chosen for the substructure and superstructure design.

The model bridge is comprised of two equal simple spans of 80 ft with seven Type III AASHTO girders spaced at 6 ft producing an overall width of 43 ft. The perspective view and the elevation view of the model bridge are presented in Figs. 3.2 and 3.3, respectively. The bridge is assumed to carry two 12-ft lanes of traffic in one direction. Clear roadway width of 40 ft from curb to curb was used in the design. The bridge girders are centered along the centerline of the bridge producing an overhang width of 3 ft 6 in. with a clear distance of 2 ft in between the centerline of the exterior girder and the gutter line on each side. The cross-section view of the model bridge is shown in Fig. 3.4.

One intermediate pier at the middle of the bridge, and two end bents at the beginning and at the end of the bridge hold up the girders, which support 8 in. thick cast-in-place concrete deck slab. Seven 18 in. square prestressed precast concrete piles spaced at 6 ft support each end bent. The pier cap is supported by two identical columns of 3 ft 6 in. diameter on two separate footings. The top of each footing is 2 ft below the ground surface. Each 10 ft by 10 ft footing is supported by four 24 in. square prestressed concrete piles with the column at the center of the footing.

Size of the end bent caps and the pier cap depends on several factors including minimum seat width required according to the AASHTO LRFD Bridge Design Specifications, beam spacing and pile spacing. The end bent cap width of 3 ft and pier cap width of 4 ft were determined to be appropriate for this model. Two columns of diameter 3 ft 6 in. were proven to be adequate to support the pier cap.

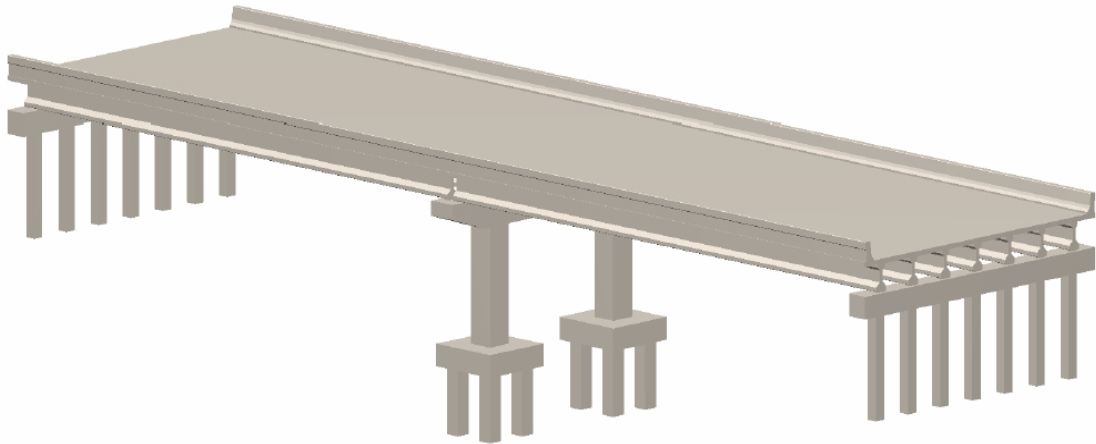


Figure 3.2: Perspective View of the Model Bridge.

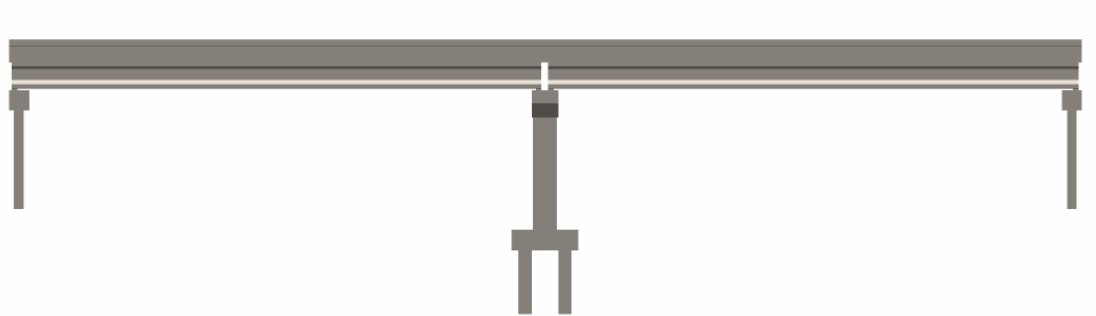


Figure 3.3: Elevation of the Model Bridge.

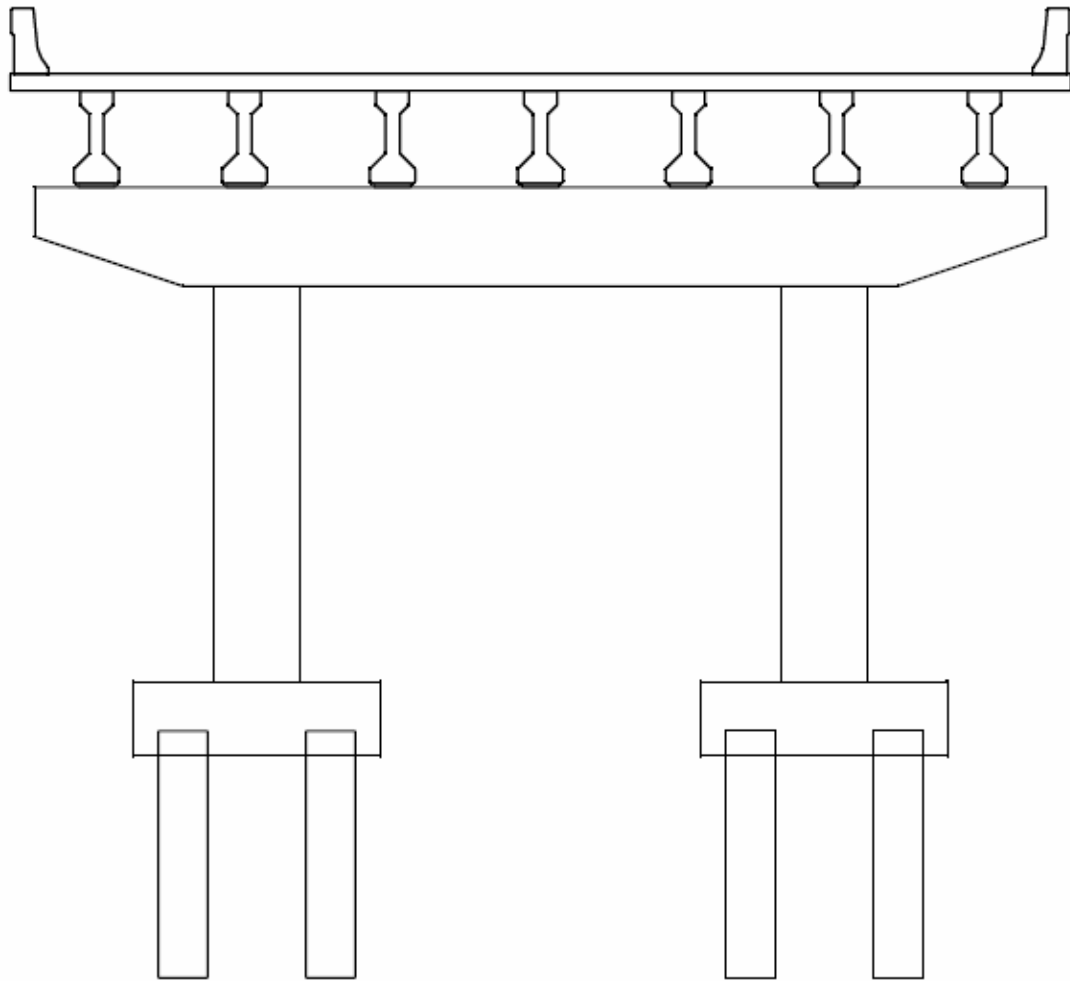


Figure 3.4: Cross Section of the Model Bridge.

3.2 Failure Criteria

Failure criteria are used in combination with information about stresses in a structure to predict the load levels a structure can withstand. For instance, maximum shear stress criteria predict failure when the applied shear stress in a structure exceeds its shear capacity. The failure criteria at the time a structure fails can be assumed as a function of the applied loads and the material property of the element. Concrete bridges are made of concrete and steel reinforcements that develop shear and flexural capacity of

a section. A universally accepted general criterion was followed throughout this research – if the applied force exceeds the capacity of the section, the component fails.

The component failure may be categorized as slight to moderate and extreme depending on the amount of damage. Minor cracking and spalling in the concrete can be easily repaired, and be considered as slight to moderate failure for which the structure may not have to be put out of service. Because of the extreme nature of blast loading, it can be assumed that failures will be extreme, which will eventually require the member, if not the whole bridge, to be fully replaced. Depending on the amount of component damage, bridge failure can be classified as partial or total failure. Partial failure will most likely cause the bridge to be put partially out of service, while total failure will definitely put the bridge completely out of service. Partially out of service means traffic will be allowed to flow over the designated part of the bridge, while repair work is ongoing. In case the bridge is completely out of service, traffic will be allowed to move through an alternate route until the replacement bridge is put into service. Individual failure and amount of damage of each bridge component will be observed and analyzed on a case-by-case basis to determine the performance of the respective members. Based on these components performance, overall bridge performance will be determined.

In case of the pier cap or column failure, there is a greater chance that the whole bridge will collapse resulting the route to be completely out of service until the bridge is completely repaired or replaced. Girders are considered as part of the deck slab support system. Individual girder failure can result in partial loss of bridge service, while more than one girder failure may force the bridge to be fully out of service. In the event of deck slab failure in between any two adjacent beams, the bridge may still be in place, and may be partially used for at least one lane of traffic movement resulting in partially out of service. Slab failure, amounting more than this specified limit, might be considered as completely out of service until a full replacement is done.

At present, the states Departments of Transportation (DOT) do not have any defined failure criteria to define a bridge as partially or completely out of service in terms of traffic movement. Failure may be caused due to damage on any one of the critical components of a bridge, such as girders, deck slab, pier cap or columns. Column or pier cap failure may initiate total collapse of the bridge, while girder or deck slab failure may

not cause complete collapse. Partial failure may place the bridge partially out of service depending on the location and amount of damage.

Failure condition due to blast loading can be reasonably categorized depending on the amount and type of damage, time to repair, and whether the bridge will be placed partially or completely out of service during emergency repair works. This will help FDOT and other engineering agencies identify the type of bridge failure, estimate approximate amount of time to repair, and maintain alternate flow of traffic during repair works.

3.2.1 Column Failure

Bridge column is an axially loaded member with eccentric forces that produce flexural and shear stress in the member. If the applied flexural and axial stress exceeds the flexural and axial capacity of the member, it fails. On the other hand, moment capacity of a column increases with the increase in applied axial force to some extent. Therefore, column capacity should be checked against moment with corresponding axial load.

Bridge column is more vulnerable to blast attack because of easy access. Therefore, it is considered the most critical element of a bridge structure in terms of failure and stability. The column is more accessible and more susceptible to damage in case of a ground based blast attack underneath the bridge, as shown in Fig. 3.5. Although one column failure may or may not initiate bridge collapse, failure of both columns will definitely collapse the entire bridge. Considering the worst-case scenario, in case of a hammerhead pier supported by a single column, the bridge will experience immediate collapse as soon as the column fails. Therefore, column is the most critical element of a bridge structure, which should be addressed with extreme importance while analyzing or designing a bridge. A column can be strengthened against sudden collapse by wrapping with carbon fibers or steel plates, which will increase its shear capacity, and to some extent, its moment capacity as well. Blast pressure decreases with the increase in distance from the point of explosion. Therefore, maintaining the required standoff distance around the column may prevent column failure due to the reduced impact of explosion.



Figure 3.5: Column Damage Due to Explosion under Bridge.
(Bridge Removals, FHWA)

3.2.2 Pier Cap Failure

A pier cap is also very important for the structural stability of a bridge. The pier cap may fail due to upward blast load caused by ground-based attack for which it is not usually designed. It may also fail because of explosion on top of the bridge. Pier cap supports the bridge superstructure through bearing pads. Failure of a pier cap will initiate the girders as well as the deck slab failure because of lack of support, which may eventually cause the bridge collapse. Pier cap may fail because of flexure or shear, if applied moment or shear due to explosion exceeds its capacity.

3.2.3 Girder Failure

Superstructure dead loads and vehicular live loads are transferred through the deck slab to the girders, and then to the substructure. Girders play an important role on securing the superstructure and substructure by creating redundancy against sudden collapse. They are more prone to damage due to blast loading from underneath the bridge than over the bridge. Girders are typically designed to withstand moments and shears caused by vertically downward loads. So, if the bridge is subjected to blast from top, for instance by a truck bomb, vertically downward forces will produce moments and shears that can be compared with the composite section properties of the deck-girder system. A possible damaged condition of a box-girder superstructure due to an explosion on top of the bridge is presented in Fig. 3.6. On the other hand, a vertically upward load, caused by blast load from underneath the bridge, will produce upward moments (negative moment) and shears. Of course, composite action of the deck-girder system will increase negative moment capacity of the section to some extent, as they are integrally built. In case of an explosion underneath the bridge, deck slab will contribute most of the resistance to the attack, while the girders will have minimal resistance unlike resistance against downward loads. If applied moments or shears exceed the respective composite capacity of the deck-girder system, slab failure will be initiated following the girder failure. Chances are that the girder failure may not initiate complete collapse of the bridge, but it may cause the bridge partially or totally out of service depending on the extent, location and the type of damage. For the purpose of this research modeling with a seven-girder bridge, it can be logically assumed that failure of any two or more girders will put the bridge completely out of service for traffic movement. Failure of any one of the seven girders may put the bridge partially out of service for emergency repair works.

3.2.4 Slab Failure

The structural element of the bridge with maximum redundancy is the deck slab. It is integrally built with the girders underneath, and secured at both edges with the traffic railing barriers. The barriers are designed in such a way that in case of a vehicular collision, barriers will fail before the deck slab failure.



Figure 3.6: Deck-Girder Failure Due to Explosion over Bridge.
(Bridge Removals, FHWA)

The deck slabs are built integrally with the supporting girders, and are more susceptible to damage in case the explosion originates underneath the bridge compared to over the bridge explosion. Because of spherical pressure profile of blast load and high redundancy of the deck slab, damage may occur on a portion of the slab only or on a localized part of the slab-girder system in case of a moderate explosion. Like other structural elements, the deck slab is also designed for moment and shear. Failure of a deck slab may initiate if applied moments or shears due to explosion exceed the capacity of the section. For the 43 ft wide model bridge being analyzed in this research, if a portion of the slab only between two adjacent girders experience moderate to severe damage, the bridge will be assumed as partially out of service. Complete loss of bridge service will be assumed for more extensive slab damage.

3.3 Model Bridge Design

Elements of the model bridge are categorized as superstructure and substructure. Superstructure includes deck slab, barrier and prestressed AASHTO Girders. Substructure is comprised of end bent cap, backwall, pier cap, column, footing and piles. All these elements of the model bridge were designed following AASHTO LRFD Bridge Design Specifications, 2nd Edition, 1999, with Interims through 2003 (AASHTO LRFD 2003). Each element has different geometric criteria to be satisfied in addition to the design requirements. All requirements, as well as any other construction related issues, were professionally followed for structural quality control.

3.3.1 Geometric Parameters

Geometric parameters play important roles in analyzing a bridge. In the model bridge, Type III AASHTO girders were spaced at 6 ft on center. The deck slab was 8 in. thick cast-in-place concrete over the girders connected with a series of vertical reinforcements. Concrete haunch was used to eliminate the gap due to beam camber between the bottom of the slab and top of the girders. The deck was integrally built with two 32 in. high FDOT standard barriers, as shown in Fig. 3.7. The girders were supported by the neoprene bearing pads designed to withstand the compressive and rotational effects due to girder loads. FDOT standard neoprene bearing pads, as presented in Fig. 3.8, were used in the model bridge. FDOT Standard Bearing Pad for Type III AASHTO girder has a longitudinal dimension of 1 ft 6 in. along the length of the cap and a transverse dimension of 10 in. Bearing pads were placed over concrete pedestals of at least 4 in thickness, and the standard geometric requirements were met throughout the entire bridge. The pedestals were made integral with the pier cap or end bent cap to accommodate the bearing pads. For Type III AASHTO girders, as shown in Fig. 3.9, pedestals were 3 ft long along the cap and 2 ft wide across the cap.

Piles were centered along the centerline of the end bent cap, and embedded 1 ft into the cap. Columns were centered along the centerline of the pier cap. Pier cap was tapered at the ends for a length of 6 ft. Each column was made integral with the footing supported by a group of 4 piles. The model bridge footing had a dimension of 10 ft by 10

ft with a depth of 3 ft, and the 24 in. square prestressed concrete piles were embedded 1 ft into the footing to secure proper connection.

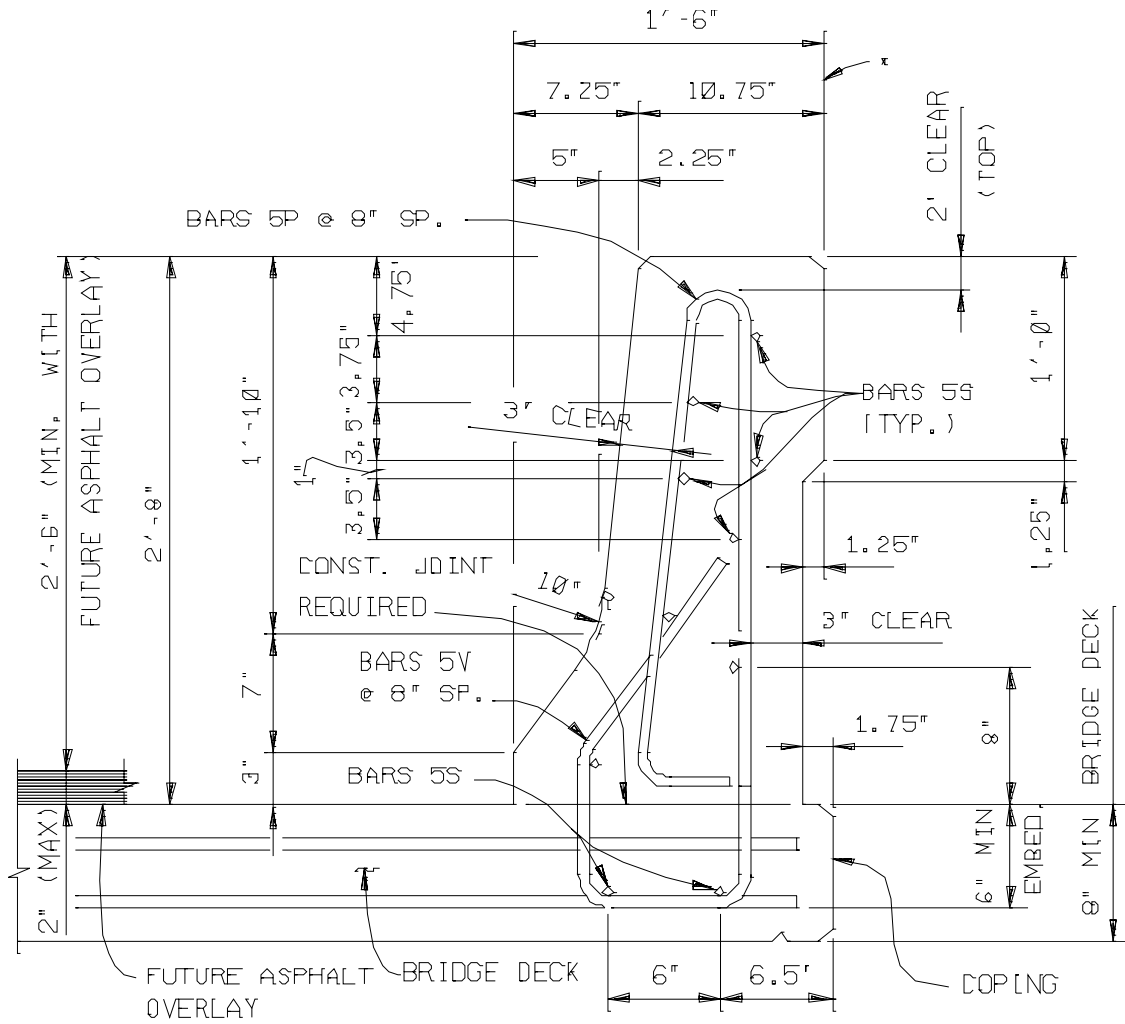


Figure 3.7: Typical Reinforcement Detail in 32 in. Barrier.

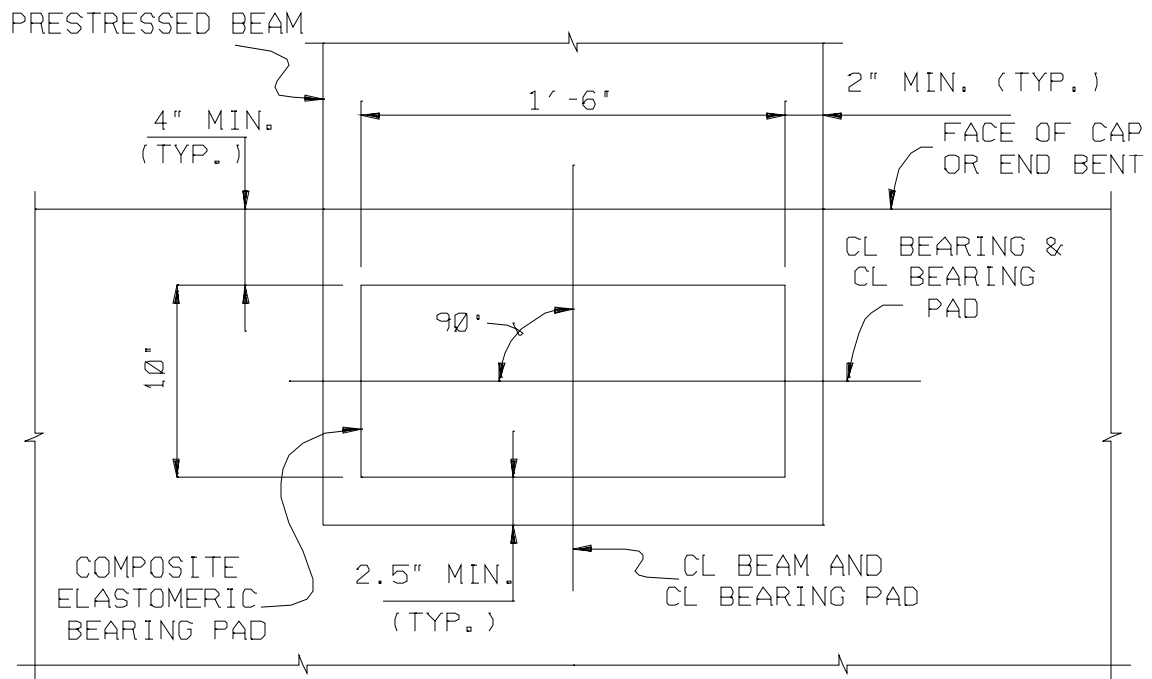


Figure 3.8: Partial Plan – Neoprene Bearing Pad.

3.3.2 Traffic Data

Traffic data play an important role in the geometric design of bridges. The proposed model bridge was assumed to have Annual Average Daily Traffic (AADT) volume of 75,000. Maximum traffic design speed over the bridge was assumed to be 70 mph, typical for interstate bridges.

3.3.3 Loads and Load Factors

AASHTO LRFD method of bridge design with appropriate load factors were used for the design of the bridge components. For permanent dead loads, weight of the bridge elements such as deck slab, girders, barriers, diaphragms, stay-in-place forms, a load factor of 1.25 was used while a factor of 1.5 was used for calculating dead load from future wearing surface. The load factor used for live load calculation was 1.75. Impact

factor of 1.33 was used for truckload, except for fatigue analysis, where the factor used was 1.15. No impact factors were used for footing or pile design because they are considered as buried structures.

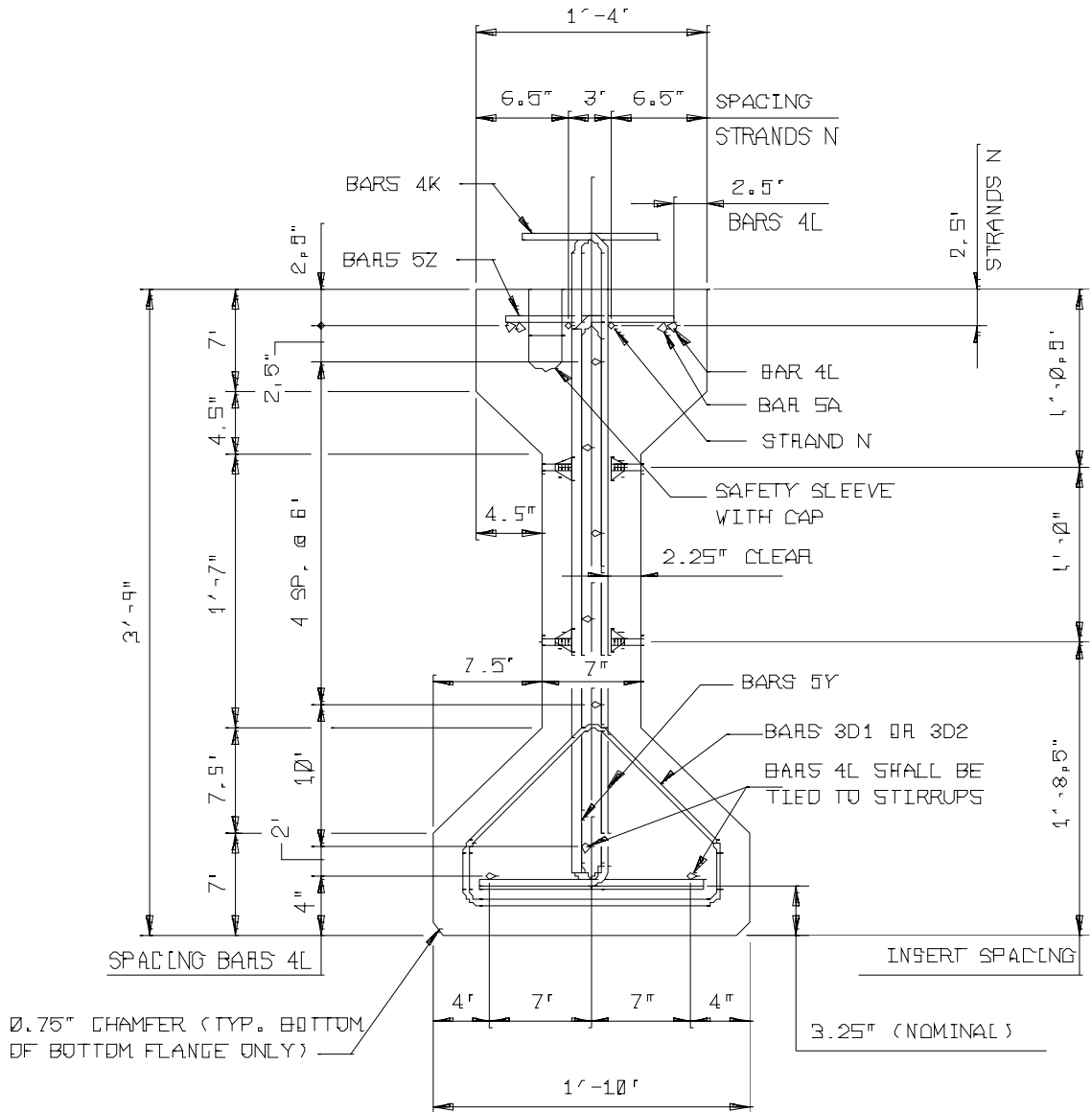


Figure 3.9: Typical Rebar Detail in Type III AASHTO Girder.

Necessary multiple presence factors were used in calculating the distribution factors for moments and shears. Those factors were already included in the distribution factors formula given in Section 4.6 of the AASHTO LRFD Bridge Design Specifications (AASHTO LRFD 2003). The bridge was analyzed with the combinations of one-, two-, or three-lane loaded; whichever produced the critical loading patterns.

3.3.4 Deck Slab Design

Following Empirical Method of the AASHTO LRFD Specifications, the deck slab was designed with #5 reinforcements spaced at 12 in. on center at top and bottom in both directions, as shown in Fig. 3.10. The AASHTO has certain criteria to be satisfied in order to use the empirical method of deck design. All required criteria were carefully examined and satisfied (calculations shown in Appendix A). The Deck slab had a clear cover of 2 in. at top and bottom. In addition to these typical reinforcements, additional reinforcements on top of the deck perpendicular to the direction of traffic were also used to secure connection between the barrier and the deck. To resist the negative flexure over the pier support, the slab was reinforced with additional steel along the direction of traffic. Barrier reinforcements were typical, as shown in Fig. 3.7, with open joint at every half span, and V-groove at every quarter span as a control joint.

3.3.5 Prestressed Girder Design

Prestressed girders were designed using FDOT LRFD Prestressed Beam Design Program. The overhang was limited to 3 ft 6 in., and all girders were equally spaced at 6 ft center to center. One interior and one exterior girder were designed and compared. The controlling girder design, in this case the exterior girder, was used for all other girder design. The girders were prestressed with ½ in. diameter 270 ksi low relaxation 30 straight strands of which 4 strands were debonded for 13 ft at each end. The details of prestressing tendon layout are presented in Fig. 3.11. The jacking force per strand was limited to 31 kips. The ratio of the ultimate moment capacity and the applied moment due to LRFD Strength I loading was 1.17. Therefore, the girders were acceptable under normal traffic loading condition. Maximum amount of cambers of 4 in. at 120 days and

4¾ in. at 240 days were within the acceptable limit. Prestressed Type III AASHTO girder design calculations are given in Appendix B.

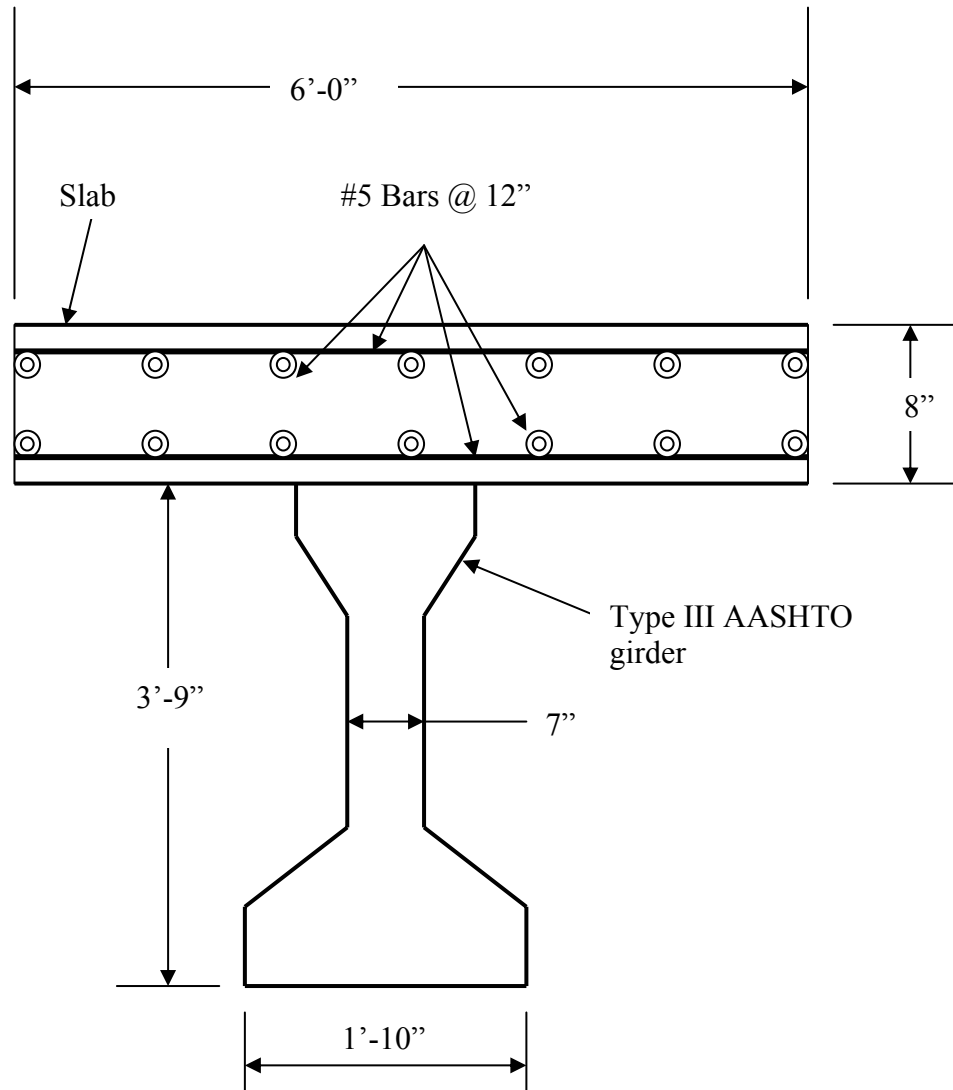


Figure 3.10: Deck Slab Reinforcement Detail.

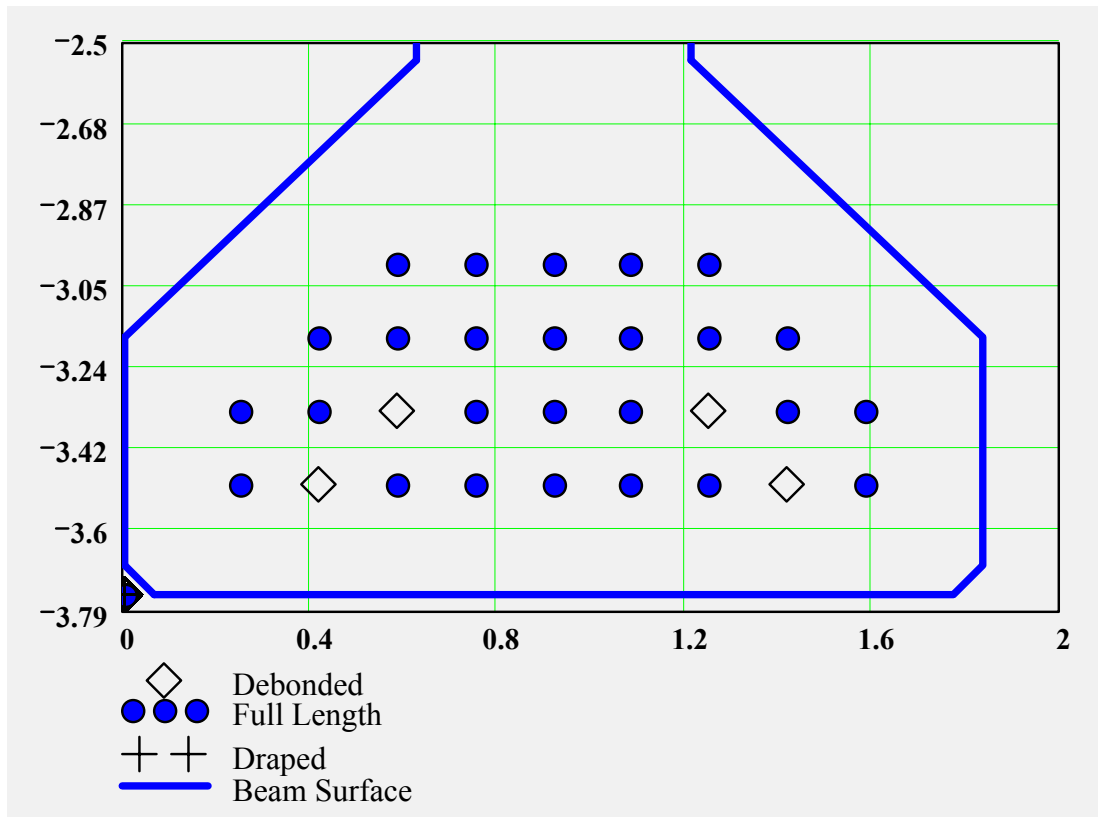


Figure 3.11: Tendon Layout in Prestressed Girder.

3.3.6 Pier Cap Design

The pier cap and the end bent cap were designed using commercially available software RC-Pier. The end bent caps will experience minimal impact of blast because of their location on top of the ground at the end of the bridge. Therefore, end bent caps were excluded from this research. The pier cap was reinforced with 13 #10 bars at top and bottom with 3 in. typical clear cover at each side, as detailed in Fig. 3.12. In addition to the flexural reinforcement, 2 #10 longitudinal reinforcement were also provided on each of the two vertical sides of the cap to satisfy longitudinal torsion requirements. Two double-legged #5 stirrups spaced at 6 in. on center were also used to satisfy vertical shear and torsion. Stirrups and the longitudinal reinforcement were checked to satisfy the

temperature and shrinkage reinforcement requirements. All the reinforcements were checked for construction related issues so that there would be no or minimum conflicts between reinforcements during construction. The ratio of the resisting moment to the applied moment caused by regular dead and live load is 1.9, which is well over the acceptable limit of 1. All related calculations on pier cap design are documented in Appendix C.

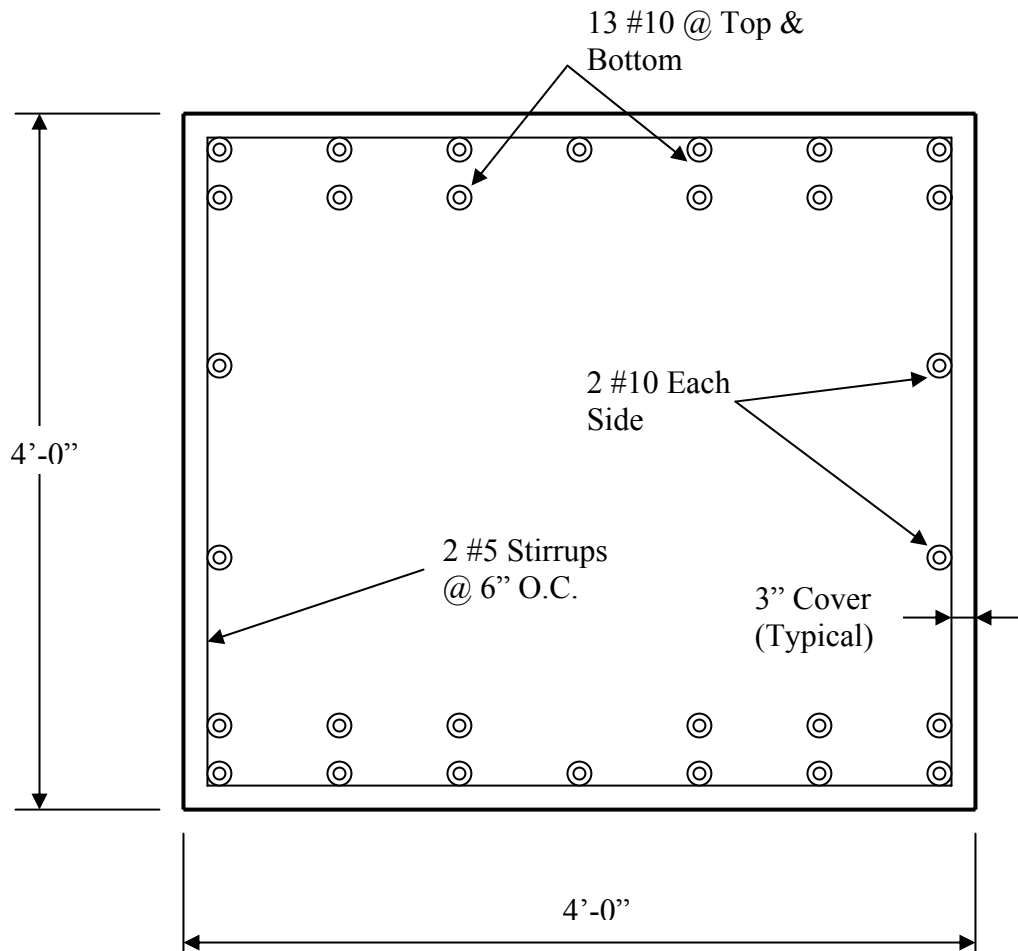


Figure 3.12: Pier Cap Reinforcement Detail.

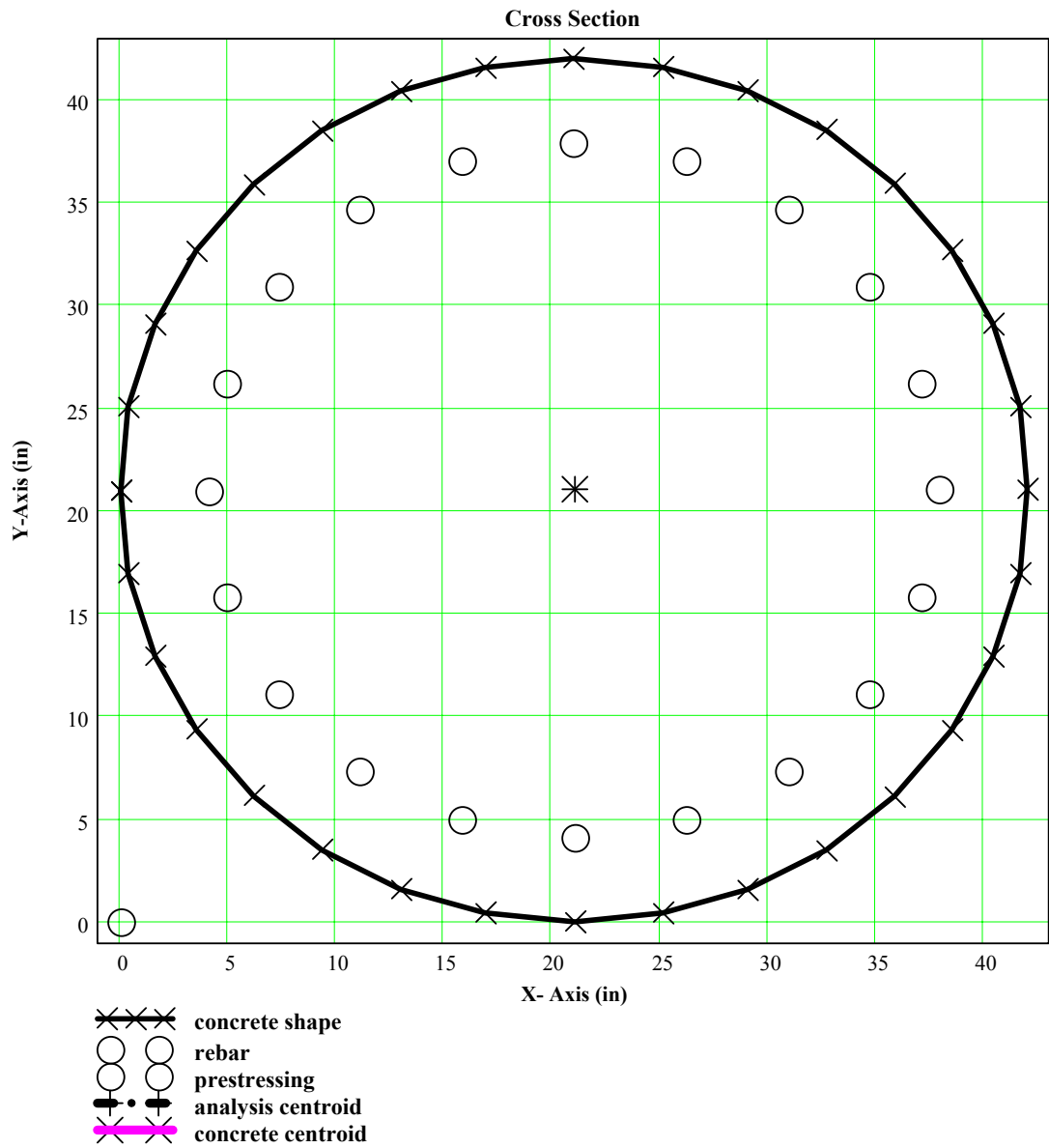


Figure 3.13: Column Reinforcement Detail.

3.3.7 Column Design

The columns and the footings were also designed using the RC-Pier software. Minimum reinforcement requirement governed in the column steel calculation. Because columns are possibly the most critical component of the bridge, they were reinforced with maximum permissible reinforcement of 20 #10 bars with #4 ties spaced at 12 in., as shown in Fig. 3.13, so that the maximum efficiency of the columns could be achieved. The ratio of the ultimate moment capacity to the applied moment was determined as 1.29, which is within the acceptable range. Footings were typically designed with required reinforcements and supported by prestressed concrete piles. It was verified that the assumed pile group was sufficient to take the loads from the footing within tolerable limits. Footings and piles were not considered as critical components of failure as they were buried underground. Since performance assessment of footing is not part of this research, only column design calculations are documented in Appendix C.

3.4 Model Bridge Capacity

The main elements of the model bridge, such as slab-girder composite, pier cap and column were analyzed under blast loading. Based on the analysis, the strength of each individual element was determined. The capacity of each element was later compared with the applied loads on the respective element to determine whether that particular element was able to withstand the loads. The respective strength of each individual element was determined using simple support condition for the girders, and fixed support condition for connection between the pier cap and the columns.

3.4.1 Prestressed Girder Capacity

The bridge may experience blast pressure from two different scenarios. The blast event may generate over or under the bridge. When the explosion occurs over the bridge, a set of vertically downward loads acts on the bridge deck. Prestressed AASHTO girders composite with the deck slab react with their fullest capacity against this set of loads. Other bridge elements, such as barriers, pier cap and columns, experience this load intensity indirectly for being interconnected with the deck slab. As girders are connected

with the deck slab through shear connectors, girder-slab section exhibits single T-beam properties, as shown in Fig. 3.14, with the girders prestressed to enhance positive moment capacity. From FDOT LRFD Prestressed Beam Design Program output (shown in Appendix B), the maximum moment capacity of the prestressed girder, as illustrated in Fig. 3.15, is 4500 kip-ft. The maximum shear force capacity of the girder determined from FDOT Prestressed Beam Program output was 278 kip, as presented in Fig. 3.16.

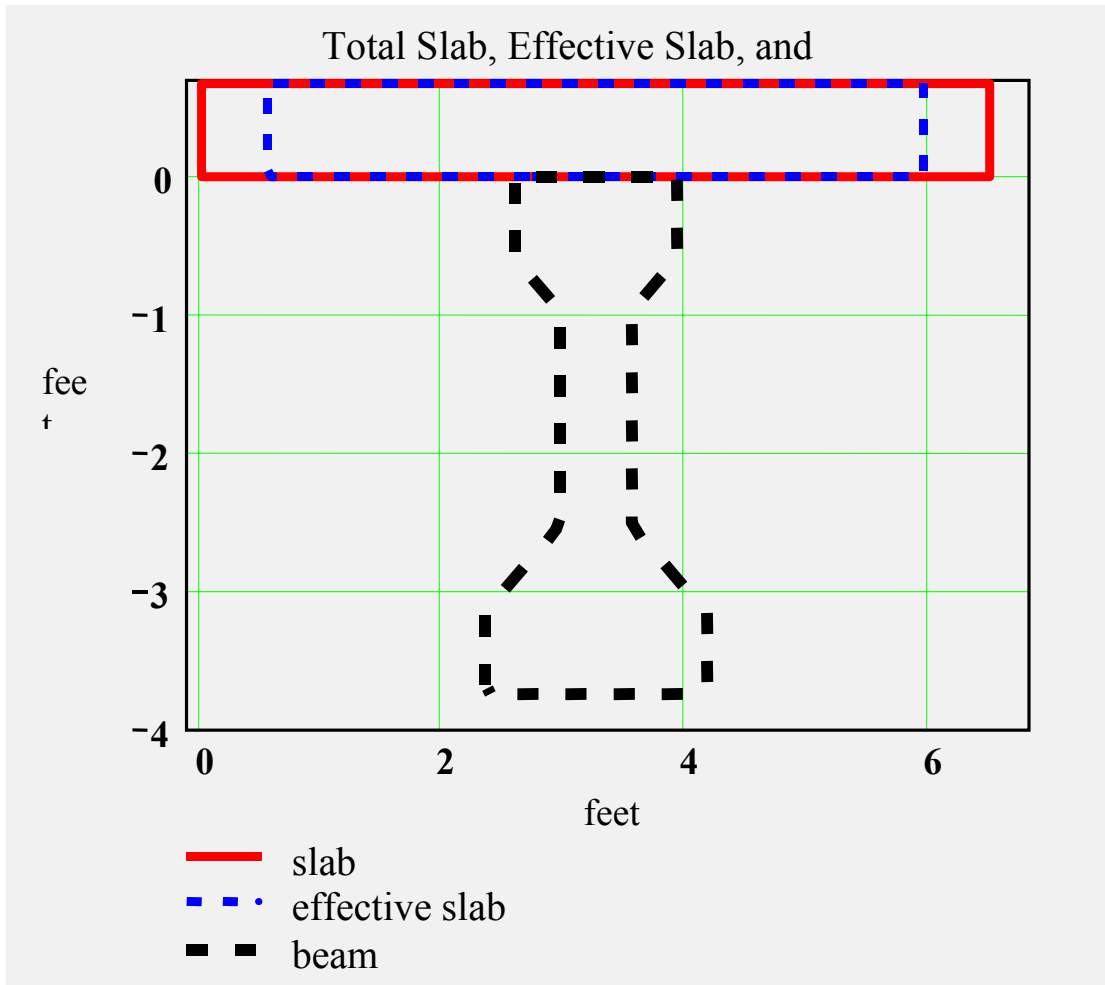


Figure 3.14: Section Properties of Beam and Slab.

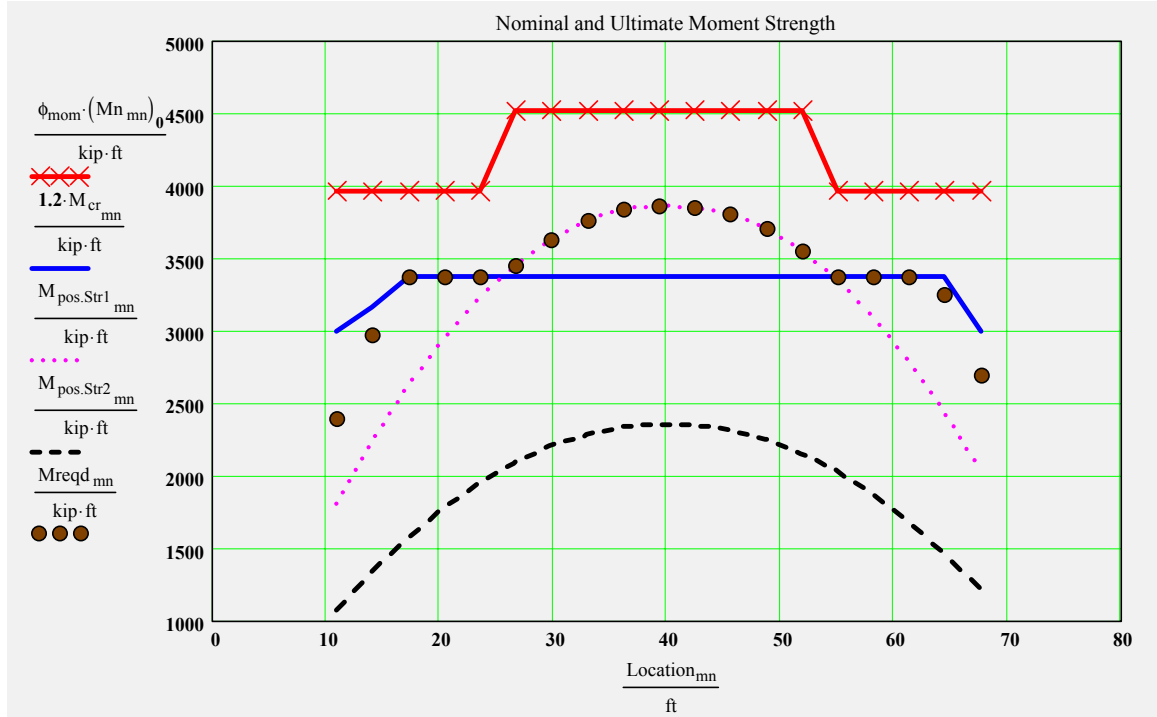


Figure 3.15: Nominal and Ultimate Moment Strength.

On the other hand, when the bridge deck experiences vertically upward loads generated through an explosion underneath the bridge, the girder-slab composite is subjected to negative moments. In this situation, the prestressing steel located near the bottom flange is ineffective in providing the needed tensile strength capacity. Only the non-prestressed longitudinal reinforcement in the slab provides limited tensile strength. Manually analyzing section properties of an inverted T-beam, as shown in Fig. 3.14, the negative moment capacity of the girder-slab composite was determined as 805 kip-ft (shown in Appendix D) after applying appropriate resistance factors. The shear capacity of the girders remains unchanged at 278 kip. All related calculations on girder capacity are shown in Section D.1 of Appendix D.

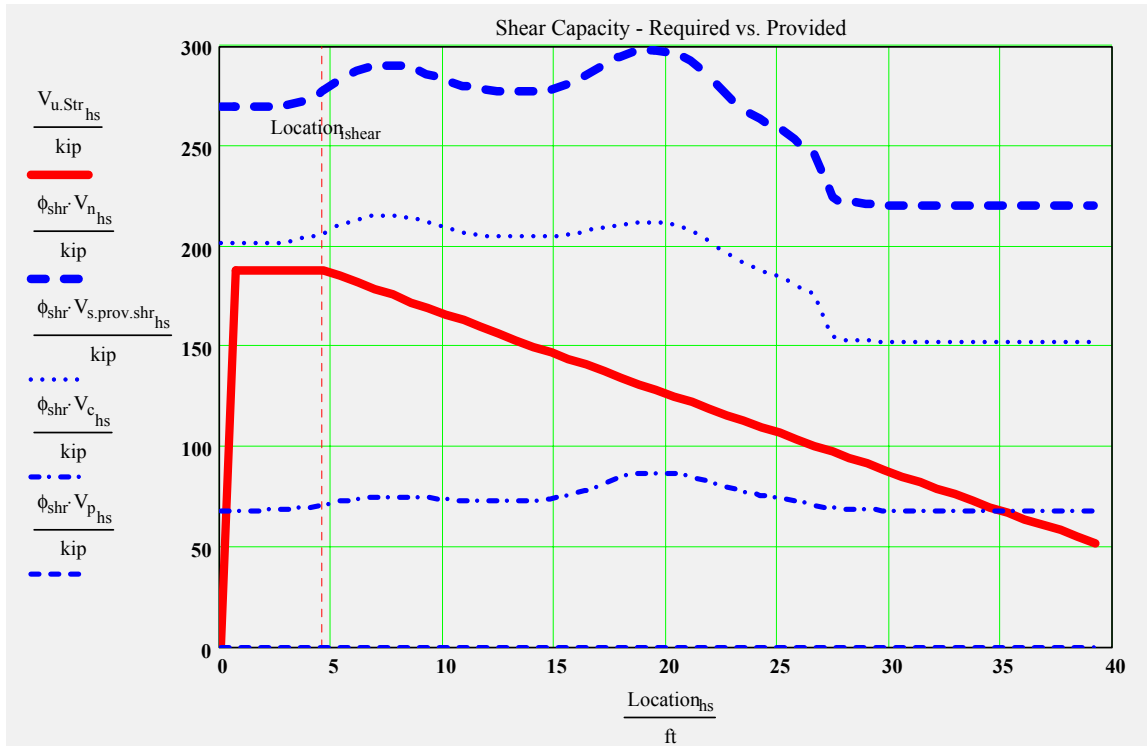


Figure 3.16: Nominal and Ultimate Shear Strength.

3.4.2 Pier Cap Capacity

The pier cap may experience two types of load, each generated due to an explosion underneath or over the bridge. When an explosion occurs right near the column base, a set of vertically upward loads acts at the bottom of the pier cap. This blast event produces a very high negative moment on the cap. In case an explosion takes place right on top of the pier cap, a very high positive moment is applied on the cap. As the pier cap was reinforced with the same amount of flexural reinforcements at top and bottom, the flexural moment capacity of the pier cap against positive or negative moment is the same. From RC-Pier pier design output (shown in Appendix C), the maximum resisting moment of the pier cap was determined as 2,953 kip-ft. The maximum shear force the pier cap can resist before failure was calculated as 772 kip, using two double-legged #5 stirrups spaced at 6 in. on center. Pier cap capacity calculations are shown in Section D.2 of Appendix D.

3.4.3 Column Capacity

The bridge columns are the most critical elements of the structure, failure of which may instantly collapse the whole bridge. Two most important scenarios of column load cases may occur when explosion takes place underneath the bridge.

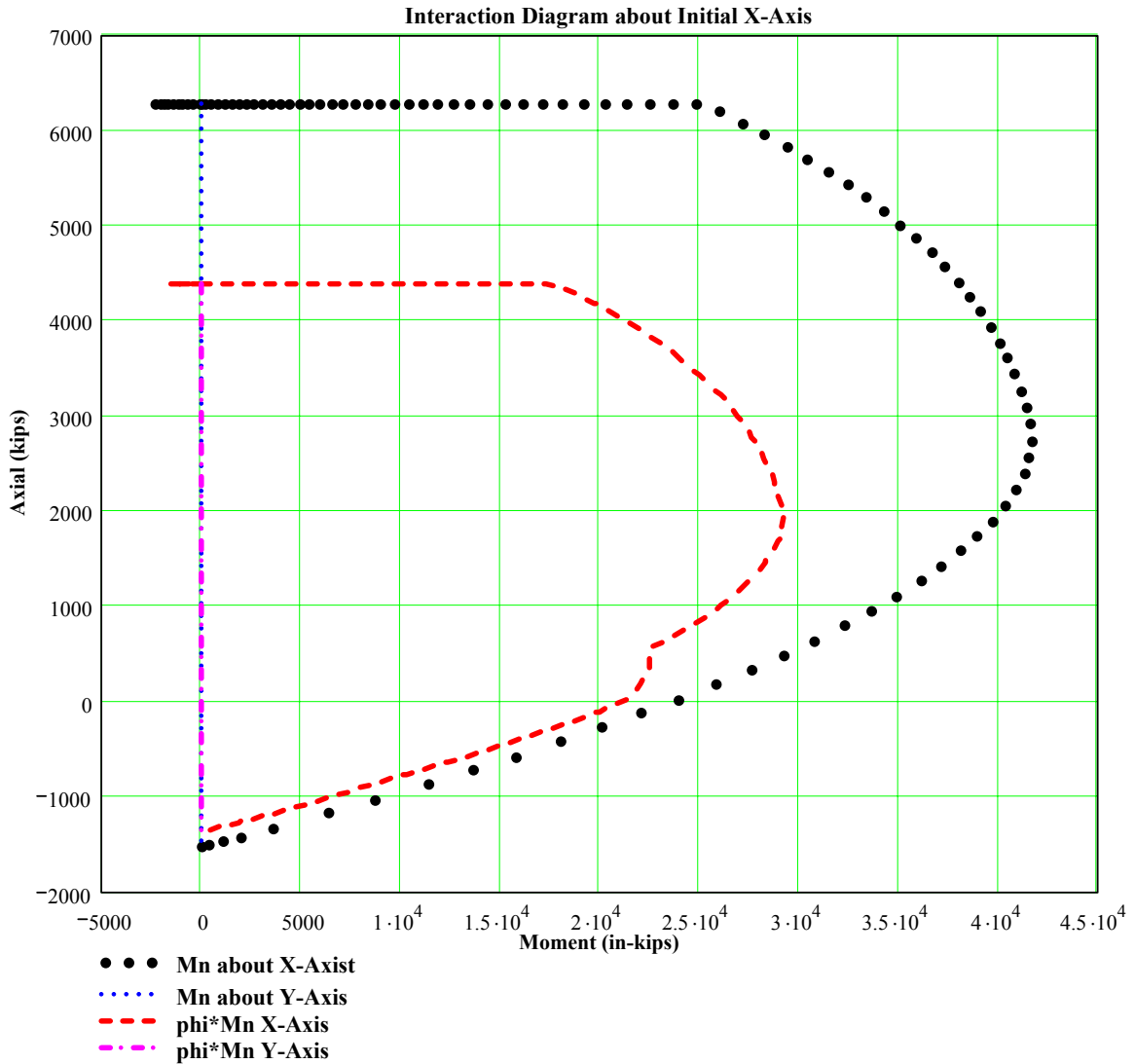


Figure 3.17: Column Interaction Diagram.

At first, if the column is easily accessible via ground or waterway, the explosion may occur right near the column, exerting a horizontal thrust on the column. The second scenario may take place if the explosion occurs right on top of the pier cap. In this scenario, the column will be subjected to loads transmitted through the pier cap.

Using the FDOT Biaxial Column Program, the maximum resisting moment and axial capacity of the column under combined compression plus bending were determined as 2,416 kip-ft. with 2,000 kips axial load. The column moment capacity decreases with increase or decrease in axial capacity, as shown in the interaction diagram of Fig. 3.17. Any applied moment beyond this range should initiate column failure, leading to a complete collapse of the bridge. Biaxial Column Program output, which was used to determine the column capacity, is shown in Section D.3 of Appendix D.

3.4.4 Assumptions and Limitations

In determining the negative moment capacity of the prestressed Type III AASHTO girders, it was assumed that only 16 in. thick bottom flange of the girder would act to resist compression, neglecting contribution of the small irregular parts of the girder. This results in a slightly conservative and simpler calculation of the girder flexural capacity.

In calculating flexural capacity of the pier cap, the effect of the longitudinal reinforcements on two sides of the cap was ignored. These reinforcements were used to satisfy the combined action of the shear and longitudinal torsion of the cap.

3.5 Blast Load

When explosives are detonated, the chemical reaction of the explosives produces a high pressure and high temperature gas. This gas pressure, also known as detonation pressure, propagates like shock and stress wave, and destroys surrounding structures. When the wave front moves forward with a spherical shape, it encounters discontinuities. At this point, some energy is transferred across and some is reflected back. During and after the stress wave propagation, high pressure and high temperature gases extend the radial cracks, any discontinuity, fracture or already weakened joints. The explosive energy always takes the path of least resistance. Once the blasted portion of the structure

is separated, no further fracturing occurs because the gas pressure escapes through the gaps. This entire process occurs within a few milliseconds (msec) from the detonation of the explosives.

The initial step in blast design or analysis is the determination of the blast load. Blasts are among the most powerful extreme loads. Even small amount of explosives can inflict sizeable amount of damage to a structure if they are set in the right location. In assessing the performance of bridges under explosion, issues that demand attention include energy absorption, safety factors, limit states, load combinations, resistance functions, structural performance considerations of critical elements, and most importantly, structural redundancy to prevent progressive collapse of the structure.

The effect of the shock wave, which travels away from the explosion faster than the speed of sound, poses the hazard at close-in locations. The shock front is similar to a moving wall of highly compressed air, and is accompanied by blast winds. When it arrives at a location, it causes a sudden rise in the normal pressure. The increase in atmospheric pressure over normal values is referred to as overpressure, and the simultaneous pressure created by the blast winds is called dynamic pressure. Both decay rapidly with time from their peak values to normal pressure, and overpressure actually sinks below the normal before equalizing back to normal atmospheric pressure. The overpressure causes hydrostatic-type loads, and the dynamic pressure causes drag or wind type loads. High reflected pressures are generated on surfaces that the shock front strikes head-on or nearly head-on. At a given distance from ground zero, overpressures and dynamic pressures decay with time but may last for several seconds. The time the reflected pressure takes to clear a point on a surface depends mainly on the distance to the closest free edge of the bridge from the point of explosion, and may take as little as one millisecond. Due to their sudden application and relatively long duration, loads produced by overpressure and dynamic pressure can be more critical than equivalent static loads, but the damaging effects of the even higher reflected pressure is reduced by their short lives (DOD, TR-62, 1976).

Blast pressure can create loads on structures that are many times greater than normal design loads, and blast winds can be much more severe than hurricanes. Dynamic pressure may continue to cause drag loads on the structural frame that is left standing. If

detonation occurs on top of the bridge, deck slab will experience the downward thrust of the overpressure, which will be transmitted to the supporting girders, pier cap and columns. Foundations will experience blast-induced vertical and overturning forces. If blast load is applied at the bottom of the bridge, pier cap, prestressed girder and deck slab will be subjected to vertically upward pressure for which they are not generally designed.

The sample pier cap and deck slab in this research were designed with the same amount of reinforcement at top and bottom. Structurally, these components are capable of resisting identical loads applied on the members either vertically downward or upward. But in case of the prestressed girders, the scenario is different. Prestressed girders are typically designed to carry only vertically downward loads, which is evident from the prestressing strand location at the bottom of the girder. When a vertically upward load is applied, it initially increases the compression at the bottom and tension at the top of the girder, which in turn makes the girders more vulnerable to damage due to unconventional loads for which they are not designed. The girders are integrally built with the deck slab at the top connected through series of vertical reinforcements. Therefore, the girder-slab composite member acts as an inverted T-beam putting the top of the slab in tension and the bottom of the girder in compression. This phenomenon changes the flexural capacity of the deck slab. Columns and foundations also experience vertically upward and lateral loads, and overturning forces. Failure is very possible unless the structural system is designed to resist these large, quickly applied loads.

Bridge structures could be completely demolished or toppled by the blast loads. Such structures would experience the combined loading conditions caused by the incident overpressure, the dynamic and highly transient reflected pressure that develops when the shock wave strikes a surface of the structure.

3.5.1 Equivalent Static Load

The method of determining equivalent blast load due to an explosion is a complex phenomenon. The blast pressure diminishes with distance from the point of explosion. In the TM 5-1300 Manual, Structures to Resist the Effects of Accidental Explosions, developed by the US Department of Defense in December 1990 (DOD 1990), an empirical formula, as shown in Eq. 3.1, was used to find the scaled distance. The amount

of blast pressure generated due to an explosion is inversely proportional to the scaled distance, which is presented in a chart in the TM 5-1300 Manual. The empirical formula to find the scaled distance, Z (ft), is:

$$Z = R/W^{(1/3)} \quad (3.1)$$

Where, R = Distance of target from point of explosion (ft), and W = Equivalent TNT weight of charge (lb).

Finding the scaled distance, Z , using the above formula for known values of R and W , amount of blast pressure can be determined from the chart showing the variation of blast pressure with scaled distance. Using this formula and the chart in TM 5-1300, Applied Research Associates, Inc (ARA, Inc) developed a computer program named ATBlast to calculate the blast loads for known values of charge weight and standoff distance. The ATBlast software is widely used and recommended by the professionals to determine the equivalent blast pressure due to an explosion. In fact, ATBlast was developed for the US General services Administration (GSA). Alex Remennikov, University of Wollongong, Australia, recommended ATBlast to evaluate blast load on structures (Remennikov 2004). Justin Domire of Pennsylvania State University used ATBlast to determine blast pressure to redesign the Silver Spring District Courthouse against blast loading (Domire 2003). Therefore, use of ATBlast software to determine blast pressure on the bridge is acceptable.

ATBlast is a software program that estimates the blast loads that develop during an open-air explosion. The program allows the user to input the minimum and maximum range, increment, explosive charge weight, and the angle of incidence. From this information, ATBlast calculates the following values: Range Distance (R , ft), Shock Front Velocity (V , ft/msec), Time of Arrival (TOA, msec), Pressure (P , psi), Impulse (I , psi-msec), and Duration (td , msec). These values can be generated for any unit incremental distance. The results are displayed in a tabular format and can be easily printed. In addition, the resulting pressure and impulse curves can be displayed graphically. ATBlast is a proprietary computer program developed by Applied Research Associates Inc., and is provided at no cost to the users.

In this research, ATBlast was used to convert blast loads into equivalent static loads. From Table 3 of the Blue Ribbon Panel Report on Bridge and Tunnel Security (BRP 2003), the highest possibility of a conventional truck bomb is with an amount of 500 lb of trinitrotoluene (TNT) explosive. This amount of TNT was used in the conversion process using ATBlast. According to the BRP recommendation, the typical barge loads vary from 2,000 to 4,000 lb of TNT, which will typically fail any AASHTO girder bridge. Therefore, no further investigation on the impact of this high amount of explosive was performed.

For an explosion underneath the bridge, it is reasonable to assume that a regular truck or any other vehicle commonly used to carry explosive charges cannot go closer than 4 ft to a bridge column, and the minimum standoff distance of 4 ft from the point of explosion to the column surface was used. The maximum range used in this model analysis is 25 ft, beyond which the impact of the explosion is assumed negligible. The minimum vertical clearance of 16 ft between the bottom of the Type III AASHTO girder and the top of the roadway underneath was considered in the analysis. The bottom of the girder and the deck slab were determined to be 13 ft and 17 ft away, respectively, from the point of explosion, considering the charge was placed on the truck bed at 3 ft above the ground. On the other hand, when explosion occurs on top of the bridge deck, the truck bed, where the explosive is placed, also acts as a barrier between the explosion and the deck surface. Considering this barrier effect and 3 ft height of the truck bed from the deck surface, it was conservatively assumed that the minimum distance between the point of explosion and the deck surface was 6 ft.

To obtain the loads to be applied on the model bridge, 500 lb of TNT with minimum and maximum range of 4 ft and 25 ft, respectively, was converted into equivalent static loads using ATBlast software analyzing at every 1 ft increment. The results from the analysis are presented in Table 3.2. The resulted static loads generated from the explosion were applied on the model bridge at different critical locations.

Figure 3.18 illustrates variation of pressure with respect to distance from the point of explosion. The closer is the explosion to structure; the more severe is the resulting pressure and the likelihood of structural damage.

Figures 3.19 and 3.20 show elevation and plan views of typical blast pressure distribution on a bridge surface. If the explosion occurs 6 ft above the deck surface, the spherical distribution of pressure extends 10 ft in each direction as shown in the figures assuming 30-degree angle of projection of the pressure wave.

Table 3.2: Equivalent Static Parameters for 500 lb of TNT Explosion

R (ft)	V (ft/sec)	TOA (msec)	P (psi)	I (psi-msec)	td (msec)
4	13.13	0.22	2511	9312	0.68
5	13.39	0.30	1884	6336	0.66
6	10.11	0.40	1480	4677	0.66
7	9.13	0.50	1198	3645	0.67
8	8.34	0.61	991	2953	0.68
9	7.69	0.73	832	2462	0.70
10	7.13	0.87	707	2098	0.73
11	6.63	1.01	607	1820	0.76
12	6.20	1.17	524	1602	0.80
13	5.81	1.34	456	1426	0.84
14	5.45	1.52	399	1283	0.89
15	5.14	1.71	351	1163	0.95
16	4.85	1.91	310	1063	1.01
17	4.58	2.13	275	977	1.08
18	4.34	2.35	245	903	1.15
19	4.12	2.59	219	839	1.23
20	3.92	2.84	197	783	1.32
21	3.74	3.11	177	733	1.41
22	3.57	3.38	161	689	1.51
23	3.42	3.67	146	650	1.61
24	3.28	3.97	133	615	1.72
25	3.15	4.29	121	583	1.84

In order to simplify the method of blast distribution, it was assumed that the blast pressure beyond this region, which diminishes with the distance, has negligible impact on the structure. Weighted average of the vertical components of these inclined pressures on

each girder was calculated according to the distribution shown in Fig. 3.20. The highest load travels the shortest distance, and is perpendicular to the surface. In this case, the highest load is 1.48 ksi generated due to an explosion of 500 lb of TNT at a height of 6 ft above the deck. Girder B, directly under the point of explosion, experiences the highest average pressure of 0.77 ksi for a length of 20 ft, which is approximately 50 percent of the peak pressure of 1.48 ksi. The adjacent girders A and C are subjected to 0.5 ksi pressure along a length of 20 ft, which is approximately 30 percent of the peak pressure of 1.48 ksi. These assumptions, named herein as 50 Percent Distribution Rule and 30 Percent Distribution Rule, respectively, were verified for three different intensity of explosions (500 lb, 100 lb and 50 lb), and found to be acceptable (calculations are presented in Appendix E.1), and were used in applying average blast pressure for different loads cases on the bridge components.

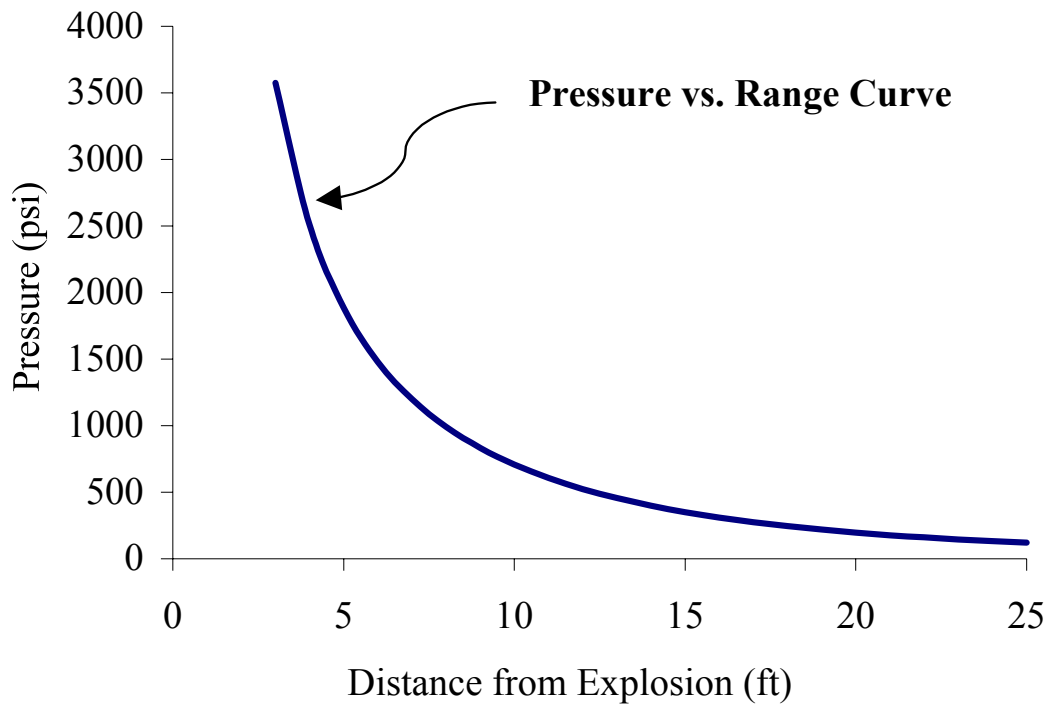


Figure 3.18: Variation of Pressure with Distance from Explosion.

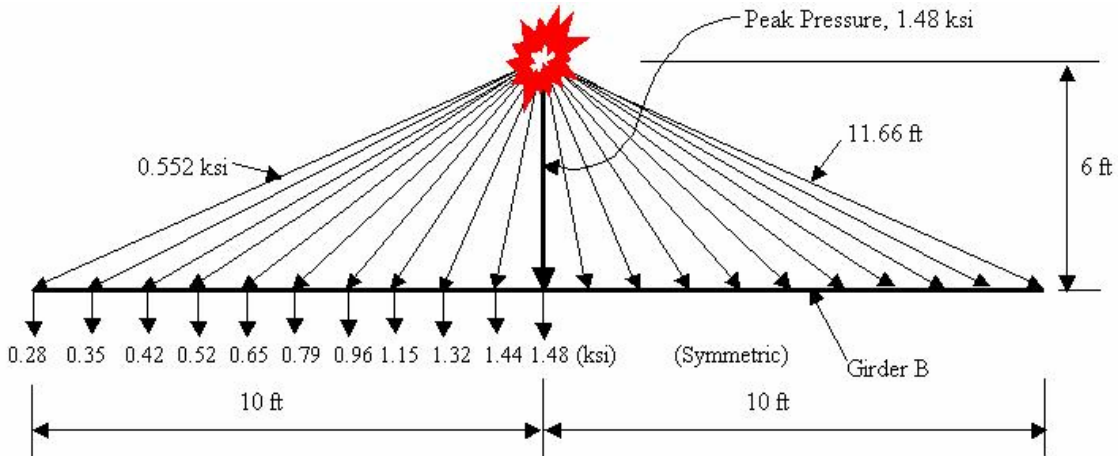


Figure 3.19: Blast Pressure Distribution on Bridge Deck (Elevation).

Following this average distribution rule, blast pressures can be applied on the critical members of the bridge for different explosion scenarios. If the explosion had occurred at a distance of 4 ft from one of the columns, approximately 1.25 ksi (50 percent of 2.5 ksi, Table 3.2) average pressure would act on the column at a distance of 4 ft from the point of explosion. If the explosion had taken place at a distance of 15 ft from the column, the column would experience an average pressure of 0.18 ksi (50 percent of 0.351 ksi). At the same time, the girder bottom at a distance of 13 ft would experience approximately 0.23 ksi (50 percent of 0.46 ksi) pressure and the slab bottom at a distance of 17 ft would take an average pressure of 0.08 ksi (30 percent of 0.275 ksi). The pier cap, which is diagonally 18 ft away from the explosion, would take 0.07 ksi (30 percent of 0.245 ksi) pressure. On the other hand, if the explosion had occurred on top of the bridge, part of the deck at 6 ft below the point of explosion would experience around 0.74 ksi (50 percent of 1.48 ksi) and 0.45 ksi (30 percent of 1.48 ksi) pressures through the closest-to-explosion beam and its adjacent beams, respectively. Depending on the amount and type of damage of the bridge components due to these loads, the bridge would be classified as partially or completely out of service.

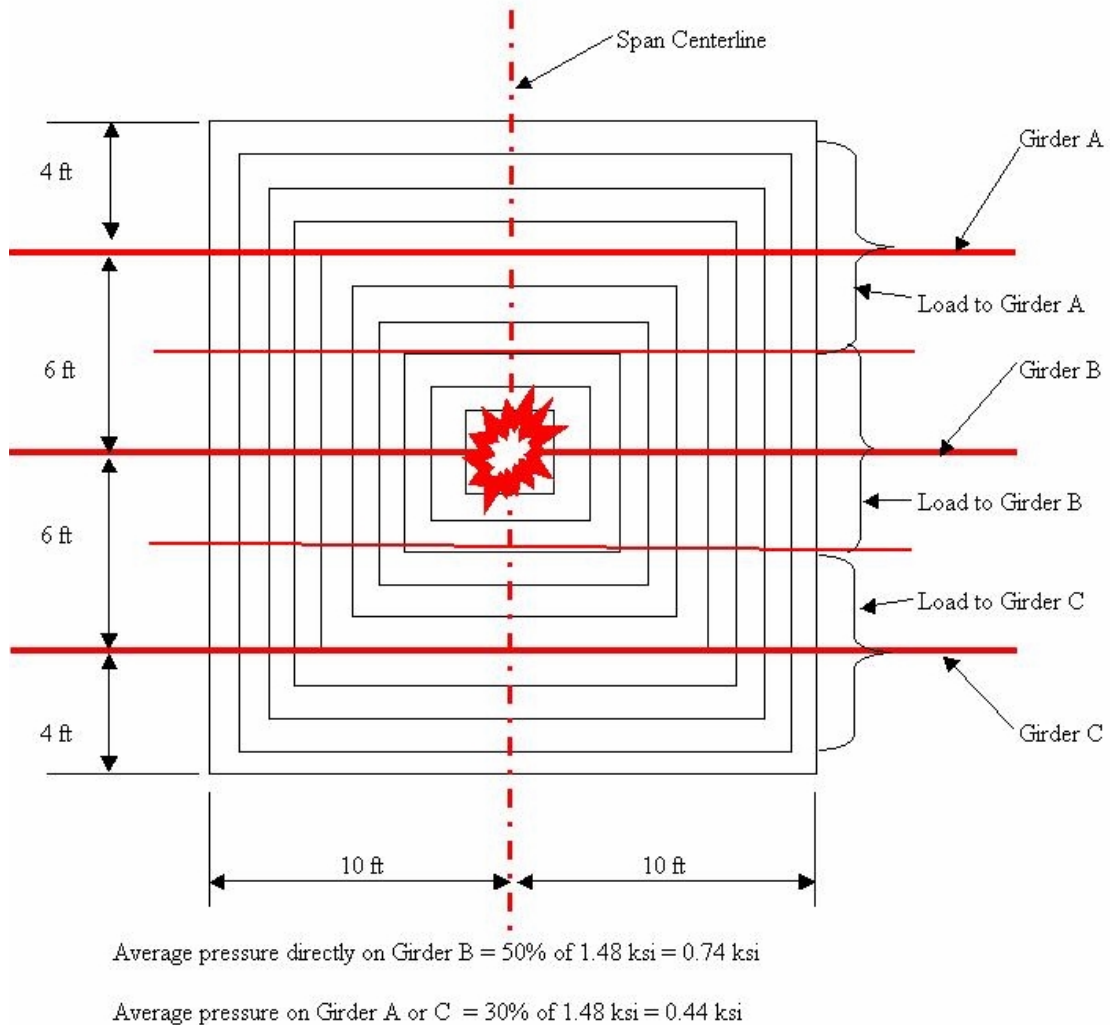


Figure 3.20: Blast Pressure Distribution on Bridge Deck (Plan).

3.5.2 Comparison of Blast and Seismic Loading

Similarities and differences between seismic and blast loading are noticeable. Both of these loads are dynamic loads and they produce dynamic structural response. The structural behavior in response to these loads is inelastic as well. The focus of structural design against these loads is on life safety as opposed to preventing structural damage. Therefore, the designs are normally performance-based that include life safety issues, progressive collapse mechanisms, ductility of certain critical components, and redundancy of the whole structure. In certain circumstances, these loads may not damage structures, but can still claim human lives and create natural hazards.

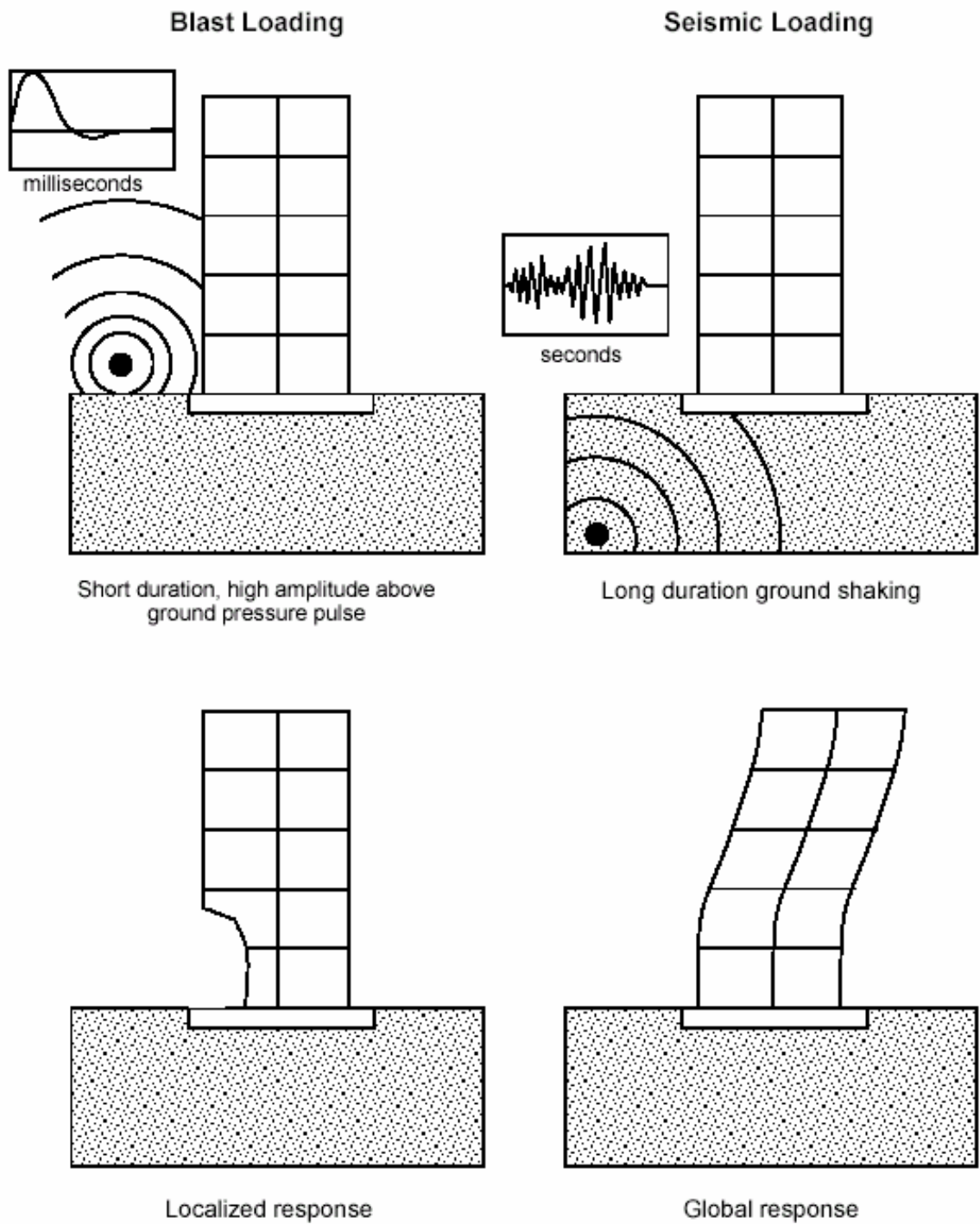


Figure 3.21: Comparison of Blast and Seismic Action on Structures.
 (NIST 2001)

Differences between these two types of loading are presented in Fig. 3.21 and summarized in Table 3.3. Blast load damages structures through propagating spherical pressure waves, while earthquake damages structures through lateral ground shaking. Spherical pressure due to explosion directly hits structures and causes failure, but seismic load causes lateral load effect on structures through ground movement.

Blast loading is of higher amplitude if it is targeted on a particular structure, while seismic loading is transferred through ground movement and is not targeted on any particular structure. Explosion can occur directly on the structure or within a very close proximity of the structure, whereas seismic epicenter develops few miles down from the earth surface. Blast loading has shorter duration compared to seismic loading. Although both of these loads are highly unpredictable in nature, seismic activity can be categorized based on geographical locations.

Table 3.3: Summary of Seismic and Blast Load Differences

Blast Load	Seismic Load
1. Damages structures through propagating spherical pressure waves.	1. Damages structures through lateral ground shaking
2. Higher amplitude if explosion is targeted on a particular structure.	2. Not targeted on any particular structure.
3. Directly hit the structure.	3. Seismic epicenter develops few miles down from the ground surface.
4. Shorter duration in terms of milliseconds.	4. Longer duration in terms of seconds.
5. Highly unpredictable.	5. Highly unpredictable, but can be precisely described in the aftermath of an earthquake.
6. More localized action.	6. More global action.
7. Does not depend on geographic location.	7. Entirely depends on geographic location.
8. Can be categorized by standoff distance and charge weight.	8. Can be categorized by geographic locations.
9. Can be prevented by implementing necessary security measures.	9. Cannot be prevented.

While magnitude of blast cannot be predicted, seismic magnitude can be precisely described in the aftermath of an earthquake. Blast loading is more localized as compared to the global nature of seismic effect. Progressive collapse of structures is the most serious consequence of explosion. Bridge girders are not typically designed to withstand upward forces that may be caused due to an explosion underneath the bridge, and very little database of blast effects on structures has been developed. Significant knowledge base exists for seismic resistant structural design, while knowledge or blast-resistant structural design is very limited.

In summary, while the effect of blast loading is localized compared with an earthquake, the ability to sustain local damage without total collapse (structural integrity) is a key similarity between seismic-resistant and blast-resistant design (NIST 2001).

There are growing interests in determining the effects of seismic design on blast resistance of structures. Robert Pekelnicky from Degenkolb Engineers presented his findings from his research in the ACI Fall 2003 Convention (Pekelnicky 2003). In his presentation, it was concluded that seismic detailing alone could provide 14 to 57 percent of additional resistance, while seismic design and detailing could generate 30 to 186 percent additional resistance. It was also mentioned that seismic design and detailing in addition to regular structural design would increase the cost at approximately 3 to 5 percent. In the ACI Fall 2003 Convention, Jack Hays from the US Army Corps of Engineers presented his preliminary findings on the Oklahoma City bombing on the Murrah Federal Building and concluded that seismic strengthening at the building exterior can improve external blast and progressive collapse resistance (Hays 2003). These studies were performed on the building structures only. Therefore, the effects of seismic design and detailing on blast resistance of bridge structures require further research.

3.6 STAAD.Pro Software

The STAAD.Pro software is the choice of 46 out of 50 leading structural engineering firms, 46 out of 50 state DOT and 7 out of the top 10 engineering universities for structural designs and analyses. It features a state-of-the-art user interface, visualization tools, powerful analysis and design engines with advanced finite element

and dynamic analysis capabilities. From model generation, analysis and design of steel, concrete, composite, timber, aluminum and cold-formed steel structures to visualization and result verification, STAAD.Pro is the professional's choice. Some of the important organizations that use the STAAD.Pro for structural analysis are: AMTRAK Engineering, Black & Veatch, Boeing Company, Exxon Corporation, FDOT, H.W. Lochner Inc, HDR Engineering Inc, HNTB Corporation, Jacobs Sverdrup, Kellogg Brown & Root, Minnesota DOT, New jersey DOT, New York DOT, Parsons Brinckerhoff Inc, Parsons Corporation, PBS&J, Port Authority of NY and NJ, RS&H Inc, Texas DOT, US Army Corps of Engineers, Virginia DOT, Walt Disney World, Weidlinger & Associates and Wilbur Smith Associates (STAAD.Pro 2004).

The STAAD.Pro software has the capability of generating 3- and 4-noded plate elements as well as 8-noded solid elements with the options of selectively releasing degrees of freedom at any node. Loads can be applied in the form of nodal loads, member loads, uniform pressure over any region, trapezoidal pressure loads, and surface expansion and temperature loads. The goal of this research was to evaluate the performance of an AASHTO girder bridge by comparing the applied bending moments and shear forces on the bridge components with their respective capacities. An extensive finite element modeling of the bridge is not necessary to perform this research. Capacities of the bridge components were determined from their individual designs, while the applied bending moments and shear forces were determined by analyzing a simple finite element model of the bridge in the STAAD.Pro. The output of this software presents the results, including moments, shears and displacements, in the tabular and graphical forms. Moreover, moments and shears, at the nodes and at any point within the element, can be easily obtained from the software output. All these features make STAAD.Pro the unique and appropriate software to analyze the model bridge used in this research.

3.7 Bridge Model

The model bridge was created using the STAAD.Pro software for analysis, as shown in Fig. 3.22. The centerlines of the elements were coded in and connected as beam elements. The deck slab was modeled as an 8 in. thick plate composed of plate elements. There were a total of 58 beam elements and 128 plate elements in the model.

Beam elements 1 to 8 and 17 to 24 formed two end bent caps, and 9 to 16 made up the pier cap. The barriers consisted of beam elements 25, 33, 34 and 42. The prestressed girders were represented by beam elements 26 to 32 in the first span and 35 to 41 in the second span. The piles, supporting the end bent caps, consisted of beam elements 43 to 49 and 52 to 58. Beam elements 50 and 51 represented the two columns supporting the pier cap.

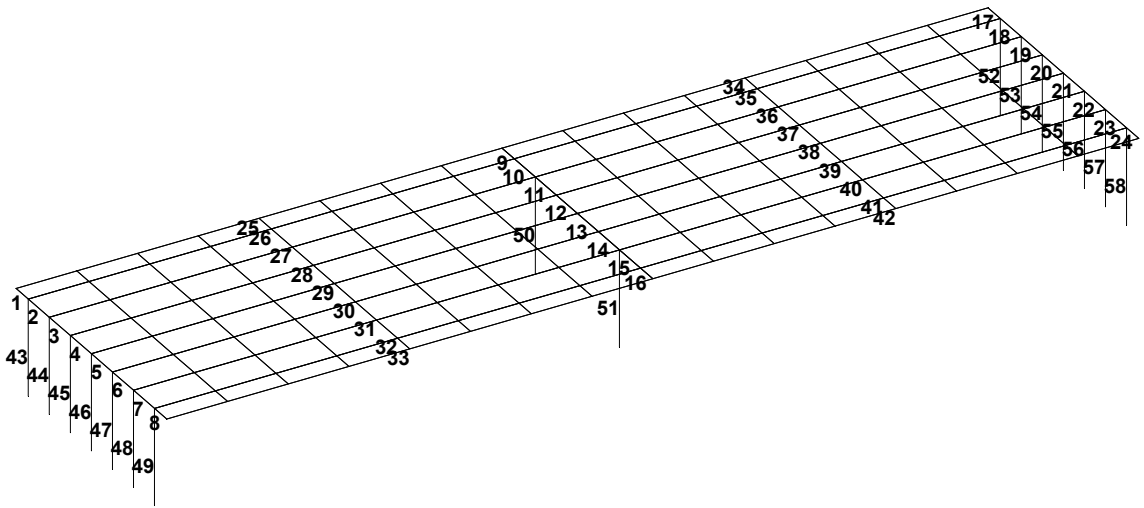


Figure 3.22: The Bridge Model in STAAD.Pro.

To simplify the calling out of the beam elements, element numbers were preceded by the name of the respective member. For example, girder 26 represented beam element 26, column 51 denoted beam element 51, and so on. Cross-sections of all the beam elements were defined as per geometry of the respective members. The equivalent area of the girders and barriers were coded in the software because of their irregular shapes to account for the dead loads. The girders were characterized as pin supported on the end bent caps. The piles and the columns were modeled as fixed supported at a depth of 16 ft

from the centerline of the cap. The deck slab was made integral with the girders to represent the composite behavior.

The girders, end bent and pier cap including the columns, and the deck slab were assumed to be made of concrete with 28-day compressive strengths of 6.5, 5.5 and 4.5 ksi, respectively, which are typically used in Florida as recommended in the FDOT Structure Design Guidelines (FDOT SDG 2004). These concretes are classified as Class V, Class IV and Class II (Bridge Deck), respectively, as per FDOT Standard Specifications for Road and Bridge Construction, 2004 (FDOT SSRBC 2004). The density for all types of concrete was assumed as 150 pcf with a Poisson's Ratio of 0.2, typical for normal weight concrete. The STAAD.Pro software requires the density input to account for the self-weight of the bridge components. Using these values, three concrete materials were defined in the STAAD.Pro bridge model input, as shown in Table 3.4. The respective modulus of elasticity for each of these three different types of concrete was calculated by using the AASHTO LRFD formula, as shown in Eq. 3.2. Although the concrete modulus of elasticity does not affect the applied moments and shears, it affects the magnitude of stiffness and displacements. Displacement and camber of girders are normally considered for traffic riding comfort, rather than predicting member efficiency. Therefore, in assessing the performance of the model bridge, displacement was not considered as a part of the analysis. Besides, as the moments and shears were considered in defining the failure criteria, the use of different concrete modulus of elasticity for different parts of the structure did not affect the performance of the bridge components.

Table 3.4: Material Properties Used

Concrete Designation	Element	28-day Compressive Strength, f_c (ksi)	Poisson's Ratio	Unit Weight, W_c (kcf)	Modulus of Elasticity, E_c (ksf)
Material 1	Girders	6.5	0.2	0.15	703,833
Material 2	End Bent Cap Pier Cap Columns	5.5	0.2	0.15	647,433
Material 3	Deck Slab	4.5	0.2	0.15	585,625

The AASHTO LRFD formula to calculate the modulus of elasticity of concrete is as follows:

$$E_c = 33,000 \times W_c^{1.5} \times f_c^{0.5} \quad (3.2)$$

Where, E_c = Modulus of Elasticity of concrete (ksi), W_c = Unit weight of concrete (kcf), and f_c = Compressive strength of concrete (ksi).

3.8 Locations of Blast Load Application

The superstructure, particularly the deck slab, is the major structural part of a bridge that is mostly affected due to possible explosion on top of the bridge. The deck slab is a highly redundant member because of the presence of alternate load paths and integral connection with the girders through the shear keys. The loads, due to an explosion on top of the bridge, were distributed on the deck slab and ultimately applied as uniformly distributed loads along the centerline of the girders. Thus, the deck slab performance was excluded from this research because of its high redundancy, localized failure potential and in order to focus on the more critical elements of failure, such as girders, pier cap and columns. The other extremely vulnerable part is the girder-bearing pad connection, where the girders just sit on top of the bearing pads. Due to this weak connection, girders are more susceptible to be displaced in case the blast originates underneath the bridge.

In case an explosion occurs on top, the bridge is expected to exhibit stronger capacity and greater redundancy, as compared to an underneath explosion. All bridge members are typically designed to resist vertically downward loads, and in some cases, horizontal loads due to earthquake. When there are scenarios of vertically upward forces acting on the bridge, the superstructure is much less safe and more prone to failure. For example, a prestressed girder is designed for positive moment with prestressing to resist downward loads. For an upward blast load, prestressing in the bottom flange is ineffective and it makes the girder more vulnerable to damage by increasing negative moment.

In most cases, blast load is unpredictable like earthquake load. While earthquake may cause definable nature of horizontal and vertical movements, blast load has no definite direction of resulting movement. It can affect the structure from any direction at

any angle of projection. Therefore, it is very difficult to characterize definite criteria for blast load direction. For the sake of simplicity, only the governing vertical or horizontal components of the inclined loads were applied on the members. All the loads were defined to act at the critical locations of the members. Upward and downward loads were applied at mid-span of the slab-girder composite system to determine the maximum moment in the girder. Downward loads were applied at the end of the span to determine maximum shear force in the girders.

As mentioned earlier, the column is the most critical element of a bridge structure in terms of failure mechanism. If any of the bridge columns supporting the pier cap fails, the bridge may collapse due to uneven support conditions. Pier cap failure may not readily initiate bridge collapse, but it may eventually occur due to unbalanced loads as a result of progressive collapse. Therefore, girder, column and pier cap performance under blast load was considered vital in this research. In order to determine the maximum applied loads on the columns and pier cap to predict their performance, a horizontal load on the column and a vertical load on the pier cap were applied simultaneously on the critical locations of the respective members.

3.9 Blast Load Cases

The typical amount of TNT explosive, used in the ATBlast software to generate the equivalent static loads, was 500 lb, as recommended by the AASHTO Blue Ribbon Panel. The explosive loads were considered as extreme event loads for which the load factor is 1.00 according to the AASHTO LRFD Bridge Design Specifications (AASHTO 2003). In addition to these blast loads, self-weight of the structure was also considered and multiplied by a factor of 1.25. The AASHTO LRFD combination of dead and live loads for extreme event cases are presented in Eq. 3.3. The truck live load was not considered in the analysis for simplicity and because of its effect is negligible compared to that of the blast load.

$$W_T = 1.25 \times DL + 0.50 \times LL + 1.00 \times EV \quad (3.3)$$

Where, W_T = Total load, DL = Dead load, LL = Truck live load, and EV = Extreme event load.

It was further assumed that the blast force projects at maximum angle of approximately 30 to 60 degree with the horizontal. Converted blast pressures, as presented in Table 3.5, were categorized into 5 different load cases depending on the location of blast, intensity and the amount applied on a specific area. The model bridge was analyzed using the STAAD.Pro software with 5 separate blast load cases applied at 5 different critical locations. The blast pressures were converted into uniformly distributed loads and applied along the centerline of the members for ease of load application on the model. The tributary distribution of blast pressures, a widely accepted method of converting pressures into uniformly distributed loads, was applied herein. The various load cases, formed by these uniformly distributed loads, are presented in the following sections, and summarized in Table 3.6.

Table 3.5: Converted Pressure for 500 lb of TNT Explosion

Range (ft)	Pressure (psi)
4	2511
5	1884
6	1480
7	1198
8	991
9	832
10	707
11	607
12	524
13	456
14	399
15	351
16	310
17	275
18	245
19	219

Table 3.6: Various Load Cases

Load Case	Location	Member Affected	Blast Set-backs
Case 1	Under the bridge, at mid-span.	Deck slab, girders	3 ft above ground.
Case 2	Over the bridge, at mid-span.	Deck slab, girders	6 ft above deck.
Case 3	Over the bridge, over pier cap.	deck slab, girders, pier cap.	6 ft above deck.
Case 4	Over the bridge, at span end.	Deck slab, girders	6 ft above deck.
Case 5	Under the bridge, at 4 ft away from column.	Column, pier cap.	3 ft above ground.

3.9.1 Load Case 1

This load case occurs when the explosion is assumed to take place beneath the bridge at girder mid-span, as shown in Fig. 3.23. When the explosion occurs underneath the bridge, the middle girder (girder 29), which is 13 ft above the explosion, experiences a vertically upward blast pressure of approximately 0.23 ksi (Table 3.5, using 50 Percent Distribution Rule) for a length of 20 ft, as per Section 3.5.1. This load was converted into a uniformly distributed load of 60.7 kip/ft using girder bottom width of 1ft 10 in. The other two girders (girders 28 and 30) experience 0.13 ksi pressure (Table 3.5, using 30 Percent Distribution Rule), which is equivalent to 34.3 k/ft, for a length of 20 ft. The portion of the slab in between two girders also experiences a portion of the blast pressure. Approximately 4 ft wide and 20 ft long portion of the slab between the two adjacent girders, located at an inclined distance of 17 ft, experiences a pressure of 0.08 ksi (Table 3.5, using 30 Percent Distribution Rule), which is equivalent to 46 k/ft equally distributed along the centerline of the girders. In the STAAD.Pro model, the total uniformly distributed load of 106.7 k/ft was applied on girder 29, and 80.3 k/ft on girders 28 and 30. These loads were applied in the middle 20 ft of the span along the centerline of the

girders to determine the maximum applied moment on the girders. The direct impact of this explosion on the pier cap and columns was neglected because of high standoff distances from these members.

Due to this pattern of blast loading, it was evident from the model analysis that girder 29 experiences the maximum effect, and the adjacent two girders, 28 and 30, are subjected to less pressure compared to girder 29. From the STAAD.Pro program output, the maximum negative moment (at girder mid-span) and shear force on girder 29 are 20,434 kip-ft and 1,281 kip, respectively. The other two adjacent girders exhibit similar reactions because the applied load is identical. Maximum negative moment and shear force on girders 28 and 30 are 15,484 kip-ft and 964 kip, respectively. The moment and shear force diagrams produced by these loads are presented in Figs. 3.24 and 3.25, respectively.

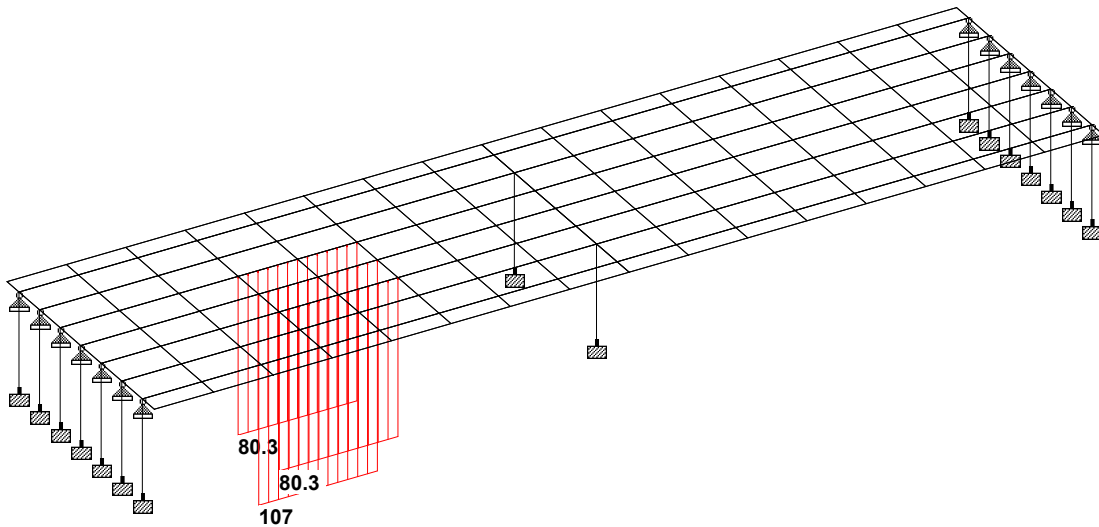


Figure 3.23: Case 1 Load on Model Bridge.

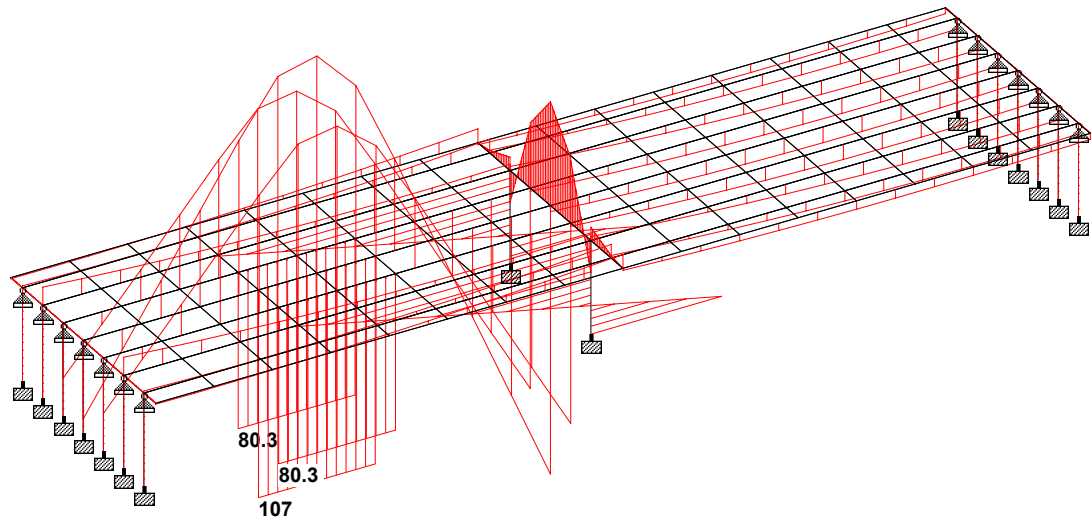


Figure 3.24: Moment Diagram for Case 1 Load.

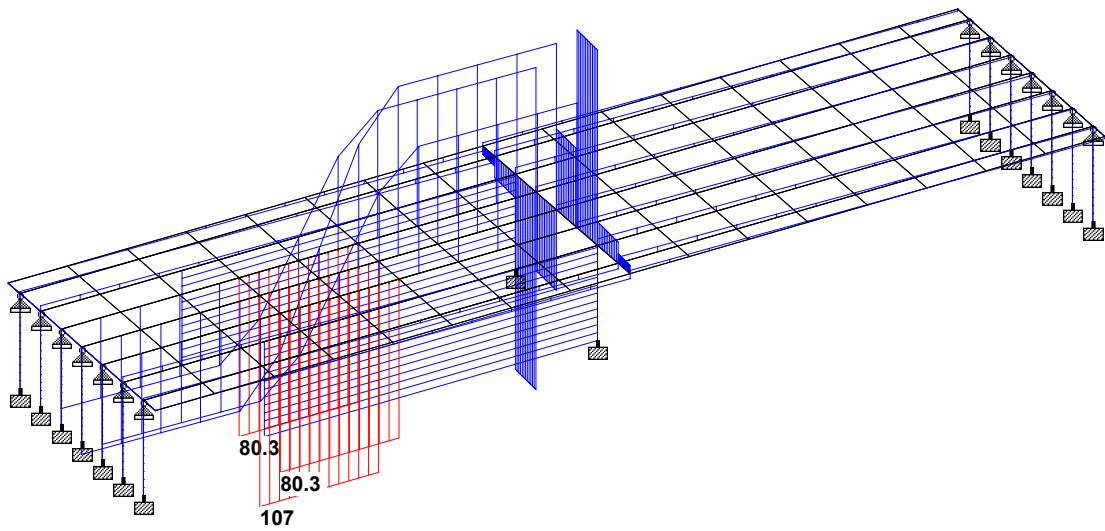


Figure 3.25: Shear Force Diagram for Case 1 Load.

A larger positive moment of 25,273 kip-ft was caused at the end of girder 29 on top of the pier cap as a result of Case 1 loads. It was due to the full continuity of the girders assumed in the STAAD.Pro model at the pier cap location. Although the actual support condition of the girders at the pier cap location is not fully continuous, some continuity exists as a result of the girder-slab composite action when the slab is continuous over the pier cap. Most importantly, a girder is more vulnerable to damage due to a bending moment at mid-span compared to that at the ends when the load is applied at the middle of the span. Therefore, in assessing the performance of a girder, only the maximum applied bending moment in between two supports was considered.

3.9.2 Load Case 2

Case 2 blast load, as shown in Fig. 3.26, was defined for an explosion occurring on the middle of the girder span 6 ft above the deck slab. Due to this explosion, it was assumed that a 20 ft by 20 ft square portion of the slab experiences a vertically downward pressure, considering the 30-degree angle of projection. The three consecutive girders (girders 28, 29 and 30), spaced at 6 ft on center, are affected as a result of this explosion. This pressure is distributed over the girder-slab composite along the centerline of the girders using 50 Percent and 30 Percent Distribution Rule established in Section 3.5.1. Using the tributary area method and the distribution rule, girder 29 is subjected to a pressure of 0.74 ksi (Table 3.5, using 50 Percent Distribution Rule), and girders 28 and 30 experience 0.44 ksi pressure (Table 3.5, using 30 Percent Distribution Rule). After converting these pressures acting on a 6 ft width of the deck, the uniformly distributed load per linear foot along the centerline of the girders was calculated as 639.36 k/ft and 380.16 k/ft over girders 29, and girders 28 and 30, respectively. In the STAAD.Pro model, uniformly distributed loads of 639.36 k/ft and 380.16 k/ft were applied on girders 29, and 28 and 30, respectively, in the middle 20 ft of the span. No direct impact on the pier cap or column due to the explosion on top of the bridge was considered.

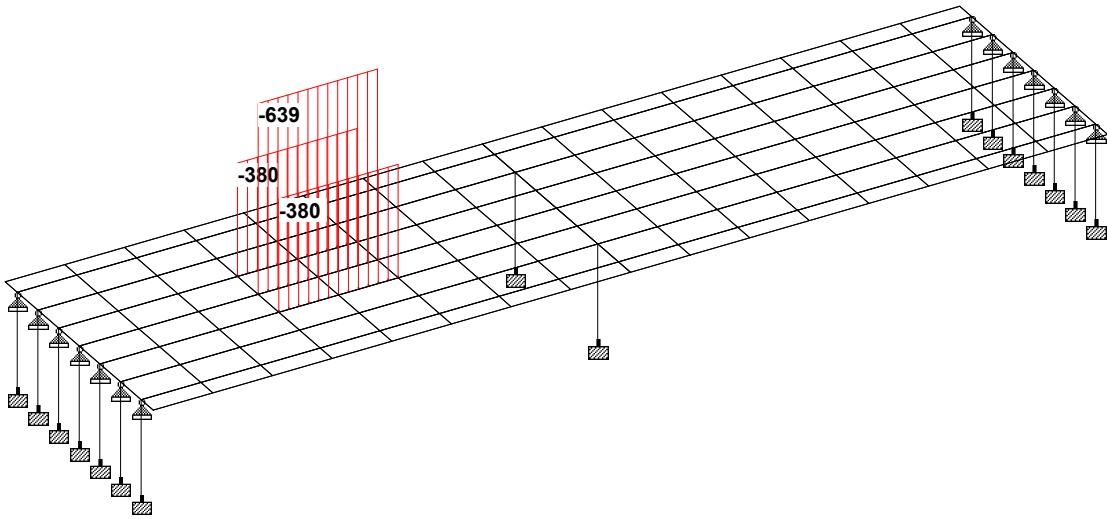


Figure 3.26: Case 2 Load on Model Bridge.

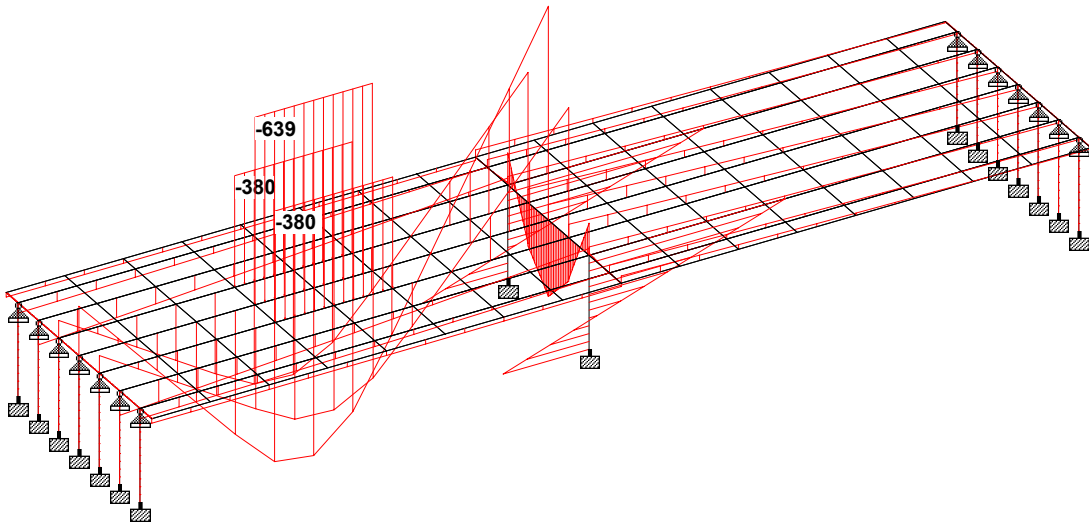


Figure 3.27: Moment Diagram for Case 2 Load.

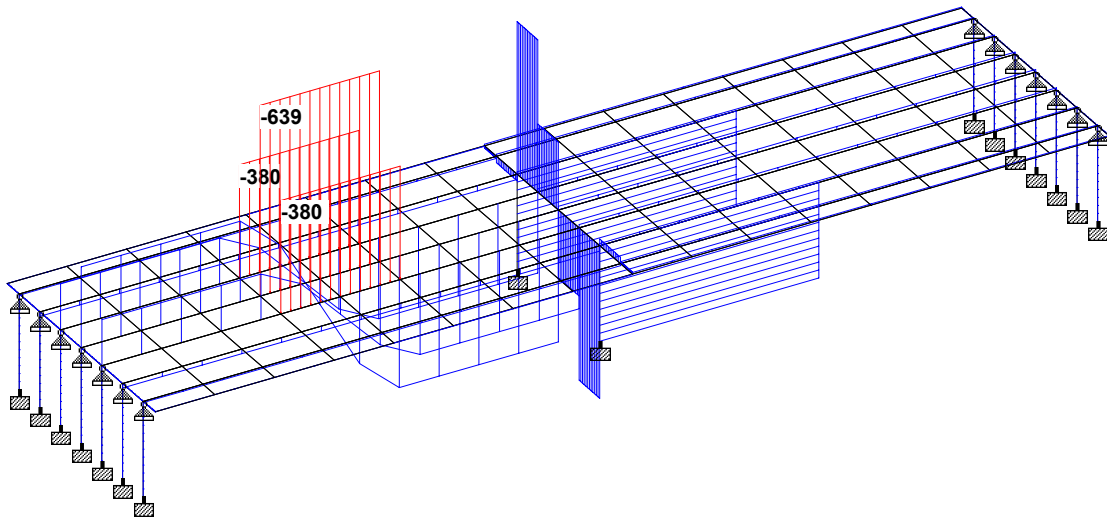


Figure 3.28: Shear Force Diagram for Case 2 Load.

The moment and shear force diagrams produced by these loads are presented in Figs. 3.27 and 3.28, respectively. Because of this pattern of blast loading, the maximum positive moment (at girder mid-span) and shear force on girder 29 are 125,716 kip-ft and 7,964 kip, respectively. The maximum positive moment and shear force on each of the girder 28 and 30 are 78,220 kip-ft and 4,885 kip, respectively. Negative moments at the girder ends were not considered, because the girders are more vulnerable to failure at the mid-span rather than at the ends, as explained in Section 3.9.1.

3.9.3 Load Case 3

Case 3 blast loads, as presented in Fig. 3.29, were identical to Case 2 loads, except that the horizontal location was changed to be on top of the pier cap. These loads were applied on the middle three girders of each span to determine the maximum effect on the pier cap and the supporting columns. Girders 29 and 38 were loaded along their centerline with 639.36 k/ft load for a length of 10 ft each way from the centerline of the pier cap. In a similar fashion, 380.16 k/ft load was applied on each of the other four girders 28, 30, 37 and 39 along their respective centerline.

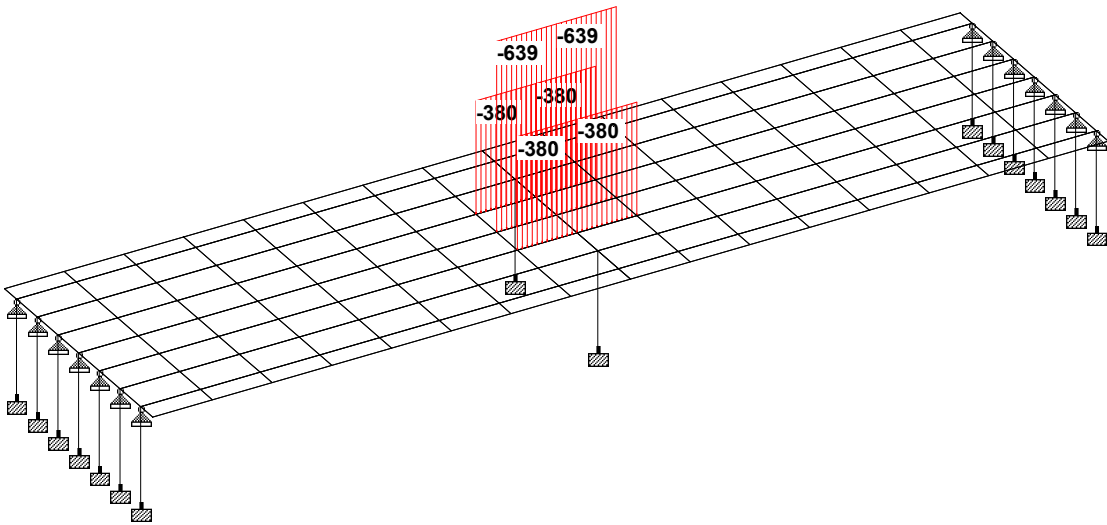


Figure 3.29: Case 3 Load on Model Bridge.

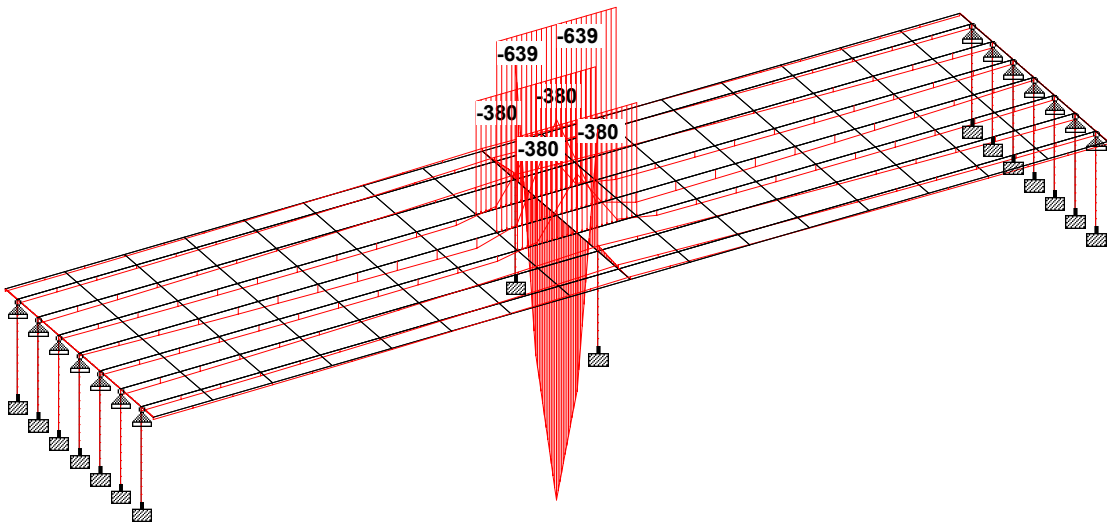


Figure 3.30: Moment Diagram for Case 3 Load.

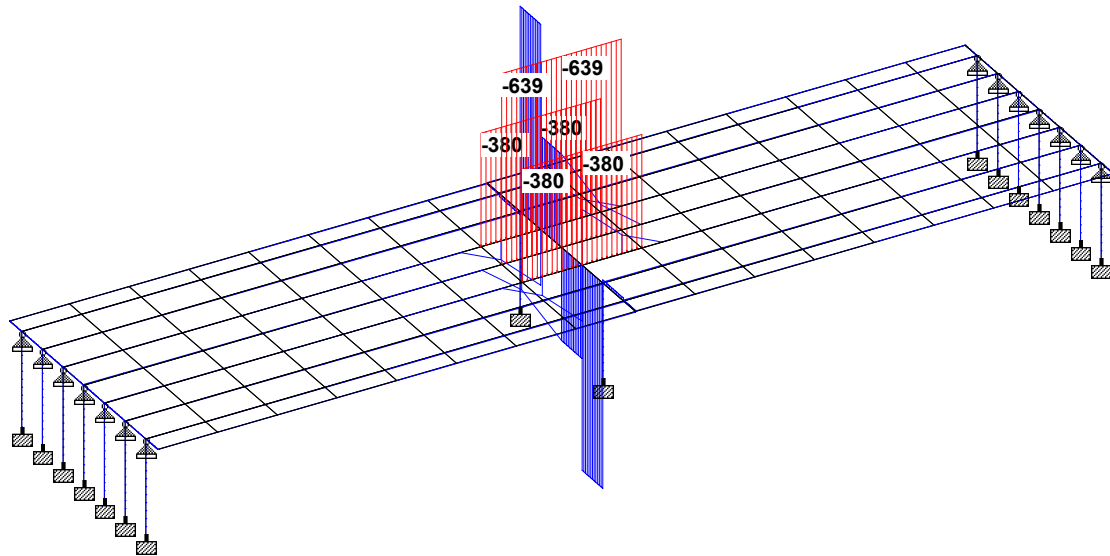


Figure 3.31: Shear Force Diagram for Case 3 Load.

After analyzing the model in the STAAD.Pro software, the maximum positive moment (at pier cap mid-span) and shear force on the pier cap, obtained from the program output, are 85,851 kip-ft and 14,096 kip, respectively. The maximum negative moment (at pier cap over column) is 85,843 kip-ft. The maximum positive moment and shear force in girders 29 and 38 are 2,987 kip-ft and 2,128 kip, respectively. Both columns (columns 50 and 51) experienced identical loads. The maximum negative moment (at column bottom) and axial load obtained in the column are 34,525 kip-ft and 3,148 kip, respectively. Column performance depends on the combined action of bending moment and corresponding axial loads, as shown in the column interaction diagram in Fig. 3.17. Figures 3.30 and 3.31 represent the bending moment and shear force diagrams, respectively, for Case 3 loads.

3.9.4 Load Case 4

Figure 3.32 shows Case 4 blast loads. Case 4 loads were defined to determine the maximum shear force in the girders. This load, identical to Case 3, was moved horizontally at the discontinued ends of the girders (girders 28, 29 and 30). These loads were applied along the centerline of girders 28, 29 and 30 for a length of 20 ft from the centerline of the end bent cap.

Figures 3.33 and 3.34 present the bending moment and shear force diagrams, respectively, for Case 4 blast loads. Because of this loading pattern, the maximum positive moment and shear force on girder 29 are 63,677 kip-ft and 10,950 kip, respectively. The maximum moment and shear force on girders 28 and 30 are 43,301 kip-ft and 6,409 kip, respectively. As a result of this load case, the end bent cap experienced high bending moment and shear force. The end bent cap is supported by multiple piles with short spans between the piles, which decreases the applied moment and increases the cap stiffness. Moreover, the bottom of the end bent cap stays in touch with the ground. These phenomena make the end bent cap less critical and more protected compared to the other elements in assessing the bridge performance. Therefore, it was excluded from this research.

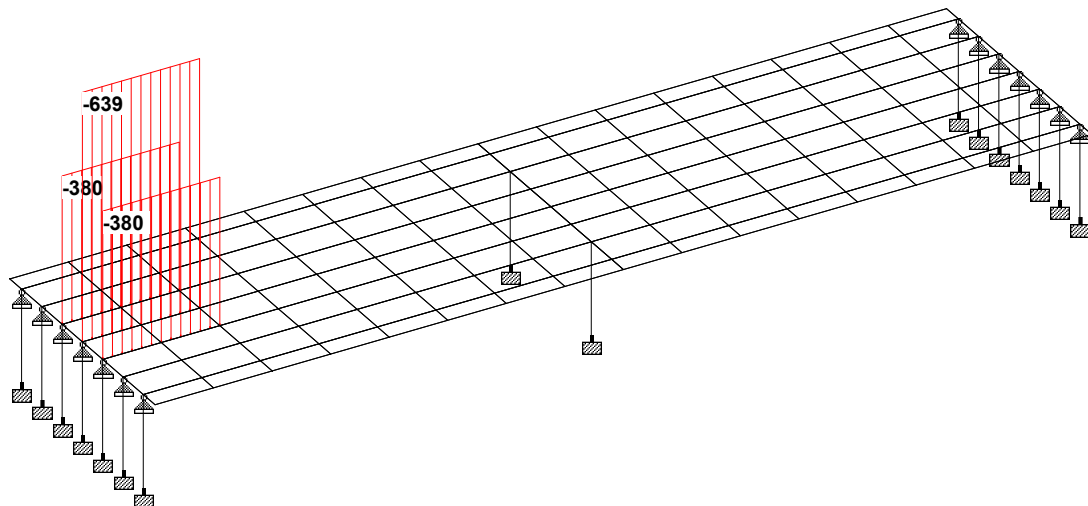


Figure 3.32: Case 4 Load on Model Bridge.

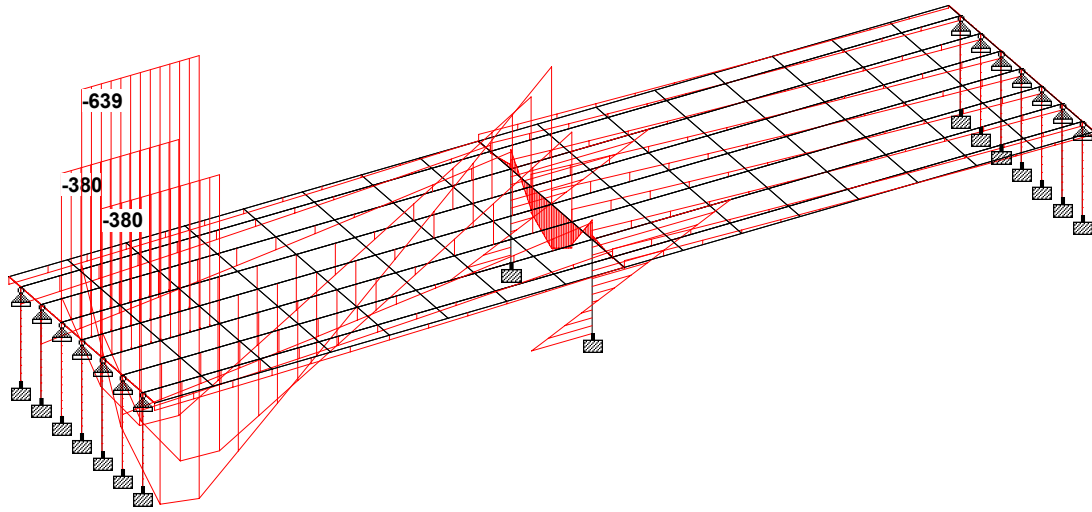


Figure 3.33: Moment Diagram for Case 4 Load.

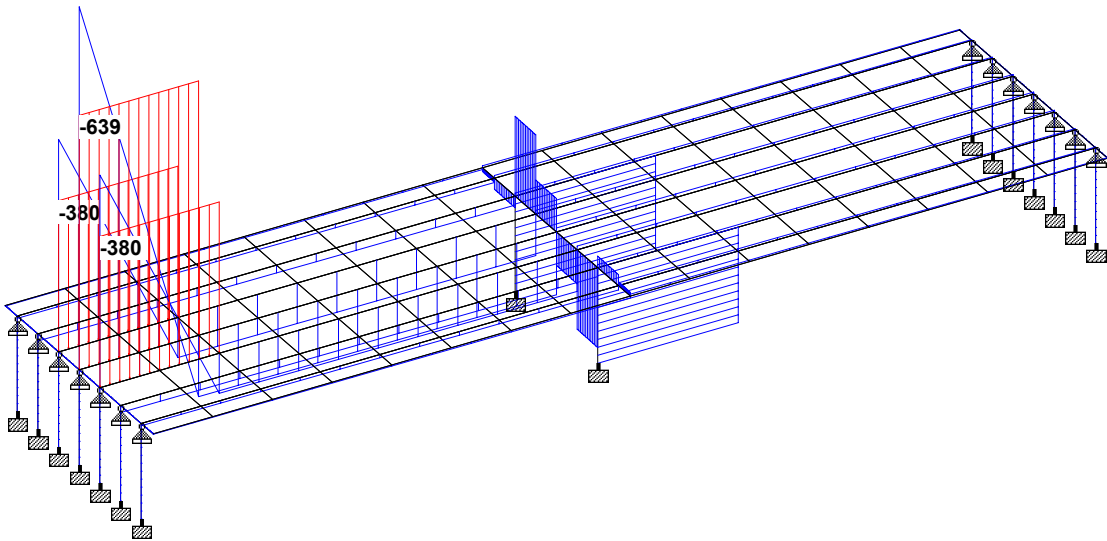


Figure 3.34: Shear Force Diagram for Case 4 Load.

3.9.5 Load Case 5

Figure 3.35 presents Case 5 blast loads on the model bridge. This load case includes horizontal pressure on the column when explosion occurs underneath the bridge at 3 ft above the ground, and at a standoff distance of 4 ft from the column surface. Because of the curved surface of the 3.5 ft diameter column, the total force intensity is less compared to that on a flat surface of equal dimension. Although the projected surface width of the circular column is 3.5 ft, as a conservative approach, the equivalent flat surface width of 3 ft was assumed for 3.5 ft diameter column to account for the reduction in the net pressure due to the curved surface. An average intensity of 1.25 ksi (Table 3.5, using 50 Percent Distribution Rule) on the equivalent flat width of 3 ft was applied on the column for a total length of 8 ft calculated on the basis of 45-degree angle of projection. The converted uniformly distributed load of 540 k/ft was applied along the centerline of column 51 for a length of 8 ft. Simultaneously, the pier cap bottom at 9 ft above the point of explosion was also subjected to a vertically upward pressure of 0.41 ksi (Table 3.5, using 50 Percent Distribution Rule) distributed over the 4 ft wide cap for a length of 18 ft. In the STAAD.Pro model, the equivalent uniformly distributed load of 236.16 k/ft was applied along the centerline of the pier cap elements 13, 14 and 15 on top of the referenced column. Although the superstructure also captured part of this explosion, it was excluded in this load case because the main purpose of this load case was to determine the performance of the substructure only. Besides, Case 1 loads were used previously to assess the superstructure behavior.

Figures 3.36 and 3.37 present the bending moment and shear force diagrams generated by Case 5 blast loads. The maximum negative bending moment and axial force produced by these loads on column 51, obtained from the STAAD.Pro output, are 11,087 kip-ft and 3,280 kip, respectively. The maximum negative bending moment and shear force on the pier cap elements are 4,820 kip-ft (element 13) and 2,057 kip (element 14), respectively.

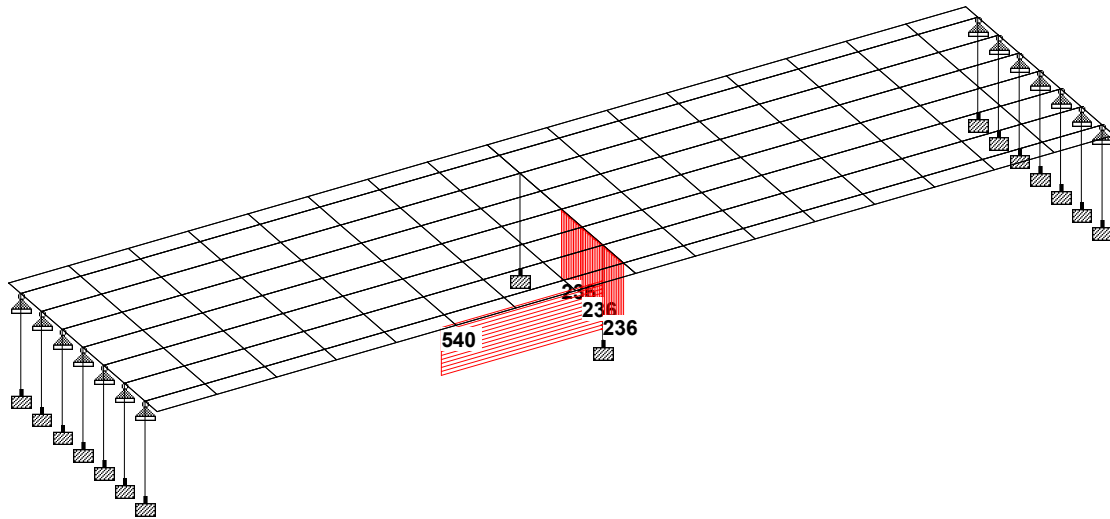


Figure 3.35: Case 5 Load on Model Bridge.

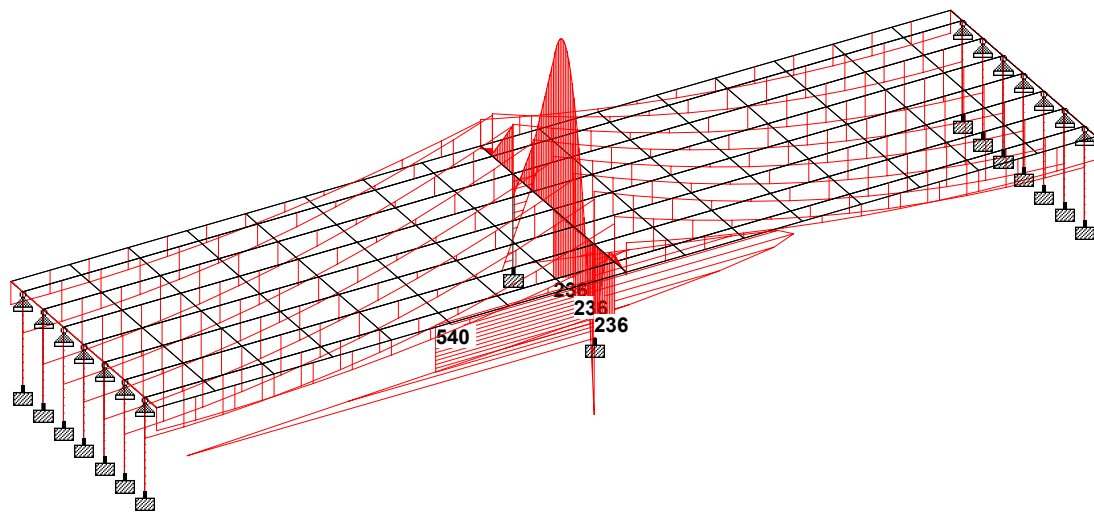


Figure 3.36: Moment Diagram for Case 5 Load.

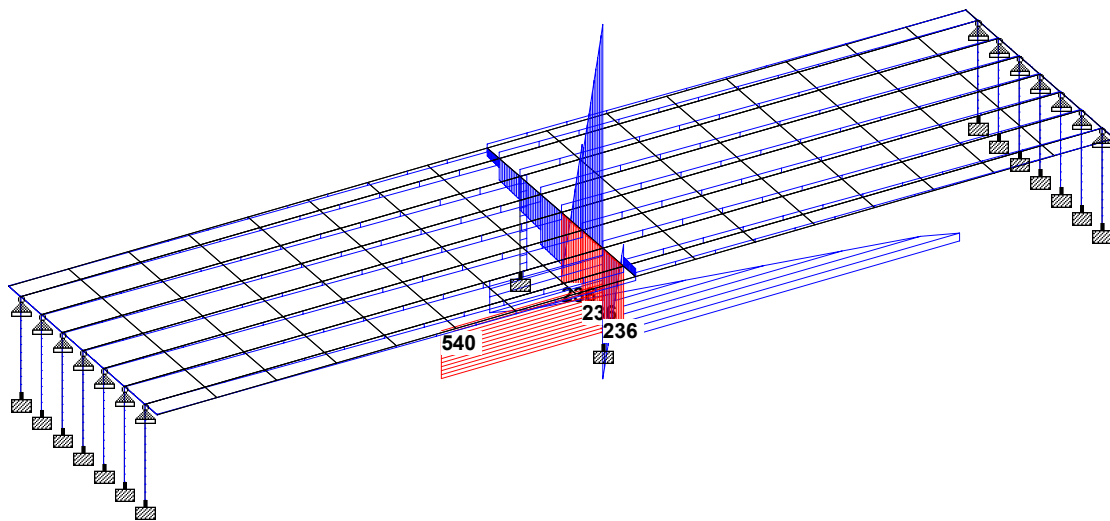


Figure 3.37: Shear Force Diagram for Case 5 Load.

3.10 Limitations of Analysis

The performance assessment of the critical members is the initial step of blast resistant bridge design. Although blast load is a dynamic load and it impacts the structure for a very short duration, equivalent static loads due to explosion were used in assessing the structural performance. There may be some minor variation in the results between equivalent static and dynamic analysis of the model bridge because of impact and sustained loading, but the overall performance of a structure would be fairly close in each of these two types of analyses. If a structure fails due to a static load, it must fail if it sustains the equivalent amount of dynamic load for any duration. Although earthquake produces dynamic load, similar analogy of converting dynamic loads into static loads has been used with acceptable accuracy for structural designs. Therefore, performance of bridge elements under equivalent static loads can be considered as reasonably similar to that under the original dynamic blast loads.

The AASHTO girders in a bridge are normally simply supported. They are, however, compositely connected through the cast-in-place slab. The deck slab was modeled with plate elements integrally connected with the girders, which resembles the actual condition. This phenomenon makes the girders partly continuous over the pier support, generating end moments. In the STAAD.Pro analysis, girders were assumed as simply supported at both end bents. Moments at the pier supports were produced because of structural continuity formed by the deck slab, which resembles the actual situation. In the static analysis of the model bridge, although no moment is generated at the simple end supports, small moments were observed at the girder ends in the STAAD.Pro output. This might happen because of the combined action of the superstructure stiffness produced by the strong framing between the deck slab and the girders, and the high dead loads of the superstructure sustained by the simple end supports. Combination of these two phenomena may generate some amount of fixity at the simple end supports, which produced those small moments.

Because of the application limitations in the structural analysis software STAAD.Pro, only the centerline of each bridge element was modeled. The equivalent area of the girders and the barriers were used in the analysis in finding applied moments and shear forces. Generally, the shape of the structure does not interfere with calculating the applied loads on the structure. The self-weight of the elements depends only on the cross-sectional area magnitudes.

All static blast loads were converted to equivalent uniformly distributed loads and applied at the centerline of each bridge element, which also did not affect the analysis.

CHAPTER 4

MODEL BRIDGE PERFORMANCE

4.1 Bridge Performance under Typical Blast Load

From the program output, the applied moments and shear forces on the critical elements of the bridge were determined, and compared with their respective capacity to assess their performance. The selected parts of the program output for different load cases are presented in Appendix F.

The performance was measured by comparing the applied moments and shear forces with the respective capacity of the members. As a general rule of analysis, if the applied load exceeds member capacity, the member can be considered as failed. The maximum applied moments, shears and the capacity of each critical member under consideration were tabulated in the member status tables with their respective survival or failure conditions. Depending on the damage and failure condition, the whole structure was identified as partially or fully out of service following failure criteria defined in Chapter 3.

After determining the effect of 500 lb of TNT explosion on the structure, several further analyses of the model bridge were performed to determine the amount of TNT the respective members could resist before failure. The amount varied depending on the standoff distance of the explosion, member type and the location of the explosion. The maximum amount of blast loads, which the typical Type III AASHTO girder, the pier cap, and the column can resist before failure, were determined by using trial and error method. Several scenarios of blast loading were considered to find these loads for each individual case.

4.1.1 Performance under Case 1 Blast Load

Table 4.1 presents the status of the critical bridge components in the aftermath of Case 1 explosion underneath the bridge. All girders in span 1 failed due to negative moments. In addition to the moment failure, girders 28, 29 and 30 also failed because of inadequate shear capacity. Apparently, girders in span 2 would survive from the explosion. The pier cap and both the columns collapsed because of very high applied moments as a result of this explosion. Although the girders in span 2 survived the direct impact of the explosion, secondary failure was expected due to the failure of the pier cap and the columns. So, there was no scope of reusing the girders for emergency works. After considering all these failures, it is evident that the model bridge underwent complete collapse, and will require immediate replacement.

Table 4.1: Member Status for Case 1 Blast Load

	Member	Bending Moment (kip-ft)		Shear/Axial* Force (kip)		Moment Failure	Shear/Axial* Failure
		Capacity	Applied	Capacity	Applied		
Span 1	Girder 26	-805	-1,036	278	43	X	
	Girder 27	-805	-1,454	278	43	X	
	Girder 28	-805	-15,484	278	964	X	X
	Girder 29	-805	-20,434	278	1,281	X	X
	Girder 30	-805	-15,484	278	964	X	X
	Girder 31	-805	-1,454	278	43	X	
	Girder 32	-805	-1,036	278	43	X	
Span 2	Girder 35	4,500	1,141	278	45		
	Girder 36	4,500	1,387	278	51		
	Girder 37	4,500	1,444	278	41		
	Girder 38	4,500	1,495	278	37		
	Girder 39	4,500	1,444	278	41		
	Girder 40	4,500	1,386	278	51		
	Girder 41	4,500	1,139	278	45		
	Pier Cap	2,953	9,772	772	1,498	X	X
	Column 50	2,416	28,124	2,000	1,235	X	
	Column 51	2,416	28,124	2,000	1,235	X	

* Axial loads for columns only.

X Denotes capacity exceeded.

4.1.2 Performance under Case 2 Blast Load

Table 4.2 shows the condition of the model bridge components after Case 2 explosion at 6 ft height above the bridge deck at mid-span. Due to this type of explosion, all girders in span 1 and 2, pier cap and columns collapsed. Very high moments and shears, generated because of this explosion, caused complete failure of all the girders. The columns experienced significant moments and axial forces far beyond their capacity, and were instantaneously grounded. Girders 27 to 31 experienced shear failure in addition to flexural failure. As a result of Case 2 blast loads, the model bridge will completely collapse and will require immediate replacement.

Table 4.2: Member Status for Case 2 Blast Load

	Member	Bending Moment (kip-ft)		Shear/Axial* Force (kip)		Moment Failure	Shear/Axial* Failure
		Capacity	Applied	Capacity	Applied		
Span 1	Girder 26	4,500	7,271	278	128	X	
	Girder 27	4,500	16,555	278	322	X	X
	Girder 28	4,500	65,033	278	4,885	X	X
	Girder 29	4,500	107,201	278	7,964	X	X
	Girder 30	4,500	65,033	278	4,885	X	X
	Girder 31	4,500	16,555	278	322	X	X
	Girder 32	4,500	7,261	278	128	X	
Span 2	Girder 35	-805	-4,971	278	121	X	
	Girder 36	-805	-5,409	278	136	X	
	Girder 37	-805	-8,772	278	195	X	
	Girder 38	-805	-10,301	278	222	X	
	Girder 39	-805	-8,772	278	195	X	
	Girder 40	-805	-5,409	278	136	X	
	Girder 41	-805	-4,970	278	121	X	
	Pier Cap	2,953	57,234	772	9,211	X	X
	Column 50	2,416	147,122	2,000	10,072	X	X
	Column 51	2,416	147,121	2,000	10,076	X	X

* Axial loads for columns only.

X Denotes capacity exceeded.

4.1.3 Performance under Case 3 Blast Load

Case 3 blast loads were applied on top of the pier cap, and the results are displayed in Table 4.3 showing the status of the model bridge components. Girders 28 to 30 and 37 to 39 failed due to the lack of shear capacity. None of the girders failed because of the applied moments. Typical shear failure produces vertical and/or diagonal cracks in the girders decreasing their end bearing capacity. On the other hand, pier cap and the columns failed due to applied moments and shears or axial forces in excess of their capacity. Four girders in each span, which survived from this explosion, were subjected to a secondary failure due to the collapse of the pier cap and the columns. As a result, the whole bridge collapsed and required immediate replacement.

Table 4.3: Member Status for Case 3 Blast Load

	Member	Bending Moment (kip-ft)		Shear/Axial* Force (kip)		Moment Failure	Shear/Axial* Failure
		Capacity	Applied	Capacity	Applied		
Span 1	Girder 26	4,500	1,204	278	60		
	Girder 27	4,500	1,751	278	71		
	Girder 28	4,500	1,820	278	3,832		X
	Girder 29	4,500	2,987	278	6,395		X
	Girder 30	4,500	1,459	278	3,832		X
	Girder 31	4,500	1,751	278	71		
	Girder 32	4,500	1,201	278	60		
Span 2	Girder 35	4,500	1,204	278	60		
	Girder 36	4,500	1,751	278	71		
	Girder 37	4,500	1,820	278	3,832		X
	Girder 38	4,500	2,987	278	6,395		X
	Girder 39	4,500	1,820	278	3,832		X
	Girder 40	4,500	1,750	278	71		
	Girder 41	4,500	1,201	278	60		
	Pier Cap	2,953	85,850	772	14,096	X	X
	Column 50	2,416	34,525	2,000	14,465	X	X
	Column 51	2,416	34,525	2,000	14,466	X	X

* Axial loads for columns only.

X Denotes capacity exceeded.

4.1.4 Performance under Case 4 Blast Load

All of the critical members of the model bridge under consideration failed due to applied moments generated from Case 4 blast loads applied on top near the end bents, as shown in Table 4.4. Girders in span 1 and span 2 failed due to very high positive and negative moments, respectively. The pier cap and the columns also collapsed because of the applied moments and corresponding shear or axial force in excess of their capacity. Therefore, the whole bridge collapsed due to Case 4 blast loads necessitating immediate replacement.

Table 4.4: Member Status for Case 4 Blast Load

	Member	Bending Moment (kip-ft)		Shear/Axial* Force (kip)		Moment Failure	Shear/Axial* Failure
		Capacity	Applied	Capacity	Applied		
Span 1	Girder 26	4,500	5,322	278	128	X	
	Girder 27	4,500	11,985	278	269	X	
	Girder 28	4,500	43,301	278	6,409	X	X
	Girder 29	4,500	65,557	278	10,950	X	X
	Girder 30	4,500	43,302	278	6,409	X	X
	Girder 31	4,500	11,985	278	269	X	
	Girder 32	4,500	5,314	278	127	X	
Span 2	Girder 35	-805	-2,237	278	83	X	
	Girder 36	-805	-2,491	278	94	X	
	Girder 37	-805	-3,504	278	113	X	
	Girder 38	-805	-3,940	278	121	X	
	Girder 39	-805	-3,504	278	113	X	
	Girder 40	-805	-2,491	278	94	X	
	Girder 41	-805	-2,236	278	83	X	
	Pier Cap	2,953	14,996	772	2,411	X	X
	Column 50	2,416	47,174	2,000	3,123	X	X
	Column 51	2,416	47,174	2,000	3,125	X	X

* Axial loads for columns only.

X Denotes capacity exceeded.

4.1.5 Performance under Case 5 Blast Load

Table 4.5 presents the status of each member under consideration due to Case 5 blast loads. These loads were applied at a standoff distance of 4 ft from the face of column 51 underneath the bridge. As a result of this explosion, girders 27 to 31 and 36 to 41 failed due to negative moments at very small margins, which indicated minor cracks on top of the bridge because of huge redundancy of the deck slab. The rest of the girders survived the explosion. Pier cap and column 51 failed while column 50 survived. No shear failure was observed in the girders due to this explosion. Because of one column failure and minor cracks on top of the bridge, the whole bridge may not immediately collapse.

Table 4.5: Member Status for Case 5 Blast Load

	Member	Bending Moment (kip-ft)		Shear/Axial* Force (kip)		Moment Failure	Shear/Axial* Failure
		Capacity	Applied	Capacity	Applied		
Span 1	Girder 26	4,500	1,111	278	57		
	Girder 27	-805	-894	278	64	X	
	Girder 28	-805	-908	278	65	X	
	Girder 29	-805	-896	278	65	X	
	Girder 30	-805	-873	278	65	X	
	Girder 31	-805	-818	278	63	X	
	Girder 32	4,500	1,110	278	57		
Span 2	Girder 35	4,500	1,105	278	58		
	Girder 36	-805	-934	278	65	X	
	Girder 37	-805	-981	278	66	X	
	Girder 38	-805	-1,005	278	67	X	
	Girder 39	-805	-1,023	278	67	X	
	Girder 40	-805	-1,017	278	66	X	
	Girder 41	-805	-863	278	59	X	
	Pier Cap	2,953	4,054	772	2,058	X	X
	Column 50	2,416	705	2,000	36		
	Column 51	2,416	11,087	2,000	3,101	X	X

* Axial loads for columns only.

X Denotes capacity exceeded.

Part of the superstructure might be reused for emergency maintenance of traffic as the traffic loads acts vertically downward, and the prestressing might still be working. Depending on the magnitude and amount of damage, the bridge was identified as partially out of service and required emergency repair works while maintaining one lane of traffic.

4.2 Blast Capacity of Bridge Elements

Because most of the load cases considered herein resulted in complete collapse of the model bridge, it may be worthwhile to determine the actual capacity of the bridge components for the chosen design. The blast capacities of the components were calculated and presented in the following sections.

4.2.1 AASHTO Girder Capacity

Only load Cases 1 and 2 locations were considered herein for the blast capacity analysis of the Type III AASHTO girders. When the explosion occurred on top of the bridge for Case 2 loads location, the blast load produced due to an explosion of only 1.7 lb of TNT (Table 4.6) at 6 ft above the bridge deck was found to be the maximum blast load the Type III AASHTO girder could resist before failure. The average pressures due to this explosion are 0.02 ksi (Table 4.6, using 50 Percent Distribution Rule) on girder 29, and 0.012 ksi (Table 4.6, using 30 Percent Distribution Rule) on girders 28 and 30. The equivalent uniformly distributed loads are 17.2 k/ft and 10.3 k/ft, respectively, applied along the centerline in the middle 20 ft of the girders.

The maximum bending moment produced on girder 29 by these loads is 4,164 kip-ft, which is less than its capacity of 4,500 kip-ft. The maximum shear force on the girder obtained from the STAAD.Pro output due to these loads is 278 kip, which is equal to its capacity. Shear capacity controlled the amount of explosive the Type III AASHTO girder could resist before failure in case the explosion occurred on top of the bridge at the girder mid-span. In general, the prestressed girders are not designed with much excess capacity beyond the minimum requirement. In this model bridge, the girders had only 17 percent more flexural capacity than required for the AASHTO Strength I loading

combination. Therefore, it appears reasonable that the girders can resist pressures caused by only 1.7 lb of TNT explosion over the bridge.

Table 4.6: Converted Pressure for 1.7 lb of TNT Explosion

Range (ft)	Pressure (psi)
4	105
5	63
6	41
7	29
8	22
9	17
10	14

In case the explosion occurred underneath the bridge (similar to load Case 1 location), the blast load produced due to an explosion of 14.5 lb of TNT underneath the bridge at 3 ft above the ground was found to be the maximum load the Type III AASHTO girder could resist before failure. The girders and the bottom of the slab were assumed to be at the height of 13 and 17 ft, respectively, above the explosion. The average pressure due to this explosion at the height of 13 ft was 0.018 ksi (Table 4.7, using 50 Percent Distribution Rule) on girder 29, and 0.01 ksi (Table 4.7, using 30 Percent Distribution Rule) on girders 28 and 30. The equivalent uniformly distributed loads due to these pressures were calculated as 4.7 k/ft and 2.6 k/ft, respectively. The bottom of the slab at the height of 17 ft above the explosion was subjected to an average pressure of 0.005 ksi (Table 4.7, using 30 Percent Distribution Rule) for a width of 4 ft in between two adjacent girders, and a length of 20 ft along the length of the bridge. The uniformly distributed load produced by this pressure was calculated as 2.8 k/ft equally distributed along the centerline of each girder. The total load applied in the middle 20 ft along the centerline of girder 29 was 7.5 k/ft, and girders 28 and 30 was 5.4 k/ft.

The maximum negative moment produced by these upward pressures on girder 29, obtained from the STAAD.Pro output, is 769 kip-ft, which is less than its capacity of 805 kip-ft. The maximum shear force produced by these loads is 84 kip, which is less than its shear capacity of 278 kip. Therefore, the model bridge Type III AASHTO girders of the chosen design can resist pressures produced by an explosion of 14.5 lb of TNT underneath the bridge.

Table 4.7: Converted Pressure for 14.5 lb of TNT Explosion

Range (ft)	Pressure (psi)
4	455
5	300
6	207
7	149
8	110
9	84
10	66
11	53
12	44
13	36
14	31
15	26
16	23
17	20
18	18

4.2.2 Pier Cap Capacity

The maximum amount of blast load that the pier cap can resist before failure was produced by an explosion of 1.7 lb of TNT at 6 ft above the bridge deck over the pier cap. For pier cap capacity, explosion occurred right on top of the pier cap, similar to the load Case 3 location. The pressures produced were converted to equivalent uniformly distributed loads, and applied on the middle three girders on each side of the pier cap for a length of 10 ft. The pressure produced due to the explosion of 1.7 lb of TNT on the

middle girder and the adjacent two girders were 0.02 ksi (Table 4.6, using 50 Percent Distribution Rule) and 0.012 ksi (Table 4.6, using 30 Percent Distribution Rule), respectively. The equivalent uniformly distributed load for 0.02 ksi pressure was calculated as 17.3 k/ft, and applied on girder 29 and 38 along their centerline for a length of 10 ft each way from the centerline of the pier cap. The equivalent uniformly distributed load for 0.012 ksi pressure was calculated as 10.4 k/ft, and applied on girder 28, 30, 37 and 39 along their respective centerline for a length of 10 ft each way from the centerline of the pier cap.

The maximum bending moment on the pier cap produced by these loads is 2,871 kip-ft, which is less than 2,953 kip-ft, the capacity of the pier cap. At the same time, the maximum amount of shear force on the pier cap as a result of this explosion, obtained from the STAAD.Pro output, is 611 kip, which is below 772 kip, the shear capacity of the pier cap. Therefore, the pier cap can resist blast pressures produced by 1.7 lb of TNT explosion.

4.2.3 Column Capacity

The column blast capacity was investigated herein for two different scenarios of explosion, on top of the bridge and under the bridge. Applying loads on top of the bridge followed the same method and analogy of Case 3 loading pattern. In the first scenario, pressure produced by the explosion of 5.7 lb of TNT 6 ft above the deck was applied on the middle girders of both spans for a length of 10 ft each way from the centerline of the pier cap. Pressure produced by the above explosion was 0.052 ksi (Table 4.8, using 50 Percent Distribution Rule) on girders 29 and 38. This load was converted to an equivalent distributed load of 44.9 k/ft and applied along the centerline of each girder. The other girders 28, 30, 37 and 39 experienced a pressure of 0.0312 ksi (Table 4.8, using 30 Percent Distribution Rule), which was converted to 26.9 k/ft and applied along the centerline of each girder.

The applied moment and axial force on the column produced by these loads are 2,338 kip-ft and 1,558 kip, respectively, which are less than its moment capacity of 2,350 kip-ft and the corresponding axial capacity of 1,600 kip. The column capacity was determined from its moment interaction diagram shown in Fig. 3.17.

Table 4.8: Converted Pressure for 5.7 lb of TNT Explosion

Range (ft)	Pressure (psi)
4	252
5	157
6	105
7	74
8	54
9	41

The second scenario, explosion underneath the bridge, followed Case 5 blast loading location. In this scenario, pressures generated by the explosion of 13 lb of TNT at a standoff distance of 4 ft from the column surface were applied on the column and the bottom of the pier cap. Column 51 at a distance of 4 ft from the point of explosion experienced a pressure of 0.21 ksi (Table 4.9, using 50 Percent Distribution Rule), and the pier cap elements 13, 14 and 15 at a distance of 9 ft from the explosion were subjected to a pressure of 0.039 ksi (Table 4.9, using 50 Percent Distribution Rule). The converted uniformly distributed loads due to these pressures were 90.7 k/ft applied on the column 4 ft above the ground for a length of 8 ft, and 22.4 k/ft applied on the pier cap for a length of 18 ft. All these loads were applied along the centerline of the elements.

Table 4.9: Converted Pressure for 13 lb of TNT Explosion

Range (ft)	Pressure (psi)
4	426
5	279
6	192
7	137
8	102
9	78
10	61

From this loading pattern, the applied moment and corresponding axial force on column 51 are 1,862 kip-ft and 255 kip, respectively, which are less than its moment capacity of 1,875 kip-ft with the corresponding axial capacity of 260 kip.

It is evident from these comparisons that the column can resist the blast pressure generated by 13 lb of TNT if it is applied underneath the bridge. When the blast generates over the bridge, it can withstand the pressure produced by 5.7 lb of TNT explosion without failure. The reason for this type of performance is the moment arms of the applied loads. Over the bridge explosion produces larger moment arm for the columns than under the bridge explosion.

4.3 Minimum Standoff Distance

Physical security of bridge components against blast loading is of great importance to highway departments and bridge engineers. One major component of this concept is placing passive standoff barriers around bridge components, which will prevent easy access to these components for blast attack purposes. Such barriers are a very economic and convenient alternative to bridge retrofit for existing bridges and design enhancement for new bridges. Standoff barriers are only applicable around bridge columns; it is not possible to provide such barriers for above-the-bridge explosion without closing one or more traffic lanes. The minimum standoff distance for a 500 lb TNT explosion near the model bridge pier was determined as follows.

A separate model was developed and analyzed herein with the blast location similar to load Case 5. By using trial and error, it was found that the model bridge column could resist blast pressures generated due to 500 lb of TNT if the explosion occurred at a distance of at least 16 ft from the face of the column. The full exposed height of the column was subjected to a horizontal blast pressure of 0.15 ksi (Table 3.5, using 50 Percent Distribution Rule) due to an explosion of 500 lb of TNT at a distance of 16 ft from the column surface. The equivalent uniformly distributed load of 64.8 k/ft, calculated for this blast pressure, was applied along the centerline of column 51 for its exposed height of 12 ft. Simultaneously, the pier cap, at a distance of 18 ft, experiences a horizontal blast pressure of 0.07 ksi (Table 3.5, using 30 Percent Distribution Rule). This blast pressure was converted to an equivalent uniformly distributed load of 40.3 k/ft, and

applied on pier cap elements 13, 14 and 15. The moment and axial force on column 51 produced by these loads are 1,969 k-ft and 607 kip, respectively. These loads are almost equal to and slightly less than the column moment capacity of 1,983 k-ft at axial loads of 610 kip. Therefore, if the standoff distance of at least 16 ft from the face of the columns is maintained, the model bridge columns are capable of resisting the blast pressure generated due to 500 lb of TNT explosion.

Logistics may or may not allow the enforcement of this minimum standoff distance for actual bridges. It may be possible to place physical barriers around the columns of bridges over waterways, if sufficient clearance can be maintained for navigational channels (if present). For bridge overpasses over land, such high standoff distances may not be feasible because they may encroach on adjacent traffic lanes or other property.

4.4 Experimental Validation

An effort was made to validate the theoretical modeling performed in this research with available experimental results. An extensive literature review was performed herein for this purpose. The search could not locate any full-scale blast load test on any bridge structures except for demolition purposes only. Some real life blast tests were conducted on experimental buildings; however, as these data are very sensitive and confidential in nature for security reasons, they are not available to the public. Several attempts were made to legally collect some blast test data in order to validate the ATBlast and STAAD.Pro models developed herein, but no viable response was received from these sources.

The performance evaluation of the AASHTO girder bridge under blast load was performed by finite element modeling of the model bridge in the STAAD.Pro. The typical blast loads were derived from the explosion of 500 lb of TNT, as recommended typical by the AASHTO Blue Ribbon Panel, using ATBlast software developed by the Applied Research Associates, Inc. (ARA).

ARA is an internationally recognized engineering and applied science firm. The company has approximately 650 employees. It offers a full range of engineering and security related services. The services include: blast consulting, blast resistant design and

assessments, retrofit designs for blast loads, security risk management training and assessments, terrorist threat/vulnerability assessments, physical and electronic security system assessments and designs, explosive testing and evaluation of products, specialty software development, accidental and intentional explosion investigations, and the development of security policies and procedures. ARA works closely with all Federal Agencies in the area of anti-terrorism and force protection. It developed the glazing hazard prediction program WINGARD for the US General Service Administration and WINLAC for the US Department of State. It has been providing weapons effects and weapon effectiveness expertise to the Department of Defense for over 40 years and working very closely with the Defense Threat Reduction Agency. The unmanned vehicles developed by ARA have been used in the Operation Iraqi Freedom. It is evident from the company profile that they are industry leader in developing software to convert blast loads into conventional static loads. Moreover, it is widely accepted that dynamic effect of earthquake is converted into static loads in designing structures to resist seismic forces. Therefore, the use of ATBlast in performing this research seems reliable.

CHAPTER 5

CONCLUSION AND RECOMMENDATIONS

5.1 Conclusion

To protect bridges from the act of terrorist explosion, blast resistant bridge design and retrofit techniques should be developed, and adopted by the applicable codes and regulatory agencies. Blast resistant bridge design is considered the most vital work that has not been addressed enough. This research may give some important insights about the performance of AASHTO type bridges, traditionally designed pier cap and columns. It will also help determine the proper methods of developing blast resistant bridge design in combination with the traditional method.

Not much work has been performed previously on blast resistant design and performance of structures under blast load. This is especially true for bridge structures. A bridge responds in different ways to the blast loads depending on the location, magnitude and the standoff distance of the explosion from the structure. Based on this research, the following conclusions were made:

1. It was found from the analytical experiments that the model bridge failed due to the typical blast load generated by an explosion of 500 lb of TNT and applied underneath or over the bridge at girder end or mid-span.
2. Part of the bridge survived the explosion when the typical blast load was applied at a location close to the column, which included blast loads applied directly on one column and a portion of the pier cap.
3. When the blast loads were applied under one span or over the pier cap, some of the girders on the other span survived the explosion. Due to the failure of the pier cap

and the column, those girders were subjected to a secondary failure as a result of the progressive collapse.

4. In case the typical loads were applied on the pier or column, the components underwent immediate failure.
5. It was determined from the research that the Type III AASHTO girders, traditionally designed pier cap and column could not withstand the impact of 500 lb of TNT.
6. In order to assess the capacity of the girders, pier cap and column, trial and error method was followed to determine the amount of TNT explosive each respective member could resist before failure.
7. It was found from the research that if the load were applied 6 ft over the bridge deck, the Type III AASHTO girders as well as the pier cap could resist only 1.7 lb of TNT explosion. For an explosion underneath the bridge, the girder could resist as much as 14.5 lb of TNT explosion. This amount is larger than that for over the bridge explosion because of the standoff distance of the explosion.
8. For over the bridge explosion, the model bridge column could resist blast pressure generated due to an explosion of only 5.7 lb of TNT, while for under the bridge explosion, it was able to resist 13 lb of TNT explosion at a standoff distance of 4 ft.
9. The model bridge column was capable of resisting blast pressure generated due to an explosion of 500 lb of TNT, if the standoff distance is at least 16 ft. So, it is evident from this research that the standoff distance plays very important and critical role in protecting the bridge structures from the act of terrorist explosions.

5.2 Recommendations and Future Research Directions

The research was performed based on the static equivalent of the blast load, which is a dynamic load with high impact. It focused on the performance of a Type III AASHTO girder bridge in terms of individual performance of its critical components. The critical components consisted of Type III AASHTO girders, pier cap and the columns. The overall bridge performance depended on the capacity of the members, amount and magnitude of the blast load, location of the explosion and the standoff

distances. Under the dynamic loading condition, the results may vary if the structure geometry, member strength, and the magnitude and point of explosion remain the same.

Based on this research, the following recommendations may be made:

1. Type III AASHTO girders, typically designed pier cap and columns are generally not capable of resisting the typical blast loads produced by an explosion of 500 lb of TNT. Blast resistant design of girders, cap and columns may be undertaken for protection of these elements in future.
2. Detailed research is warranted to develop appropriate means and methods to protect the critical elements of existing bridge structures from future explosive impact.
3. Deck slab was excluded from this research in order to focus on the performance of the critical components only. Future research may be undertaken to determine the performance of typical deck slab and to develop blast resistant design of deck slab. Parametric research may be performed by varying the deck thickness, and using fiber reinforced polymer (FRP) to strengthen its flexural and shear capacity against typical explosive loads.
4. The effect of bearing pad seat width, and connection between the girder and the cap were not included in the research. Further research is necessary to determine the effect of connections in response to blast loading. If the blast load is applied underneath the bridge, connections may have a vital role in protecting the bridge structures from sudden collapse due to girder dislocation. Moreover, the connections may help evenly distribute the blast pressure through the entire length of the girders.
5. The connection between the girders and the slab needs more extensive research. As the girder-slab composite performs worse against negative moments as compared to positive moments due to traditional downward loads, research may be conducted to determine the methods of strengthening girders against negative moments.
6. Prestressing of girder only increases its strength against traditional vertically downward loads. Future research may be undertaken to determine methods of prestressing and post-tensioning that will increase positive as well as the negative moment capacity of the girders.

7. The shear strength of the AASHTO girder might be a major concern in developing blast resistant design. It was found from this research that, in some instances, a girder failed due to inadequate shear capacity before it failed because of applied moments. Therefore, more research is necessary to identify method of increasing shear capacity of the AASHTO girders. Parametric research can be conducted by thickening the girder web with varying amount of reinforcements to determine maximum shear capacity.
8. It was observed from the research that typically designed pier cap and columns perform better under explosion than the prestressed AASHTO girders, although not strong enough to withstand the typical blast load. Future research is recommended to determine methods of strengthening pier cap and columns against the typical blast loads. Caps designed with FRP along with traditional reinforcements, with prestressing and post-tensioning, may be investigated to determine their performance against typical explosion.
9. This research was based on the equivalent static loads for dynamic blast pressures. Finite element model analysis of the entire bridge and its components is recommended to determine performance under dynamic loads using LS-DYNA, ABAQUS, etc.
10. Due to unavailability of real life blast load test data on structures (because of their sensitivity and confidentiality), experimental validation of the theoretical findings was not possible herein. Validation of the static and dynamic experiments can be achieved by comparing analytical data with the real life data.
11. Standoff distance plays a major role in protecting the structure against failure. Appropriate means and methods of increasing standoff distances are necessary to be developed through further research in order to protect the existing and future bridges from terrorist explosion.
12. Effect of carbon fiber wrapping on bridge elements may be investigated to determine their performance and behavior against blast loading. Other possible methods of strengthening the bridge components may be investigated as well.
13. This research was performed on a Type III AASHTO girder bridge. Future research may be conducted on other AASHTO girder bridges, Bulb-Tee bridges, and

segmental bridges to determine their performance and to establish blast resistant bridge design. Research may be conducted to assess the performance of the cable-stayed and suspension bridges under dynamic blast loading. Moreover, immediate research should be carried out to determine the methods to retrofit the existing cable-stayed and suspension bridges against typical explosion.

14. Research should be conducted to determine the effect of seismic retrofit, design and detail in the blast resistance of bridges.
15. An additional column may be added to a two-column pier cap with the same design as if it were designed for two columns. This will enhance the efficiency of the pier cap in terms of reduced applied moments, and the additional column will act to support the pier cap in case one of the columns fails due to explosion.
16. The required standoff distance can be achieved through the combination of establishing several precautionary measures, such as regular video surveillance near important and critical bridges, putting barricades around the piers ensuring the required standoff distance, and placing regulatory traffic signs prohibiting normal or emergency parking of vehicles at or near the piers.

<u>AASHTO LRFD Criteria</u>	<u>Condition Satisfied (Yes/No)</u>
10. Specified 28-day concrete strength is not less than 4.0 ksi. Deck concrete strength = 4.5 ksi > 4 ksi.	Yes
11. Deck is made composite with the supporting structural components.	Yes

All required conditions satisfied. So, Empirical Design Method can be used.

MAIN REINFORCEMENTS: (As per Empirical Design)

Use #5 bars @ 12 in on center at top and bottom in each direction.

Use additional 2 ~ #5 bars perpendicular to the traffic at 4 in. nominal spacing at the top of the slab overhang extended upto first interior beam.

OVER PIER: (From SDG 4.2.6)

Use 35 ft long #5 bars placed symmetrically about the centerline of the pier with alternate bars staggered 5 ft.

APPENDIX B. PRESTRESSED GIRDER DESIGN

LRFD English Prestressed Beam Design Program – Exterior Beam design

Project = "Model Bridge" **DesignedBy** = "Anwar" **Date** = "12/04"

Legend Tan = DataEntry Yellow = CheckValues Grey = Comments + Graphs

The CR values displayed are Capacity Ratios which give the ratio of the provided capacity divided by the required

☞ Reference: C:\FDOT_STR\Programs\LRFDpbeamE1.85\ProgramFiles\section1.mcd(R

Bridge Layout and Dimensions

Comment = "Type III Ext 80 ft span"

filename = "C:\fdot_str\programs\LRFDpbeamE1.85\Type III Ext 80 ft span.dat"

The top of the precast beam is the location of the origin

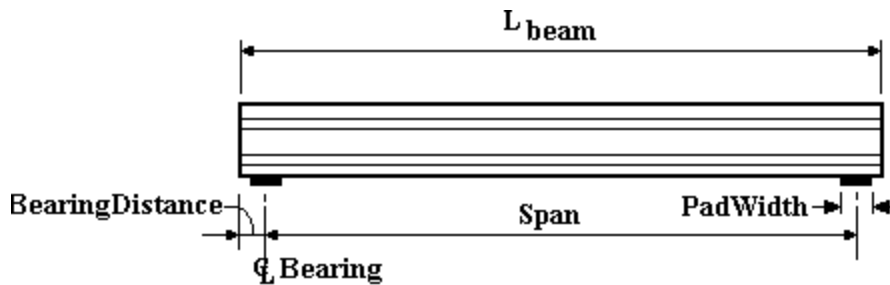


Figure B.1: Typical Beam Elevation

DataMessage = "This is a Single Web Beam Design, AASHTO LRFD used to Calculate Distribution Factors "

$L_{beam} = 80$ ft $BearingDistance = 8$ in $Span = 78.67$ ft $PadWidth = 10$ in

WRITEPRN("coord.dat") := $\frac{BeamType}{ft}$ WRITEPRN("location.dat") := $\frac{Location}{ft}$

Overhang = 3.5 ft BeamSpacing = 6 ft $t_{slab} = 8$ in $h_{buildup} = 0$ in

Skew = 0 deg $t_{integral.ws} = 0.5$ in NumberOfBeams = 7 $t_{slab.delta} = 0$ in

BeamTypeTog = "III"

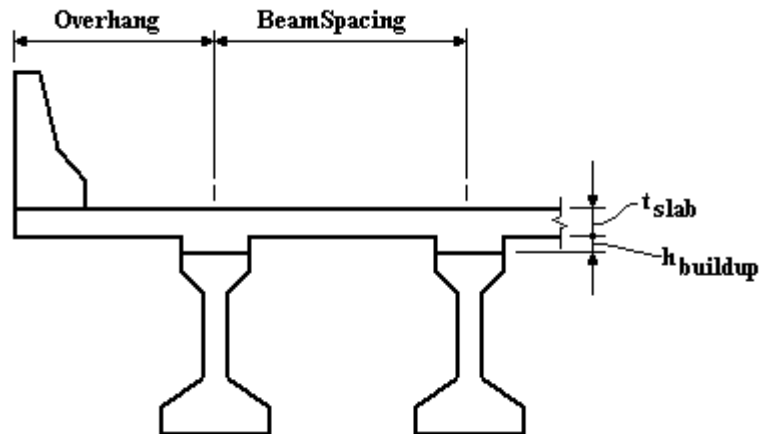


Figure B.2: Partial Superstructure Section

These are typically the FDOT designations found in our standards. The user can also create a coordinate file for a custom shape. In all cases the top of the beam is at the $y=0$ ordinate.

BeamPosition = "exterior"

For calculating distribution factors must be either interior or exterior

SectionType = "transformed" $b_e = 6.5$ ft

effective slab width LRFD 4.6.2.6

user_g_mom $\equiv 0$ user_g_shear $\equiv 0$

If user_g_mom (the moment distribution factor) or user_g_shear (the shear distribution factor) is set to zero the program's calculated value will be used. If they are other than zero then this user inputted value will be used.

Section Properties - Beam and Slab

Material Properties - Concrete

Corrosion Classification Environment = "moderately"

density of slab concrete $\gamma_{slab} = 0.15 \frac{\text{kip}}{\text{ft}^3}$

strength of slab concrete $f_{c,slab} = 4.5$ ksi

density of beam concrete $\gamma_{beam} = 0.15 \frac{\text{kip}}{\text{ft}^3}$

strength of beam concrete $f_{c,beam} = 6.5$ ksi

release beam strength $f_{ci,beam} = 5$ ksi

weight of future wearing surface Weight_{future.ws} = $0.015 \frac{\text{kip}}{\text{ft}^2}$

initial conc. modulus of elasticity $E_{ci} = 3663$ ksi
 used in distribution calculation $n_d = 1.202$
 concrete modulus of elasticity $E_c = 4176$ ksi
 type of coarse aggregate, either "Florida" or "Standard" AggregateType = "Florida"
 relative humidity $H = 75$
 Material Properties - Prestressing Tendons and Mild Steel
 tendon ultimate tensile strength $f_{pu} = 270$ ksi
 tendon modulus of elasticity $E_p = 28500$ ksi
 time in days between jacking and transfer $t_j = 1.5$
 ratio of tendon modulus to beam concrete modulus $n_p = 6.825$
 mild steel yield strength $f_y = 60$ ksi
 mild steel modulus of elasticity $E_s = 29000$ ksi
 ratio of rebar modulus to beam concrete modulus $n_m = 6.944$
 d distance from top of slab to centroid of slab reinf. $d_{slab.rebar} = 4$ in
 area per unit width of longitudinal slab reinf. $A_{slab.rebar} = 0.62 \frac{\text{in}^2}{\text{ft}}$
 d distance from top of beam to centroid of mild flexural tension reinf. $d_{long} = 0$ in
 area of mild reinf lumped at centroid of bar locations $A_{s.long} = 0 \text{ in}^2$

Permit Loads

Number of wheel loads that comprise the permit truck PermitAxles = 2

PermitUniformLoad = $0 \frac{\text{lb}}{\text{ft}}$ PermitAxleLoad^T = (8 32) kip

PermitAxleSpacing^T = (0 14 0) ft

Loads - Release, Non composite, Composite, and Live Load (truck and lane)

$w_{beam} = 0.583 \frac{\text{kip}}{\text{ft}}$ $\max(M_{release}) = 466.4$ kip·ft

note: at release, span length is the full length of the beam

$w_{slab} = 0.691 \frac{\text{kip}}{\text{ft}}$ $w_{beam} = 0.583 \frac{\text{kip}}{\text{ft}}$ $w_{forms} = 0.047 \frac{\text{kip}}{\text{ft}}$ $w_{noncomposite} = 1.32 \frac{\text{kip}}{\text{ft}}$

(w_{slab} includes buildup)

Add_w_noncomp $\equiv 0 \cdot \frac{\text{kip}}{\text{ft}}$

$\max(M_{dl.non.comp}) = 1021.1$ kip·ft $\max(V_{dl.non.comp}) = 51.9$ kip $w_{barrier} = 0.182 \frac{\text{kip}}{\text{ft}}$

$w_{future.ws} = 0.079 \frac{\text{kip}}{\text{ft}}$ $w_{composite} = 0.26 \frac{\text{kip}}{\text{ft}}$ Add_w_comp $\equiv 0 \cdot \frac{\text{kip}}{\text{ft}}$

$\max(M_{dl.comp}) = 202$ kip·ft $\max(V_{dl.comp}) = 10$ kip
 $\max(M_{dist.live.pos}) = 1323.9$ kip·ft (includes impact)
 $\max(V_{dist.live.pos}) = 72$ kip (includes impact)

Live load distribution factors

BeamPosition = "exterior" $g_{\text{shear}} = 0.658$ $g_{\text{mom}} = 0.658$ Reaction_{LL} = 72.957 kip

(service value includes truck impact)

Reaction_{DL} = 63.265 kip (service value)

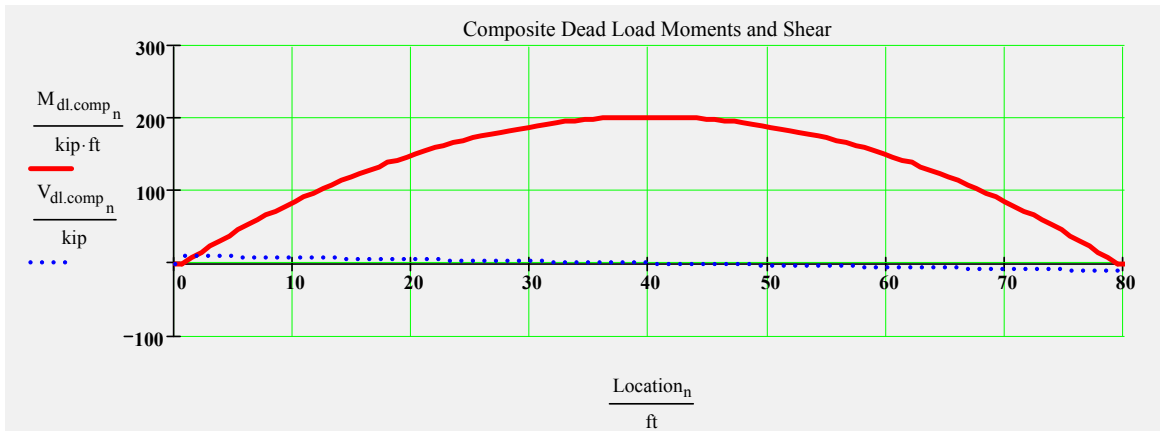


Figure B.3: Composite Dead Load Moments and Shear

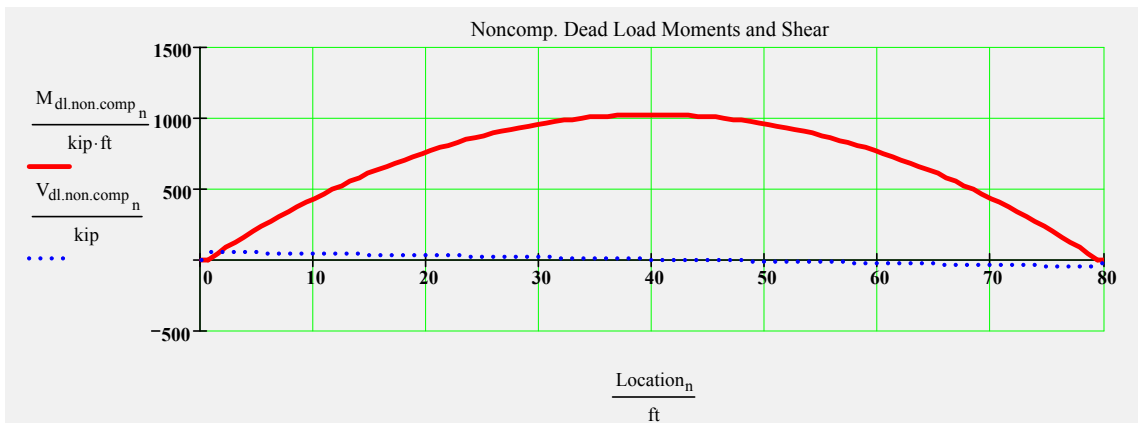


Figure B.4: Non-Composite Dead Load Moments and Shear

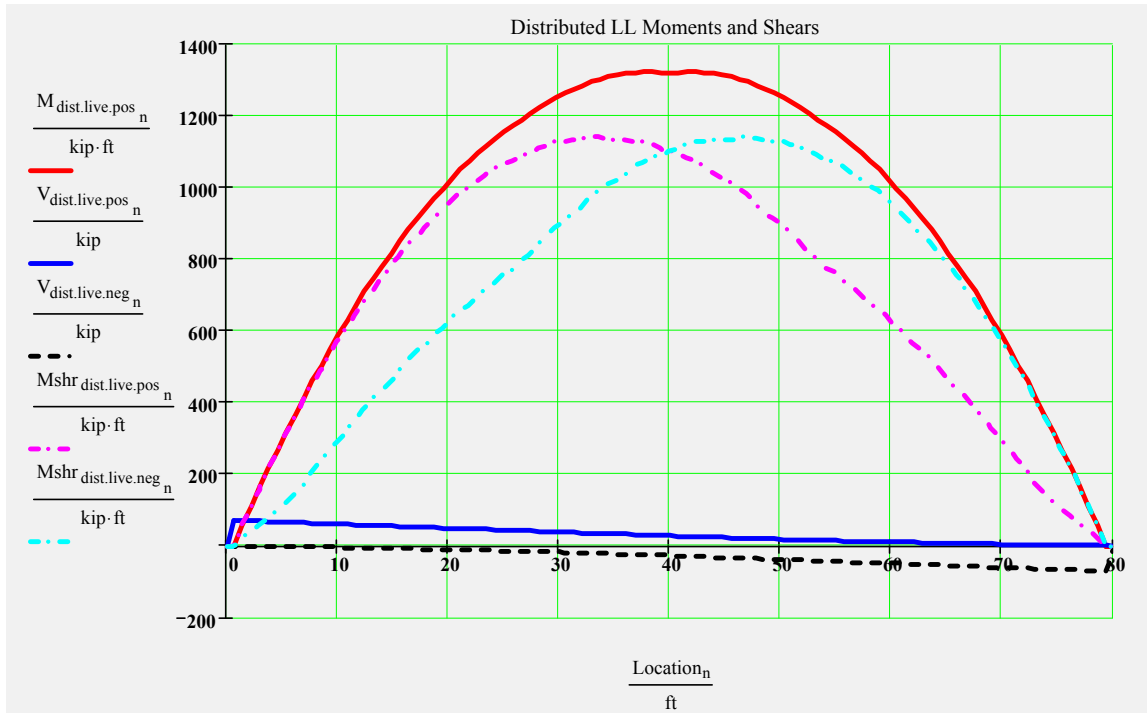


Figure B.5: Distributed Live Load Moments and Shear

A suggested method of iteration is to fill the beam with tendons beginning in the middle of the bottom row, filling the row outward, then continuing on to the middle of the next lowest row. Typically, the minimum number of tendon is reached when midspan tensile stress is below the LRFD Service III Limit stress. Next, tendons should be debonded in pairs according to the Structures Design Guidelines until the end compression stress are below the LRFD Service I Limit stress. These two limits typically control the design (see graph below).

Design Prestress Tendon Geometry



```
Stranddata := | a ← READPRN("tendsect.dat")
              | w ← READPRN("strand.dat")
              | x ← READPRN("area.dat")
              | y ← READPRN("shield.dat")
              | z ← READPRN("distance.dat")
              | (w x y z a)
```

*Double click on the **Strand Geometry** icon to specify type, location, size, and debonding of strands. Then click on **Stranddata** and press F9 to read in the data.*

Strand Geometry

☞ Reference: C:\FDOT_STR\Programs\LRFPbeamE1.85\ProgramFiles\section2.mcd(R
 Summary of Initial Compression and Final Tension Prestress for Iteration Purposes.
 These two stress checks usually control . See graphs in proceeding sections for full
 details.

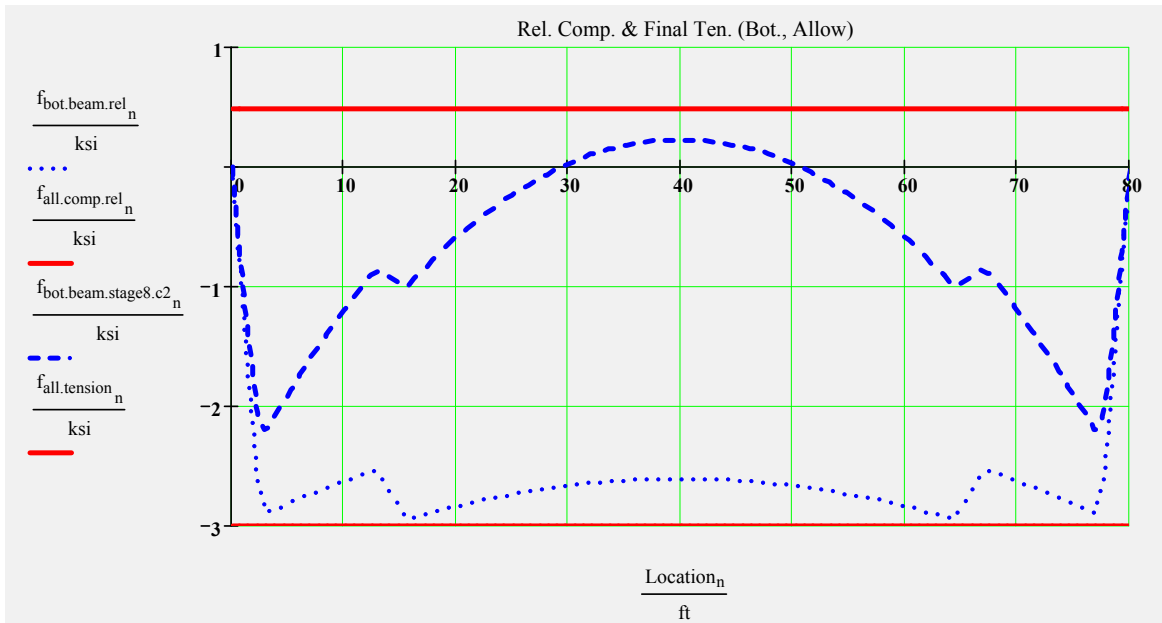


Figure B.6: Compression at Release and Final Tension

$$\min(CR_{f_{comp.rel}}) = 1.015 \quad \text{Check}_{f_{comp.rel}} = \text{"OK"} \quad \min(CR_{f_{tension.stage8}}) = 2.232$$

$$\text{Check}_{f_{tension.stage8}} = \text{"OK"}$$

check strand pattern for debonding limits (per row and total) and for debonded strands on outside edge of strand patter. Check0 - No Debonded tendon on outside row, Check1 - less than 40 percent Debonded in any row, Check2 - less than 25 percent Debonded total

$$\text{CheckPattern}_0 = \text{"OK"} \quad \text{CheckPattern}_1 = \text{"OK"} \quad \text{CheckPattern}_2 = \text{"OK"}$$

Section and tendon properties

$$\text{Concrete area of beam} \quad A_{beam} = 3.887 \text{ ft}^2$$

$$\text{Gross Moment of Inertia of Beam} \quad I_{beam} = 1.252 \times 10^5 \text{ in}^4$$

$$\text{Gross Moment of Inertia Composite Section} \quad I_{comp} = 3.503 \times 10^5 \text{ in}^4$$

$$\text{Dist. from top of beam to CG of composite section} \quad y_{comp} = -10.902 \text{ in}$$

$$\text{Concrete area of deck slab} \quad A_{deck} = 3.606 \text{ ft}^2$$

total area of strands

$$A_{ps} = 4.6 \text{ in}^2$$

diameter of Prestressing strand

$$d_{b,ps} = 0.5 \text{ in}$$

0 - low lax 1 - stress relieved

$$\text{min}(\text{PrestressType}) = 0$$

tendon yield strength

$$f_{py} = 243 \text{ ksi}$$

prestress jacking stress

$$f_{pj} = 203 \text{ ksi}$$

$$L_{\text{shielding}}^T = (13 \ 0 \ 13 \ 0 \ 0 \ 0) \text{ ft}$$

$$A_{ps,row}^T = (0.3 \ 1.1 \ 0.3 \ 1.1 \ 1.1 \ 0.8) \text{ in}^2$$

	0	1	2	3	4	5	6	7	8
0	-3.5	-3.5	-3.5	-3.5	-3.5	-3.5	-3.5	-3.5	-3.5
1	-3.5	-3.5	-3.5	-3.5	-3.5	-3.5	-3.5	-3.5	-3.5
$d_{ps,row} =$	2	-3.333	-3.333	-3.333	-3.333	-3.333	-3.333	-3.333	-3.333
	3	-3.333	-3.333	-3.333	-3.333	-3.333	-3.333	-3.333	-3.333
	4	-3.167	-3.167	-3.167	-3.167	-3.167	-3.167	-3.167	-3.167
	5	-3	-3	-3	-3	-3	-3	-3	-3

Tendon Layout

$$\text{TotalNumberOfTendons} = 30$$

$$\text{NumberOfDebondedTendons} = 4$$

$$\text{NumberOfDrapedTendons} = 0$$

$$\text{StrandSize} = "1/2 \text{ in low lax}"$$

$$\text{StrandArea} = 0.153 \text{ in}^2$$

$$\text{JackingForceper.strand} = 30.983 \text{ kip}$$

SERVICE LIMIT STATE

$$\text{max}(M_{\text{pos.Ser1}}) = 2545 \text{ kip-ft}$$

$$\text{max}(M_{\text{pos.Ser3}}) = 2281 \text{ kip-ft}$$

Prestress Losses (LRFD 5.9.5)

$$f_{pj} = 202.5 \text{ ksi}$$

$$\Delta f_{pR1} = -2.2 \text{ ksi}$$

$$\Delta f_{pES} = -17.7 \text{ ksi}$$

$$\Delta f_{pi} = -20 \text{ ksi}$$

$$f_{pi} = 183 \text{ ksi}$$

$$\Delta f_{pCR} = -20.7 \text{ ksi}$$

$$\Delta f_{pSR} = -5.8 \text{ ksi}$$

$$\Delta f_{pR2} = -2.3 \text{ ksi}$$

$$\Delta f_{pTot} = -49 \text{ ksi}$$

$$f_{pe} = 154 \text{ ksi}$$

percentages

$$\frac{\Delta f_{pi}}{f_{pj}} = -9.843 \%$$

$$\frac{f_{pi}}{f_{pj}} = 90.157 \%$$

$$\frac{\Delta f_{pTot}}{f_{pj}} = -24.033 \%$$

$$\frac{f_{pe}}{f_{pj}} = 75.967 \%$$

Stress Limitations for P/S tendons (LRFD 5.9.3)

$$\text{Check}_{f_{pt}} = \text{"OK"}$$

$$0.8 f_{py} = 194 \text{ ksi}$$

$$\text{Check}_{f_{pe}} = \text{"OK"}$$

Stress Limitations for Concrete - Release and Final (LRFD 5.9.4)Release



Figure B.7: Top, Bottom and Allowable Release Stresses

$$\min(\text{CR}_{f_{\text{tension.rel}}}) = 1.349$$

Check_ $f_{\text{tension.rel}}$ = "OK"

$$\min(\text{CR}_{f_{\text{comp.rel}}}) = 1.015$$

Check_ $f_{\text{comp.rel}}$ = "OK"

Final

$$\min(\text{CR}_{f_{\text{tension.stage8}}}) = 2.232$$

Check_ $f_{\text{tension.stage8}}$ = "OK"

(Service III , PS + DL +LL*0.8)

$$\min(\text{CR}_{f_{\text{comp.stage8.c1}}}) = 1.772$$

Check_ $f_{\text{comp.stage8.c1}}$ = "OK"

(Service I , PS + DL)

$$\min(\text{CR}_{f_{\text{comp.stage8.c2}}}) = 1.837$$

Check_ $f_{\text{comp.stage8.c2}}$ = "OK"

(Service I , PS + DL +LL)

$$\min(\text{CR}_{f_{\text{comp.stage8.c3}}}) = 2.002$$

Check_ $f_{\text{comp.stage8.c3}}$ = "OK"

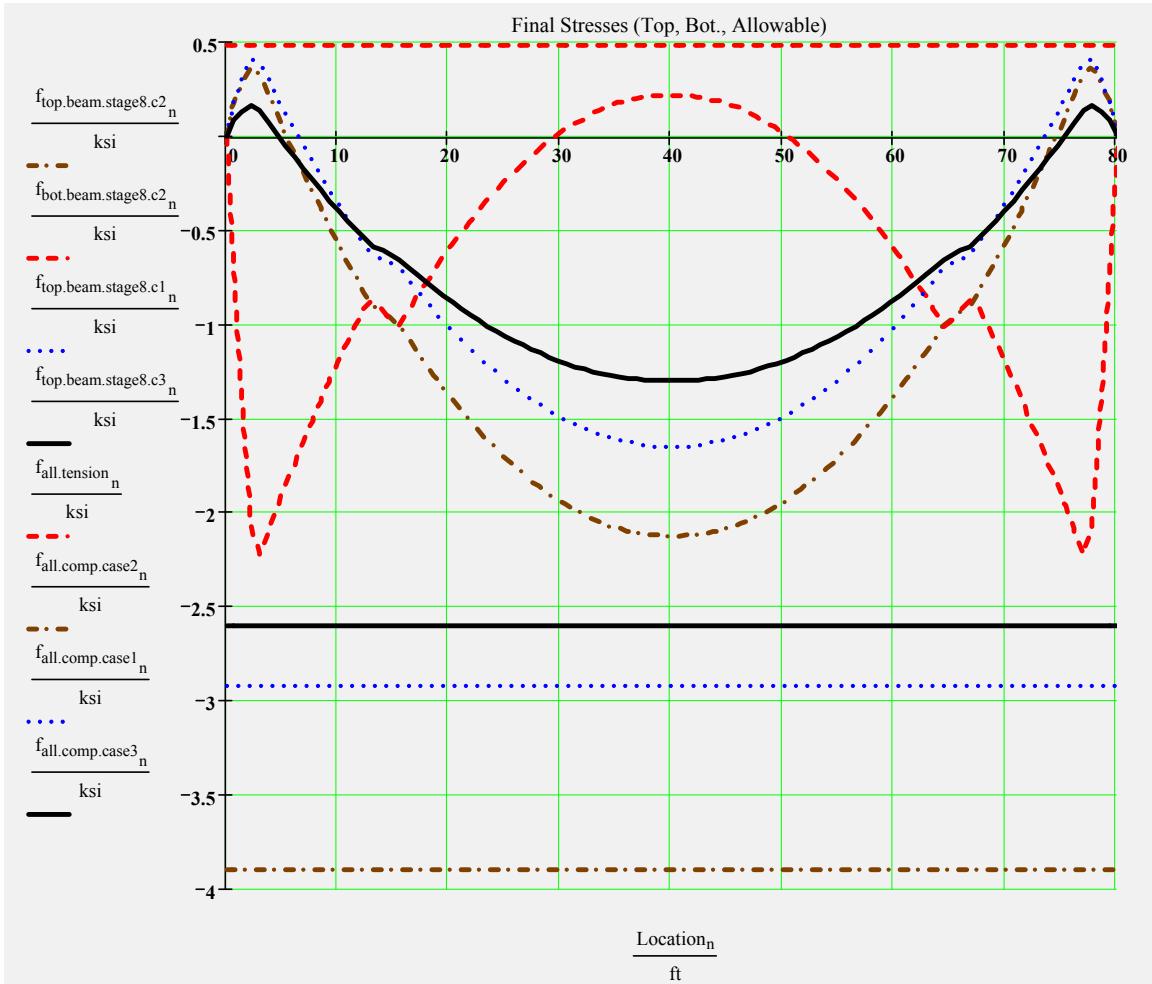


Figure B.8: Top, Bottom and Allowable Final Stresses

(Service I , (PS + DL)*0.5 +LL)
 Summary of Values at Midspan
 Compression stresses are negative
 and tensile stresses are positive

Stage	Top of Beam (ksi)	Bott of Beam (ksi)
1	-0.157	-2.614
2	-0.287	-2.131
4	-0.251	-2.159
6	-1.578	-1.134
8	-2.123	0.216

Stage 1 ---> At release with the span length equal to the length of the beam. Prestress losses are elastic shortening and overnight relax

Stage 2 ---> Same as release with the addition of the remaining prestress losses applied to the transformed beam

Stage 4 ---> Same as stage 2 with supports changed from the end of the beam to the bearing locations

Stage 6 ---> Stage 4 with the addition of non-composite dead load excluding beam weight, which has been included since Stage 1

Stage 8 ---> Stage 6 with the addition of composite dead load and live loads applied to the composite section

$$\text{PrestressForce} = \left(\begin{array}{l} \text{"Condition " } \\ \text{"Release" } \\ \text{"Final (about composite centroid)" } \end{array} \begin{array}{l} \text{"Axial (kip)" } \\ -832.9851 \\ -706.0957 \end{array} \begin{array}{l} \text{"Moment (kip*ft)" } \\ -1031.7259 \\ -1659.586 \end{array} \right)$$

$$\text{Properties} = \left(\begin{array}{l} \text{"Section " } \\ \text{"Net Beam " } \\ \text{"Transformed Beam " } \\ \text{"Composite " } \end{array} \begin{array}{l} \text{"Area (in^2)" } \\ 555.13 \\ 586.46 \\ 1129.61 \end{array} \begin{array}{l} \text{"Inertia (in^4)" } \\ 124211.81 \\ 130903.6 \\ 377370.57 \end{array} \begin{array}{l} \text{"distance to centroid from top of bm)" } \\ -24.6 \\ -25.4 \\ -11.26 \end{array} \right)$$

$$\text{ServiceMoments} = \left(\begin{array}{l} \text{"Type " } \\ \text{"Release" } \\ \text{"Non-composite (includes bm wt.)" } \\ \text{"Composite" } \\ \text{"Distributed Live Load" } \end{array} \begin{array}{l} \text{"Value (kip*ft)" } \\ 466.4 \\ 1021.1 \\ 202.1 \\ 1320.1 \end{array} \right)$$

Camber and Shrinkage and dead Load Deflections

$$\text{SlopeData} = \left(\begin{array}{l} \text{"Stage" } \\ \text{"Release" } \\ \text{"30 Days" } \\ \text{"60 Days" } \\ \text{"120 Days" } \\ \text{"240 Days" } \\ \text{"non-comp DL" } \\ \text{"comp DL" } \end{array} \begin{array}{l} \text{"Change in L @ Top (in)" } \\ 0.034 \\ -0.044 \\ -0.093 \\ -0.149 \\ -0.2 \\ -0.2 \\ -0.011 \end{array} \begin{array}{l} \text{"Change in L @ Bot. (in)" } \\ -0.694 \\ -1.303 \\ -1.549 \\ -1.845 \\ -2.165 \\ 0.155 \\ 0.033 \end{array} \begin{array}{l} \text{"Slope at End (deg)" } \\ 0.464 \\ 0.803 \\ 0.928 \\ 1.081 \\ 1.253 \\ -0.226 \\ -0.028 \end{array} \begin{array}{l} \text{"midspan defl (in)" } \\ 1.892 \\ 3.274 \\ 3.784 \\ 4.409 \\ 5.109 \\ -1.162 \\ -0.143 \end{array} \right)$$

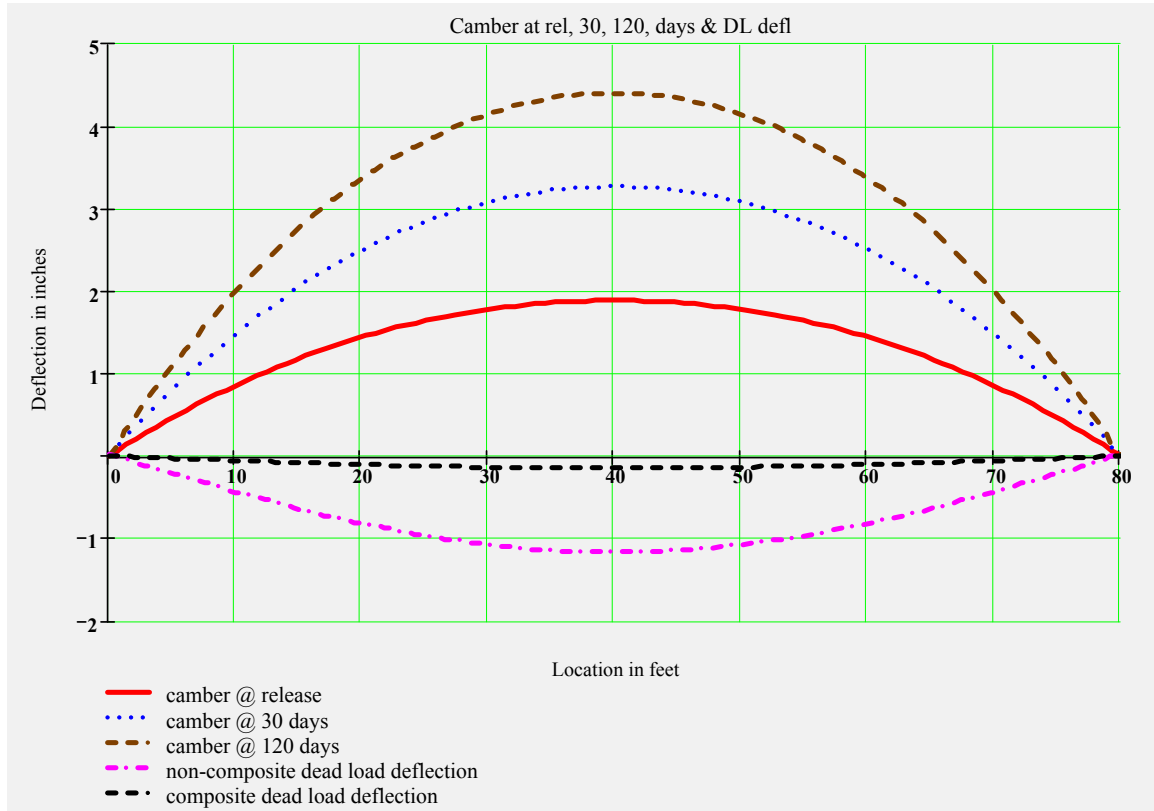


Figure B.9: Camber and Dead Load Deflection

STRENGTH LIMIT STATE

☞ Reference:C:\FDOT_STR\Programs\LRFDPbeamE1.85\ProgramFiles\section3.mcd(R

Moment Nominal Resistance versus Ultimate Strength Cases I and II

$\max(M_{pos.Str1}) = 3859 \text{ kip}\cdot\text{ft}$ $\min(CR_{Str1.mom}) = 1.17$ CheckMomentCapacity = "OK"

Strength Shear and Associated Moment

$\max(V_{u.Str}) = 188 \text{ kip}$ $\max(M_{shr_{u.Str}}) = 3514 \text{ kip}\cdot\text{ft}$

Check and Design Shear, Interface and Anchorage Reinforcement

The interface_factor accounts for situations where not all of the shear reinforcing is embedded in the poured in place slab

Locally assigned stirrup sizes and spacings (Values less than 0 are ignored)

To change the values from the input file enter the new values into the vectors below.

Input only those that you wish to change, values that are less than one will not alter the original input values.

user_A stirrup nspacings :=

XX·in ²
XX·in ²
XX·in ²
XX·in ²
XX·in ²

user_s nspacings := user_NumberSpaces nspacings := interface_factor nspacings :=

XX·in	XX	0.5
XX·in	XX	1
XX·in	XX	1
XX·in	XX	1
XX·in	XX	1

- A stirrup
- S1 stirrup
- S2 stirrup
- S3 stirrup
- S4 stirrup

☞ Reference: C:\FDOT_STR\Programs\LRFPbeamE1.85\ProgramFiles\section4.mcd(R
 Stirrup sizes and spacings used in analysis

- A stirrup
- S1 stirrup
- S2 stirrup
- S3 stirrup
- S4 stirrup

$$s = \begin{pmatrix} 3 \\ 9 \\ 9 \\ 9 \\ 10 \end{pmatrix} \text{ in}$$

$$\text{NumberSpaces} = \begin{pmatrix} 5 \\ 10 \\ 10 \\ 14 \\ 15.7 \end{pmatrix}$$

$$A_{\text{stirrup}} = \begin{pmatrix} 0.62 \\ 0.31 \\ 0.31 \\ 0.31 \\ 0.31 \end{pmatrix} \text{ in}^2$$

EndCover = 2 in

The number of spaces for the S4 stirrup is calculated by the program to complete the half beam length

$\min(\text{CRShearCapacity}) = 1.475$ CheckShearCapacity = "OK"

$\min(\text{CRStirArea}) = 1.761$ CheckStirArea = "OK"

$\min(\text{CRStirrupArea}) = 3.294$ CheckMinStirArea = "OK"

CheckMaxStirSpacing = "OK" CheckAnchorageSteel = "OK"

Check Longitudinal Steel

$$\min(\text{CR}_{\text{LongSteel}}) = 1.298$$

CheckLongSteel = "OK"

If NG can also adjust with

shear reinforcing

Check Interface Steel

Typically shear steel is extended up into the deck slab. These calculations are based on that assumption that the shear steel functions as interface reinforcing. The `interface_factor` can be used to adjust this assumption

MinInterfaceReinfReqd = "Yes"

If $A_{vf.design}$ or $A_{vf.min}$ is greater than $0 \text{ in}^2/\text{ft}$, interface steel is required.

$$A_{vf.min} = 0.16 \frac{\text{in}^2}{\text{ft}}$$

$$\max(A_{vf.des}) = 0.7 \frac{\text{in}^2}{\text{ft}}$$

MinLegsPerRow = 0

CheckInterfaceSpacing = "OK"

$$\text{CheckInterfaceSteel} := \text{if} \left(\frac{\text{TotalInterfaceSteelProvided}}{\text{TotalInterfaceSteelRequired} + 0.001 \cdot \text{in}^2} \geq 1, \text{"OK"}, \text{"No Good"} \right)$$

CheckInterfaceSteel = "OK"

Check Anchorage Steel for Bursting and Calculate Confinement Steel

CheckAnchorageSteel = "OK" use #3 bars @ 6 in for confinement

TotalNoConfineBars = 24 value includes bars at both ends

Summary of Design Checks

AcceptInteriorM = "OK" AcceptExteriorM = "OK" AcceptInteriorV = "OK" Check_f_{pt} = "OK"

Check_f_{pe} = "OK" Check_f_{tension.rel} = "OK" Check_f_{comp.rel} = "OK"

Check_f_{tension.stage8} = "OK"

Check_f_{comp.stage8.c1} = "OK" Check_f_{comp.stage8.c2} = "OK" Check_f_{comp.stage8.c3} = "OK"

CheckMomentCapacity = "OK" CheckMaxCapacity = "OK" CheckStirArea = "OK"

CheckShearCapacity = "OK" CheckMinStirArea = "OK" CheckMaxStirSpacing = "OK"

CheckLongSteel = "OK" CheckInterfaceSpacing = "OK" CheckAnchorageSteel = "OK"

CheckMaxReinforcement = "OK" WRITEPRN(filename) := data_{mod} CheckInterfaceSteel = "OK"

CheckStrandFit = "OK" TotalCheck = "OK" WRITEPRN("psbeam.inp") := data_{mod}

APPENDIX C. PIER CAP AND COLUMN DESIGN

PROJECT DATA

=====

Project : Model Bridge Type III AASHTO girder Bridge
 User Job No.:
 State : FL
 Comments : Pier Cap, Column Design and Footing (Not required) Design

PIER GEOMETRY

=====

Pier Type: Multi Column

Cap Shape: Tapered Top Elevations: start = 100.00 ft end = 100.00 ft
 Depth(Z) = 48.00 in Skew angle = 0.00 Reduction of I = 1.000
 Length(X) = 41.00 ft Non tapered length = 29.00 ft
 Height max(Y) = 48.00 in Height min(Y) = 24.00 in

Column Shape : Round
 Number of columns: 2

Column number 1:

Location from the left edge of the cap(X): 9.00 ft
 Elevations: bottom = 80.00 ft top = 99.00 ft Reduction of I = 1.000
 Column section dimensions:
 Diameter = 42.00 in

Column number 2:

Location from the left edge of the cap(X): 32.00 ft
 Elevations: bottom = 80.00 ft top = 99.00 ft Reduction of I = 1.000
 Column section dimensions:
 Diameter = 42.00 in

STRUCTURE MODEL

=====

FRAME Model:

	Member	Node	Hinge	Check Pt	Dist(ft)	Memb length(ft)
Column No. 1	1	1	-		0.00	
		2	-		19.00	19.00
Column No. 2	2	3	-		0.00	
		4	-		19.00	19.00
Cap	3	5	-		0.00	
	4	6	-		2.50	2.50
		6	-		2.50	
		7	-		6.00	3.50
	5	7	-		6.00	
		8	-		8.50	2.50
	6	8	-		8.50	
		2	-		9.00	0.50
	7	2	-		9.00	
		9	-		14.50	5.50
	8	9	-		14.50	
		10	-		20.50	6.00
	9	10	-		20.50	
		11	-		26.50	6.00
	10	11	-		26.50	
		4	-		32.00	5.50
	11	4	-		32.00	
		12	-		32.50	0.50
	12	12	-		32.50	
		13	-		35.00	2.50
	13	13	-		35.00	
		14	-		38.50	3.50

14	14	-	38.50	
15	15	-	41.00	2.50

Node coordinates:

Number	X(ft)	Y(ft)	Node type
1	9.00	80.00	fixed at ground
2	9.00	99.00	column-cap
3	32.00	80.00	fixed at ground
4	32.00	99.00	column-cap
5	0.00	99.00	
6	2.50	99.00	bearing
7	6.00	99.00	
8	8.50	99.00	bearing
9	14.50	99.00	bearing
10	20.50	99.00	bearing
11	26.50	99.00	bearing
12	32.50	99.00	bearing
13	35.00	99.00	
14	38.50	99.00	bearing
15	41.00	99.00	

SUPERSTRUCTURE INFO

=====

Total number of spans: 2 Span number rear to current pier: 1
 Number of traffic lanes: 3

Beam: height = 45.00 in section area = 560.00 in²
 Barrier height = 32.00 in Depth of slab = 8.00 in

Span	Forward	Rear
Overall width	43.00 ft	43.00 ft
Curbs width	40.00 ft	40.00 ft
Span Length	80.00 ft	80.00 ft

BEARING POINTS

=====

Number of bearing lines: 2

First bearing line Eccentricity = 1.00 ft

Point	Distance ft
1	2.50
2	8.50
3	14.50
4	20.50
5	26.50
6	32.50
7	38.50

Second bearing line Eccentricity = -1.00 ft

Point	Distance ft
1	2.50
2	8.50
3	14.50
4	20.50
5	26.50
6	32.50
7	38.50

MATERIAL PROPERTIES

=====

	Cap	Column	Footing
Concrete Type	normal	normal	normal
Concrete Strength (psi)	5500.00	5500.00	5500.00
Concrete Density (lb/ft ³)	150.00	150.00	150.00
Concrete Modulus Ec (ksi)	4496.10	4496.10	4496.10
Steel Strength Fy (ksi)	60.00	60.00	60.00

DESIGN PARAMETERS
=====

AASHTO LRFD Code
Resistance factors for reinf. concrete: Multi presence factors for live
load:

Flexure and tension	0.90	1 Lane	1.20
Shear and torsion (normal)	0.90	2 Lanes	1.00
(lightweight)	0.70	3 Lanes	0.85
Axial compression (ties)	0.75	more than 3 Lanes	0.65
Axial compression (spiral)	0.75		
Compression in STM	0.70		

Eta factor:

	Service	Fatigue	Strength	Extreme event
Cap	1.00	1.00	1.00	1.00
Column	1.00	1.00	1.00	1.00
Footing	1.00	1.00	1.00	1.00

Dynamic load allowance IM:

	Truck	Lane	Fatigue
Cap	0.33	0.00	0.15
Column	0.33	0.00	0.15
Footing	0.00	0.00	0.00

	Crack control factor kip/ft	Min clear cover in
Cap	170.00	3.00
Column	170.00	3.00
Footing	130.00	4.00

Degree of fixity in foundations for Moment Magnify Method: R = 5.00

LOADS
=====

Load Cases: 34

Loadcase ID: DC1 Name:
Multiplier = 1.000

Auto generation details:

Generated Dead Load
Slab weight = 150.00 pcf Girder weight = 150.00 pcf
Wearing weight = Not included Barrier load = 2378.00 plf

Loadcase ID: DW1 Name:
Multiplier = 1.000

Auto generation details:

Generated Dead Load
Slab weight = Not included Girder weight = Not included
Wearing weight = 600.00 plf Barrier load = Not included

Loadcase ID: BR1 Name:
Multiplier = 1.000

Loadcase ID: CT1 Name:
Multiplier = 1.000

Column loads:

Col #	Type	Dir	Mag1	y1/L	Mag2	y2/L
1	Force	X	400.000	kip 0.23	----	----

Auto generation details:

Generated Live Load
 Library load: Design Truck + Lane Load
 Number of loaded lanes = all combinations
 Total number of considered truck positions = 6548

Selected load Cases:

STRENGTH GROUP I
 SERVICE GROUP I
 EXTREME EVENT GROUP II
 FATIGUE

CAP DESIGN

=====

Code: AASHTO LRFD
 Units: US

DESIGN PARAMETERS:

=====

f'c = 5500.0 psi fy = 60000.0 psi
 phi flex = 0.90 phi shear = 0.90
 Ec = 4496.1 ksi Es = 29000.0 ksi
 crack control factor z = 170.00 kips / in
 Concrete Type : Normal Weight.

CAP GEOMETRY:

=====

Tapered Cap : Length(X) = 41.00 ft Depth(Z) = 48.00 in

REINFORCEMENT:

=====

	Bar size	Quantity	Bar dist. in	As total in^2	From ft	To ft	Hook
TOP	# 10	7	4.26	8.890	0.00	41.00	None
	# 10	6	8.26	7.620	0.00	41.00	None
BOTTOM	# 10	4	8.26	5.080	0.00	41.00	None
	# 10	6	4.26	7.620	0.00	41.00	None

Stirrups size: # 5

FLEXURE DESIGN:

=====

Span 1: From 0.00 ft To 9.00 ft											
Loc eff	AbsLoc	H	Mmax	Mr	Comb	Asb-req	Asb-prv	Asb-eff	Ast-req	Ast-prv	Ast- eff
ft	ft	in	kips-ft	kips-ft		in^2	in^2	in^2	in^2	in^2	in^2
0.0	0.0	24	0.0	0.0	0	1.06	12.70*	0.00*	1.06	16.51*	
0.00*			0.0	0.0	0	1.06	12.70*	0.00*	1.06	16.51*	
0.00*											
2.5	2.5	34	0.0	1206.8	121	1.50	12.70	9.38	1.50	16.51	
16.51			-5.7	-1113.6	1	1.50	12.70	12.70	1.50	16.51	
8.71											
6.0	6.0	48	0.0	2346.6	124	2.11	12.70	12.70	2.11	16.51	
16.51			-559.5	-2952.9	11	2.11	12.70	12.70	4.00	16.51	
16.51											
8.5	8.5	48	0.0	2346.6	124	2.11	12.70	12.70	2.11	16.51	
16.51			-975.7	-2952.9	11	2.11	12.70	12.70	5.54	16.51	
16.51											
9.0	9.0	48	0.0	2346.6	124	2.11	12.70	12.70	2.11	16.51	
16.51											

16.51 -1130.5 -2952.9 11 2.11 12.70 12.70 6.12 16.51

Span 2: From 9.00 ft To 32.00 ft

Loc eff	AbsLoc	H	Mmax	Mr	Comb	Asb-req	Asb-prv	Asb-eff	Ast-req	Ast-prv	Ast- eff
ft	ft	in	kips-ft	kips-ft		in ²	in ²	in ²	in ²	in ²	in ²
0.0	9.0	48	108.1	2346.6	124	2.11	12.70	12.70	2.11	16.51	
16.51			-1036.4	-2952.9	16	2.11	12.70	12.70	5.60	16.51	
16.51	5.5	48	715.0	2346.6	17	5.10	12.70	12.70	2.11	16.51	
16.51			-495.0	-2952.9	131	2.11	12.70	12.70	3.53	16.51	
16.51	11.5	48	1229.9	2346.6	7	6.63	12.70	12.70	2.11	16.51	
16.51			-398.7	-2952.9	123	2.11	12.70	12.70	2.84	16.51	
16.51	17.5	48	715.0	2346.6	26	5.10	12.70	12.70	2.11	16.51	
16.51			-495.0	-2952.9	124	2.11	12.70	12.70	3.53	16.51	
16.51	23.0	48	108.1	2346.6	131	2.11	12.70	12.70	2.11	16.51	
16.51			-1036.4	-2952.9	28	2.11	12.70	12.70	5.60	16.51	
16.51											

Span 3: From 32.00 ft To 41.00 ft

Loc eff	AbsLoc	H	Mmax	Mr	Comb	Asb-req	Asb-prv	Asb-eff	Ast-req	Ast-prv	Ast- eff
ft	ft	in	kips-ft	kips-ft		in ²	in ²	in ²	in ²	in ²	in ²
0.0	32.0	48	0.0	2346.6	121	2.11	12.70	12.70	2.11	16.51	
16.51			-1130.5	-2952.9	4	2.11	12.70	12.70	6.12	16.51	
16.51	0.5	48	0.0	2346.6	121	2.11	12.70	12.70	2.11	16.51	
16.51			-975.7	-2952.9	4	2.11	12.70	12.70	5.54	16.51	
16.51	3.0	48	0.0	2346.6	121	2.11	12.70	12.70	2.11	16.51	
16.51			-559.5	-2952.9	4	2.11	12.70	12.70	4.00	16.51	
16.51	6.5	34	0.0	1206.8	121	1.50	12.70	9.38	1.50	16.51	
16.51			-5.7	-1113.6	1	1.50	12.70	12.70	1.50	16.51	
8.71	9.0	24	0.0	0.0	0	1.06	12.70*	0.00*	1.06	16.51*	
0.00*			0.0	0.0	0	1.06	12.70*	0.00*	1.06	16.51*	
0.00*											

Note:

* The provided reinforcement is not adequate, either less than required or larger than maximum allowed.

** The section can not be designed. Required spacing of bars violated.

SHEAR DESIGN:

=====

Simplified Method used for design.

Span 1: From 0.00 ft To 9.00 ft

Loc Smax ft in	AbsLoc ft	Pos	Vu kips	Comb	Tu kips-ft	Comb	phi*Vc kips	T-lim kips-ft	Avs/s <----	2Ats/s in^2/ft	Av/s -->	Alx in^2

0.00	0.00	R	0.0	1	0.0	1	114.7	50.7	0.00	0.00	0.00	0.00
14.3												
2.50	2.50	L	4.5	1	0.0	1	171.3	89.3	0.00	0.00	0.00	0.00
21.4												
		R	153.8	11	117.5	14	171.3	89.3	0.35	0.37	0.71	0.00
21.4												
6.00	6.00	L	162.7	11	117.5	13	254.3	152.0	0.71	0.00	0.71	0.00
24.0												
		R	162.7	11	117.5	14	254.3	152.0	0.71	0.00	0.71	0.00
24.0												
8.50	8.50	L	170.2	11	117.5	13	254.3	152.0	0.71	0.00	0.71	0.00
24.0												
		R	308.7	11	229.6	14	254.3	152.0	0.30	0.46	0.77	0.00
24.0												
9.00	9.00	L	310.2	11	229.6	13	254.3	152.0	0.31	0.46	0.78	0.00
24.0												

Span 2: From 9.00 ft To 32.00 ft

Loc Smax ft in	AbsLoc ft	Pos	Vu kips	Comb	Tu kips-ft	Comb	phi*Vc kips	T-lim kips-ft	Avs/s <----	2Ats/s in^2/ft	Av/s -->	Alx in^2

0.00	9.00	R	246.1	15	198.0	9	254.3	152.0	0.31	0.40	0.71	0.00
24.0												
5.50	14.50	L	229.6	15	198.0	12	254.3	152.0	0.31	0.40	0.71	0.00
24.0												
		R	137.9	18	160.8	21	254.3	152.0	0.39	0.32	0.71	0.00
24.0												
11.50	20.50	L	119.9	18	160.8	19	254.3	152.0	0.39	0.32	0.71	0.00
24.0												
		R	119.9	24	160.8	25	254.3	152.0	0.39	0.32	0.71	0.00
24.0												
17.50	26.50	L	137.9	24	160.8	23	254.3	152.0	0.39	0.32	0.71	0.00
24.0												
		R	229.6	27	198.0	5	254.3	152.0	0.31	0.40	0.71	0.00
24.0												
23.00	32.00	L	246.1	27	198.0	2	254.3	152.0	0.31	0.40	0.71	0.00
24.0												

Span 3: From 32.00 ft To 41.00 ft

Loc Smax ft in	AbsLoc ft	Pos	Vu kips	Comb	Tu kips-ft	Comb	phi*Vc kips	T-lim kips-ft	Avs/s <----	2Ats/s in^2/ft	Av/s -->	Alx in^2

0.00	32.00	R	310.2	4	229.6	30	254.3	152.0	0.31	0.46	0.78	0.00
24.0												
0.50	32.50	L	308.7	4	229.6	29	254.3	152.0	0.30	0.46	0.77	0.00
24.0												
		R	170.2	4	117.5	30	254.3	152.0	0.71	0.00	0.71	0.00
24.0												
3.00	35.00	L	162.7	4	117.5	29	254.3	152.0	0.71	0.00	0.71	0.00
24.0												
		R	162.7	4	117.5	30	254.3	152.0	0.71	0.00	0.71	0.00
24.0												
6.50	38.50	L	153.8	4	117.5	29	171.3	89.3	0.35	0.37	0.71	0.00
21.4												
		R	4.5	1	0.0	1	171.3	89.3	0.00	0.00	0.00	0.00
21.4												
9.00	41.00	L	0.0	1	0.0	1	114.7	50.7	0.00	0.00	0.00	0.00
14.3												

Note:

* Required shear resistance provided by shear reinforcement is greater than maximum allowed.

- Pos is the design position. L suggests the calculation is done at immediate left

- of "Loc" and R suggests at immediate right of it.
- T-lim is the limiting value of torsion for the concrete section. If actual torsion is higher than this value, torsional steel has to be provided.
 - Avs/s is the required area of steel per unit length for shear force.
 - 2Ats/s is the required area of steel per unit length for two legs of torsional reinforcement.
 - Av/s is the total required area of steel per unit length due to shear plus torsion.
 - Alx is the EFFECTIVE longitudinal steel required in addition to the PROVIDED EFFECTIVE flexural steel.

CRACKING/FATIGUE CHECK:
=====

Span 1: From 0.00 ft To 9.00 ft

Loc ft	AbsLoc ft	H in	Cracking				Fatigue			
			fs-t fs-b ksi	ratio ratio	fs-t fs-b	Comb Comb	fs-t fs-b ksi	ratio ratio	fs-t fs-b	Comb Comb
0.00	0.0	24.0	0.0	0.00	0	0.0	0.00	0		
2.50	2.5	34.0	0.0	0.00	0	0.0	0.00	0		
6.00	6.0	48.0	0.2	0.01	241	0.0	0.00	0		
8.50	8.5	48.0	0.0	0.00	0	0.0	0.00	0		
9.00	9.0	48.0	6.3	0.17	251	4.2	0.18	551		
			0.0	0.00	0	0.0	0.00	0		
			11.0	0.31	251	7.2	0.31	551		
			0.0	0.00	0	0.0	0.00	0		
			12.8	0.36	251	8.3	0.36	551		
			0.0	0.00	0	0.0	0.00	0		

Span 2: From 9.00 ft To 32.00 ft

Loc ft	AbsLoc ft	H in	Cracking				Fatigue			
			fs-t fs-b ksi	ratio ratio	fs-t fs-b	Comb Comb	fs-t fs-b ksi	ratio ratio	fs-t fs-b	Comb Comb
0.00	9.0	48.0	11.8	0.33	256	7.8	0.34	556		
			0.5	0.01	244	4.1	0.18	544		
5.50	14.5	48.0	5.2	0.14	251	5.5	0.24	551		
			10.3	0.29	257	8.2	0.36	546		
11.50	20.5	48.0	3.7	0.10	243	5.9	0.26	543		
			17.8	0.50	247	12.8	0.57	547		
17.50	26.5	48.0	5.2	0.14	244	5.5	0.24	544		
			10.3	0.29	266	8.2	0.36	550		
23.00	32.0	48.0	11.8	0.33	268	7.8	0.34	568		
			0.5	0.01	251	4.1	0.18	551		

Span 3: From 32.00 ft To 41.00 ft

Loc ft	AbsLoc ft	H in	Cracking				Fatigue			
			fs-t fs-b ksi	ratio ratio	fs-t fs-b	Comb Comb	fs-t fs-b ksi	ratio ratio	fs-t fs-b	Comb Comb
0.00	32.0	48.0	12.8	0.36	244	8.3	0.36	544		
			0.0	0.00	0	0.0	0.00	0		
0.50	32.5	48.0	11.0	0.31	244	7.2	0.31	544		
			0.0	0.00	0	0.0	0.00	0		
3.00	35.0	48.0	6.3	0.17	244	4.2	0.18	544		
			0.0	0.00	0	0.0	0.00	0		
6.50	38.5	34.0	0.2	0.01	241	0.0	0.00	0		
			0.0	0.00	0	0.0	0.00	0		
9.00	41.0	24.0	0.0	0.00	0	0.0	0.00	0		
			0.0	0.00	0	0.0	0.00	0		

Note:
* Cracking / fatigue checking failed.

COLUMN DESIGN - Column: 1

Column Type: Round D = 42.00 in

Code: AASHTO LRFD
 Units: US
 Design/Analysis Method: No Slenderness Considered.

Design Parameters:

```

=====
f'c = 5500.0 psi      fy = 60000.0 psi
phi flex = 0.90      phi axial = 0.75
Ec = 4496.1 ksi      Es = 29000 ksi
Concrete Type : Normal Weight.
    
```

Reinforcement:

=====

Reinforcement Pattern:

Layer	Dir	Size	No. bars	Bar Dist. in
1	X	10	20	4.14

Main bars summary: Ties size: # 4
 20 # 10 bars

Total number of bars in the column: 20

Design values used - (e-min effect included).

```

=====
(global coordinates)
Loc      Comb      Fx      Fy      Fz      Mx      My      Mz
ft              kips    kips    kips    kips-ft kips-ft kips-ft
-----
80.00    10        35.7    307.6    -0.0    -47.7    0.2    -223.7
99.00    10       -35.7    278.8     0.0     43.2    0.2    -455.0
80.00    424     -383.0    42.2    -0.0     -6.5    0.5    1374.6
99.00    424     -17.0    21.4     0.0     3.3    0.5     50.2
    
```

Column Design

=====

Loc ft	Comb	Pu kips	Mux kips-ft	Muz kips-ft	pMn kips-ft	C in	Incl deg	pPn/Pu	pMn/Mu
80.00	424	42.2	6.5	1374.6	1776.7	10.11	89.7	1.00	1.29
99.00	10	278.8	43.2	455.0	1883.5	11.55	84.6	1.00	4.12

Note:

- * The provided reinforcement is not adequate.
- ** Minimum/Maximum requirement for reinforcement ratio or bar spacing violated.

COLUMN DESIGN - Column: 2

Column Type: Round D = 42.00 in

Code: AASHTO LRFD
 Units: US
 Design/Analysis Method: No Slenderness Considered.

Design Parameters:

```

=====
f'c = 5500.0 psi      fy = 60000.0 psi
phi flex = 0.90      phi axial = 0.75
Ec = 4496.1 ksi      Es = 29000 ksi
Concrete Type : Normal Weight.
    
```

Reinforcement:

=====

Reinforcement Pattern:

Layer	Dir	Size	No. bars	Bar Dist. in
1	X	10	20	4.14

Main bars summary: Ties size: # 4
 20 # 10 bars

Total number of bars in the column: 20

Design values used - (e-min effect included).

=====

(global coordinates)

Loc ft	Comb	Fx kips	Fy kips	Fz kips	Mx kips-ft	My kips-ft	Mz kips-ft
80.00	6	-35.7	307.6	-0.0	-47.7	-0.2	223.7
99.00	6	35.7	278.8	0.0	43.2	-0.2	455.0
80.00	307	-32.5	163.3	0.0	-25.3	0.0	296.8
99.00	307	32.5	134.5	0.0	20.8	0.0	320.1

Column Design

=====

Loc ft	Comb	Pu kips	Mux kips-ft	Muz kips-ft	pMn kips-ft	C in	Incl deg	pPn/Pu	pMn/Mu
80.00	307	163.3	25.3	296.8	1827.4	10.81	85.1	1.00	6.13
99.00	6	278.8	43.2	455.0	1883.5	11.55	84.6	1.00	4.12

Note:

- * The provided reinforcement is not adequate.
- ** Minimum/Maximum requirement for reinforcement ratio or bar spacing violated.

APPENDIX D. MEMBER CAPACITY CALCULATIONS

D.1 Prestressed Girder Capacity

Type III AASHTO girder Moment Capacity:

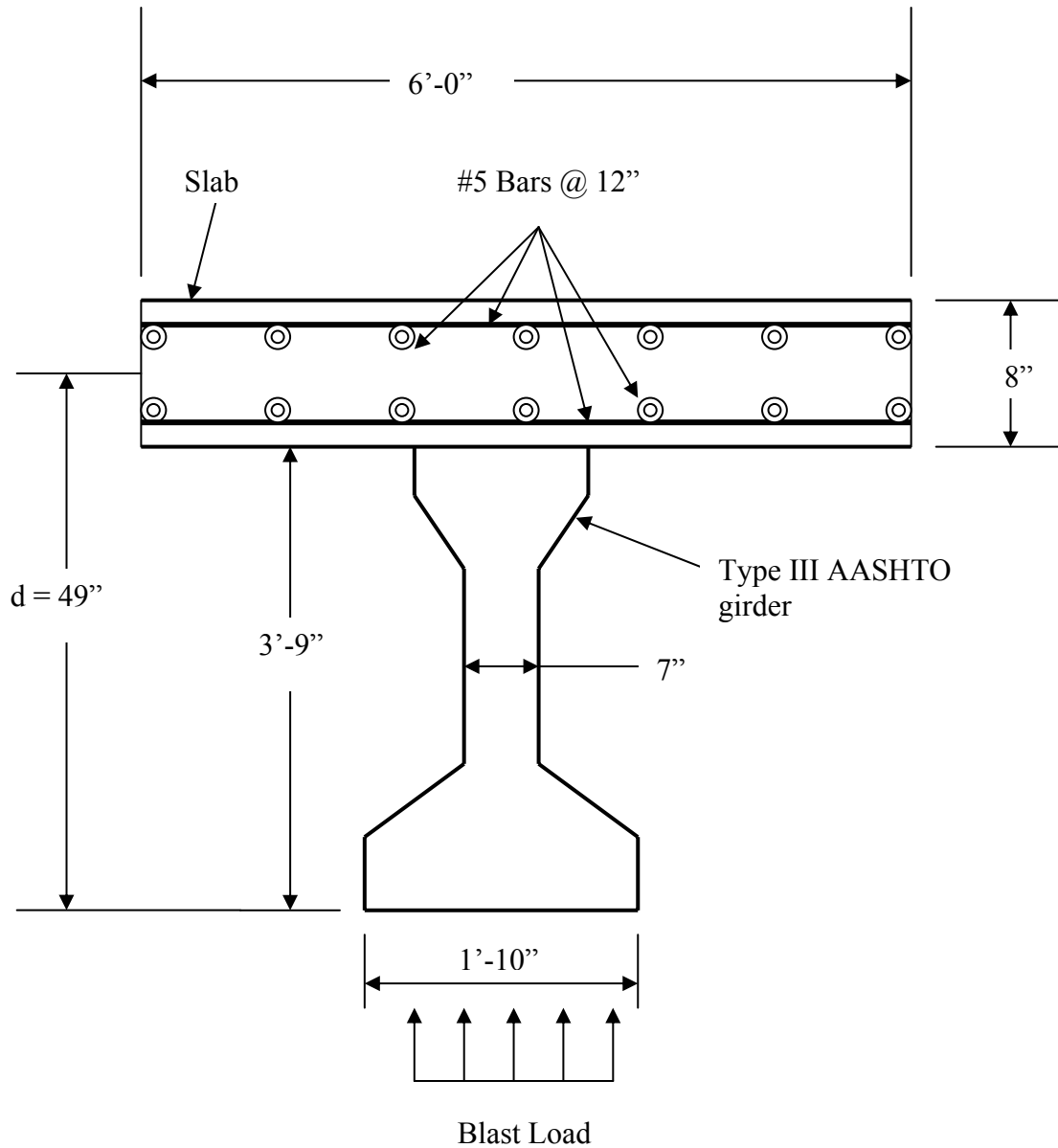


Figure D.1: Blast Load for Negative Moment Capacity

$$\text{kip} \equiv 1000 \cdot \text{lb}$$

$$\text{ksi} \equiv \frac{\text{kip}}{\text{in}^2}$$

Positive Moment Capacity:

From Appendix B: Prestressed Girder Design,
Girder moment capacity, $\phi \cdot M_n = 4500 \cdot \text{kip} \cdot \text{ft}$

Negative Moment Capacity:

$$\phi := 0.9$$

$$f_c := 6.5 \cdot \text{ksi}$$

$$f_y := 60 \cdot \text{ksi}$$

$$b := 22 \cdot \text{in}$$

$$d := 49 \cdot \text{in}$$

$$A_s := 12 \cdot (0.31) \cdot \text{in}^2$$

$$A_s = 3.72 \text{ in}^2$$

Depth of compression block

$$a := \frac{A_s \cdot f_y}{0.85 \cdot f_c \cdot b}$$

$$a = 1.836 \text{ in}$$

$$\phi M_n := \phi \cdot A_s \cdot f_y \cdot \left(d - \frac{a}{2} \right)$$

$$\phi M_n = 805 \text{ kip} \cdot \text{ft}$$

Negative moment capacity of Type III AASHTO girder, $\phi M_n = 805 \text{ kip} \cdot \text{ft}$

D.2 Pier Cap Capacity

Moment Capacity:

From RC-Pier program output in Appendix C: Pier Cap and Column Design,

Positive or negative moment capacity (as top and bottom reinforcements are the same) of pier cap,

$$\phi M_n = 2,953 \text{ kip-ft (Section – Flexure Design)}$$

Shear Capacity:

From RC-Pier program output in Appendix C: Pier Cap and Column Design,

Shear force taken by concrete, $\phi V_c = 254 \text{ kip}$

Shear force taken by steel, $V_s = A_s * f_y * d / S$

Here, $A_s = 2 * 2 * 0.31 = 1.24 \text{ in.}^2$, $f_y = 60 \text{ ksi}$, $d = 41.74 \text{ in.}$, $S = 6 \text{ in.}$

$$\phi V_n = \phi V_c + V_s = 254 + (1.24 * 60 * 41.74 / 6) = 772 \text{ kip.}$$

D.3 Column Capacity

Interaction Diagram of Concrete Column:

Data

constants

$\text{kip} \equiv 1000 \cdot \text{lbf}$ $\text{ksi} \equiv 1000 \cdot \text{psi}$ $\text{data} := \text{READPRN}(\text{"values.out"})$

$\text{StressStrain} := \text{READPRN}(\text{"strline.out"})$

$\phi_{\text{axial}} := \text{data}_5$ $\phi_{\text{flexure}} := \text{data}_4$ $\phi_{\text{axial}} = 0.7$ $\phi_{\text{flexure}} = 0.9$

materials

$f'_c := \text{data}_0 \cdot \text{ksi}$ $E_s := \text{data}_1 \cdot \text{ksi}$ $F_y := \text{data}_2 \cdot \text{ksi}$ $E_p := \text{data}_6 \cdot \text{ksi}$ $f_{pe} := \text{data}_7 \cdot \text{ksi}$

$f'_c = 5.5 \text{ ksi}$ $E_s = 2.9 \times 10^4 \text{ ksi}$ $F_y = 60 \text{ ksi}$ $E_p = 0 \text{ ksi}$ $f_{pe} = 0 \text{ ksi}$

$\text{PhiType} := \text{data}_8$ $\text{TieType} := \text{data}_9$ $\text{PhiType} = 0$ $\text{TieType} = 0$

0 indicates std AASHTO 1 indicates ACI App B

0 indicates std 1 indicates spiral

analysis locations

$\text{divs} := \text{data}_3$ (min value is 3) $\text{divs} = 8$ $\text{vdiv} := 10$ $\text{contour} = \blacksquare$

shape contour rebar locations

$\text{contour} := \text{READPRN}(\text{"contour.out"})$ $\text{rebar} := \text{READPRN}(\text{"rebar.out"})$ $\text{bar}_{\text{area}} := \text{rebar}_{0,2}$

$\text{bar}_{\text{area}} = 1.27 \text{ (in}^2\text{)}$

loads

$\text{bar}_{\text{type}} := \text{rebar}_{0,3}$ $\text{bar}_{\text{type}} = 0$

0 mild steel 1 lo lax 2 stress rel 3 A722 bar 4 user def

$\text{loads} := \text{READPRN}(\text{"loads.out"})$ $\text{user}_{\text{axial}} := (\text{loads}^{(0)})$ $\text{user}_{\text{mom.y}} := (\text{loads}^{(1)})$

$\text{user}_{\text{mom.x}} := (\text{loads}^{(2)})$

file name

$\text{filename} := \text{vec2str}(\text{READPRN}(\text{"filename.out"}))$ $\text{ext} := \text{"cld"}$ $\text{filename} := \text{concat}(\text{filename}, \text{ext})$

```

tmparray:=
| for i ∈ 0.. vdiv
|   for j ∈ 0.. 4
|     tmp1,j ← 0
|   tmp

```

$\text{strength}_{(\text{divs}-1)} := \text{tmparray}$ $\text{ia} := 0.. (\text{divs} - 1)$ $\text{th}_{\text{ia}} := \text{ia} \cdot \left(\frac{2}{\text{divs}} \cdot \pi \right)$

$\text{strength}_{\text{ia}} := \text{fInteractioninc} \left(\text{contour}, \text{rebar}, \frac{F_y}{\text{ksi}}, \frac{f'_c}{\text{ksi}}, \text{th}_{\text{ia}}, \text{vdiv} \right)$

```

strength := cnt ← 0
           i ← 0
           while i ≤ last(strength)
             if strengthi ≠ 0
               anscnt ← strengthi
               cnt ← cnt + 1
             i ← i + 1
           ans
intershape := sum ← strength0
            for k ∈ 1..(last(strength))
              sum ← stack(sum, strengthk)
            sum

ia := 0..(rows(strength) - 1)   xi := intershape<0>   yi := intershape<1>   zi := intershape<2>

top := max(contour<1>) + 1       rside := max(contour<0>) + 1       bott := min(contour<1>) - 1
lside := min(contour<0>) - 1

centroidanalysis := fPlasticCentroid( rebar, fConcCentroid(contour, 0), 0,  $\frac{F_y}{ksi}$ ,  $\frac{f_c}{ksi}$ , Prop(fPropCoord(contour))0 )
centroidanalysis = (21 21)      location of centroid used for analysis
centconc := fConcCentroid(contour, 0)   centconc = (21 21)
gross centroid area := Prop(fPropCoord(contour))0
area = 1376.55731
gross area

```

```

strength =
  {102,5}
  {102,5}
  {102,5}
  {102,5}
  {102,5}
  {102,5}
  {102,5}
  {102,5}

```

```

fPhiFactor(st, cr, fc) :=
  fPhiFactorACIB(
    cprop ← fPropCoord(cr)
    st) := lastr ← rows(st)
    area ← Prop(cprop)
    for j ∈ 0..(lastr - 1)
    cv ← 0.1 · area · fc
        if stj,4 < 0.002
    lastr ← rows(st)
    for j ∈ 0..(lastr - 1)
    resj,0 ← stj,0 · φaxial
    if stj,0 ≥ cv
    resj,1 ← stj,1 · φaxial
    resj,2 ← stj,2 · φaxial
    resj,3 ← stj,3 · φaxial
    if [(stj,4 ≥ 0.002) ∧ (stj,4 ≤ 0.005)]
    resj,2 ← stj,2 · φaxial0.002
    phi ←  $\frac{st_{j,2} \cdot \phi_{axial}^{0.002}}{0.003} \cdot (\phi_{flexure} - \phi_{axial}) + \phi_{axial}$ 
    if stj,0 ≤ 0
    resj,0 ← stj,0 · phi
    resj,1 ← stj,1 · phi
    resj,2 ← stj,2 · phi
    resj,3 ← stj,3 · phi
    if (stj,0 < cv) ∧ (stj,0 > 0)
    resj,0 ← stj,0 · φflexure
    cv ← stj,0
    phi ←  $\frac{res_{j,0}}{cv} \cdot st_{j,1} \cdot (\phi_{flexure} - \phi_{axial}) + \phi_{axial}$ 
    resj,0 ← stj,0 · phi
    resj,1 ← stj,1 · phi
    resj,2 ← stj,2 · phi
    resj,3 ← stj,3
  res

```

```

capacityia :=
  ans ← fPhiFactor(
    strengthia, contour,  $\frac{f_c}{ksi}$ ) if PhiType = 0
  ans ← fPhiFactorACIB(strengthia) otherwise
  ans

```

```

FactoredCapacity =
  sum ← capacity0
  for k ∈ 1..(rows(strength) - 1)
  sum ← stack(sum, capacityk)
  sum

```

```
capx := FactoredCapacity<0>
```

```
capy := FactoredCapacity<1>
```

```
capz := FactoredCapacity<2>
```

```

fPlane(ux, s) := for j ∈ 0..(rows(ux) - 1)
  for k ∈ 0..(rows(s) - 1)
    tmp ← sk
    if uxj > tmp0,0
      resk,0 ← 0
      resk,1 ← 0
      resk,2 ← 0
      continue
    for z ∈ 1..(rows(tmp) - 1)
      if (tmpz,0 ≤ uxj) · (tmpz-1,0 > uxj)
        resk,0 ←  $\frac{ux_j - tmp_{z-1,0}}{tmp_{z,0} - tmp_{z-1,0}} \cdot (tmp_{z,1} - tmp_{z-1,1}) + tmp_{z-1,1}$ 
        resk,1 ←  $\frac{ux_j - tmp_{z-1,0}}{tmp_{z,0} - tmp_{z-1,0}} \cdot (tmp_{z,2} - tmp_{z-1,2}) + tmp_{z-1,2}$ 
        resk,2 ←  $\frac{ux_j - tmp_{z-1,0}}{tmp_{z,0} - tmp_{z-1,0}} \cdot (tmp_{z,3} - tmp_{z-1,3}) + tmp_{z-1,3}$ 
        break
      resk+1,0 ← res0,0
      resk+1,1 ← res0,1
      resk+1,2 ← res0,2
    ansj ← res
  ans

```

Moment_{failure} := **fPlane**(user_{axial}, strength)

Moment_{envl} := **fPlane**(user_{axial}, capacity)

Moment_{envl} = ({9,3})

```

fClosePoint(c, fy, x1, y1, z1) := lastr ← rows(c) - 1
                                x1 ← x1 · 1000
                                for j ∈ 0..lastr
                                  x0 ← cj,0 · 1000
                                  if j = 0
                                    res ← cj,3
                                    distmin ←  $\left[ \frac{(c_{j,1} \cdot z1 - c_{j,2} \cdot y1)^2 + (c_{j,2} \cdot x1 - x0 \cdot z1)^2 + (x0 \cdot y1 - c_{j,1} \cdot x1)^2}{x1^2 + y1^2 + z1^2} \right]^{0.5}$ 
                                    continue
                                  continue if x0 < x1
                                  if x1 ≤ 0
                                    res ← fy
                                    break
                                  dist ←  $\left[ \frac{(c_{j,1} \cdot z1 - c_{j,2} \cdot y1)^2 + (c_{j,2} \cdot x1 - x0 \cdot z1)^2 + (x0 \cdot y1 - c_{j,1} \cdot x1)^2}{x1^2 + y1^2 + z1^2} \right]^{0.5}$ 
                                  if dist < distmin
                                    distmin ← dist
                                    res ← cj,3
                                res

```

inv := 0..rows(user_axial) - 1

SpliceStress_{inv} := fClosePoint $\left(\text{intershape}, \frac{F_y}{\text{ksi}}, \text{user_axial}_{\text{inv}}, \text{user_mom.y}_{\text{inv}}, \text{user_mom.x}_{\text{inv}} \right)$

SpliceStress = (0)

user_axial = (1000)

user_mom.y = (0)

user_mom.x = (0)

point := 0

user_axial_{point} = 1000

SpliceStress_{point} = 0

(pos. value indicates tension)

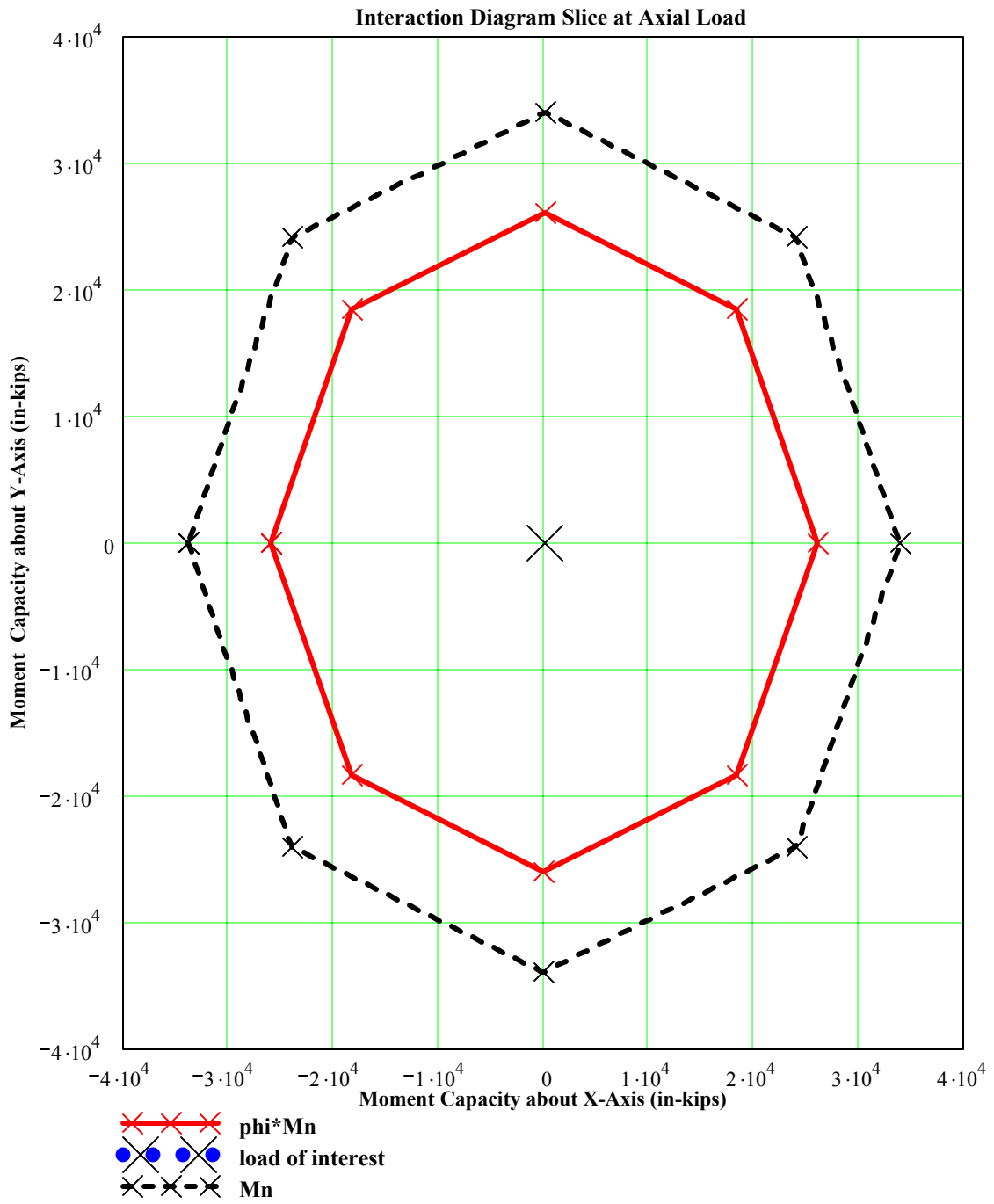


Figure D.2: Interaction Diagram Slice at Axial Load

Note: phi * Mn is incorrect for Moment envelope slices not centered around 0.0
 This note should typically only apply to sections with large eccentric prestressing
mid := 0

data₀ := $\frac{E_s}{\text{ksi}}$ data₁ := $\frac{F_y}{\text{ksi}}$ data₂ := $\frac{f'_c}{\text{ksi}}$ data₃ := contour data₄ := rebar
data₅ := strength data₆ := centconc data₇ := area data₈ := centroidanalysis
data₉ := divs data₁₀ := ϕ_{axial} data₁₁ := ϕ_{flexure} data₁₂ := $\frac{E_p}{\text{ksi}}$ data₁₃ := f_{pe}
data₁₄ := TieType data₁₅ := PhiType WRITEPRN(filename) := data

APPENDIX E. BLAST DISTRIBUTION

E.1 Distribution of Blast Loading

Simulation 1:

Explosive Amount = 500 lb TNT

Angle of Inclination = 90 deg

$Y := 6 \quad i := 0, 1..9 \quad k := 0, 1..22$

$\text{ksi} := \frac{\text{kip}}{\text{in}^2} \quad \text{kip} \equiv 1000 \text{ lb}$

$$X_i := i + 1 \quad d_i := \sqrt{Y^2 + (X_i)^2}$$

$$\theta_i := \text{asin}\left(\frac{Y}{d_i}\right)$$

Blast pressure from 3 ft to 25 ft range

d =

	0
0	6.083
1	6.325
2	6.708
3	7.211
4	7.81
5	8.485
6	9.22
7	10
8	10.817
9	11.662

θ =

	0
0	80.538
1	71.565
2	63.435
3	56.31
4	50.194
5	45
6	40.601
7	36.87
8	33.69
9	30.964

deg

F :=

3.576
2.511
1.884
1.480
1.198
0.991
0.832
0.707
0.606
0.524
0.456
0.398
0.350
0.309
0.275
0.245
0.219
0.196
0.177
0.161
0.145
0.132
0.121

Average Pressure:

$$\begin{aligned}
 P_0 &:= \left[F_3 - (F_3 - F_4) \cdot (d_0 - 6) \right] \cdot \sin(\theta_0) & P_0 &= 1.437 \\
 P_1 &:= \left[F_3 - (F_3 - F_4) \cdot (d_1 - 6) \right] \cdot \sin(\theta_1) & P_1 &= 1.317 \\
 P_2 &:= \left[F_3 - (F_3 - F_4) \cdot (d_2 - 6) \right] \cdot \sin(\theta_2) & P_2 &= 1.145 \\
 P_3 &:= \left[F_4 - (F_4 - F_5) \cdot (d_3 - 7) \right] \cdot \sin(\theta_3) & P_3 &= 0.96 \\
 P_4 &:= \left[F_4 - (F_4 - F_5) \cdot (d_4 - 7) \right] \cdot \sin(\theta_4) & P_4 &= 0.791 \\
 P_5 &:= \left[F_5 - (F_5 - F_6) \cdot (d_5 - 8) \right] \cdot \sin(\theta_5) & P_5 &= 0.646 \\
 P_6 &:= \left[F_6 - (F_6 - F_7) \cdot (d_6 - 9) \right] \cdot \sin(\theta_6) & P_6 &= 0.524 \\
 P_7 &:= F_7 \cdot \sin(\theta_7) & P_7 &= 0.424 \\
 P_8 &:= \left[F_7 - (F_7 - F_8) \cdot (d_8 - 10) \right] \cdot \sin(\theta_8) & P_8 &= 0.346 \\
 P_9 &:= \left[F_8 - (F_8 - F_9) \cdot (d_9 - 11) \right] \cdot \sin(\theta_9) & P_9 &= 0.284
 \end{aligned}$$

$$\text{Load}_{\text{Beam29}} := \left[P_0 \cdot 4 + P_1 \cdot 12 + P_2 \cdot 20 + (P_3 + P_4 + P_5 + P_6 + P_7 + P_8 + P_9) \cdot 12 \right] \cdot 144 \frac{\text{kip}}{20 \cdot \text{ft}}$$

$$\text{Load}_{\text{Beam29}} = 664 \frac{\text{kip}}{\text{ft}}$$

$$\text{Load}_{\text{Beam30}} := (P_3 \cdot 8 + P_4 \cdot 12 + P_5 \cdot 16 + P_6 \cdot 20 + P_7 \cdot 24 + P_8 \cdot 28 + P_9 \cdot 12) \cdot 144 \frac{\text{kip}}{20 \cdot \text{ft}}$$

$$\text{Load}_{\text{Beam30}} = 441 \frac{\text{kip}}{\text{ft}}$$

$$\text{Pressure}_{\text{Beam29}} := \frac{\text{Load}_{\text{Beam29}}}{6 \cdot \text{ft}}$$

$$\text{Pressure}_{\text{Beam29}} = 0.77 \text{ksi}$$

Which is approximately 50 percent of maximum pressure of 1.48 ksi

$$\text{Pressure}_{\text{Beam30}} := \frac{\text{Load}_{\text{Beam30}}}{6 \cdot \text{ft}}$$

$$\text{Pressure}_{\text{Beam30}} = 0.51 \text{ksi}$$

Which is approximately 30 percent of maximum pressure of 1.48 ksi

Simulation 2:

Explosive Amount = 100 lb TNT

Angle of Inclination = 90 deg.

$$Y := 6$$

$$i := 0, 1..9$$

$$X_i := i + 1$$

$$d_i := \sqrt{Y^2 + (X_i)^2}$$

$$\theta_i := \text{asin}\left(\frac{Y}{d_i}\right)$$

Blast pressure from 3 ft to 25 ft range

	0		0		(1.821)
d =	0	6.083	0	80.538	1.237
	1	6.325	1	71.565	0.898
	2	6.708	2	63.435	0.679
	3	7.211	3	56.31	0.526
	4	7.81	4	50.194	0.416
	5	8.485	5	45	0.334
	6	9.22	6	40.601	0.271
	7	10	7	36.87	0.223
	8	10.817	8	33.69	0.186
	9	11.662	9	30.964	0.156
					0.133
					0.114
					0.098
					0.085
					0.075
					0.066
					0.059
					0.052
					0.047
					0.042
					0.038
					0.035

Average Pressure:

$P_0 := [F_3 - (F_3 - F_4) \cdot (d_0 - 6)] \cdot \sin(\theta_0)$	$P_0 = 0.657$
$P_1 := [F_3 - (F_3 - F_4) \cdot (d_1 - 6)] \cdot \sin(\theta_1)$	$P_1 = 0.597$
$P_2 := [F_3 - (F_3 - F_4) \cdot (d_2 - 6)] \cdot \sin(\theta_2)$	$P_2 = 0.51$
$P_3 := [F_4 - (F_4 - F_5) \cdot (d_3 - 7)] \cdot \sin(\theta_3)$	$P_3 = 0.418$
$P_4 := [F_4 - (F_4 - F_5) \cdot (d_4 - 7)] \cdot \sin(\theta_4)$	$P_4 = 0.336$
$P_5 := [F_5 - (F_5 - F_6) \cdot (d_5 - 8)] \cdot \sin(\theta_5)$	$P_5 = 0.266$
$P_6 := [F_6 - (F_6 - F_7) \cdot (d_6 - 9)] \cdot \sin(\theta_6)$	$P_6 = 0.208$
$P_7 := F_7 \cdot \sin(\theta_7)$	$P_7 = 0.163$
$P_8 := [F_7 - (F_7 - F_8) \cdot (d_8 - 10)] \cdot \sin(\theta_8)$	$P_8 = 0.129$
$P_9 := [F_8 - (F_8 - F_9) \cdot (d_9 - 11)] \cdot \sin(\theta_9)$	$P_9 = 0.102$

$$\text{Load}_{\text{Beam29}} := \left[P_0 \cdot 4 + P_1 \cdot 12 + P_2 \cdot 20 + (P_3 + P_4 + P_5 + P_6 + P_7 + P_8 + P_9) \cdot 12 \right] \cdot 144 \frac{\text{kip}}{20 \cdot \text{ft}}$$

$$\text{Load}_{\text{Beam29}} = 284 \frac{\text{kip}}{\text{ft}}$$

$$\text{Load}_{\text{Beam30}} := (P_3 \cdot 8 + P_4 \cdot 12 + P_5 \cdot 16 + P_6 \cdot 20 + P_7 \cdot 24 + P_8 \cdot 28 + P_9 \cdot 12) \cdot 144 \frac{\text{kip}}{20 \cdot \text{ft}}$$

$$\text{Load}_{\text{Beam30}} = 177 \frac{\text{kip}}{\text{ft}}$$

$$\text{Pressure}_{\text{Beam29}} := \frac{\text{Load}_{\text{Beam29}}}{6 \cdot \text{ft}} \quad \text{Pressure}_{\text{Beam29}} = 0.329 \text{ksi}$$

Which is approximately 50 percent of maximum pressure of 0.679 ksi

$$\text{Pressure}_{\text{Beam30}} := \frac{\text{Load}_{\text{Beam30}}}{6 \cdot \text{ft}} \quad \text{Pressure}_{\text{Beam30}} = 0.204 \text{ksi}$$

Which is approximately 30 percent of maximum pressure of 0.679 ksi

Simulation 3:

Explosive Amount = 50 lb TNT

Angle of Inclination = 90 deg

Y := 6 i := 0, 1..9

$$X_i := i + 1 \quad d_i := \sqrt{Y^2 + (X_i)^2} \quad \theta_i := \text{asin}\left(\frac{Y}{d_i}\right)$$

	0
0	6.083
1	6.325
2	6.708
3	7.211
d = 4	7.81
5	8.485
6	9.22
7	10
8	10.817
9	11.662

	0
0	80.538
1	71.565
2	63.435
3	56.31
θ = 4	50.194
5	45
6	40.601
7	36.87
8	33.69
9	30.964

deg

F :=

- 1.337
- 0.888
- 0.627
- 0.460
- 0.347
- 0.267
- 0.210
- 0.167
- 0.136
- 0.112
- 0.093
- 0.078
- 0.067
- 0.058
- 0.050
- 0.044
- 0.039
- 0.034
- 0.031
- 0.028
- 0.025
- 0.023
- 0.021

Average Pressure:

$$\begin{aligned}
 P_0 &:= \left[F_3 - (F_3 - F_4) \cdot (d_0 - 6) \right] \cdot \sin(\theta_0) & P_0 &= 0.445 \\
 P_1 &:= \left[F_3 - (F_3 - F_4) \cdot (d_1 - 6) \right] \cdot \sin(\theta_1) & P_1 &= 0.402 \\
 P_2 &:= \left[F_3 - (F_3 - F_4) \cdot (d_2 - 6) \right] \cdot \sin(\theta_2) & P_2 &= 0.34 \\
 P_3 &:= \left[F_4 - (F_4 - F_5) \cdot (d_3 - 7) \right] \cdot \sin(\theta_3) & P_3 &= 0.275 \\
 P_4 &:= \left[F_4 - (F_4 - F_5) \cdot (d_4 - 7) \right] \cdot \sin(\theta_4) & P_4 &= 0.217 \\
 P_5 &:= \left[F_5 - (F_5 - F_6) \cdot (d_5 - 8) \right] \cdot \sin(\theta_5) & P_5 &= 0.169 \\
 P_6 &:= \left[F_6 - (F_6 - F_7) \cdot (d_6 - 9) \right] \cdot \sin(\theta_6) & P_6 &= 0.131 \\
 P_7 &:= F_7 \cdot \sin(\theta_7) & P_7 &= 0.1 \\
 P_8 &:= \left[F_7 - (F_7 - F_8) \cdot (d_8 - 10) \right] \cdot \sin(\theta_8) & P_8 &= 0.079 \\
 P_9 &:= \left[F_8 - (F_8 - F_9) \cdot (d_9 - 11) \right] \cdot \sin(\theta_9) & P_9 &= 0.062
 \end{aligned}$$

$$\text{Load}_{\text{Beam29}} := \left[P_0 \cdot 4 + P_1 \cdot 12 + P_2 \cdot 20 + (P_3 + P_4 + P_5 + P_6 + P_7 + P_8 + P_9) \cdot 12 \right] \cdot 144 \frac{\text{kip}}{20 \cdot \text{ft}}$$

$$\text{Load}_{\text{Beam29}} = 186 \frac{\text{kip}}{\text{ft}}$$

$$\text{Load}_{\text{Beam30}} := (P_3 \cdot 8 + P_4 \cdot 12 + P_5 \cdot 16 + P_6 \cdot 20 + P_7 \cdot 24 + P_8 \cdot 28 + P_9 \cdot 12) \cdot 144 \frac{\text{kip}}{20 \cdot \text{ft}}$$

$$\text{Load}_{\text{Beam30}} = 111 \frac{\text{kip}}{\text{ft}}$$

$$\text{Pressure}_{\text{Beam29}} := \frac{\text{Load}_{\text{Beam29}}}{6 \cdot \text{ft}} \quad \text{Pressure}_{\text{Beam29}} = 0.215 \text{ksi}$$

Which is approximately 50 percent of maximum pressure of 0.460 ksi

$$\text{Pressure}_{\text{Beam30}} := \frac{\text{Load}_{\text{Beam30}}}{6 \cdot \text{ft}} \quad \text{Pressure}_{\text{Beam30}} = 0.129 \text{ksi}$$

Which is approximately 30 percent of maximum pressure of 0.460 ksi

It was concluded from these analyses that the average pressure directly under the point of explosion is 50 percent of the peak pressure, which was designated as “50 Percent Distribution Rule,” and the average pressure at 6 ft away from the point of explosion is 30 percent of the peak pressure, which is designated as “30 Percent Distribution Rule.”

APPENDIX F. MODEL ANALYSIS RESULTS

F.1 Selected Output of Case 1 Blast Load

```
STAAD SPACE
START JOB INFORMATION
JOB NAME RESEARCH
JOB CLIENT FAMU-FSU COLLEGE OF ENGINEERING
JOB NO 1
JOB PART MODEL BRIDGE ANALYSIS
JOB REF LRFD
JOB COMMENT APPLY CASE 1 UNIFORM BLAST LOAD.
ENGINEER NAME ANWAR
ENGINEER DATE 07-FEB-05
END JOB INFORMATION
INPUT WIDTH 79
UNIT FEET KIP
JOINT COORDINATES
1 0 100 0; 2 0 100 3.5; 3 0 100 9.5; 4 0 100 15.5; 5 0 100 21.5; 6 0 100 27.5;
7 0 100 33.5; 8 0 100 39.5; 9 0 100 43; 10 80 100 0; 11 80 100 3.5;
12 80 100 9.5; 13 80 100 15.5; 14 80 100 21.5; 15 80 100 27.5; 16 80 100 33.5;
17 80 100 39.5; 18 80 100 43; 19 160 100 0; 20 160 100 3.5; 21 160 100 9.5;
22 160 100 15.5; 23 160 100 21.5; 24 160 100 27.5; 25 160 100 33.5;
26 160 100 39.5; 27 160 100 43; 28 0 84 3.5; 29 0 84 9.5; 30 0 84 15.5;
31 0 84 21.5; 32 0 84 27.5; 33 0 84 33.5; 34 0 84 39.5; 35 80 84 9.5;
36 80 84 33.5; 37 160 84 3.5; 38 160 84 9.5; 39 160 84 15.5; 40 160 84 21.5;
41 160 84 27.5; 42 160 84 33.5; 43 160 84 39.5; 44 0 100 0.01; 45 0 100 3.51;
46 0 100 9.51; 47 0 100 15.51; 48 0 100 21.51; 49 0 100 27.51;
50 0 100 33.51; 51 0 100 39.51; 52 0 100 42.99; 53 160 100 0.01;
54 160 100 3.51; 55 160 100 9.51; 56 160 100 15.51; 57 160 100 21.51;
58 160 100 27.51; 59 160 100 33.51; 60 160 100 39.51; 61 160 100 42.99;
MEMBER INCIDENCES
1 1 2; 2 2 3; 3 3 4; 4 4 5; 5 5 6; 6 6 7; 7 7 8; 8 8 9; 9 10 11; 10 11 12;
11 12 13; 12 13 14; 13 14 15; 14 15 16; 15 16 17; 16 17 18; 17 19 20; 18 20 21;
19 21 22; 20 22 23; 21 23 24; 22 24 25; 23 25 26; 24 26 27; 25 44 10; 26 45 11;
27 46 12; 28 47 13; 29 48 14; 30 49 15; 31 50 16; 32 51 17; 33 52 18; 34 10 53;
35 11 54; 36 12 55; 37 13 56; 38 14 57; 39 15 58; 40 16 59; 41 17 60; 42 18 61;
43 2 28; 44 3 29; 45 4 30; 46 5 31; 47 6 32; 48 7 33; 49 8 34; 50 12 35;
51 16 36; 52 20 37; 53 21 38; 54 22 39; 55 23 40; 56 24 41; 57 25 42; 58 26 43;
DEFINE MESH
A JOINT 44
B JOINT 45
C JOINT 51
D JOINT 52
E JOINT 61
F JOINT 60
G JOINT 54
H JOINT 53
GENERATE ELEMENT
MESH ABGH 1 16
MESH BCFG 6 16
MESH CDEF 1 16
ELEMENT PROPERTY
59 TO 186 TH 0.667
MEMBER PROPERTY
43 TO 49 52 TO 58 PRIS YD 1.5 ZD 1.5
1 TO 8 17 TO 24 PRIS YD 3 ZD 3
```

```

9 TO 16 PRIS YD 4 ZD 4
50 51 PRIS YD 3.5
26 TO 32 35 TO 41 PRIS YD 1.972 ZD 1.972
25 33 34 42 PRIS YD 2.67 ZD 1
DEFINE MATERIAL START
ISOTROPIC MATERIAL1
E 703803
POISSON 0.2
DENSITY 0.15
DAMP 2.8026e-044
ISOTROPIC MATERIAL2
E 647432
POISSON 0.2
DENSITY 0.15
DAMP 2.8026e-044
ISOTROPIC MATERIAL3
E 585625
POISSON 0.2
DENSITY 0.15
DAMP 2.8026e-044
END DEFINE MATERIAL
CONSTANTS
MATERIAL MATERIAL1 MEMB 26 TO 32 35 TO 41
MATERIAL MATERIAL2 MEMB 1 TO 24 43 TO 49 50 51 52 TO 58
MATERIAL MATERIAL3 MEMB 25 33 34 42 59 TO 186
SUPPORTS
28 TO 43 FIXED
45 TO 51 54 TO 60 PINNED
LOAD 1 CASE 1
MEMBER LOAD
29 UNI GY 106.7 30 50
28 30 UNI GY 80.3 30 50
SELFWEIGHT Y -1.25
PERFORM ANALYSIS
PRINT MEMBER FORCES ALL
PRINT FORCE ENVELOPE ALL
PRINT JOINT DISPLACEMENTS ALL
PRINT SUPPORT REACTION ALL
FINISH

```

P R O B L E M S T A T I S T I C S

```

-----
NUMBER OF JOINTS/MEMBER+ELEMENTS/SUPPORTS =   196/   186/   30
ORIGINAL/FINAL BAND-WIDTH=   136/   28/   174 DOF
TOTAL PRIMARY LOAD CASES =    1, TOTAL DEGREES OF FREEDOM =   1080
SIZE OF STIFFNESS MATRIX =    188 DOUBLE   KILO-WORDS
REQRD/AVAIL. DISK SPACE =   14.8/138998.7 MB,   EXMEM =   804.7 MB

```

MEMBER END FORCES STRUCTURE TYPE = SPACE

ALL UNITS ARE -- KIP FEET

MEMBER	LOAD	JT	AXIAL	SHEAR-Y	SHEAR-Z	TORSION	MOM-Y	MOM-Z
9	1	10	0.00	-62.34	129.63	1502.88	-13.98	-6.28
		11	0.00	72.84	-129.63	-1502.88	-439.74	-230.28
10	1	11	0.02	-161.06	687.50	2555.01	341.45	253.29
		12	-0.02	179.06	-687.50	-2555.01	-4466.45	-1273.67

11	1	12	-409.00	-1479.73	-888.90	30906.69	4434.84	-3033.45
		13	409.00	1497.73	888.90	-30906.69	898.55	-5898.94
12	1	13	-408.99	-594.08	-234.69	12345.40	-839.39	6150.18
		14	408.99	612.08	234.69	-12345.40	2247.52	-9768.67
13	1	14	-408.99	612.82	234.70	-12345.37	-2247.52	9772.01
		15	408.99	-594.82	-234.70	12345.37	839.32	-6149.09
14	1	15	-409.00	1498.48	888.91	-30906.89	-898.48	5902.80
		16	409.00	-1480.48	-888.91	30906.89	-4434.98	3034.08
15	1	16	0.02	178.94	-687.50	-2555.45	4466.60	1272.87
		17	-0.02	-160.94	687.50	2555.45	-341.63	-253.25
16	1	17	0.00	72.79	-129.68	-1502.64	439.92	230.06
		18	0.00	-62.29	129.68	1502.64	13.98	6.33
50	1	12	-1234.75	-2526.94	409.04	-24.24	-4486.25	-28123.73
		35	1205.89	2526.94	-409.04	24.24	-2058.32	-12307.26
51	1	16	-1235.65	-2526.93	-409.04	24.26	4486.28	-28123.63
		36	1206.79	2526.93	409.04	-24.26	2058.30	-12307.23

***** END OF LATEST ANALYSIS RESULT *****

MEMB	DISTANCE		FY	LD	MZ	LD	FZ	LD	MY	LD
26	0.00	MAX	15.24	1	193.12	1	-0.89	1	22.07	1
		MIN	15.24	1	193.12	1	-0.89	1	22.07	1
	6.67	MAX	10.38	1	107.69	1	-0.89	1	16.16	1
		MIN	10.38	1	107.69	1	-0.89	1	16.16	1
	13.33	MAX	5.52	1	54.67	1	-0.89	1	10.26	1
		MIN	5.52	1	54.67	1	-0.89	1	10.26	1
	20.00	MAX	0.66	1	34.06	1	-0.89	1	4.35	1
		MIN	0.66	1	34.06	1	-0.89	1	4.35	1
	26.67	MAX	-4.20	1	45.86	1	-0.89	1	-1.55	1
		MIN	-4.20	1	45.86	1	-0.89	1	-1.55	1
	33.33	MAX	-9.06	1	90.06	1	-0.89	1	-7.46	1
		MIN	-9.06	1	90.06	1	-0.89	1	-7.46	1
	40.00	MAX	-13.92	1	166.67	1	-0.89	1	-13.36	1
		MIN	-13.92	1	166.67	1	-0.89	1	-13.36	1
	46.67	MAX	-18.78	1	275.68	1	-0.89	1	-19.26	1
		MIN	-18.78	1	275.68	1	-0.89	1	-19.26	1
	53.33	MAX	-23.64	1	417.10	1	-0.89	1	-25.17	1
		MIN	-23.64	1	417.10	1	-0.89	1	-25.17	1
	60.00	MAX	-28.50	1	590.93	1	-0.89	1	-31.07	1
		MIN	-28.50	1	590.93	1	-0.89	1	-31.07	1
	66.67	MAX	-33.37	1	797.17	1	-0.89	1	-36.98	1
		MIN	-33.37	1	797.17	1	-0.89	1	-36.98	1
	73.33	MAX	-38.23	1	1035.81	1	-0.89	1	-42.88	1
		MIN	-38.23	1	1035.81	1	-0.89	1	-42.88	1
	80.00	MAX	-43.09	1	1306.86	1	-0.89	1	-48.79	1
		MIN	-43.09	1	1306.86	1	-0.89	1	-48.79	1
27	0.00	MAX	43.18	1	1725.64	1	-0.05	1	0.54	1
		MIN	43.18	1	1725.64	1	-0.05	1	0.54	1
	6.67	MAX	38.32	1	1453.99	1	-0.05	1	0.22	1
		MIN	38.32	1	1453.99	1	-0.05	1	0.22	1
	13.33	MAX	33.45	1	1214.76	1	-0.05	1	-0.10	1
		MIN	33.45	1	1214.76	1	-0.05	1	-0.10	1
	20.00	MAX	28.59	1	1007.93	1	-0.05	1	-0.43	1
		MIN	28.59	1	1007.93	1	-0.05	1	-0.43	1

	26.67	MAX	23.73	1	833.50	1	-0.05	1	-0.75	1
		MIN	23.73	1	833.50	1	-0.05	1	-0.75	1
	33.33	MAX	18.87	1	691.49	1	-0.05	1	-1.07	1
		MIN	18.87	1	691.49	1	-0.05	1	-1.07	1
	40.00	MAX	14.01	1	581.88	1	-0.05	1	-1.39	1
		MIN	14.01	1	581.88	1	-0.05	1	-1.39	1
	46.67	MAX	9.15	1	504.67	1	-0.05	1	-1.71	1
		MIN	9.15	1	504.67	1	-0.05	1	-1.71	1
	53.33	MAX	4.29	1	459.88	1	-0.05	1	-2.03	1
		MIN	4.29	1	459.88	1	-0.05	1	-2.03	1
	60.00	MAX	-0.57	1	447.49	1	-0.05	1	-2.35	1
		MIN	-0.57	1	447.49	1	-0.05	1	-2.35	1
	66.67	MAX	-5.43	1	467.50	1	-0.05	1	-2.68	1
		MIN	-5.43	1	467.50	1	-0.05	1	-2.68	1
	73.33	MAX	-10.29	1	519.93	1	-0.05	1	-3.00	1
		MIN	-10.29	1	519.93	1	-0.05	1	-3.00	1
	80.00	MAX	-15.15	1	604.75	1	-0.05	1	-3.32	1
		MIN	-15.15	1	604.75	1	-0.05	1	-3.32	1
28	0.00	MAX	-603.18	1	-5211.50	1	0.56	1	-14.76	1
		MIN	-603.18	1	-5211.50	1	0.56	1	-14.76	1
	6.67	MAX	-608.04	1	-1174.12	1	0.56	1	-11.05	1
		MIN	-608.04	1	-1174.12	1	0.56	1	-11.05	1
	13.33	MAX	-612.90	1	2895.68	1	0.56	1	-7.34	1
		MIN	-612.90	1	2895.68	1	0.56	1	-7.34	1
	20.00	MAX	-617.76	1	6997.87	1	0.56	1	-3.63	1
		MIN	-617.76	1	6997.87	1	0.56	1	-3.63	1
	26.67	MAX	-622.62	1	11132.48	1	0.56	1	0.08	1
		MIN	-622.62	1	11132.48	1	0.56	1	0.08	1
	33.33	MAX	-359.82	1	14853.38	1	0.56	1	3.79	1
		MIN	-359.82	1	14853.38	1	0.56	1	3.79	1
	40.00	MAX	170.66	1	15483.91	1	0.56	1	7.50	1
		MIN	170.66	1	15483.91	1	0.56	1	7.50	1
	46.67	MAX	701.13	1	12577.95	1	0.56	1	11.21	1
		MIN	701.13	1	12577.95	1	0.56	1	11.21	1
	53.33	MAX	963.94	1	6581.63	1	0.56	1	14.92	1
		MIN	963.94	1	6581.63	1	0.56	1	14.92	1
	60.00	MAX	959.07	1	171.60	1	0.56	1	18.63	1
		MIN	959.07	1	171.60	1	0.56	1	18.63	1
	66.67	MAX	954.21	1	-6206.03	1	0.56	1	22.34	1
		MIN	954.21	1	-6206.03	1	0.56	1	22.34	1
	73.33	MAX	949.35	1	-12551.25	1	0.56	1	26.05	1
		MIN	949.35	1	-12551.25	1	0.56	1	26.05	1
	80.00	MAX	944.49	1	-18864.06	1	0.56	1	29.76	1
		MIN	944.49	1	-18864.06	1	0.56	1	29.76	1
29	0.00	MAX	-814.21	1	-7382.94	1	0.00	1	0.00	1
		MIN	-814.21	1	-7382.94	1	0.00	1	0.00	1
	6.67	MAX	-819.07	1	-1938.69	1	0.00	1	0.00	1
		MIN	-819.07	1	-1938.69	1	0.00	1	0.00	1
	13.33	MAX	-823.93	1	3537.96	1	0.00	1	0.00	1
		MIN	-823.93	1	3537.96	1	0.00	1	0.00	1
	20.00	MAX	-828.79	1	9047.01	1	0.00	1	0.00	1
		MIN	-828.79	1	9047.01	1	0.00	1	0.00	1
	26.67	MAX	-833.65	1	14588.48	1	0.00	1	0.00	1
		MIN	-833.65	1	14588.48	1	0.00	1	0.00	1
	33.33	MAX	-482.84	1	19569.57	1	0.00	1	0.00	1
		MIN	-482.84	1	19569.57	1	0.00	1	0.00	1
	40.00	MAX	223.63	1	20433.63	1	0.00	1	0.00	1
		MIN	223.63	1	20433.63	1	0.00	1	0.00	1
	46.67	MAX	930.10	1	16587.87	1	0.00	1	0.00	1
		MIN	930.10	1	16587.87	1	0.00	1	0.00	1
	53.33	MAX	1280.91	1	8625.07	1	0.00	1	0.00	1

		MIN	1280.91	1	8625.07	1	0.00	1	0.00	1
60.00		MAX	1276.05	1	101.90	1	0.00	1	0.00	1
		MIN	1276.05	1	101.90	1	0.00	1	0.00	1
66.67		MAX	1271.18	1	-8388.87	1	0.00	1	0.00	1
		MIN	1271.18	1	-8388.87	1	0.00	1	0.00	1
73.33		MAX	1266.32	1	-16847.22	1	0.00	1	0.00	1
		MIN	1266.32	1	-16847.22	1	0.00	1	0.00	1
80.00		MAX	1261.46	1	-25273.18	1	0.00	1	0.00	1
		MIN	1261.46	1	-25273.18	1	0.00	1	0.00	1
30	0.00	MAX	-603.17	1	-5211.06	1	-0.56	1	14.76	1
		MIN	-603.17	1	-5211.06	1	-0.56	1	14.76	1
	6.67	MAX	-608.03	1	-1173.73	1	-0.56	1	11.05	1
		MIN	-608.03	1	-1173.73	1	-0.56	1	11.05	1
	13.33	MAX	-612.89	1	2896.00	1	-0.56	1	7.34	1
		MIN	-612.89	1	2896.00	1	-0.56	1	7.34	1
	20.00	MAX	-617.75	1	6998.14	1	-0.56	1	3.63	1
		MIN	-617.75	1	6998.14	1	-0.56	1	3.63	1
	26.67	MAX	-622.61	1	11132.69	1	-0.56	1	-0.08	1
		MIN	-622.61	1	11132.69	1	-0.56	1	-0.08	1
	33.33	MAX	-359.81	1	14853.53	1	-0.56	1	-3.79	1
		MIN	-359.81	1	14853.53	1	-0.56	1	-3.79	1
	40.00	MAX	170.67	1	15484.00	1	-0.56	1	-7.50	1
		MIN	170.67	1	15484.00	1	-0.56	1	-7.50	1
	46.67	MAX	701.14	1	12577.99	1	-0.56	1	-11.21	1
		MIN	701.14	1	12577.99	1	-0.56	1	-11.21	1
	53.33	MAX	963.94	1	6581.61	1	-0.56	1	-14.92	1
		MIN	963.94	1	6581.61	1	-0.56	1	-14.92	1
	60.00	MAX	959.08	1	171.52	1	-0.56	1	-18.63	1
		MIN	959.08	1	171.52	1	-0.56	1	-18.63	1
	66.67	MAX	954.22	1	-6206.16	1	-0.56	1	-22.34	1
		MIN	954.22	1	-6206.16	1	-0.56	1	-22.34	1
	73.33	MAX	949.36	1	-12551.44	1	-0.56	1	-26.05	1
		MIN	949.36	1	-12551.44	1	-0.56	1	-26.05	1
	80.00	MAX	944.50	1	-18864.30	1	-0.56	1	-29.76	1
		MIN	944.50	1	-18864.30	1	-0.56	1	-29.76	1
31	0.00	MAX	43.19	1	1726.40	1	0.05	1	-0.54	1
		MIN	43.19	1	1726.40	1	0.05	1	-0.54	1
	6.67	MAX	38.33	1	1454.66	1	0.05	1	-0.22	1
		MIN	38.33	1	1454.66	1	0.05	1	-0.22	1
	13.33	MAX	33.47	1	1215.32	1	0.05	1	0.10	1
		MIN	33.47	1	1215.32	1	0.05	1	0.10	1
	20.00	MAX	28.61	1	1008.40	1	0.05	1	0.43	1
		MIN	28.61	1	1008.40	1	0.05	1	0.43	1
	26.67	MAX	23.75	1	833.87	1	0.05	1	0.75	1
		MIN	23.75	1	833.87	1	0.05	1	0.75	1
	33.33	MAX	18.89	1	691.76	1	0.05	1	1.07	1
		MIN	18.89	1	691.76	1	0.05	1	1.07	1
	40.00	MAX	14.03	1	582.05	1	0.05	1	1.39	1
		MIN	14.03	1	582.05	1	0.05	1	1.39	1
	46.67	MAX	9.16	1	504.75	1	0.05	1	1.71	1
		MIN	9.16	1	504.75	1	0.05	1	1.71	1
	53.33	MAX	4.30	1	459.85	1	0.05	1	2.03	1
		MIN	4.30	1	459.85	1	0.05	1	2.03	1
	60.00	MAX	-0.56	1	447.36	1	0.05	1	2.35	1
		MIN	-0.56	1	447.36	1	0.05	1	2.35	1
	66.67	MAX	-5.42	1	467.28	1	0.05	1	2.68	1
		MIN	-5.42	1	467.28	1	0.05	1	2.68	1
	73.33	MAX	-10.28	1	519.61	1	0.05	1	3.00	1
		MIN	-10.28	1	519.61	1	0.05	1	3.00	1
	80.00	MAX	-15.14	1	604.34	1	0.05	1	3.32	1
		MIN	-15.14	1	604.34	1	0.05	1	3.32	1

32	0.00	MAX	15.27	1	194.46	1	0.89	1	-22.06	1
		MIN	15.27	1	194.46	1	0.89	1	-22.06	1
	6.67	MAX	10.41	1	108.86	1	0.89	1	-16.16	1
		MIN	10.41	1	108.86	1	0.89	1	-16.16	1
	13.33	MAX	5.55	1	55.67	1	0.89	1	-10.25	1
		MIN	5.55	1	55.67	1	0.89	1	-10.25	1
	20.00	MAX	0.69	1	34.89	1	0.89	1	-4.35	1
		MIN	0.69	1	34.89	1	0.89	1	-4.35	1
	26.67	MAX	-4.17	1	46.51	1	0.89	1	1.56	1
		MIN	-4.17	1	46.51	1	0.89	1	1.56	1
	33.33	MAX	-9.04	1	90.54	1	0.89	1	7.46	1
		MIN	-9.04	1	90.54	1	0.89	1	7.46	1
	40.00	MAX	-13.90	1	166.98	1	0.89	1	13.36	1
		MIN	-13.90	1	166.98	1	0.89	1	13.36	1
	46.67	MAX	-18.76	1	275.82	1	0.89	1	19.27	1
		MIN	-18.76	1	275.82	1	0.89	1	19.27	1
	53.33	MAX	-23.62	1	417.07	1	0.89	1	25.17	1
		MIN	-23.62	1	417.07	1	0.89	1	25.17	1
	60.00	MAX	-28.48	1	590.73	1	0.89	1	31.08	1
		MIN	-28.48	1	590.73	1	0.89	1	31.08	1
	66.67	MAX	-33.34	1	796.79	1	0.89	1	36.98	1
		MIN	-33.34	1	796.79	1	0.89	1	36.98	1
	73.33	MAX	-38.20	1	1035.26	1	0.89	1	42.88	1
		MIN	-38.20	1	1035.26	1	0.89	1	42.88	1
	80.00	MAX	-43.06	1	1306.14	1	0.89	1	48.79	1
		MIN	-43.06	1	1306.14	1	0.89	1	48.79	1
35	0.00	MAX	45.14	1	254.74	1	-0.90	1	49.50	1
		MIN	45.14	1	254.74	1	-0.90	1	49.50	1
	6.67	MAX	40.28	1	-29.97	1	-0.90	1	43.48	1
		MIN	40.28	1	-29.97	1	-0.90	1	43.48	1
	13.33	MAX	35.41	1	-282.27	1	-0.90	1	37.47	1
		MIN	35.41	1	-282.27	1	-0.90	1	37.47	1
	20.00	MAX	30.55	1	-502.16	1	-0.90	1	31.45	1
		MIN	30.55	1	-502.16	1	-0.90	1	31.45	1
	26.67	MAX	25.69	1	-689.65	1	-0.90	1	25.43	1
		MIN	25.69	1	-689.65	1	-0.90	1	25.43	1
	33.33	MAX	20.83	1	-844.73	1	-0.90	1	19.41	1
		MIN	20.83	1	-844.73	1	-0.90	1	19.41	1
	40.00	MAX	15.97	1	-967.40	1	-0.90	1	13.40	1
		MIN	15.97	1	-967.40	1	-0.90	1	13.40	1
	46.67	MAX	11.11	1	-1057.67	1	-0.90	1	7.38	1
		MIN	11.11	1	-1057.67	1	-0.90	1	7.38	1
	53.33	MAX	6.25	1	-1115.53	1	-0.90	1	1.36	1
		MIN	6.25	1	-1115.53	1	-0.90	1	1.36	1
	60.00	MAX	1.39	1	-1140.99	1	-0.90	1	-4.66	1
		MIN	1.39	1	-1140.99	1	-0.90	1	-4.66	1
	66.67	MAX	-3.47	1	-1134.03	1	-0.90	1	-10.67	1
		MIN	-3.47	1	-1134.03	1	-0.90	1	-10.67	1
	73.33	MAX	-8.33	1	-1094.68	1	-0.90	1	-16.69	1
		MIN	-8.33	1	-1094.68	1	-0.90	1	-16.69	1
	80.00	MAX	-13.20	1	-1022.91	1	-0.90	1	-22.71	1
		MIN	-13.20	1	-1022.91	1	-0.90	1	-22.71	1
36	0.00	MAX	50.76	1	376.84	1	-0.07	1	4.05	1
		MIN	50.76	1	376.84	1	-0.07	1	4.05	1
	6.67	MAX	45.90	1	54.64	1	-0.07	1	3.61	1
		MIN	45.90	1	54.64	1	-0.07	1	3.61	1
	13.33	MAX	41.04	1	-235.16	1	-0.07	1	3.17	1
		MIN	41.04	1	-235.16	1	-0.07	1	3.17	1
	20.00	MAX	36.18	1	-492.56	1	-0.07	1	2.73	1

		MIN	36.18	1	-492.56	1	-0.07	1	2.73	1
26.67		MAX	31.32	1	-717.54	1	-0.07	1	2.29	1
		MIN	31.32	1	-717.54	1	-0.07	1	2.29	1
33.33		MAX	26.46	1	-910.12	1	-0.07	1	1.86	1
		MIN	26.46	1	-910.12	1	-0.07	1	1.86	1
40.00		MAX	21.60	1	-1070.30	1	-0.07	1	1.42	1
		MIN	21.60	1	-1070.30	1	-0.07	1	1.42	1
46.67		MAX	16.73	1	-1198.06	1	-0.07	1	0.98	1
		MIN	16.73	1	-1198.06	1	-0.07	1	0.98	1
53.33		MAX	11.87	1	-1293.43	1	-0.07	1	0.54	1
		MIN	11.87	1	-1293.43	1	-0.07	1	0.54	1
60.00		MAX	7.01	1	-1356.38	1	-0.07	1	0.11	1
		MIN	7.01	1	-1356.38	1	-0.07	1	0.11	1
66.67		MAX	2.15	1	-1386.93	1	-0.07	1	-0.33	1
		MIN	2.15	1	-1386.93	1	-0.07	1	-0.33	1
73.33		MAX	-2.71	1	-1385.07	1	-0.07	1	-0.77	1
		MIN	-2.71	1	-1385.07	1	-0.07	1	-0.77	1
80.00		MAX	-7.57	1	-1350.80	1	-0.07	1	-1.21	1
		MIN	-7.57	1	-1350.80	1	-0.07	1	-1.21	1
37	0.00	MAX	40.84	1	-302.73	1	0.55	1	-29.40	1
		MIN	40.84	1	-302.73	1	0.55	1	-29.40	1
	6.67	MAX	35.98	1	-558.82	1	0.55	1	-25.75	1
		MIN	35.98	1	-558.82	1	0.55	1	-25.75	1
	13.33	MAX	31.12	1	-782.49	1	0.55	1	-22.09	1
		MIN	31.12	1	-782.49	1	0.55	1	-22.09	1
	20.00	MAX	26.26	1	-973.76	1	0.55	1	-18.44	1
		MIN	26.26	1	-973.76	1	0.55	1	-18.44	1
	26.67	MAX	21.40	1	-1132.62	1	0.55	1	-14.79	1
		MIN	21.40	1	-1132.62	1	0.55	1	-14.79	1
	33.33	MAX	16.54	1	-1259.08	1	0.55	1	-11.14	1
		MIN	16.54	1	-1259.08	1	0.55	1	-11.14	1
	40.00	MAX	11.68	1	-1353.13	1	0.55	1	-7.48	1
		MIN	11.68	1	-1353.13	1	0.55	1	-7.48	1
	46.67	MAX	6.82	1	-1414.77	1	0.55	1	-3.83	1
		MIN	6.82	1	-1414.77	1	0.55	1	-3.83	1
	53.33	MAX	1.96	1	-1444.01	1	0.55	1	-0.18	1
		MIN	1.96	1	-1444.01	1	0.55	1	-0.18	1
	60.00	MAX	-2.91	1	-1440.84	1	0.55	1	3.47	1
		MIN	-2.91	1	-1440.84	1	0.55	1	3.47	1
	66.67	MAX	-7.77	1	-1405.27	1	0.55	1	7.12	1
		MIN	-7.77	1	-1405.27	1	0.55	1	7.12	1
	73.33	MAX	-12.63	1	-1337.28	1	0.55	1	10.78	1
		MIN	-12.63	1	-1337.28	1	0.55	1	10.78	1
	80.00	MAX	-17.49	1	-1236.89	1	0.55	1	14.43	1
		MIN	-17.49	1	-1236.89	1	0.55	1	14.43	1
38	0.00	MAX	36.56	1	-582.40	1	0.00	1	0.00	1
		MIN	36.56	1	-582.40	1	0.00	1	0.00	1
	6.67	MAX	31.70	1	-809.92	1	0.00	1	0.00	1
		MIN	31.70	1	-809.92	1	0.00	1	0.00	1
	13.33	MAX	26.84	1	-1005.04	1	0.00	1	0.00	1
		MIN	26.84	1	-1005.04	1	0.00	1	0.00	1
	20.00	MAX	21.98	1	-1167.74	1	0.00	1	0.00	1
		MIN	21.98	1	-1167.74	1	0.00	1	0.00	1
	26.67	MAX	17.11	1	-1298.05	1	0.00	1	0.00	1
		MIN	17.11	1	-1298.05	1	0.00	1	0.00	1
	33.33	MAX	12.25	1	-1395.94	1	0.00	1	0.00	1
		MIN	12.25	1	-1395.94	1	0.00	1	0.00	1
	40.00	MAX	7.39	1	-1461.43	1	0.00	1	0.00	1
		MIN	7.39	1	-1461.43	1	0.00	1	0.00	1
	46.67	MAX	2.53	1	-1494.52	1	0.00	1	0.00	1
		MIN	2.53	1	-1494.52	1	0.00	1	0.00	1

	53.33	MAX	-2.33	1	-1495.19	1	0.00	1	0.00	1
		MIN	-2.33	1	-1495.19	1	0.00	1	0.00	1
	60.00	MAX	-7.19	1	-1463.46	1	0.00	1	0.00	1
		MIN	-7.19	1	-1463.46	1	0.00	1	0.00	1
	66.67	MAX	-12.05	1	-1399.32	1	0.00	1	0.00	1
		MIN	-12.05	1	-1399.32	1	0.00	1	0.00	1
	73.33	MAX	-16.91	1	-1302.78	1	0.00	1	0.00	1
		MIN	-16.91	1	-1302.78	1	0.00	1	0.00	1
	80.00	MAX	-21.77	1	-1173.83	1	0.00	1	0.00	1
		MIN	-21.77	1	-1173.83	1	0.00	1	0.00	1
39	0.00	MAX	40.84	1	-302.83	1	-0.55	1	29.40	1
		MIN	40.84	1	-302.83	1	-0.55	1	29.40	1
	6.67	MAX	35.98	1	-558.89	1	-0.55	1	25.74	1
		MIN	35.98	1	-558.89	1	-0.55	1	25.74	1
	13.33	MAX	31.12	1	-782.55	1	-0.55	1	22.09	1
		MIN	31.12	1	-782.55	1	-0.55	1	22.09	1
	20.00	MAX	26.26	1	-973.80	1	-0.55	1	18.44	1
		MIN	26.26	1	-973.80	1	-0.55	1	18.44	1
	26.67	MAX	21.40	1	-1132.64	1	-0.55	1	14.79	1
		MIN	21.40	1	-1132.64	1	-0.55	1	14.79	1
	33.33	MAX	16.54	1	-1259.08	1	-0.55	1	11.14	1
		MIN	16.54	1	-1259.08	1	-0.55	1	11.14	1
	40.00	MAX	11.67	1	-1353.11	1	-0.55	1	7.49	1
		MIN	11.67	1	-1353.11	1	-0.55	1	7.49	1
	46.67	MAX	6.81	1	-1414.74	1	-0.55	1	3.83	1
		MIN	6.81	1	-1414.74	1	-0.55	1	3.83	1
	53.33	MAX	1.95	1	-1443.95	1	-0.55	1	0.18	1
		MIN	1.95	1	-1443.95	1	-0.55	1	0.18	1
	60.00	MAX	-2.91	1	-1440.76	1	-0.55	1	-3.47	1
		MIN	-2.91	1	-1440.76	1	-0.55	1	-3.47	1
	66.67	MAX	-7.77	1	-1405.17	1	-0.55	1	-7.12	1
		MIN	-7.77	1	-1405.17	1	-0.55	1	-7.12	1
	73.33	MAX	-12.63	1	-1337.17	1	-0.55	1	-10.77	1
		MIN	-12.63	1	-1337.17	1	-0.55	1	-10.77	1
	80.00	MAX	-17.49	1	-1236.76	1	-0.55	1	-14.43	1
		MIN	-17.49	1	-1236.76	1	-0.55	1	-14.43	1
40	0.00	MAX	50.75	1	376.50	1	0.07	1	-4.05	1
		MIN	50.75	1	376.50	1	0.07	1	-4.05	1
	6.67	MAX	45.89	1	54.37	1	0.07	1	-3.61	1
		MIN	45.89	1	54.37	1	0.07	1	-3.61	1
	13.33	MAX	41.03	1	-235.34	1	0.07	1	-3.17	1
		MIN	41.03	1	-235.34	1	0.07	1	-3.17	1
	20.00	MAX	36.17	1	-492.66	1	0.07	1	-2.73	1
		MIN	36.17	1	-492.66	1	0.07	1	-2.73	1
	26.67	MAX	31.31	1	-717.56	1	0.07	1	-2.30	1
		MIN	31.31	1	-717.56	1	0.07	1	-2.30	1
	33.33	MAX	26.44	1	-910.06	1	0.07	1	-1.86	1
		MIN	26.44	1	-910.06	1	0.07	1	-1.86	1
	40.00	MAX	21.58	1	-1070.15	1	0.07	1	-1.42	1
		MIN	21.58	1	-1070.15	1	0.07	1	-1.42	1
	46.67	MAX	16.72	1	-1197.84	1	0.07	1	-0.98	1
		MIN	16.72	1	-1197.84	1	0.07	1	-0.98	1
	53.33	MAX	11.86	1	-1293.12	1	0.07	1	-0.54	1
		MIN	11.86	1	-1293.12	1	0.07	1	-0.54	1
	60.00	MAX	7.00	1	-1355.99	1	0.07	1	-0.11	1
		MIN	7.00	1	-1355.99	1	0.07	1	-0.11	1
	66.67	MAX	2.14	1	-1386.46	1	0.07	1	0.33	1
		MIN	2.14	1	-1386.46	1	0.07	1	0.33	1
	73.33	MAX	-2.72	1	-1384.52	1	0.07	1	0.77	1
		MIN	-2.72	1	-1384.52	1	0.07	1	0.77	1
	80.00	MAX	-7.58	1	-1350.17	1	0.07	1	1.21	1

		MIN	-7.58	1	-1350.17	1	0.07	1	1.21	1
41	0.00	MAX	45.08	1	253.31	1	0.90	1	-49.50	1
		MIN	45.08	1	253.31	1	0.90	1	-49.50	1
	6.67	MAX	40.22	1	-31.04	1	0.90	1	-43.49	1
		MIN	40.22	1	-31.04	1	0.90	1	-43.49	1
	13.33	MAX	35.36	1	-282.99	1	0.90	1	-37.47	1
		MIN	35.36	1	-282.99	1	0.90	1	-37.47	1
	20.00	MAX	30.50	1	-502.53	1	0.90	1	-31.45	1
		MIN	30.50	1	-502.53	1	0.90	1	-31.45	1
	26.67	MAX	25.64	1	-689.66	1	0.90	1	-25.43	1
		MIN	25.64	1	-689.66	1	0.90	1	-25.43	1
	33.33	MAX	20.78	1	-844.39	1	0.90	1	-19.42	1
		MIN	20.78	1	-844.39	1	0.90	1	-19.42	1
	40.00	MAX	15.92	1	-966.71	1	0.90	1	-13.40	1
		MIN	15.92	1	-966.71	1	0.90	1	-13.40	1
	46.67	MAX	11.06	1	-1056.62	1	0.90	1	-7.38	1
		MIN	11.06	1	-1056.62	1	0.90	1	-7.38	1
	53.33	MAX	6.20	1	-1114.13	1	0.90	1	-1.37	1
		MIN	6.20	1	-1114.13	1	0.90	1	-1.37	1
	60.00	MAX	1.33	1	-1139.23	1	0.90	1	4.65	1
		MIN	1.33	1	-1139.23	1	0.90	1	4.65	1
	66.67	MAX	-3.53	1	-1131.93	1	0.90	1	10.67	1
		MIN	-3.53	1	-1131.93	1	0.90	1	10.67	1
	73.33	MAX	-8.39	1	-1092.21	1	0.90	1	16.69	1
		MIN	-8.39	1	-1092.21	1	0.90	1	16.69	1
	80.00	MAX	-13.25	1	-1020.09	1	0.90	1	22.70	1
		MIN	-13.25	1	-1020.09	1	0.90	1	22.70	1
50	0.00	MAX	-2526.94	1	-28123.73	1	409.04	1	-4486.25	1
		MIN	-2526.94	1	-28123.73	1	409.04	1	-4486.25	1
	1.33	MAX	-2526.94	1	-24754.48	1	409.04	1	-3940.87	1
		MIN	-2526.94	1	-24754.48	1	409.04	1	-3940.87	1
	2.67	MAX	-2526.94	1	-21385.23	1	409.04	1	-3395.49	1
		MIN	-2526.94	1	-21385.23	1	409.04	1	-3395.49	1
	4.00	MAX	-2526.94	1	-18015.98	1	409.04	1	-2850.11	1
		MIN	-2526.94	1	-18015.98	1	409.04	1	-2850.11	1
	5.33	MAX	-2526.94	1	-14646.74	1	409.04	1	-2304.73	1
		MIN	-2526.94	1	-14646.74	1	409.04	1	-2304.73	1
	6.67	MAX	-2526.94	1	-11277.49	1	409.04	1	-1759.35	1
		MIN	-2526.94	1	-11277.49	1	409.04	1	-1759.35	1
	8.00	MAX	-2526.94	1	-7908.24	1	409.04	1	-1213.96	1
		MIN	-2526.94	1	-7908.24	1	409.04	1	-1213.96	1
	9.33	MAX	-2526.94	1	-4538.99	1	409.04	1	-668.58	1
		MIN	-2526.94	1	-4538.99	1	409.04	1	-668.58	1
	10.67	MAX	-2526.94	1	-1169.74	1	409.04	1	-123.20	1
		MIN	-2526.94	1	-1169.74	1	409.04	1	-123.20	1
	12.00	MAX	-2526.94	1	2199.51	1	409.04	1	422.18	1
		MIN	-2526.94	1	2199.51	1	409.04	1	422.18	1
	13.33	MAX	-2526.94	1	5568.76	1	409.04	1	967.56	1
		MIN	-2526.94	1	5568.76	1	409.04	1	967.56	1
	14.67	MAX	-2526.94	1	8938.01	1	409.04	1	1512.94	1
		MIN	-2526.94	1	8938.01	1	409.04	1	1512.94	1
	16.00	MAX	-2526.94	1	12307.26	1	409.04	1	2058.32	1
		MIN	-2526.94	1	12307.26	1	409.04	1	2058.32	1
51	0.00	MAX	-2526.93	1	-28123.63	1	-409.04	1	4486.28	1
		MIN	-2526.93	1	-28123.63	1	-409.04	1	4486.28	1
	1.33	MAX	-2526.93	1	-24754.40	1	-409.04	1	3940.90	1
		MIN	-2526.93	1	-24754.40	1	-409.04	1	3940.90	1
	2.67	MAX	-2526.93	1	-21385.16	1	-409.04	1	3395.52	1
		MIN	-2526.93	1	-21385.16	1	-409.04	1	3395.52	1
	4.00	MAX	-2526.93	1	-18015.92	1	-409.04	1	2850.14	1

	MIN	-2526.93	1	-18015.92	1	-409.04	1	2850.14	1
5.33	MAX	-2526.93	1	-14646.68	1	-409.04	1	2304.76	1
	MIN	-2526.93	1	-14646.68	1	-409.04	1	2304.76	1
6.67	MAX	-2526.93	1	-11277.44	1	-409.04	1	1759.37	1
	MIN	-2526.93	1	-11277.44	1	-409.04	1	1759.37	1
8.00	MAX	-2526.93	1	-7908.20	1	-409.04	1	1213.99	1
	MIN	-2526.93	1	-7908.20	1	-409.04	1	1213.99	1
9.33	MAX	-2526.93	1	-4538.96	1	-409.04	1	668.61	1
	MIN	-2526.93	1	-4538.96	1	-409.04	1	668.61	1
10.67	MAX	-2526.93	1	-1169.73	1	-409.04	1	123.23	1
	MIN	-2526.93	1	-1169.73	1	-409.04	1	123.23	1
12.00	MAX	-2526.93	1	2199.51	1	-409.04	1	-422.15	1
	MIN	-2526.93	1	2199.51	1	-409.04	1	-422.15	1
13.33	MAX	-2526.93	1	5568.75	1	-409.04	1	-967.53	1
	MIN	-2526.93	1	5568.75	1	-409.04	1	-967.53	1
14.67	MAX	-2526.93	1	8937.99	1	-409.04	1	-1512.92	1
	MIN	-2526.93	1	8937.99	1	-409.04	1	-1512.92	1
16.00	MAX	-2526.93	1	12307.23	1	-409.04	1	-2058.30	1
	MIN	-2526.93	1	12307.23	1	-409.04	1	-2058.30	1

F.2 Selected Output of Case 2 Blast Load

```

STAAD SPACE
START JOB INFORMATION
JOB NAME RESEARCH
JOB CLIENT FAMU-FSU COLLEGE OF ENGINEERING
JOB NO 1
JOB PART MODEL BRIDGE ANALYSIS
JOB REF LRFD
JOB COMMENT APPLY CASE 2 UNIFORM BLAST LOAD.
ENGINEER NAME ANWAR
ENGINEER DATE 07-FEB-05
END JOB INFORMATION
INPUT WIDTH 79
UNIT FEET KIP
JOINT COORDINATES
1 0 100 0; 2 0 100 3.5; 3 0 100 9.5; 4 0 100 15.5; 5 0 100 21.5; 6 0 100 27.5;
7 0 100 33.5; 8 0 100 39.5; 9 0 100 43; 10 80 100 0; 11 80 100 3.5;
12 80 100 9.5; 13 80 100 15.5; 14 80 100 21.5; 15 80 100 27.5; 16 80 100 33.5;
17 80 100 39.5; 18 80 100 43; 19 160 100 0; 20 160 100 3.5; 21 160 100 9.5;
22 160 100 15.5; 23 160 100 21.5; 24 160 100 27.5; 25 160 100 33.5;
26 160 100 39.5; 27 160 100 43; 28 0 84 3.5; 29 0 84 9.5; 30 0 84 15.5;
31 0 84 21.5; 32 0 84 27.5; 33 0 84 33.5; 34 0 84 39.5; 35 80 84 9.5;
36 80 84 33.5; 37 160 84 3.5; 38 160 84 9.5; 39 160 84 15.5; 40 160 84 21.5;
41 160 84 27.5; 42 160 84 33.5; 43 160 84 39.5; 44 0 100 0.01; 45 0 100 3.51;
46 0 100 9.51; 47 0 100 15.51; 48 0 100 21.51; 49 0 100 27.51;
50 0 100 33.51; 51 0 100 39.51; 52 0 100 42.99; 53 160 100 0.01;
54 160 100 3.51; 55 160 100 9.51; 56 160 100 15.51; 57 160 100 21.51;
58 160 100 27.51; 59 160 100 33.51; 60 160 100 39.51; 61 160 100 42.99;
MEMBER INCIDENCES
1 1 2; 2 2 3; 3 3 4; 4 4 5; 5 5 6; 6 6 7; 7 7 8; 8 8 9; 9 10 11; 10 11 12;
11 12 13; 12 13 14; 13 14 15; 14 15 16; 15 16 17; 16 17 18; 17 19 20; 18 20 21;
19 21 22; 20 22 23; 21 23 24; 22 24 25; 23 25 26; 24 26 27; 25 44 10; 26 45 11;
27 46 12; 28 47 13; 29 48 14; 30 49 15; 31 50 16; 32 51 17; 33 52 18; 34 10 53;
35 11 54; 36 12 55; 37 13 56; 38 14 57; 39 15 58; 40 16 59; 41 17 60; 42 18 61;
43 2 28; 44 3 29; 45 4 30; 46 5 31; 47 6 32; 48 7 33; 49 8 34; 50 12 35;
51 16 36; 52 20 37; 53 21 38; 54 22 39; 55 23 40; 56 24 41; 57 25 42; 58 26 43;
DEFINE MESH
A JOINT 44

```

```

B JOINT 45
C JOINT 51
D JOINT 52
E JOINT 61
F JOINT 60
G JOINT 54
H JOINT 53
GENERATE ELEMENT
MESH ABGH 1 16
MESH BCFG 6 16
MESH CDEF 1 16
ELEMENT PROPERTY
59 TO 186 TH 0.667
MEMBER PROPERTY
43 TO 49 52 TO 58 PRIS YD 1.5 ZD 1.5
1 TO 8 17 TO 24 PRIS YD 3 ZD 3
9 TO 16 PRIS YD 4 ZD 4
50 51 PRIS YD 3.5
26 TO 32 35 TO 41 PRIS YD 1.972 ZD 1.972
25 33 34 42 PRIS YD 2.67 ZD 1
DEFINE MATERIAL START
ISOTROPIC MATERIAL1
E 703803
POISSON 0.2
DENSITY 0.15
DAMP 2.8026e-044
ISOTROPIC MATERIAL2
E 647432
POISSON 0.2
DENSITY 0.15
DAMP 2.8026e-044
ISOTROPIC MATERIAL3
E 585625
POISSON 0.2
DENSITY 0.15
DAMP 2.8026e-044
END DEFINE MATERIAL
CONSTANTS
MATERIAL MATERIAL1 MEMB 26 TO 32 35 TO 41
MATERIAL MATERIAL2 MEMB 1 TO 24 43 TO 49 50 51 52 TO 58
MATERIAL MATERIAL3 MEMB 25 33 34 42 59 TO 186
SUPPORTS
28 TO 43 FIXED
45 TO 51 54 TO 60 PINNED
LOAD 1 CASE 2
MEMBER LOAD
29 UNI GY -639.36 30 50
28 30 UNI GY -380.16 30 50
SELFWEIGHT Y -1.25
PERFORM ANALYSIS
PRINT MEMBER FORCES ALL
PRINT FORCE ENVELOPE ALL
PRINT JOINT DISPLACEMENTS ALL
PRINT SUPPORT REACTION ALL
FINISH

```

P R O B L E M S T A T I S T I C S

```

-----
NUMBER OF JOINTS/MEMBER+ELEMENTS/SUPPORTS =   196/   186/   30
ORIGINAL/FINAL BAND-WIDTH=   136/    28/   174 DOF
TOTAL PRIMARY LOAD CASES =     1, TOTAL DEGREES OF FREEDOM =   1080
SIZE OF STIFFNESS MATRIX =     188 DOUBLE KILO-WORDS

```

REQRD/AVAIL. DISK SPACE = 14.8/138998.5 MB, EXMEM = 797.2 MB

MEMBER END FORCES STRUCTURE TYPE = SPACE

ALL UNITS ARE -- KIP FEET

MEMBER	LOAD	JT	AXIAL	SHEAR-Y	SHEAR-Z	TORSION	MOM-Y	MOM-Z
9	1	10	-0.01	-130.08	-678.14	-7865.94	73.11	-399.03
		11	0.01	140.58	678.14	7865.94	2300.38	-74.63
10	1	11	-0.10	-389.86	-3596.47	-13472.20	-1786.22	-620.52
		12	0.10	407.86	3596.47	13472.20	23365.04	-1772.65
11	1	12	2116.37	9206.60	4650.03	-161779.48	-23199.69	24019.77
		13	-2116.37	-9188.60	-4650.03	161779.48	-4700.50	31165.84
12	1	13	2116.32	4108.47	1227.71	-74255.78	4391.04	-32614.76
		14	-2116.32	-4090.47	-1227.71	74255.78	-11757.30	57211.55
13	1	14	2116.32	-4095.08	-1227.77	74255.64	11757.29	-57234.34
		15	-2116.32	4113.08	1227.77	-74255.64	-4390.67	32609.84
14	1	15	2116.37	-9193.25	-4650.09	161780.59	4700.13	-31190.08
		16	-2116.37	9211.25	4650.09	-161780.59	23200.38	-24023.42
15	1	16	-0.10	407.52	3596.45	13474.55	-23365.82	1772.39
		17	0.10	-389.52	-3596.45	-13474.55	1787.13	618.71
16	1	17	-0.01	140.50	678.41	7864.79	-2301.30	75.29
		18	0.01	-130.00	-678.41	-7864.79	-73.13	398.10
50	1	12	10072.32	13218.98	-2116.56	126.83	23214.05	147121.67
		35	-10101.18	-13218.98	2116.56	-126.83	10650.91	64382.09
51	1	16	10076.62	13218.94	2116.56	-126.91	-23214.40	147121.12
		36	-10105.48	-13218.94	-2116.56	126.91	-10650.58	64381.90

***** END OF LATEST ANALYSIS RESULT *****

MEMBER FORCE ENVELOPE

MEMB	DISTANCE		FY	LD	MZ	LD	FZ	LD	MY	LD
26	0.00	MAX	-69.69	1	-7751.78	1	4.63	1	-115.45	1
		MIN	-69.69	1	-7751.78	1	4.63	1	-115.45	1
	6.67	MAX	-74.55	1	-7270.97	1	4.63	1	-84.56	1
		MIN	-74.55	1	-7270.97	1	4.63	1	-84.56	1
	13.33	MAX	-79.41	1	-6757.74	1	4.63	1	-53.67	1
		MIN	-79.41	1	-6757.74	1	4.63	1	-53.67	1
	20.00	MAX	-84.27	1	-6212.11	1	4.63	1	-22.78	1
		MIN	-84.27	1	-6212.11	1	4.63	1	-22.78	1
	26.67	MAX	-89.14	1	-5634.08	1	4.63	1	8.11	1
		MIN	-89.14	1	-5634.08	1	4.63	1	8.11	1
	33.33	MAX	-94.00	1	-5023.63	1	4.63	1	39.00	1
		MIN	-94.00	1	-5023.63	1	4.63	1	39.00	1
	40.00	MAX	-98.86	1	-4380.79	1	4.63	1	69.89	1
		MIN	-98.86	1	-4380.79	1	4.63	1	69.89	1
	46.67	MAX	-103.72	1	-3705.53	1	4.63	1	100.78	1
		MIN	-103.72	1	-3705.53	1	4.63	1	100.78	1
	53.33	MAX	-108.58	1	-2997.87	1	4.63	1	131.67	1
		MIN	-108.58	1	-2997.87	1	4.63	1	131.67	1

	60.00	MAX	-113.44	1	-2257.80	1	4.63	1	162.56	1
		MIN	-113.44	1	-2257.80	1	4.63	1	162.56	1
	66.67	MAX	-118.30	1	-1485.32	1	4.63	1	193.45	1
		MIN	-118.30	1	-1485.32	1	4.63	1	193.45	1
	73.33	MAX	-123.16	1	-680.44	1	4.63	1	224.34	1
		MIN	-123.16	1	-680.44	1	4.63	1	224.34	1
	80.00	MAX	-128.02	1	156.85	1	4.63	1	255.23	1
		MIN	-128.02	1	156.85	1	4.63	1	255.23	1
27	0.00	MAX	-263.86	1	-18330.51	1	0.25	1	-2.84	1
		MIN	-263.86	1	-18330.51	1	0.25	1	-2.84	1
	6.67	MAX	-268.72	1	-16555.25	1	0.25	1	-1.15	1
		MIN	-268.72	1	-16555.25	1	0.25	1	-1.15	1
	13.33	MAX	-273.58	1	-14747.60	1	0.25	1	0.53	1
		MIN	-273.58	1	-14747.60	1	0.25	1	0.53	1
	20.00	MAX	-278.44	1	-12907.53	1	0.25	1	2.22	1
		MIN	-278.44	1	-12907.53	1	0.25	1	2.22	1
	26.67	MAX	-283.30	1	-11035.06	1	0.25	1	3.90	1
		MIN	-283.30	1	-11035.06	1	0.25	1	3.90	1
	33.33	MAX	-288.16	1	-9130.19	1	0.25	1	5.59	1
		MIN	-288.16	1	-9130.19	1	0.25	1	5.59	1
	40.00	MAX	-293.02	1	-7192.90	1	0.25	1	7.27	1
		MIN	-293.02	1	-7192.90	1	0.25	1	7.27	1
	46.67	MAX	-297.88	1	-5223.21	1	0.25	1	8.96	1
		MIN	-297.88	1	-5223.21	1	0.25	1	8.96	1
	53.33	MAX	-302.74	1	-3221.11	1	0.25	1	10.64	1
		MIN	-302.74	1	-3221.11	1	0.25	1	10.64	1
	60.00	MAX	-307.61	1	-1186.61	1	0.25	1	12.33	1
		MIN	-307.61	1	-1186.61	1	0.25	1	12.33	1
	66.67	MAX	-312.47	1	880.30	1	0.25	1	14.01	1
		MIN	-312.47	1	880.30	1	0.25	1	14.01	1
	73.33	MAX	-317.33	1	2979.61	1	0.25	1	15.69	1
		MIN	-317.33	1	2979.61	1	0.25	1	15.69	1
	80.00	MAX	-322.19	1	5111.34	1	0.25	1	17.38	1
		MIN	-322.19	1	5111.34	1	0.25	1	17.38	1
28	0.00	MAX	2776.71	1	13257.60	1	-2.91	1	77.19	1
		MIN	2776.71	1	13257.60	1	-2.91	1	77.19	1
	6.67	MAX	2771.85	1	-5237.62	1	-2.91	1	57.79	1
		MIN	2771.85	1	-5237.62	1	-2.91	1	57.79	1
	13.33	MAX	2766.99	1	-23700.44	1	-2.91	1	38.38	1
		MIN	2766.99	1	-23700.44	1	-2.91	1	38.38	1
	20.00	MAX	2762.13	1	-42130.84	1	-2.91	1	18.98	1
		MIN	2762.13	1	-42130.84	1	-2.91	1	18.98	1
	26.67	MAX	2757.27	1	-60528.84	1	-2.91	1	-0.43	1
		MIN	2757.27	1	-60528.84	1	-2.91	1	-0.43	1
	33.33	MAX	1485.21	1	-76782.44	1	-2.91	1	-19.83	1
		MIN	1485.21	1	-76782.44	1	-2.91	1	-19.83	1
	40.00	MAX	-1054.05	1	-78219.62	1	-2.91	1	-39.24	1
		MIN	-1054.05	1	-78219.62	1	-2.91	1	-39.24	1
	46.67	MAX	-3593.31	1	-62728.40	1	-2.91	1	-58.64	1
		MIN	-3593.31	1	-62728.40	1	-2.91	1	-58.64	1
	53.33	MAX	-4865.37	1	-32420.78	1	-2.91	1	-78.04	1
		MIN	-4865.37	1	-32420.78	1	-2.91	1	-78.04	1
	60.00	MAX	-4870.24	1	31.26	1	-2.91	1	-97.45	1
		MIN	-4870.24	1	31.26	1	-2.91	1	-97.45	1
	66.67	MAX	-4875.10	1	32515.70	1	-2.91	1	-116.85	1
		MIN	-4875.10	1	32515.70	1	-2.91	1	-116.85	1
	73.33	MAX	-4879.96	1	65032.54	1	-2.91	1	-136.26	1
		MIN	-4879.96	1	65032.54	1	-2.91	1	-136.26	1
	80.00	MAX	-4884.82	1	97581.80	1	-2.91	1	-155.66	1
		MIN	-4884.82	1	97581.80	1	-2.91	1	-155.66	1

29	0.00	MAX	4881.95	1	37010.62	1	0.00	1	0.00	1	
		MIN	4881.95	1	37010.62	1	0.00	1	0.00	1	
	6.67	MAX	4877.09	1	4480.47	1	0.00	1	0.00	1	
		MIN	4877.09	1	4480.47	1	0.00	1	0.00	1	
	13.33	MAX	4872.23	1	-28017.28	1	0.00	1	0.00	1	
		MIN	4872.23	1	-28017.28	1	0.00	1	0.00	1	
	20.00	MAX	4867.37	1	-60482.62	1	0.00	1	0.00	1	
		MIN	4867.37	1	-60482.62	1	0.00	1	0.00	1	
	26.67	MAX	4862.51	1	-92915.55	1	0.00	1	0.00	1	
		MIN	4862.51	1	-92915.55	1	0.00	1	0.00	1	
	33.33	MAX	2726.45	1	-121764.08	1	0.00	1	0.00	1	
		MIN	2726.45	1	-121764.08	1	0.00	1	0.00	1	
	40.00	MAX	-1540.81	1	-125716.19	1	0.00	1	0.00	1	
		MIN	-1540.81	1	-125716.19	1	0.00	1	0.00	1	
	46.67	MAX	-5808.07	1	-101219.91	1	0.00	1	0.00	1	
		MIN	-5808.07	1	-101219.91	1	0.00	1	0.00	1	
	53.33	MAX	-7944.13	1	-51827.21	1	0.00	1	0.00	1	
		MIN	-7944.13	1	-51827.21	1	0.00	1	0.00	1	
	60.00	MAX	-7949.00	1	1149.89	1	0.00	1	0.00	1	
		MIN	-7949.00	1	1149.89	1	0.00	1	0.00	1	
	66.67	MAX	-7953.86	1	54159.40	1	0.00	1	0.00	1	
		MIN	-7953.86	1	54159.40	1	0.00	1	0.00	1	
	73.33	MAX	-7958.72	1	107201.31	1	0.00	1	0.00	1	
		MIN	-7958.72	1	107201.31	1	0.00	1	0.00	1	
	80.00	MAX	-7963.58	1	160275.67	1	0.00	1	0.00	1	
		MIN	-7963.58	1	160275.67	1	0.00	1	0.00	1	
	30	0.00	MAX	2776.68	1	13256.09	1	2.91	1	-77.19	1
			MIN	2776.68	1	13256.09	1	2.91	1	-77.19	1
		6.67	MAX	2771.82	1	-5238.93	1	2.91	1	-57.78	1
			MIN	2771.82	1	-5238.93	1	2.91	1	-57.78	1
		13.33	MAX	2766.96	1	-23701.54	1	2.91	1	-38.38	1
			MIN	2766.96	1	-23701.54	1	2.91	1	-38.38	1
20.00		MAX	2762.10	1	-42131.75	1	2.91	1	-18.97	1	
		MIN	2762.10	1	-42131.75	1	2.91	1	-18.97	1	
26.67		MAX	2757.24	1	-60529.55	1	2.91	1	0.43	1	
		MIN	2757.24	1	-60529.55	1	2.91	1	0.43	1	
33.33		MAX	1485.18	1	-76782.94	1	2.91	1	19.83	1	
		MIN	1485.18	1	-76782.94	1	2.91	1	19.83	1	
40.00		MAX	-1054.08	1	-78219.92	1	2.91	1	39.24	1	
		MIN	-1054.08	1	-78219.92	1	2.91	1	39.24	1	
46.67		MAX	-3593.34	1	-62728.50	1	2.91	1	58.64	1	
		MIN	-3593.34	1	-62728.50	1	2.91	1	58.64	1	
53.33		MAX	-4865.40	1	-32420.67	1	2.91	1	78.05	1	
		MIN	-4865.40	1	-32420.67	1	2.91	1	78.05	1	
60.00		MAX	-4870.27	1	31.56	1	2.91	1	97.45	1	
		MIN	-4870.27	1	31.56	1	2.91	1	97.45	1	
66.67		MAX	-4875.13	1	32516.21	1	2.91	1	116.86	1	
		MIN	-4875.13	1	32516.21	1	2.91	1	116.86	1	
73.33		MAX	-4879.99	1	65033.26	1	2.91	1	136.26	1	
		MIN	-4879.99	1	65033.26	1	2.91	1	136.26	1	
80.00		MAX	-4884.85	1	97582.71	1	2.91	1	155.67	1	
		MIN	-4884.85	1	97582.71	1	2.91	1	155.67	1	
31		0.00	MAX	-263.86	1	-18330.59	1	-0.25	1	2.83	1
			MIN	-263.86	1	-18330.59	1	-0.25	1	2.83	1
		6.67	MAX	-268.72	1	-16555.31	1	-0.25	1	1.15	1
			MIN	-268.72	1	-16555.31	1	-0.25	1	1.15	1
		13.33	MAX	-273.58	1	-14747.63	1	-0.25	1	-0.53	1
			MIN	-273.58	1	-14747.63	1	-0.25	1	-0.53	1
	20.00	MAX	-278.44	1	-12907.54	1	-0.25	1	-2.22	1	
		MIN	-278.44	1	-12907.54	1	-0.25	1	-2.22	1	
	26.67	MAX	-283.31	1	-11035.04	1	-0.25	1	-3.90	1	

		MIN	-283.31	1	-11035.04	1	-0.25	1	-3.90	1
33.33		MAX	-288.17	1	-9130.14	1	-0.25	1	-5.59	1
		MIN	-288.17	1	-9130.14	1	-0.25	1	-5.59	1
40.00		MAX	-293.03	1	-7192.83	1	-0.25	1	-7.27	1
		MIN	-293.03	1	-7192.83	1	-0.25	1	-7.27	1
46.67		MAX	-297.89	1	-5223.11	1	-0.25	1	-8.96	1
		MIN	-297.89	1	-5223.11	1	-0.25	1	-8.96	1
53.33		MAX	-302.75	1	-3220.99	1	-0.25	1	-10.64	1
		MIN	-302.75	1	-3220.99	1	-0.25	1	-10.64	1
60.00		MAX	-307.61	1	-1186.46	1	-0.25	1	-12.32	1
		MIN	-307.61	1	-1186.46	1	-0.25	1	-12.32	1
66.67		MAX	-312.47	1	880.48	1	-0.25	1	-14.01	1
		MIN	-312.47	1	880.48	1	-0.25	1	-14.01	1
73.33		MAX	-317.33	1	2979.82	1	-0.25	1	-15.69	1
		MIN	-317.33	1	2979.82	1	-0.25	1	-15.69	1
80.00		MAX	-322.19	1	5111.57	1	-0.25	1	-17.38	1
		MIN	-322.19	1	5111.57	1	-0.25	1	-17.38	1
32	0.00	MAX	-69.49	1	-7740.74	1	-4.63	1	115.41	1
		MIN	-69.49	1	-7740.74	1	-4.63	1	115.41	1
	6.67	MAX	-74.35	1	-7261.28	1	-4.63	1	84.53	1
		MIN	-74.35	1	-7261.28	1	-4.63	1	84.53	1
	13.33	MAX	-79.21	1	-6749.42	1	-4.63	1	53.64	1
		MIN	-79.21	1	-6749.42	1	-4.63	1	53.64	1
	20.00	MAX	-84.07	1	-6205.15	1	-4.63	1	22.75	1
		MIN	-84.07	1	-6205.15	1	-4.63	1	22.75	1
	26.67	MAX	-88.93	1	-5628.47	1	-4.63	1	-8.13	1
		MIN	-88.93	1	-5628.47	1	-4.63	1	-8.13	1
	33.33	MAX	-93.79	1	-5019.39	1	-4.63	1	-39.02	1
		MIN	-93.79	1	-5019.39	1	-4.63	1	-39.02	1
	40.00	MAX	-98.65	1	-4377.90	1	-4.63	1	-69.91	1
		MIN	-98.65	1	-4377.90	1	-4.63	1	-69.91	1
	46.67	MAX	-103.51	1	-3704.00	1	-4.63	1	-100.80	1
		MIN	-103.51	1	-3704.00	1	-4.63	1	-100.80	1
	53.33	MAX	-108.38	1	-2997.70	1	-4.63	1	-131.68	1
		MIN	-108.38	1	-2997.70	1	-4.63	1	-131.68	1
	60.00	MAX	-113.24	1	-2258.99	1	-4.63	1	-162.57	1
		MIN	-113.24	1	-2258.99	1	-4.63	1	-162.57	1
	66.67	MAX	-118.10	1	-1487.88	1	-4.63	1	-193.46	1
		MIN	-118.10	1	-1487.88	1	-4.63	1	-193.46	1
	73.33	MAX	-122.96	1	-684.36	1	-4.63	1	-224.34	1
		MIN	-122.96	1	-684.36	1	-4.63	1	-224.34	1
	80.00	MAX	-127.82	1	151.57	1	-4.63	1	-255.23	1
		MIN	-127.82	1	151.57	1	-4.63	1	-255.23	1
35	0.00	MAX	121.26	1	5763.02	1	4.72	1	-258.93	1
		MIN	121.26	1	5763.02	1	4.72	1	-258.93	1
	6.67	MAX	116.39	1	4970.86	1	4.72	1	-227.45	1
		MIN	116.39	1	4970.86	1	4.72	1	-227.45	1
	13.33	MAX	111.53	1	4211.10	1	4.72	1	-195.98	1
		MIN	111.53	1	4211.10	1	4.72	1	-195.98	1
	20.00	MAX	106.67	1	3483.75	1	4.72	1	-164.50	1
		MIN	106.67	1	3483.75	1	4.72	1	-164.50	1
	26.67	MAX	101.81	1	2788.80	1	4.72	1	-133.03	1
		MIN	101.81	1	2788.80	1	4.72	1	-133.03	1
	33.33	MAX	96.95	1	2126.27	1	4.72	1	-101.55	1
		MIN	96.95	1	2126.27	1	4.72	1	-101.55	1
	40.00	MAX	92.09	1	1496.13	1	4.72	1	-70.08	1
		MIN	92.09	1	1496.13	1	4.72	1	-70.08	1
	46.67	MAX	87.23	1	898.41	1	4.72	1	-38.60	1
		MIN	87.23	1	898.41	1	4.72	1	-38.60	1
	53.33	MAX	82.37	1	333.09	1	4.72	1	-7.13	1
		MIN	82.37	1	333.09	1	4.72	1	-7.13	1

	60.00	MAX	77.51	1	-199.82	1	4.72	1	24.35	1
		MIN	77.51	1	-199.82	1	4.72	1	24.35	1
	66.67	MAX	72.65	1	-700.32	1	4.72	1	55.82	1
		MIN	72.65	1	-700.32	1	4.72	1	55.82	1
	73.33	MAX	67.78	1	-1168.42	1	4.72	1	87.30	1
		MIN	67.78	1	-1168.42	1	4.72	1	87.30	1
	80.00	MAX	62.92	1	-1604.11	1	4.72	1	118.77	1
		MIN	62.92	1	-1604.11	1	4.72	1	118.77	1
36	0.00	MAX	135.67	1	6296.78	1	0.34	1	-21.14	1
		MIN	135.67	1	6296.78	1	0.34	1	-21.14	1
	6.67	MAX	130.81	1	5408.54	1	0.34	1	-18.85	1
		MIN	130.81	1	5408.54	1	0.34	1	-18.85	1
	13.33	MAX	125.95	1	4552.70	1	0.34	1	-16.57	1
		MIN	125.95	1	4552.70	1	0.34	1	-16.57	1
	20.00	MAX	121.08	1	3729.27	1	0.34	1	-14.28	1
		MIN	121.08	1	3729.27	1	0.34	1	-14.28	1
	26.67	MAX	116.22	1	2938.24	1	0.34	1	-12.00	1
		MIN	116.22	1	2938.24	1	0.34	1	-12.00	1
	33.33	MAX	111.36	1	2179.63	1	0.34	1	-9.71	1
		MIN	111.36	1	2179.63	1	0.34	1	-9.71	1
	40.00	MAX	106.50	1	1453.41	1	0.34	1	-7.42	1
		MIN	106.50	1	1453.41	1	0.34	1	-7.42	1
	46.67	MAX	101.64	1	759.61	1	0.34	1	-5.14	1
		MIN	101.64	1	759.61	1	0.34	1	-5.14	1
	53.33	MAX	96.78	1	98.21	1	0.34	1	-2.85	1
		MIN	96.78	1	98.21	1	0.34	1	-2.85	1
	60.00	MAX	91.92	1	-530.78	1	0.34	1	-0.56	1
		MIN	91.92	1	-530.78	1	0.34	1	-0.56	1
	66.67	MAX	87.06	1	-1127.37	1	0.34	1	1.72	1
		MIN	87.06	1	-1127.37	1	0.34	1	1.72	1
	73.33	MAX	82.20	1	-1691.55	1	0.34	1	4.01	1
		MIN	82.20	1	-1691.55	1	0.34	1	4.01	1
	80.00	MAX	77.34	1	-2223.32	1	0.34	1	6.29	1
		MIN	77.34	1	-2223.32	1	0.34	1	6.29	1
37	0.00	MAX	195.32	1	10057.87	1	-2.87	1	153.80	1
		MIN	195.32	1	10057.87	1	-2.87	1	153.80	1
	6.67	MAX	190.46	1	8771.95	1	-2.87	1	134.69	1
		MIN	190.46	1	8771.95	1	-2.87	1	134.69	1
	13.33	MAX	185.60	1	7518.45	1	-2.87	1	115.58	1
		MIN	185.60	1	7518.45	1	-2.87	1	115.58	1
	20.00	MAX	180.73	1	6297.35	1	-2.87	1	96.48	1
		MIN	180.73	1	6297.35	1	-2.87	1	96.48	1
	26.67	MAX	175.87	1	5108.65	1	-2.87	1	77.37	1
		MIN	175.87	1	5108.65	1	-2.87	1	77.37	1
	33.33	MAX	171.01	1	3952.36	1	-2.87	1	58.26	1
		MIN	171.01	1	3952.36	1	-2.87	1	58.26	1
	40.00	MAX	166.15	1	2828.48	1	-2.87	1	39.15	1
		MIN	166.15	1	2828.48	1	-2.87	1	39.15	1
	46.67	MAX	161.29	1	1737.01	1	-2.87	1	20.05	1
		MIN	161.29	1	1737.01	1	-2.87	1	20.05	1
	53.33	MAX	156.43	1	677.94	1	-2.87	1	0.94	1
		MIN	156.43	1	677.94	1	-2.87	1	0.94	1
	60.00	MAX	151.57	1	-348.72	1	-2.87	1	-18.17	1
		MIN	151.57	1	-348.72	1	-2.87	1	-18.17	1
	66.67	MAX	146.71	1	-1342.97	1	-2.87	1	-37.28	1
		MIN	146.71	1	-1342.97	1	-2.87	1	-37.28	1
	73.33	MAX	141.85	1	-2304.82	1	-2.87	1	-56.38	1
		MIN	141.85	1	-2304.82	1	-2.87	1	-56.38	1
	80.00	MAX	136.99	1	-3234.26	1	-2.87	1	-75.49	1
		MIN	136.99	1	-3234.26	1	-2.87	1	-75.49	1

38	0.00	MAX	221.97	1	11764.24	1	0.00	1	0.00	1
		MIN	221.97	1	11764.24	1	0.00	1	0.00	1
6.67	MAX	217.11	1	10300.64	1	0.00	1	0.00	1	
		MIN	217.11	1	10300.64	1	0.00	1	0.00	1
13.33	MAX	212.25	1	8869.45	1	0.00	1	0.00	1	
		MIN	212.25	1	8869.45	1	0.00	1	0.00	1
20.00	MAX	207.39	1	7470.66	1	0.00	1	0.00	1	
		MIN	207.39	1	7470.66	1	0.00	1	0.00	1
26.67	MAX	202.53	1	6104.28	1	0.00	1	0.00	1	
		MIN	202.53	1	6104.28	1	0.00	1	0.00	1
33.33	MAX	197.67	1	4770.31	1	0.00	1	0.00	1	
		MIN	197.67	1	4770.31	1	0.00	1	0.00	1
40.00	MAX	192.80	1	3468.74	1	0.00	1	0.00	1	
		MIN	192.80	1	3468.74	1	0.00	1	0.00	1
46.67	MAX	187.94	1	2199.58	1	0.00	1	0.00	1	
		MIN	187.94	1	2199.58	1	0.00	1	0.00	1
53.33	MAX	183.08	1	962.83	1	0.00	1	0.00	1	
		MIN	183.08	1	962.83	1	0.00	1	0.00	1
60.00	MAX	178.22	1	-241.52	1	0.00	1	0.00	1	
		MIN	178.22	1	-241.52	1	0.00	1	0.00	1
66.67	MAX	173.36	1	-1413.46	1	0.00	1	-0.01	1	
		MIN	173.36	1	-1413.46	1	0.00	1	-0.01	1
73.33	MAX	168.50	1	-2552.99	1	0.00	1	-0.01	1	
		MIN	168.50	1	-2552.99	1	0.00	1	-0.01	1
80.00	MAX	163.64	1	-3660.12	1	0.00	1	-0.01	1	
		MIN	163.64	1	-3660.12	1	0.00	1	-0.01	1
39	0.00	MAX	195.32	1	10057.99	1	2.87	1	-153.79	1
		MIN	195.32	1	10057.99	1	2.87	1	-153.79	1
6.67	MAX	190.46	1	8772.07	1	2.87	1	-134.68	1	
		MIN	190.46	1	8772.07	1	2.87	1	-134.68	1
13.33	MAX	185.60	1	7518.56	1	2.87	1	-115.58	1	
		MIN	185.60	1	7518.56	1	2.87	1	-115.58	1
20.00	MAX	180.74	1	6297.45	1	2.87	1	-96.47	1	
		MIN	180.74	1	6297.45	1	2.87	1	-96.47	1
26.67	MAX	175.87	1	5108.76	1	2.87	1	-77.37	1	
		MIN	175.87	1	5108.76	1	2.87	1	-77.37	1
33.33	MAX	171.01	1	3952.47	1	2.87	1	-58.26	1	
		MIN	171.01	1	3952.47	1	2.87	1	-58.26	1
40.00	MAX	166.15	1	2828.58	1	2.87	1	-39.16	1	
		MIN	166.15	1	2828.58	1	2.87	1	-39.16	1
46.67	MAX	161.29	1	1737.10	1	2.87	1	-20.05	1	
		MIN	161.29	1	1737.10	1	2.87	1	-20.05	1
53.33	MAX	156.43	1	678.03	1	2.87	1	-0.95	1	
		MIN	156.43	1	678.03	1	2.87	1	-0.95	1
60.00	MAX	151.57	1	-348.63	1	2.87	1	18.16	1	
		MIN	151.57	1	-348.63	1	2.87	1	18.16	1
66.67	MAX	146.71	1	-1342.89	1	2.87	1	37.27	1	
		MIN	146.71	1	-1342.89	1	2.87	1	37.27	1
73.33	MAX	141.85	1	-2304.75	1	2.87	1	56.37	1	
		MIN	141.85	1	-2304.75	1	2.87	1	56.37	1
80.00	MAX	136.99	1	-3234.19	1	2.87	1	75.48	1	
		MIN	136.99	1	-3234.19	1	2.87	1	75.48	1
40	0.00	MAX	135.66	1	6296.65	1	-0.34	1	21.15	1
		MIN	135.66	1	6296.65	1	-0.34	1	21.15	1
6.67	MAX	130.80	1	5408.46	1	-0.34	1	18.86	1	
		MIN	130.80	1	5408.46	1	-0.34	1	18.86	1
13.33	MAX	125.94	1	4552.68	1	-0.34	1	16.58	1	
		MIN	125.94	1	4552.68	1	-0.34	1	16.58	1
20.00	MAX	121.08	1	3729.31	1	-0.34	1	14.29	1	
		MIN	121.08	1	3729.31	1	-0.34	1	14.29	1
26.67	MAX	116.21	1	2938.34	1	-0.34	1	12.00	1	
		MIN	116.21	1	2938.34	1	-0.34	1	12.00	1

	33.33	MAX	111.35	1	2179.78	1	-0.34	1	9.71	1
		MIN	111.35	1	2179.78	1	-0.34	1	9.71	1
	40.00	MAX	106.49	1	1453.63	1	-0.34	1	7.42	1
		MIN	106.49	1	1453.63	1	-0.34	1	7.42	1
	46.67	MAX	101.63	1	759.88	1	-0.34	1	5.14	1
		MIN	101.63	1	759.88	1	-0.34	1	5.14	1
	53.33	MAX	96.77	1	98.54	1	-0.34	1	2.85	1
		MIN	96.77	1	98.54	1	-0.34	1	2.85	1
	60.00	MAX	91.91	1	-530.39	1	-0.34	1	0.56	1
		MIN	91.91	1	-530.39	1	-0.34	1	0.56	1
	66.67	MAX	87.05	1	-1126.92	1	-0.34	1	-1.73	1
		MIN	87.05	1	-1126.92	1	-0.34	1	-1.73	1
	73.33	MAX	82.19	1	-1691.04	1	-0.34	1	-4.01	1
		MIN	82.19	1	-1691.04	1	-0.34	1	-4.01	1
	80.00	MAX	77.33	1	-2222.75	1	-0.34	1	-6.30	1
		MIN	77.33	1	-2222.75	1	-0.34	1	-6.30	1
41	0.00	MAX	121.19	1	5761.42	1	-4.72	1	258.94	1
		MIN	121.19	1	5761.42	1	-4.72	1	258.94	1
	6.67	MAX	116.33	1	4969.68	1	-4.72	1	227.46	1
		MIN	116.33	1	4969.68	1	-4.72	1	227.46	1
	13.33	MAX	111.47	1	4210.34	1	-4.72	1	195.99	1
		MIN	111.47	1	4210.34	1	-4.72	1	195.99	1
	20.00	MAX	106.61	1	3483.40	1	-4.72	1	164.52	1
		MIN	106.61	1	3483.40	1	-4.72	1	164.52	1
	26.67	MAX	101.75	1	2788.87	1	-4.72	1	133.04	1
		MIN	101.75	1	2788.87	1	-4.72	1	133.04	1
	33.33	MAX	96.89	1	2126.75	1	-4.72	1	101.57	1
		MIN	96.89	1	2126.75	1	-4.72	1	101.57	1
	40.00	MAX	92.03	1	1497.04	1	-4.72	1	70.09	1
		MIN	92.03	1	1497.04	1	-4.72	1	70.09	1
	46.67	MAX	87.17	1	899.73	1	-4.72	1	38.62	1
		MIN	87.17	1	899.73	1	-4.72	1	38.62	1
	53.33	MAX	82.30	1	334.83	1	-4.72	1	7.15	1
		MIN	82.30	1	334.83	1	-4.72	1	7.15	1
	60.00	MAX	77.44	1	-197.67	1	-4.72	1	-24.33	1
		MIN	77.44	1	-197.67	1	-4.72	1	-24.33	1
	66.67	MAX	72.58	1	-697.76	1	-4.72	1	-55.80	1
		MIN	72.58	1	-697.76	1	-4.72	1	-55.80	1
	73.33	MAX	67.72	1	-1165.44	1	-4.72	1	-87.28	1
		MIN	67.72	1	-1165.44	1	-4.72	1	-87.28	1
	80.00	MAX	62.86	1	-1600.71	1	-4.72	1	-118.75	1
		MIN	62.86	1	-1600.71	1	-4.72	1	-118.75	1
50	0.00	MAX	13218.98	1	147121.67	1	-2116.56	1	23214.05	1
		MIN	13218.98	1	147121.67	1	-2116.56	1	23214.05	1
	1.33	MAX	13218.98	1	129496.36	1	-2116.56	1	20391.97	1
		MIN	13218.98	1	129496.36	1	-2116.56	1	20391.97	1
	2.67	MAX	13218.98	1	111871.05	1	-2116.56	1	17569.89	1
		MIN	13218.98	1	111871.05	1	-2116.56	1	17569.89	1
	4.00	MAX	13218.98	1	94245.73	1	-2116.56	1	14747.81	1
		MIN	13218.98	1	94245.73	1	-2116.56	1	14747.81	1
	5.33	MAX	13218.98	1	76620.42	1	-2116.56	1	11925.73	1
		MIN	13218.98	1	76620.42	1	-2116.56	1	11925.73	1
	6.67	MAX	13218.98	1	58995.11	1	-2116.56	1	9103.65	1
		MIN	13218.98	1	58995.11	1	-2116.56	1	9103.65	1
	8.00	MAX	13218.98	1	41369.79	1	-2116.56	1	6281.57	1
		MIN	13218.98	1	41369.79	1	-2116.56	1	6281.57	1
	9.33	MAX	13218.98	1	23744.48	1	-2116.56	1	3459.49	1
		MIN	13218.98	1	23744.48	1	-2116.56	1	3459.49	1
	10.67	MAX	13218.98	1	6119.17	1	-2116.56	1	637.41	1
		MIN	13218.98	1	6119.17	1	-2116.56	1	637.41	1
	12.00	MAX	13218.98	1	-11506.15	1	-2116.56	1	-2184.67	1

		MIN	13218.98	1	-11506.15	1	-2116.56	1	-2184.67	1
13.33		MAX	13218.98	1	-29131.46	1	-2116.56	1	-5006.75	1
		MIN	13218.98	1	-29131.46	1	-2116.56	1	-5006.75	1
14.67		MAX	13218.98	1	-46756.77	1	-2116.56	1	-7828.83	1
		MIN	13218.98	1	-46756.77	1	-2116.56	1	-7828.83	1
16.00		MAX	13218.98	1	-64382.09	1	-2116.56	1	-10650.91	1
		MIN	13218.98	1	-64382.09	1	-2116.56	1	-10650.91	1
51	0.00	MAX	13218.94	1	147121.12	1	2116.56	1	-23214.40	1
		MIN	13218.94	1	147121.12	1	2116.56	1	-23214.40	1
	1.33	MAX	13218.94	1	129495.88	1	2116.56	1	-20392.32	1
		MIN	13218.94	1	129495.88	1	2116.56	1	-20392.32	1
	2.67	MAX	13218.94	1	111870.62	1	2116.56	1	-17570.24	1
		MIN	13218.94	1	111870.62	1	2116.56	1	-17570.24	1
	4.00	MAX	13218.94	1	94245.38	1	2116.56	1	-14748.16	1
		MIN	13218.94	1	94245.38	1	2116.56	1	-14748.16	1
	5.33	MAX	13218.94	1	76620.12	1	2116.56	1	-11926.07	1
		MIN	13218.94	1	76620.12	1	2116.56	1	-11926.07	1
	6.67	MAX	13218.94	1	58994.87	1	2116.56	1	-9103.99	1
		MIN	13218.94	1	58994.87	1	2116.56	1	-9103.99	1
	8.00	MAX	13218.94	1	41369.62	1	2116.56	1	-6281.91	1
		MIN	13218.94	1	41369.62	1	2116.56	1	-6281.91	1
	9.33	MAX	13218.94	1	23744.37	1	2116.56	1	-3459.83	1
		MIN	13218.94	1	23744.37	1	2116.56	1	-3459.83	1
	10.67	MAX	13218.94	1	6119.11	1	2116.56	1	-637.75	1
		MIN	13218.94	1	6119.11	1	2116.56	1	-637.75	1
	12.00	MAX	13218.94	1	-11506.14	1	2116.56	1	2184.33	1
		MIN	13218.94	1	-11506.14	1	2116.56	1	2184.33	1
	13.33	MAX	13218.94	1	-29131.39	1	2116.56	1	5006.42	1
		MIN	13218.94	1	-29131.39	1	2116.56	1	5006.42	1
	14.67	MAX	13218.94	1	-46756.64	1	2116.56	1	7828.50	1
		MIN	13218.94	1	-46756.64	1	2116.56	1	7828.50	1
	16.00	MAX	13218.94	1	-64381.90	1	2116.56	1	10650.58	1
		MIN	13218.94	1	-64381.90	1	2116.56	1	10650.58	1

F.3 Selected Output of Case 3 Blast Load

```

STAAD SPACE
START JOB INFORMATION
JOB NAME RESEARCH
JOB CLIENT FAMU-FSU COLLEGE OF ENGINEERING
JOB NO 1
JOB PART MODEL BRIDGE ANALYSIS
JOB REF LRFD
JOB COMMENT APPLY CASE 3 UNIFORM BLAST LOAD.
ENGINEER NAME ANWAR
ENGINEER DATE 07-FEB-05
END JOB INFORMATION
INPUT WIDTH 79
UNIT FEET KIP
JOINT COORDINATES
1 0 100 0; 2 0 100 3.5; 3 0 100 9.5; 4 0 100 15.5; 5 0 100 21.5; 6 0 100 27.5;
7 0 100 33.5; 8 0 100 39.5; 9 0 100 43; 10 80 100 0; 11 80 100 3.5;
12 80 100 9.5; 13 80 100 15.5; 14 80 100 21.5; 15 80 100 27.5; 16 80 100 33.5;
17 80 100 39.5; 18 80 100 43; 19 160 100 0; 20 160 100 3.5; 21 160 100 9.5;
22 160 100 15.5; 23 160 100 21.5; 24 160 100 27.5; 25 160 100 33.5;
26 160 100 39.5; 27 160 100 43; 28 0 84 3.5; 29 0 84 9.5; 30 0 84 15.5;
31 0 84 21.5; 32 0 84 27.5; 33 0 84 33.5; 34 0 84 39.5; 35 80 84 9.5;
36 80 84 33.5; 37 160 84 3.5; 38 160 84 9.5; 39 160 84 15.5; 40 160 84 21.5;

```

41 160 84 27.5; 42 160 84 33.5; 43 160 84 39.5; 44 0 100 0.01; 45 0 100 3.51;
 46 0 100 9.51; 47 0 100 15.51; 48 0 100 21.51; 49 0 100 27.51;
 50 0 100 33.51; 51 0 100 39.51; 52 0 100 42.99; 53 160 100 0.01;
 54 160 100 3.51; 55 160 100 9.51; 56 160 100 15.51; 57 160 100 21.51;
 58 160 100 27.51; 59 160 100 33.51; 60 160 100 39.51; 61 160 100 42.99;
 MEMBER INCIDENCES
 1 1 2; 2 2 3; 3 3 4; 4 4 5; 5 5 6; 6 6 7; 7 7 8; 8 8 9; 9 10 11; 10 11 12;
 11 12 13; 12 13 14; 13 14 15; 14 15 16; 15 16 17; 16 17 18; 17 19 20; 18 20 21;
 19 21 22; 20 22 23; 21 23 24; 22 24 25; 23 25 26; 24 26 27; 25 44 10; 26 45 11;
 27 46 12; 28 47 13; 29 48 14; 30 49 15; 31 50 16; 32 51 17; 33 52 18; 34 10 53;
 35 11 54; 36 12 55; 37 13 56; 38 14 57; 39 15 58; 40 16 59; 41 17 60; 42 18 61;
 43 2 28; 44 3 29; 45 4 30; 46 5 31; 47 6 32; 48 7 33; 49 8 34; 50 12 35;
 51 16 36; 52 20 37; 53 21 38; 54 22 39; 55 23 40; 56 24 41; 57 25 42; 58 26 43;
 DEFINE MESH
 A JOINT 44
 B JOINT 45
 C JOINT 51
 D JOINT 52
 E JOINT 61
 F JOINT 60
 G JOINT 54
 H JOINT 53
 GENERATE ELEMENT
 MESH ABGH 1 16
 MESH BCFG 6 16
 MESH CDEF 1 16
 ELEMENT PROPERTY
 59 TO 186 TH 0.667
 MEMBER PROPERTY
 43 TO 49 52 TO 58 PRIS YD 1.5 ZD 1.5
 1 TO 8 17 TO 24 PRIS YD 3 ZD 3
 9 TO 16 PRIS YD 4 ZD 4
 50 51 PRIS YD 3.5
 26 TO 32 35 TO 41 PRIS YD 1.972 ZD 1.972
 25 33 34 42 PRIS YD 2.67 ZD 1
 DEFINE MATERIAL START
 ISOTROPIC MATERIAL1
 E 703803
 POISSON 0.2
 DENSITY 0.15
 DAMP 2.8026e-044
 ISOTROPIC MATERIAL2
 E 647432
 POISSON 0.2
 DENSITY 0.15
 DAMP 2.8026e-044
 ISOTROPIC MATERIAL3
 E 585625
 POISSON 0.2
 DENSITY 0.15
 DAMP 2.8026e-044
 END DEFINE MATERIAL
 CONSTANTS
 MATERIAL MATERIAL1 MEMB 26 TO 32 35 TO 41
 MATERIAL MATERIAL2 MEMB 1 TO 24 43 TO 49 50 51 52 TO 58
 MATERIAL MATERIAL3 MEMB 25 33 34 42 59 TO 186
 SUPPORTS
 28 TO 43 FIXED
 45 TO 51 54 TO 60 PINNED
 LOAD 1 CASE 3
 MEMBER LOAD
 29 UNI GY -639.36 70 80
 38 UNI GY -639.36 0 10

28 30 UNI GY -380.16 70 80
 37 39 UNI GY -380.16 0 10
 SELFWEIGHT Y -1.25
 PERFORM ANALYSIS
 PRINT MEMBER FORCES ALL
 PRINT FORCE ENVELOPE ALL
 PRINT JOINT DISPLACEMENTS ALL
 PRINT SUPPORT REACTION ALL
 FINISH

P R O B L E M S T A T I S T I C S

NUMBER OF JOINTS/MEMBER+ELEMENTS/SUPPORTS = 196/ 186/ 30
 ORIGINAL/FINAL BAND-WIDTH= 136/ 28/ 174 DOF
 TOTAL PRIMARY LOAD CASES = 1, TOTAL DEGREES OF FREEDOM = 1080
 SIZE OF STIFFNESS MATRIX = 188 DOUBLE KILO-WORDS
 REQRD/AVAIL. DISK SPACE = 14.8/138998.3 MB, EXMEM = 795.6 MB

MEMBER END FORCES STRUCTURE TYPE = SPACE

ALL UNITS ARE -- KIP FEET

MEMBER	LOAD	JT	AXIAL	SHEAR-Y	SHEAR-Z	TORSION	MOM-Y	MOM-Z
9	1	10	-0.02	-78.89	0.00	0.00	0.00	-0.67
		11	0.02	89.39	0.00	0.00	0.00	-293.80
10	1	11	-0.15	-210.08	0.00	0.00	0.00	536.40
		12	0.15	228.08	0.00	0.00	0.00	-1850.85
11	1	12	3147.57	14094.65	0.00	0.00	0.00	36759.23
		13	-3147.57	-14076.65	0.00	0.00	0.00	47754.67
12	1	13	3147.51	6412.46	0.00	0.00	0.00	-47422.56
		14	-3147.51	-6394.46	0.00	0.00	0.00	85843.33
13	1	14	3147.51	-6395.87	0.00	0.00	0.00	-85850.71
		15	-3147.51	6413.87	0.00	0.00	0.00	47421.51
14	1	15	3147.57	-14078.06	0.00	0.00	0.00	-47762.82
		16	-3147.57	14096.06	0.00	0.00	0.00	-36759.55
15	1	16	-0.15	227.91	0.00	0.00	0.00	1850.10
		17	0.15	-209.91	0.00	0.00	0.00	-536.64
16	1	17	-0.02	89.33	0.00	0.00	0.00	293.77
		18	0.02	-78.83	0.00	0.00	0.00	0.51
50	1	12	14464.62	0.00	-3147.86	0.00	34525.28	0.00
		35	-14493.49	0.00	3147.86	0.00	15840.43	0.00
51	1	16	14465.86	0.00	3147.86	0.00	-34525.48	0.00
		36	-14494.72	0.00	-3147.86	0.00	-15840.24	0.00

***** END OF LATEST ANALYSIS RESULT *****

MEMBER FORCE ENVELOPE

MEMB	DISTANCE	FY	LD	MZ	LD	FZ	LD	MY	LD
26	0.00 MAX	-2.01	1	-1233.60	1	-0.07	1	2.48	1

		MIN	-2.01	1	-1233.60	1	-0.07	1	2.48	1
	6.67	MAX	-6.87	1	-1203.97	1	-0.07	1	2.04	1
		MIN	-6.87	1	-1203.97	1	-0.07	1	2.04	1
	13.33	MAX	-11.74	1	-1141.94	1	-0.07	1	1.60	1
		MIN	-11.74	1	-1141.94	1	-0.07	1	1.60	1
	20.00	MAX	-16.60	1	-1047.50	1	-0.07	1	1.17	1
		MIN	-16.60	1	-1047.50	1	-0.07	1	1.17	1
	26.67	MAX	-21.46	1	-920.66	1	-0.07	1	0.73	1
		MIN	-21.46	1	-920.66	1	-0.07	1	0.73	1
	33.33	MAX	-26.32	1	-761.41	1	-0.07	1	0.30	1
		MIN	-26.32	1	-761.41	1	-0.07	1	0.30	1
	40.00	MAX	-31.18	1	-569.75	1	-0.07	1	-0.14	1
		MIN	-31.18	1	-569.75	1	-0.07	1	-0.14	1
	46.67	MAX	-36.04	1	-345.69	1	-0.07	1	-0.57	1
		MIN	-36.04	1	-345.69	1	-0.07	1	-0.57	1
	53.33	MAX	-40.90	1	-89.22	1	-0.07	1	-1.01	1
		MIN	-40.90	1	-89.22	1	-0.07	1	-1.01	1
	60.00	MAX	-45.76	1	199.66	1	-0.07	1	-1.44	1
		MIN	-45.76	1	199.66	1	-0.07	1	-1.44	1
	66.67	MAX	-50.62	1	520.95	1	-0.07	1	-1.88	1
		MIN	-50.62	1	520.95	1	-0.07	1	-1.88	1
	73.33	MAX	-55.48	1	874.64	1	-0.07	1	-2.32	1
		MIN	-55.48	1	874.64	1	-0.07	1	-2.32	1
	80.00	MAX	-60.35	1	1260.73	1	-0.07	1	-2.75	1
		MIN	-60.35	1	1260.73	1	-0.07	1	-2.75	1
27	0.00	MAX	-12.62	1	-1850.91	1	-0.07	1	2.57	1
		MIN	-12.62	1	-1850.91	1	-0.07	1	2.57	1
	6.67	MAX	-17.48	1	-1750.59	1	-0.07	1	2.13	1
		MIN	-17.48	1	-1750.59	1	-0.07	1	2.13	1
	13.33	MAX	-22.34	1	-1617.87	1	-0.07	1	1.68	1
		MIN	-22.34	1	-1617.87	1	-0.07	1	1.68	1
	20.00	MAX	-27.20	1	-1452.74	1	-0.07	1	1.23	1
		MIN	-27.20	1	-1452.74	1	-0.07	1	1.23	1
	26.67	MAX	-32.06	1	-1255.20	1	-0.07	1	0.78	1
		MIN	-32.06	1	-1255.20	1	-0.07	1	0.78	1
	33.33	MAX	-36.92	1	-1025.25	1	-0.07	1	0.34	1
		MIN	-36.92	1	-1025.25	1	-0.07	1	0.34	1
	40.00	MAX	-41.78	1	-762.90	1	-0.07	1	-0.11	1
		MIN	-41.78	1	-762.90	1	-0.07	1	-0.11	1
	46.67	MAX	-46.64	1	-468.14	1	-0.07	1	-0.56	1
		MIN	-46.64	1	-468.14	1	-0.07	1	-0.56	1
	53.33	MAX	-51.51	1	-140.98	1	-0.07	1	-1.01	1
		MIN	-51.51	1	-140.98	1	-0.07	1	-1.01	1
	60.00	MAX	-56.37	1	218.59	1	-0.07	1	-1.46	1
		MIN	-56.37	1	218.59	1	-0.07	1	-1.46	1
	66.67	MAX	-61.23	1	610.57	1	-0.07	1	-1.90	1
		MIN	-61.23	1	610.57	1	-0.07	1	-1.90	1
	73.33	MAX	-66.09	1	1034.96	1	-0.07	1	-2.35	1
		MIN	-66.09	1	1034.96	1	-0.07	1	-2.35	1
	80.00	MAX	-70.95	1	1491.75	1	-0.07	1	-2.80	1
		MIN	-70.95	1	1491.75	1	-0.07	1	-2.80	1
28	0.00	MAX	27.84	1	-1289.82	1	-0.03	1	1.27	1
		MIN	27.84	1	-1289.82	1	-0.03	1	1.27	1
	6.67	MAX	22.98	1	-1459.19	1	-0.03	1	1.05	1
		MIN	22.98	1	-1459.19	1	-0.03	1	1.05	1
	13.33	MAX	18.11	1	-1596.16	1	-0.03	1	0.82	1
		MIN	18.11	1	-1596.16	1	-0.03	1	0.82	1
	20.00	MAX	13.25	1	-1700.72	1	-0.03	1	0.60	1
		MIN	13.25	1	-1700.72	1	-0.03	1	0.60	1
	26.67	MAX	8.39	1	-1772.88	1	-0.03	1	0.38	1
		MIN	8.39	1	-1772.88	1	-0.03	1	0.38	1

	33.33	MAX	3.53	1	-1812.62	1	-0.03	1	0.16	1
		MIN	3.53	1	-1812.62	1	-0.03	1	0.16	1
	40.00	MAX	-1.33	1	-1819.96	1	-0.03	1	-0.06	1
		MIN	-1.33	1	-1819.96	1	-0.03	1	-0.06	1
	46.67	MAX	-6.19	1	-1794.90	1	-0.03	1	-0.28	1
		MIN	-6.19	1	-1794.90	1	-0.03	1	-0.28	1
	53.33	MAX	-11.05	1	-1737.43	1	-0.03	1	-0.50	1
		MIN	-11.05	1	-1737.43	1	-0.03	1	-0.50	1
	60.00	MAX	-15.91	1	-1647.55	1	-0.03	1	-0.73	1
		MIN	-15.91	1	-1647.55	1	-0.03	1	-0.73	1
	66.67	MAX	-20.77	1	-1525.26	1	-0.03	1	-0.95	1
		MIN	-20.77	1	-1525.26	1	-0.03	1	-0.95	1
	73.33	MAX	-1292.83	1	741.43	1	-0.03	1	-1.17	1
		MIN	-1292.83	1	741.43	1	-0.03	1	-1.17	1
	80.00	MAX	-3832.10	1	17824.53	1	-0.03	1	-1.39	1
29	0.00	MAX	56.77	1	-822.46	1	0.00	1	0.00	1
		MIN	56.77	1	-822.46	1	0.00	1	0.00	1
	6.67	MAX	51.91	1	-1184.72	1	0.00	1	0.00	1
		MIN	51.91	1	-1184.72	1	0.00	1	0.00	1
	13.33	MAX	47.05	1	-1514.56	1	0.00	1	0.00	1
		MIN	47.05	1	-1514.56	1	0.00	1	0.00	1
	20.00	MAX	42.19	1	-1812.00	1	0.00	1	0.00	1
		MIN	42.19	1	-1812.00	1	0.00	1	0.00	1
	26.67	MAX	37.32	1	-2077.03	1	0.00	1	0.00	1
		MIN	37.32	1	-2077.03	1	0.00	1	0.00	1
	33.33	MAX	32.46	1	-2309.66	1	0.00	1	0.00	1
		MIN	32.46	1	-2309.66	1	0.00	1	0.00	1
	40.00	MAX	27.60	1	-2509.88	1	0.00	1	0.00	1
		MIN	27.60	1	-2509.88	1	0.00	1	0.00	1
	46.67	MAX	22.74	1	-2677.69	1	0.00	1	0.00	1
		MIN	22.74	1	-2677.69	1	0.00	1	0.00	1
	53.33	MAX	17.88	1	-2813.09	1	0.00	1	0.00	1
		MIN	17.88	1	-2813.09	1	0.00	1	0.00	1
	60.00	MAX	13.02	1	-2916.09	1	0.00	1	0.00	1
		MIN	13.02	1	-2916.09	1	0.00	1	0.00	1
	66.67	MAX	8.16	1	-2986.69	1	0.00	1	0.00	1
		MIN	8.16	1	-2986.69	1	0.00	1	0.00	1
	73.33	MAX	-2127.90	1	527.13	1	0.00	1	0.00	1
		MIN	-2127.90	1	527.13	1	0.00	1	0.00	1
	80.00	MAX	-6395.16	1	28937.35	1	0.00	1	0.00	1
		MIN	-6395.16	1	28937.35	1	0.00	1	0.00	1
30	0.00	MAX	27.83	1	-1289.77	1	0.03	1	-1.27	1
		MIN	27.83	1	-1289.77	1	0.03	1	-1.27	1
	6.67	MAX	22.97	1	-1459.13	1	0.03	1	-1.05	1
		MIN	22.97	1	-1459.13	1	0.03	1	-1.05	1
	13.33	MAX	18.11	1	-1596.09	1	0.03	1	-0.83	1
		MIN	18.11	1	-1596.09	1	0.03	1	-0.83	1
	20.00	MAX	13.25	1	-1700.63	1	0.03	1	-0.60	1
		MIN	13.25	1	-1700.63	1	0.03	1	-0.60	1
	26.67	MAX	8.39	1	-1772.77	1	0.03	1	-0.38	1
		MIN	8.39	1	-1772.77	1	0.03	1	-0.38	1
	33.33	MAX	3.53	1	-1812.51	1	0.03	1	-0.16	1
		MIN	3.53	1	-1812.51	1	0.03	1	-0.16	1
	40.00	MAX	-1.33	1	-1819.83	1	0.03	1	0.06	1
		MIN	-1.33	1	-1819.83	1	0.03	1	0.06	1
	46.67	MAX	-6.19	1	-1794.75	1	0.03	1	0.28	1
		MIN	-6.19	1	-1794.75	1	0.03	1	0.28	1
	53.33	MAX	-11.05	1	-1737.27	1	0.03	1	0.51	1
		MIN	-11.05	1	-1737.27	1	0.03	1	0.51	1
	60.00	MAX	-15.91	1	-1647.38	1	0.03	1	0.73	1
		MIN	-15.91	1	-1647.38	1	0.03	1	0.73	1

	66.67	MAX	-20.78	1	-1525.08	1	0.03	1	0.95	1
		MIN	-20.78	1	-1525.08	1	0.03	1	0.95	1
	73.33	MAX	-1292.84	1	741.63	1	0.03	1	1.17	1
		MIN	-1292.84	1	741.63	1	0.03	1	1.17	1
	80.00	MAX	-3832.10	1	17824.74	1	0.03	1	1.39	1
		MIN	-3832.10	1	17824.74	1	0.03	1	1.39	1
31	0.00	MAX	-12.61	1	-1850.35	1	0.07	1	-2.58	1
		MIN	-12.61	1	-1850.35	1	0.07	1	-2.58	1
	6.67	MAX	-17.47	1	-1750.08	1	0.07	1	-2.13	1
		MIN	-17.47	1	-1750.08	1	0.07	1	-2.13	1
	13.33	MAX	-22.33	1	-1617.41	1	0.07	1	-1.68	1
		MIN	-22.33	1	-1617.41	1	0.07	1	-1.68	1
	20.00	MAX	-27.19	1	-1452.32	1	0.07	1	-1.23	1
		MIN	-27.19	1	-1452.32	1	0.07	1	-1.23	1
	26.67	MAX	-32.05	1	-1254.83	1	0.07	1	-0.78	1
		MIN	-32.05	1	-1254.83	1	0.07	1	-0.78	1
	33.33	MAX	-36.92	1	-1024.93	1	0.07	1	-0.34	1
		MIN	-36.92	1	-1024.93	1	0.07	1	-0.34	1
	40.00	MAX	-41.78	1	-762.63	1	0.07	1	0.11	1
		MIN	-41.78	1	-762.63	1	0.07	1	0.11	1
	46.67	MAX	-46.64	1	-467.92	1	0.07	1	0.56	1
		MIN	-46.64	1	-467.92	1	0.07	1	0.56	1
	53.33	MAX	-51.50	1	-140.80	1	0.07	1	1.01	1
		MIN	-51.50	1	-140.80	1	0.07	1	1.01	1
	60.00	MAX	-56.36	1	218.72	1	0.07	1	1.46	1
		MIN	-56.36	1	218.72	1	0.07	1	1.46	1
	66.67	MAX	-61.22	1	610.65	1	0.07	1	1.91	1
		MIN	-61.22	1	610.65	1	0.07	1	1.91	1
	73.33	MAX	-66.08	1	1034.98	1	0.07	1	2.35	1
		MIN	-66.08	1	1034.98	1	0.07	1	2.35	1
	80.00	MAX	-70.94	1	1491.73	1	0.07	1	2.80	1
		MIN	-70.94	1	1491.73	1	0.07	1	2.80	1
32	0.00	MAX	-1.96	1	-1230.49	1	0.07	1	-2.48	1
		MIN	-1.96	1	-1230.49	1	0.07	1	-2.48	1
	6.67	MAX	-6.82	1	-1201.23	1	0.07	1	-2.04	1
		MIN	-6.82	1	-1201.23	1	0.07	1	-2.04	1
	13.33	MAX	-11.68	1	-1139.57	1	0.07	1	-1.61	1
		MIN	-11.68	1	-1139.57	1	0.07	1	-1.61	1
	20.00	MAX	-16.54	1	-1045.50	1	0.07	1	-1.17	1
		MIN	-16.54	1	-1045.50	1	0.07	1	-1.17	1
	26.67	MAX	-21.40	1	-919.02	1	0.07	1	-0.73	1
		MIN	-21.40	1	-919.02	1	0.07	1	-0.73	1
	33.33	MAX	-26.26	1	-760.13	1	0.07	1	-0.30	1
		MIN	-26.26	1	-760.13	1	0.07	1	-0.30	1
	40.00	MAX	-31.12	1	-568.84	1	0.07	1	0.14	1
		MIN	-31.12	1	-568.84	1	0.07	1	0.14	1
	46.67	MAX	-35.99	1	-345.15	1	0.07	1	0.57	1
		MIN	-35.99	1	-345.15	1	0.07	1	0.57	1
	53.33	MAX	-40.85	1	-89.04	1	0.07	1	1.01	1
		MIN	-40.85	1	-89.04	1	0.07	1	1.01	1
	60.00	MAX	-45.71	1	199.47	1	0.07	1	1.45	1
		MIN	-45.71	1	199.47	1	0.07	1	1.45	1
	66.67	MAX	-50.57	1	520.39	1	0.07	1	1.88	1
		MIN	-50.57	1	520.39	1	0.07	1	1.88	1
	73.33	MAX	-55.43	1	873.71	1	0.07	1	2.32	1
		MIN	-55.43	1	873.71	1	0.07	1	2.32	1
	80.00	MAX	-60.29	1	1259.44	1	0.07	1	2.75	1
		MIN	-60.29	1	1259.44	1	0.07	1	2.75	1
35	0.00	MAX	60.35	1	1260.73	1	0.07	1	-2.75	1
		MIN	60.35	1	1260.73	1	0.07	1	-2.75	1

	6.67	MAX	55.48	1	874.64	1	0.07	1	-2.32	1
		MIN	55.48	1	874.64	1	0.07	1	-2.32	1
	13.33	MAX	50.62	1	520.95	1	0.07	1	-1.88	1
		MIN	50.62	1	520.95	1	0.07	1	-1.88	1
	20.00	MAX	45.76	1	199.66	1	0.07	1	-1.44	1
		MIN	45.76	1	199.66	1	0.07	1	-1.44	1
	26.67	MAX	40.90	1	-89.21	1	0.07	1	-1.01	1
		MIN	40.90	1	-89.21	1	0.07	1	-1.01	1
	33.33	MAX	36.04	1	-345.69	1	0.07	1	-0.57	1
		MIN	36.04	1	-345.69	1	0.07	1	-0.57	1
	40.00	MAX	31.18	1	-569.75	1	0.07	1	-0.14	1
		MIN	31.18	1	-569.75	1	0.07	1	-0.14	1
	46.67	MAX	26.32	1	-761.41	1	0.07	1	0.30	1
		MIN	26.32	1	-761.41	1	0.07	1	0.30	1
	53.33	MAX	21.46	1	-920.66	1	0.07	1	0.73	1
		MIN	21.46	1	-920.66	1	0.07	1	0.73	1
	60.00	MAX	16.60	1	-1047.50	1	0.07	1	1.17	1
		MIN	16.60	1	-1047.50	1	0.07	1	1.17	1
	66.67	MAX	11.74	1	-1141.94	1	0.07	1	1.60	1
		MIN	11.74	1	-1141.94	1	0.07	1	1.60	1
	73.33	MAX	6.87	1	-1203.97	1	0.07	1	2.04	1
		MIN	6.87	1	-1203.97	1	0.07	1	2.04	1
	80.00	MAX	2.01	1	-1233.60	1	0.07	1	2.48	1
		MIN	2.01	1	-1233.60	1	0.07	1	2.48	1
36	0.00	MAX	70.95	1	1491.75	1	0.07	1	-2.80	1
		MIN	70.95	1	1491.75	1	0.07	1	-2.80	1
	6.67	MAX	66.09	1	1034.96	1	0.07	1	-2.35	1
		MIN	66.09	1	1034.96	1	0.07	1	-2.35	1
	13.33	MAX	61.23	1	610.57	1	0.07	1	-1.90	1
		MIN	61.23	1	610.57	1	0.07	1	-1.90	1
	20.00	MAX	56.37	1	218.59	1	0.07	1	-1.46	1
		MIN	56.37	1	218.59	1	0.07	1	-1.46	1
	26.67	MAX	51.51	1	-140.98	1	0.07	1	-1.01	1
		MIN	51.51	1	-140.98	1	0.07	1	-1.01	1
	33.33	MAX	46.64	1	-468.14	1	0.07	1	-0.56	1
		MIN	46.64	1	-468.14	1	0.07	1	-0.56	1
	40.00	MAX	41.78	1	-762.90	1	0.07	1	-0.11	1
		MIN	41.78	1	-762.90	1	0.07	1	-0.11	1
	46.67	MAX	36.92	1	-1025.25	1	0.07	1	0.34	1
		MIN	36.92	1	-1025.25	1	0.07	1	0.34	1
	53.33	MAX	32.06	1	-1255.20	1	0.07	1	0.78	1
		MIN	32.06	1	-1255.20	1	0.07	1	0.78	1
	60.00	MAX	27.20	1	-1452.74	1	0.07	1	1.23	1
		MIN	27.20	1	-1452.74	1	0.07	1	1.23	1
	66.67	MAX	22.34	1	-1617.87	1	0.07	1	1.68	1
		MIN	22.34	1	-1617.87	1	0.07	1	1.68	1
	73.33	MAX	17.48	1	-1750.59	1	0.07	1	2.13	1
		MIN	17.48	1	-1750.59	1	0.07	1	2.13	1
	80.00	MAX	12.62	1	-1850.91	1	0.07	1	2.57	1
		MIN	12.62	1	-1850.91	1	0.07	1	2.57	1
37	0.00	MAX	3832.10	1	17824.52	1	0.03	1	-1.39	1
		MIN	3832.10	1	17824.52	1	0.03	1	-1.39	1
	6.67	MAX	1292.83	1	741.43	1	0.03	1	-1.17	1
		MIN	1292.83	1	741.43	1	0.03	1	-1.17	1
	13.33	MAX	20.77	1	-1525.27	1	0.03	1	-0.95	1
		MIN	20.77	1	-1525.27	1	0.03	1	-0.95	1
	20.00	MAX	15.91	1	-1647.55	1	0.03	1	-0.73	1
		MIN	15.91	1	-1647.55	1	0.03	1	-0.73	1
	26.67	MAX	11.05	1	-1737.43	1	0.03	1	-0.50	1
		MIN	11.05	1	-1737.43	1	0.03	1	-0.50	1
	33.33	MAX	6.19	1	-1794.90	1	0.03	1	-0.28	1

		MIN	6.19	1	-1794.90	1	0.03	1	-0.28	1
40.00		MAX	1.33	1	-1819.97	1	0.03	1	-0.06	1
		MIN	1.33	1	-1819.97	1	0.03	1	-0.06	1
46.67		MAX	-3.53	1	-1812.63	1	0.03	1	0.16	1
		MIN	-3.53	1	-1812.63	1	0.03	1	0.16	1
53.33		MAX	-8.39	1	-1772.88	1	0.03	1	0.38	1
		MIN	-8.39	1	-1772.88	1	0.03	1	0.38	1
60.00		MAX	-13.25	1	-1700.72	1	0.03	1	0.60	1
		MIN	-13.25	1	-1700.72	1	0.03	1	0.60	1
66.67		MAX	-18.11	1	-1596.16	1	0.03	1	0.82	1
		MIN	-18.11	1	-1596.16	1	0.03	1	0.82	1
73.33		MAX	-22.98	1	-1459.20	1	0.03	1	1.05	1
		MIN	-22.98	1	-1459.20	1	0.03	1	1.05	1
80.00		MAX	-27.84	1	-1289.82	1	0.03	1	1.27	1
		MIN	-27.84	1	-1289.82	1	0.03	1	1.27	1
38	0.00	MAX	6395.16	1	28937.34	1	0.00	1	0.00	1
		MIN	6395.16	1	28937.34	1	0.00	1	0.00	1
	6.67	MAX	2127.90	1	527.13	1	0.00	1	0.00	1
		MIN	2127.90	1	527.13	1	0.00	1	0.00	1
	13.33	MAX	-8.16	1	-2986.68	1	0.00	1	0.00	1
		MIN	-8.16	1	-2986.68	1	0.00	1	0.00	1
	20.00	MAX	-13.02	1	-2916.09	1	0.00	1	0.00	1
		MIN	-13.02	1	-2916.09	1	0.00	1	0.00	1
	26.67	MAX	-17.88	1	-2813.09	1	0.00	1	0.00	1
		MIN	-17.88	1	-2813.09	1	0.00	1	0.00	1
	33.33	MAX	-22.74	1	-2677.68	1	0.00	1	0.00	1
		MIN	-22.74	1	-2677.68	1	0.00	1	0.00	1
	40.00	MAX	-27.60	1	-2509.86	1	0.00	1	0.00	1
		MIN	-27.60	1	-2509.86	1	0.00	1	0.00	1
	46.67	MAX	-32.46	1	-2309.64	1	0.00	1	0.00	1
		MIN	-32.46	1	-2309.64	1	0.00	1	0.00	1
	53.33	MAX	-37.32	1	-2077.01	1	0.00	1	0.00	1
		MIN	-37.32	1	-2077.01	1	0.00	1	0.00	1
	60.00	MAX	-42.19	1	-1811.98	1	0.00	1	0.00	1
		MIN	-42.19	1	-1811.98	1	0.00	1	0.00	1
	66.67	MAX	-47.05	1	-1514.54	1	0.00	1	0.00	1
		MIN	-47.05	1	-1514.54	1	0.00	1	0.00	1
	73.33	MAX	-51.91	1	-1184.69	1	0.00	1	0.00	1
		MIN	-51.91	1	-1184.69	1	0.00	1	0.00	1
	80.00	MAX	-56.77	1	-822.46	1	0.00	1	0.00	1
		MIN	-56.77	1	-822.46	1	0.00	1	0.00	1
39	0.00	MAX	3832.10	1	17824.74	1	-0.03	1	1.39	1
		MIN	3832.10	1	17824.74	1	-0.03	1	1.39	1
	6.67	MAX	1292.84	1	741.63	1	-0.03	1	1.17	1
		MIN	1292.84	1	741.63	1	-0.03	1	1.17	1
	13.33	MAX	20.78	1	-1525.08	1	-0.03	1	0.95	1
		MIN	20.78	1	-1525.08	1	-0.03	1	0.95	1
	20.00	MAX	15.91	1	-1647.38	1	-0.03	1	0.73	1
		MIN	15.91	1	-1647.38	1	-0.03	1	0.73	1
	26.67	MAX	11.05	1	-1737.27	1	-0.03	1	0.51	1
		MIN	11.05	1	-1737.27	1	-0.03	1	0.51	1
	33.33	MAX	6.19	1	-1794.76	1	-0.03	1	0.28	1
		MIN	6.19	1	-1794.76	1	-0.03	1	0.28	1
	40.00	MAX	1.33	1	-1819.84	1	-0.03	1	0.06	1
		MIN	1.33	1	-1819.84	1	-0.03	1	0.06	1
	46.67	MAX	-3.53	1	-1812.51	1	-0.03	1	-0.16	1
		MIN	-3.53	1	-1812.51	1	-0.03	1	-0.16	1
	53.33	MAX	-8.39	1	-1772.78	1	-0.03	1	-0.38	1
		MIN	-8.39	1	-1772.78	1	-0.03	1	-0.38	1
	60.00	MAX	-13.25	1	-1700.64	1	-0.03	1	-0.60	1
		MIN	-13.25	1	-1700.64	1	-0.03	1	-0.60	1

	66.67	MAX	-18.11	1	-1596.09	1	-0.03	1	-0.83	1
		MIN	-18.11	1	-1596.09	1	-0.03	1	-0.83	1
	73.33	MAX	-22.97	1	-1459.14	1	-0.03	1	-1.05	1
		MIN	-22.97	1	-1459.14	1	-0.03	1	-1.05	1
	80.00	MAX	-27.83	1	-1289.77	1	-0.03	1	-1.27	1
		MIN	-27.83	1	-1289.77	1	-0.03	1	-1.27	1
40	0.00	MAX	70.94	1	1491.73	1	-0.07	1	2.80	1
		MIN	70.94	1	1491.73	1	-0.07	1	2.80	1
	6.67	MAX	66.08	1	1034.99	1	-0.07	1	2.35	1
		MIN	66.08	1	1034.99	1	-0.07	1	2.35	1
	13.33	MAX	61.22	1	610.65	1	-0.07	1	1.91	1
		MIN	61.22	1	610.65	1	-0.07	1	1.91	1
	20.00	MAX	56.36	1	218.72	1	-0.07	1	1.46	1
		MIN	56.36	1	218.72	1	-0.07	1	1.46	1
	26.67	MAX	51.50	1	-140.80	1	-0.07	1	1.01	1
		MIN	51.50	1	-140.80	1	-0.07	1	1.01	1
	33.33	MAX	46.64	1	-467.92	1	-0.07	1	0.56	1
		MIN	46.64	1	-467.92	1	-0.07	1	0.56	1
	40.00	MAX	41.78	1	-762.63	1	-0.07	1	0.11	1
		MIN	41.78	1	-762.63	1	-0.07	1	0.11	1
	46.67	MAX	36.92	1	-1024.93	1	-0.07	1	-0.34	1
		MIN	36.92	1	-1024.93	1	-0.07	1	-0.34	1
	53.33	MAX	32.05	1	-1254.83	1	-0.07	1	-0.78	1
		MIN	32.05	1	-1254.83	1	-0.07	1	-0.78	1
	60.00	MAX	27.19	1	-1452.32	1	-0.07	1	-1.23	1
		MIN	27.19	1	-1452.32	1	-0.07	1	-1.23	1
	66.67	MAX	22.33	1	-1617.41	1	-0.07	1	-1.68	1
		MIN	22.33	1	-1617.41	1	-0.07	1	-1.68	1
	73.33	MAX	17.47	1	-1750.08	1	-0.07	1	-2.13	1
		MIN	17.47	1	-1750.08	1	-0.07	1	-2.13	1
	80.00	MAX	12.61	1	-1850.35	1	-0.07	1	-2.58	1
		MIN	12.61	1	-1850.35	1	-0.07	1	-2.58	1
41	0.00	MAX	60.29	1	1259.44	1	-0.07	1	2.75	1
		MIN	60.29	1	1259.44	1	-0.07	1	2.75	1
	6.67	MAX	55.43	1	873.71	1	-0.07	1	2.32	1
		MIN	55.43	1	873.71	1	-0.07	1	2.32	1
	13.33	MAX	50.57	1	520.39	1	-0.07	1	1.88	1
		MIN	50.57	1	520.39	1	-0.07	1	1.88	1
	20.00	MAX	45.71	1	199.47	1	-0.07	1	1.45	1
		MIN	45.71	1	199.47	1	-0.07	1	1.45	1
	26.67	MAX	40.85	1	-89.04	1	-0.07	1	1.01	1
		MIN	40.85	1	-89.04	1	-0.07	1	1.01	1
	33.33	MAX	35.99	1	-345.15	1	-0.07	1	0.57	1
		MIN	35.99	1	-345.15	1	-0.07	1	0.57	1
	40.00	MAX	31.12	1	-568.84	1	-0.07	1	0.14	1
		MIN	31.12	1	-568.84	1	-0.07	1	0.14	1
	46.67	MAX	26.26	1	-760.13	1	-0.07	1	-0.30	1
		MIN	26.26	1	-760.13	1	-0.07	1	-0.30	1
	53.33	MAX	21.40	1	-919.02	1	-0.07	1	-0.73	1
		MIN	21.40	1	-919.02	1	-0.07	1	-0.73	1
	60.00	MAX	16.54	1	-1045.50	1	-0.07	1	-1.17	1
		MIN	16.54	1	-1045.50	1	-0.07	1	-1.17	1
	66.67	MAX	11.68	1	-1139.57	1	-0.07	1	-1.61	1
		MIN	11.68	1	-1139.57	1	-0.07	1	-1.61	1
	73.33	MAX	6.82	1	-1201.23	1	-0.07	1	-2.04	1
		MIN	6.82	1	-1201.23	1	-0.07	1	-2.04	1
	80.00	MAX	1.96	1	-1230.49	1	-0.07	1	-2.48	1
		MIN	1.96	1	-1230.49	1	-0.07	1	-2.48	1
50	0.00	MAX	0.00	1	0.00	1	-3147.86	1	34525.28	1
		MIN	0.00	1	0.00	1	-3147.86	1	34525.28	1

	1.33	MAX	0.00	1	0.00	1	-3147.86	1	30328.14	1
		MIN	0.00	1	0.00	1	-3147.86	1	30328.14	1
	2.67	MAX	0.00	1	0.00	1	-3147.86	1	26131.00	1
		MIN	0.00	1	0.00	1	-3147.86	1	26131.00	1
	4.00	MAX	0.00	1	0.00	1	-3147.86	1	21933.86	1
		MIN	0.00	1	0.00	1	-3147.86	1	21933.86	1
	5.33	MAX	0.00	1	0.00	1	-3147.86	1	17736.71	1
		MIN	0.00	1	0.00	1	-3147.86	1	17736.71	1
	6.67	MAX	0.00	1	0.00	1	-3147.86	1	13539.57	1
		MIN	0.00	1	0.00	1	-3147.86	1	13539.57	1
	8.00	MAX	0.00	1	0.00	1	-3147.86	1	9342.43	1
		MIN	0.00	1	0.00	1	-3147.86	1	9342.43	1
	9.33	MAX	0.00	1	0.00	1	-3147.86	1	5145.28	1
		MIN	0.00	1	0.00	1	-3147.86	1	5145.28	1
	10.67	MAX	0.00	1	0.00	1	-3147.86	1	948.14	1
		MIN	0.00	1	0.00	1	-3147.86	1	948.14	1
	12.00	MAX	0.00	1	0.00	1	-3147.86	1	-3249.00	1
		MIN	0.00	1	0.00	1	-3147.86	1	-3249.00	1
	13.33	MAX	0.00	1	0.00	1	-3147.86	1	-7446.14	1
		MIN	0.00	1	0.00	1	-3147.86	1	-7446.14	1
	14.67	MAX	0.00	1	0.00	1	-3147.86	1	-11643.29	1
		MIN	0.00	1	0.00	1	-3147.86	1	-11643.29	1
	16.00	MAX	0.00	1	0.00	1	-3147.86	1	-15840.43	1
		MIN	0.00	1	0.00	1	-3147.86	1	-15840.43	1
51	0.00	MAX	0.00	1	0.00	1	3147.86	1	-34525.48	1
		MIN	0.00	1	0.00	1	3147.86	1	-34525.48	1
	1.33	MAX	0.00	1	0.00	1	3147.86	1	-30328.34	1
		MIN	0.00	1	0.00	1	3147.86	1	-30328.34	1
	2.67	MAX	0.00	1	0.00	1	3147.86	1	-26131.20	1
		MIN	0.00	1	0.00	1	3147.86	1	-26131.20	1
	4.00	MAX	0.00	1	0.00	1	3147.86	1	-21934.05	1
		MIN	0.00	1	0.00	1	3147.86	1	-21934.05	1
	5.33	MAX	0.00	1	0.00	1	3147.86	1	-17736.91	1
		MIN	0.00	1	0.00	1	3147.86	1	-17736.91	1
	6.67	MAX	0.00	1	0.00	1	3147.86	1	-13539.77	1
		MIN	0.00	1	0.00	1	3147.86	1	-13539.77	1
	8.00	MAX	0.00	1	0.00	1	3147.86	1	-9342.62	1
		MIN	0.00	1	0.00	1	3147.86	1	-9342.62	1
	9.33	MAX	0.00	1	0.00	1	3147.86	1	-5145.48	1
		MIN	0.00	1	0.00	1	3147.86	1	-5145.48	1
	10.67	MAX	0.00	1	0.00	1	3147.86	1	-948.34	1
		MIN	0.00	1	0.00	1	3147.86	1	-948.34	1
	12.00	MAX	0.00	1	0.00	1	3147.86	1	3248.81	1
		MIN	0.00	1	0.00	1	3147.86	1	3248.81	1
	13.33	MAX	0.00	1	0.00	1	3147.86	1	7445.95	1
		MIN	0.00	1	0.00	1	3147.86	1	7445.95	1
	14.67	MAX	0.00	1	0.00	1	3147.86	1	11643.10	1
		MIN	0.00	1	0.00	1	3147.86	1	11643.10	1
	16.00	MAX	0.00	1	0.00	1	3147.86	1	15840.24	1
		MIN	0.00	1	0.00	1	3147.86	1	15840.24	1

F.4 Selected Output of Case 4 Blast Load

STAAD SPACE
 START JOB INFORMATION
 JOB NAME RESEARCH
 JOB CLIENT FAMU-FSU COLLEGE OF ENGINEERING
 JOB NO 1

```

JOB PART MODEL BRIDGE ANALYSIS
JOB REF LRFD
JOB COMMENT APPLY CASE 4 UNIFORM BLAST LOAD.
ENGINEER NAME ANWAR
ENGINEER DATE 07-FEB-05
END JOB INFORMATION
INPUT WIDTH 79
UNIT FEET KIP
JOINT COORDINATES
1 0 100 0; 2 0 100 3.5; 3 0 100 9.5; 4 0 100 15.5; 5 0 100 21.5; 6 0 100 27.5;
7 0 100 33.5; 8 0 100 39.5; 9 0 100 43; 10 80 100 0; 11 80 100 3.5;
12 80 100 9.5; 13 80 100 15.5; 14 80 100 21.5; 15 80 100 27.5; 16 80 100 33.5;
17 80 100 39.5; 18 80 100 43; 19 160 100 0; 20 160 100 3.5; 21 160 100 9.5;
22 160 100 15.5; 23 160 100 21.5; 24 160 100 27.5; 25 160 100 33.5;
26 160 100 39.5; 27 160 100 43; 28 0 84 3.5; 29 0 84 9.5; 30 0 84 15.5;
31 0 84 21.5; 32 0 84 27.5; 33 0 84 33.5; 34 0 84 39.5; 35 80 84 9.5;
36 80 84 33.5; 37 160 84 3.5; 38 160 84 9.5; 39 160 84 15.5; 40 160 84 21.5;
41 160 84 27.5; 42 160 84 33.5; 43 160 84 39.5; 44 0 100 0.01; 45 0 100 3.51;
46 0 100 9.51; 47 0 100 15.51; 48 0 100 21.51; 49 0 100 27.51;
50 0 100 33.51; 51 0 100 39.51; 52 0 100 42.99; 53 160 100 0.01;
54 160 100 3.51; 55 160 100 9.51; 56 160 100 15.51; 57 160 100 21.51;
58 160 100 27.51; 59 160 100 33.51; 60 160 100 39.51; 61 160 100 42.99;
MEMBER INCIDENCES
1 1 2; 2 2 3; 3 3 4; 4 4 5; 5 5 6; 6 6 7; 7 7 8; 8 8 9; 9 10 11; 10 11 12;
11 12 13; 12 13 14; 13 14 15; 14 15 16; 15 16 17; 16 17 18; 17 19 20; 18 20 21;
19 21 22; 20 22 23; 21 23 24; 22 24 25; 23 25 26; 24 26 27; 25 44 10; 26 45 11;
27 46 12; 28 47 13; 29 48 14; 30 49 15; 31 50 16; 32 51 17; 33 52 18; 34 10 53;
35 11 54; 36 12 55; 37 13 56; 38 14 57; 39 15 58; 40 16 59; 41 17 60; 42 18 61;
43 2 28; 44 3 29; 45 4 30; 46 5 31; 47 6 32; 48 7 33; 49 8 34; 50 12 35;
51 16 36; 52 20 37; 53 21 38; 54 22 39; 55 23 40; 56 24 41; 57 25 42; 58 26 43;
DEFINE MESH
A JOINT 44
B JOINT 45
C JOINT 51
D JOINT 52
E JOINT 61
F JOINT 60
G JOINT 54
H JOINT 53
GENERATE ELEMENT
MESH ABGH 1 16
MESH BCFG 6 16
MESH CDEF 1 16
ELEMENT PROPERTY
59 TO 186 TH 0.667
MEMBER PROPERTY
43 TO 49 52 TO 58 PRIS YD 1.5 ZD 1.5
1 TO 8 17 TO 24 PRIS YD 3 ZD 3
9 TO 16 PRIS YD 4 ZD 4
50 51 PRIS YD 3.5
26 TO 32 35 TO 41 PRIS YD 1.972 ZD 1.972
25 33 34 42 PRIS YD 2.67 ZD 1
DEFINE MATERIAL START
ISOTROPIC MATERIAL1
E 703803
POISSON 0.2
DENSITY 0.15
DAMP 2.8026e-044
ISOTROPIC MATERIAL2
E 647432
POISSON 0.2
DENSITY 0.15
DAMP 2.8026e-044

```

```

ISOTROPIC MATERIAL3
E 585625
POISSON 0.2
DENSITY 0.15
DAMP 2.8026e-044
END DEFINE MATERIAL
CONSTANTS
MATERIAL MATERIAL1 MEMB 26 TO 32 35 TO 41
MATERIAL MATERIAL2 MEMB 1 TO 24 43 TO 49 50 51 52 TO 58
MATERIAL MATERIAL3 MEMB 25 33 34 42 59 TO 186
SUPPORTS
28 TO 43 FIXED
45 TO 51 54 TO 60 PINNED
LOAD 1 CASE 4
MEMBER LOAD
29 UNI GY -639.36 0 20
28 30 UNI GY -380.16 0 20
SELFWEIGHT Y -1.25
PERFORM ANALYSIS
PRINT MEMBER FORCES ALL
PRINT FORCE ENVELOPE ALL
PRINT JOINT DISPLACEMENTS ALL
PRINT SUPPORT REACTION ALL
FINISH

```

P R O B L E M S T A T I S T I C S

```

-----
NUMBER OF JOINTS/MEMBER+ELEMENTS/SUPPORTS =   196/   186/   30
ORIGINAL/FINAL BAND-WIDTH=   136/   28/   174 DOF
TOTAL PRIMARY LOAD CASES =   1, TOTAL DEGREES OF FREEDOM =   1080
SIZE OF STIFFNESS MATRIX =   188 DOUBLE   KILO-WORDS
REQRD/AVAIL. DISK SPACE =   14.8/138998.1 MB,   EXMEM =   794.5 MB

```

MEMBER END FORCES STRUCTURE TYPE = SPACE

ALL UNITS ARE -- KIP FEET

MEMBER	LOAD	JT	AXIAL	SHEAR-Y	SHEAR-Z	TORSION	MOM-Y	MOM-Z
9	1	10	0.00	-112.70	-217.44	-2202.80	23.44	-330.76
		11	0.00	123.20	217.44	2202.80	737.61	-82.08
10	1	11	-0.03	-333.59	-1153.20	-2907.90	-572.75	-555.77
		12	0.03	351.59	1153.20	2907.90	7491.95	-1499.76
11	1	12	545.51	2408.93	1491.02	-47389.38	-7438.93	6655.44
		13	-545.51	-2390.93	-1491.02	47389.38	-1507.20	7744.16
12	1	13	545.50	1025.11	393.66	-21063.93	1407.97	-8891.53
		14	-545.50	-1007.11	-393.66	21063.93	-3769.95	14988.22
13	1	14	545.50	-1008.79	-393.68	21063.82	3769.94	-14995.64
		15	-545.50	1026.79	393.68	-21063.82	-1407.86	8888.92
14	1	15	545.51	-2392.62	-1491.03	47390.11	1507.09	-7751.94
		16	-545.51	2410.62	1491.03	-47390.11	7439.12	-6657.80
15	1	16	-0.03	351.29	1153.19	2909.48	-7492.17	1499.38
		17	0.03	-333.29	-1153.19	-2909.48	573.04	554.39
16	1	17	0.00	123.13	217.53	2202.05	-737.90	82.52
		18	0.00	-112.63	-217.53	-2202.05	-23.45	330.07

50	1	12	3123.74	4238.64	-545.56	40.67	5983.63	47174.27
		35	-3152.60	-4238.64	545.56	-40.67	2745.31	20643.98
51	1	16	3125.12	4238.61	545.56	-40.69	-5983.64	47173.89
		36	-3153.99	-4238.61	-545.56	40.69	-2745.31	20643.84

***** END OF LATEST ANALYSIS RESULT *****

MEMBER FORCE ENVELOPE

MEMB	DISTANCE		FY	LD	MZ	LD	FZ	LD	MY	LD
26	0.00	MAX	-69.17	1	-5798.86	1	1.49	1	-37.12	1
		MIN	-69.17	1	-5798.86	1	1.49	1	-37.12	1
	6.67	MAX	-74.04	1	-5321.50	1	1.49	1	-27.20	1
		MIN	-74.04	1	-5321.50	1	1.49	1	-27.20	1
	13.33	MAX	-78.90	1	-4811.73	1	1.49	1	-17.28	1
		MIN	-78.90	1	-4811.73	1	1.49	1	-17.28	1
	20.00	MAX	-83.76	1	-4269.55	1	1.49	1	-7.35	1
		MIN	-83.76	1	-4269.55	1	1.49	1	-7.35	1
	26.67	MAX	-88.62	1	-3694.97	1	1.49	1	2.57	1
		MIN	-88.62	1	-3694.97	1	1.49	1	2.57	1
	33.33	MAX	-93.48	1	-3087.98	1	1.49	1	12.49	1
		MIN	-93.48	1	-3087.98	1	1.49	1	12.49	1
	40.00	MAX	-98.34	1	-2448.58	1	1.49	1	22.42	1
		MIN	-98.34	1	-2448.58	1	1.49	1	22.42	1
	46.67	MAX	-103.20	1	-1776.78	1	1.49	1	32.34	1
		MIN	-103.20	1	-1776.78	1	1.49	1	32.34	1
	53.33	MAX	-108.06	1	-1072.57	1	1.49	1	42.26	1
		MIN	-108.06	1	-1072.57	1	1.49	1	42.26	1
	60.00	MAX	-112.92	1	-335.95	1	1.49	1	52.19	1
		MIN	-112.92	1	-335.95	1	1.49	1	52.19	1
66.67	MAX	-117.78	1	433.07	1	1.49	1	62.11	1	
	MIN	-117.78	1	433.07	1	1.49	1	62.11	1	
73.33	MAX	-122.64	1	1234.50	1	1.49	1	72.03	1	
	MIN	-122.64	1	1234.50	1	1.49	1	72.03	1	
80.00	MAX	-127.51	1	2068.34	1	1.49	1	81.96	1	
	MIN	-127.51	1	2068.34	1	1.49	1	81.96	1	
27	0.00	MAX	-210.85	1	-13406.53	1	0.08	1	-1.02	1
		MIN	-210.85	1	-13406.53	1	0.08	1	-1.02	1
	6.67	MAX	-215.71	1	-11984.65	1	0.08	1	-0.46	1
		MIN	-215.71	1	-11984.65	1	0.08	1	-0.46	1
	13.33	MAX	-220.57	1	-10530.38	1	0.08	1	0.10	1
		MIN	-220.57	1	-10530.38	1	0.08	1	0.10	1
	20.00	MAX	-225.43	1	-9043.69	1	0.08	1	0.66	1
		MIN	-225.43	1	-9043.69	1	0.08	1	0.66	1
	26.67	MAX	-230.29	1	-7524.60	1	0.08	1	1.22	1
		MIN	-230.29	1	-7524.60	1	0.08	1	1.22	1
	33.33	MAX	-235.16	1	-5973.10	1	0.08	1	1.78	1
		MIN	-235.16	1	-5973.10	1	0.08	1	1.78	1
	40.00	MAX	-240.02	1	-4389.20	1	0.08	1	2.34	1
		MIN	-240.02	1	-4389.20	1	0.08	1	2.34	1
	46.67	MAX	-244.88	1	-2772.89	1	0.08	1	2.90	1
		MIN	-244.88	1	-2772.89	1	0.08	1	2.90	1
	53.33	MAX	-249.74	1	-1124.17	1	0.08	1	3.45	1
		MIN	-249.74	1	-1124.17	1	0.08	1	3.45	1
	60.00	MAX	-254.60	1	556.95	1	0.08	1	4.01	1
		MIN	-254.60	1	556.95	1	0.08	1	4.01	1
66.67	MAX	-259.46	1	2270.48	1	0.08	1	4.57	1	
	MIN	-259.46	1	2270.48	1	0.08	1	4.57	1	

	73.33	MAX	-264.32	1	4016.41	1	0.08	1	5.13	1
		MIN	-264.32	1	4016.41	1	0.08	1	5.13	1
	80.00	MAX	-269.18	1	5794.76	1	0.08	1	5.69	1
		MIN	-269.18	1	5794.76	1	0.08	1	5.69	1
28	0.00	MAX	6408.54	1	8691.70	1	-0.93	1	24.70	1
		MIN	6408.54	1	8691.70	1	-0.93	1	24.70	1
	6.67	MAX	3869.28	1	-25567.71	1	-0.93	1	18.49	1
		MIN	3869.28	1	-25567.71	1	-0.93	1	18.49	1
	13.33	MAX	1330.02	1	-42898.71	1	-0.93	1	12.27	1
		MIN	1330.02	1	-42898.71	1	-0.93	1	12.27	1
	20.00	MAX	-1209.24	1	-43301.31	1	-0.93	1	6.06	1
		MIN	-1209.24	1	-43301.31	1	-0.93	1	6.06	1
	26.67	MAX	-1214.10	1	-35223.50	1	-0.93	1	-0.15	1
		MIN	-1214.10	1	-35223.50	1	-0.93	1	-0.15	1
	33.33	MAX	-1218.96	1	-27113.29	1	-0.93	1	-6.37	1
		MIN	-1218.96	1	-27113.29	1	-0.93	1	-6.37	1
	40.00	MAX	-1223.82	1	-18970.66	1	-0.93	1	-12.58	1
		MIN	-1223.82	1	-18970.66	1	-0.93	1	-12.58	1
	46.67	MAX	-1228.69	1	-10795.63	1	-0.93	1	-18.79	1
		MIN	-1228.69	1	-10795.63	1	-0.93	1	-18.79	1
	53.33	MAX	-1233.55	1	-2588.20	1	-0.93	1	-25.00	1
		MIN	-1233.55	1	-2588.20	1	-0.93	1	-25.00	1
	60.00	MAX	-1238.41	1	5651.65	1	-0.93	1	-31.22	1
		MIN	-1238.41	1	5651.65	1	-0.93	1	-31.22	1
	66.67	MAX	-1243.27	1	13923.89	1	-0.93	1	-37.43	1
		MIN	-1243.27	1	13923.89	1	-0.93	1	-37.43	1
	73.33	MAX	-1248.13	1	22228.55	1	-0.93	1	-43.64	1
		MIN	-1248.13	1	22228.55	1	-0.93	1	-43.64	1
	80.00	MAX	-1252.99	1	30565.60	1	-0.93	1	-49.85	1
29	0.00	MAX	10950.13	1	25428.22	1	0.00	1	0.00	1
		MIN	10950.13	1	25428.22	1	0.00	1	0.00	1
	6.67	MAX	6682.87	1	-33348.44	1	0.00	1	0.00	1
		MIN	6682.87	1	-33348.44	1	0.00	1	0.00	1
	13.33	MAX	2415.61	1	-63676.69	1	0.00	1	0.00	1
		MIN	2415.61	1	-63676.69	1	0.00	1	0.00	1
	20.00	MAX	-1851.65	1	-65556.53	1	0.00	1	0.00	1
		MIN	-1851.65	1	-65556.53	1	0.00	1	0.00	1
	26.67	MAX	-1856.51	1	-53195.97	1	0.00	1	0.00	1
		MIN	-1856.51	1	-53195.97	1	0.00	1	0.00	1
	33.33	MAX	-1861.38	1	-40803.00	1	0.00	1	0.00	1
		MIN	-1861.38	1	-40803.00	1	0.00	1	0.00	1
	40.00	MAX	-1866.24	1	-28377.62	1	0.00	1	0.00	1
		MIN	-1866.24	1	-28377.62	1	0.00	1	0.00	1
	46.67	MAX	-1871.10	1	-15919.84	1	0.00	1	0.00	1
		MIN	-1871.10	1	-15919.84	1	0.00	1	0.00	1
	53.33	MAX	-1875.96	1	-3429.65	1	0.00	1	0.00	1
		MIN	-1875.96	1	-3429.65	1	0.00	1	0.00	1
	60.00	MAX	-1880.82	1	9092.95	1	0.00	1	0.00	1
		MIN	-1880.82	1	9092.95	1	0.00	1	0.00	1
	66.67	MAX	-1885.68	1	21647.95	1	0.00	1	0.00	1
		MIN	-1885.68	1	21647.95	1	0.00	1	0.00	1
	73.33	MAX	-1890.54	1	34235.36	1	0.00	1	0.00	1
		MIN	-1890.54	1	34235.36	1	0.00	1	0.00	1
	80.00	MAX	-1895.40	1	46855.12	1	0.00	1	0.00	1
		MIN	-1895.40	1	46855.12	1	0.00	1	0.00	1
30	0.00	MAX	6408.52	1	8690.71	1	0.93	1	-24.70	1
		MIN	6408.52	1	8690.71	1	0.93	1	-24.70	1
	6.67	MAX	3869.26	1	-25568.58	1	0.93	1	-18.48	1
		MIN	3869.26	1	-25568.58	1	0.93	1	-18.48	1

	13.33	MAX	1330.00	1	-42899.45	1	0.93	1	-12.27	1
		MIN	1330.00	1	-42899.45	1	0.93	1	-12.27	1
	20.00	MAX	-1209.26	1	-43301.92	1	0.93	1	-6.06	1
		MIN	-1209.26	1	-43301.92	1	0.93	1	-6.06	1
	26.67	MAX	-1214.12	1	-35223.98	1	0.93	1	0.15	1
		MIN	-1214.12	1	-35223.98	1	0.93	1	0.15	1
	33.33	MAX	-1218.98	1	-27113.64	1	0.93	1	6.37	1
		MIN	-1218.98	1	-27113.64	1	0.93	1	6.37	1
	40.00	MAX	-1223.84	1	-18970.89	1	0.93	1	12.58	1
		MIN	-1223.84	1	-18970.89	1	0.93	1	12.58	1
	46.67	MAX	-1228.70	1	-10795.74	1	0.93	1	18.79	1
		MIN	-1228.70	1	-10795.74	1	0.93	1	18.79	1
	53.33	MAX	-1233.57	1	-2588.17	1	0.93	1	25.00	1
		MIN	-1233.57	1	-2588.17	1	0.93	1	25.00	1
	60.00	MAX	-1238.43	1	5651.80	1	0.93	1	31.22	1
		MIN	-1238.43	1	5651.80	1	0.93	1	31.22	1
	66.67	MAX	-1243.29	1	13924.17	1	0.93	1	37.43	1
		MIN	-1243.29	1	13924.17	1	0.93	1	37.43	1
	73.33	MAX	-1248.15	1	22228.95	1	0.93	1	43.64	1
		MIN	-1248.15	1	22228.95	1	0.93	1	43.64	1
	80.00	MAX	-1253.01	1	30566.14	1	0.93	1	49.85	1
		MIN	-1253.01	1	30566.14	1	0.93	1	49.85	1
31	0.00	MAX	-210.85	1	-13406.38	1	-0.08	1	1.02	1
		MIN	-210.85	1	-13406.38	1	-0.08	1	1.02	1
	6.67	MAX	-215.71	1	-11984.53	1	-0.08	1	0.46	1
		MIN	-215.71	1	-11984.53	1	-0.08	1	0.46	1
	13.33	MAX	-220.57	1	-10530.26	1	-0.08	1	-0.10	1
		MIN	-220.57	1	-10530.26	1	-0.08	1	-0.10	1
	20.00	MAX	-225.43	1	-9043.59	1	-0.08	1	-0.66	1
		MIN	-225.43	1	-9043.59	1	-0.08	1	-0.66	1
	26.67	MAX	-230.29	1	-7524.51	1	-0.08	1	-1.22	1
		MIN	-230.29	1	-7524.51	1	-0.08	1	-1.22	1
	33.33	MAX	-235.15	1	-5973.03	1	-0.08	1	-1.78	1
		MIN	-235.15	1	-5973.03	1	-0.08	1	-1.78	1
	40.00	MAX	-240.01	1	-4389.14	1	-0.08	1	-2.34	1
		MIN	-240.01	1	-4389.14	1	-0.08	1	-2.34	1
	46.67	MAX	-244.88	1	-2772.84	1	-0.08	1	-2.90	1
		MIN	-244.88	1	-2772.84	1	-0.08	1	-2.90	1
	53.33	MAX	-249.74	1	-1124.14	1	-0.08	1	-3.45	1
		MIN	-249.74	1	-1124.14	1	-0.08	1	-3.45	1
	60.00	MAX	-254.60	1	556.97	1	-0.08	1	-4.01	1
		MIN	-254.60	1	556.97	1	-0.08	1	-4.01	1
	66.67	MAX	-259.46	1	2270.49	1	-0.08	1	-4.57	1
		MIN	-259.46	1	2270.49	1	-0.08	1	-4.57	1
	73.33	MAX	-264.32	1	4016.41	1	-0.08	1	-5.13	1
		MIN	-264.32	1	4016.41	1	-0.08	1	-5.13	1
	80.00	MAX	-269.18	1	5794.74	1	-0.08	1	-5.69	1
		MIN	-269.18	1	5794.74	1	-0.08	1	-5.69	1
32	0.00	MAX	-69.02	1	-5790.33	1	-1.49	1	37.11	1
		MIN	-69.02	1	-5790.33	1	-1.49	1	37.11	1
	6.67	MAX	-73.88	1	-5314.03	1	-1.49	1	27.19	1
		MIN	-73.88	1	-5314.03	1	-1.49	1	27.19	1
	13.33	MAX	-78.74	1	-4805.31	1	-1.49	1	17.27	1
		MIN	-78.74	1	-4805.31	1	-1.49	1	17.27	1
	20.00	MAX	-83.60	1	-4264.20	1	-1.49	1	7.35	1
		MIN	-83.60	1	-4264.20	1	-1.49	1	7.35	1
	26.67	MAX	-88.46	1	-3690.67	1	-1.49	1	-2.58	1
		MIN	-88.46	1	-3690.67	1	-1.49	1	-2.58	1
	33.33	MAX	-93.32	1	-3084.74	1	-1.49	1	-12.50	1
		MIN	-93.32	1	-3084.74	1	-1.49	1	-12.50	1
	40.00	MAX	-98.18	1	-2446.40	1	-1.49	1	-22.42	1

		MIN	-98.18	1	-2446.40	1	-1.49	1	-22.42	1
46.67		MAX	-103.04	1	-1775.66	1	-1.49	1	-32.34	1
		MIN	-103.04	1	-1775.66	1	-1.49	1	-32.34	1
53.33		MAX	-107.90	1	-1072.51	1	-1.49	1	-42.27	1
		MIN	-107.90	1	-1072.51	1	-1.49	1	-42.27	1
60.00		MAX	-112.76	1	-336.95	1	-1.49	1	-52.19	1
		MIN	-112.76	1	-336.95	1	-1.49	1	-52.19	1
66.67		MAX	-117.63	1	431.02	1	-1.49	1	-62.11	1
		MIN	-117.63	1	431.02	1	-1.49	1	-62.11	1
73.33		MAX	-122.49	1	1231.39	1	-1.49	1	-72.03	1
		MIN	-122.49	1	1231.39	1	-1.49	1	-72.03	1
80.00		MAX	-127.35	1	2064.16	1	-1.49	1	-81.96	1
		MIN	-127.35	1	2064.16	1	-1.49	1	-81.96	1
35	0.00	MAX	82.88	1	2773.37	1	1.51	1	-82.91	1
		MIN	82.88	1	2773.37	1	1.51	1	-82.91	1
	6.67	MAX	78.02	1	2237.04	1	1.51	1	-72.84	1
		MIN	78.02	1	2237.04	1	1.51	1	-72.84	1
	13.33	MAX	73.16	1	1733.13	1	1.51	1	-62.76	1
		MIN	73.16	1	1733.13	1	1.51	1	-62.76	1
	20.00	MAX	68.30	1	1261.62	1	1.51	1	-52.69	1
		MIN	68.30	1	1261.62	1	1.51	1	-52.69	1
	26.67	MAX	63.43	1	822.52	1	1.51	1	-42.61	1
		MIN	63.43	1	822.52	1	1.51	1	-42.61	1
	33.33	MAX	58.57	1	415.82	1	1.51	1	-32.54	1
		MIN	58.57	1	415.82	1	1.51	1	-32.54	1
	40.00	MAX	53.71	1	41.53	1	1.51	1	-22.46	1
		MIN	53.71	1	41.53	1	1.51	1	-22.46	1
	46.67	MAX	48.85	1	-300.35	1	1.51	1	-12.39	1
		MIN	48.85	1	-300.35	1	1.51	1	-12.39	1
	53.33	MAX	43.99	1	-609.83	1	1.51	1	-2.32	1
		MIN	43.99	1	-609.83	1	1.51	1	-2.32	1
	60.00	MAX	39.13	1	-886.90	1	1.51	1	7.76	1
		MIN	39.13	1	-886.90	1	1.51	1	7.76	1
	66.67	MAX	34.27	1	-1131.56	1	1.51	1	17.83	1
		MIN	34.27	1	-1131.56	1	1.51	1	17.83	1
	73.33	MAX	29.41	1	-1343.82	1	1.51	1	27.91	1
		MIN	29.41	1	-1343.82	1	1.51	1	27.91	1
	80.00	MAX	24.55	1	-1523.67	1	1.51	1	37.98	1
36	0.00	MAX	94.04	1	3101.86	1	0.11	1	-6.66	1
		MIN	94.04	1	3101.86	1	0.11	1	-6.66	1
	6.67	MAX	89.18	1	2491.15	1	0.11	1	-5.95	1
		MIN	89.18	1	2491.15	1	0.11	1	-5.95	1
	13.33	MAX	84.32	1	1912.84	1	0.11	1	-5.23	1
		MIN	84.32	1	1912.84	1	0.11	1	-5.23	1
	20.00	MAX	79.45	1	1366.94	1	0.11	1	-4.52	1
		MIN	79.45	1	1366.94	1	0.11	1	-4.52	1
	26.67	MAX	74.59	1	853.45	1	0.11	1	-3.80	1
		MIN	74.59	1	853.45	1	0.11	1	-3.80	1
	33.33	MAX	69.73	1	372.36	1	0.11	1	-3.09	1
		MIN	69.73	1	372.36	1	0.11	1	-3.09	1
	40.00	MAX	64.87	1	-76.31	1	0.11	1	-2.38	1
		MIN	64.87	1	-76.31	1	0.11	1	-2.38	1
	46.67	MAX	60.01	1	-492.59	1	0.11	1	-1.66	1
		MIN	60.01	1	-492.59	1	0.11	1	-1.66	1
	53.33	MAX	55.15	1	-876.45	1	0.11	1	-0.95	1
		MIN	55.15	1	-876.45	1	0.11	1	-0.95	1
	60.00	MAX	50.29	1	-1227.91	1	0.11	1	-0.23	1
		MIN	50.29	1	-1227.91	1	0.11	1	-0.23	1
	66.67	MAX	45.43	1	-1546.96	1	0.11	1	0.48	1
		MIN	45.43	1	-1546.96	1	0.11	1	0.48	1
	73.33	MAX	40.57	1	-1833.61	1	0.11	1	1.20	1

		MIN	40.57	1	-1833.61	1	0.11	1	1.20	1
80.00		MAX	35.71	1	-2087.85	1	0.11	1	1.91	1
		MIN	35.71	1	-2087.85	1	0.11	1	1.91	1
37	0.00	MAX	112.83	1	4240.00	1	-0.92	1	49.37	1
		MIN	112.83	1	4240.00	1	-0.92	1	49.37	1
	6.67	MAX	107.97	1	3504.01	1	-0.92	1	43.24	1
		MIN	107.97	1	3504.01	1	-0.92	1	43.24	1
	13.33	MAX	103.11	1	2800.43	1	-0.92	1	37.10	1
		MIN	103.11	1	2800.43	1	-0.92	1	37.10	1
	20.00	MAX	98.25	1	2129.25	1	-0.92	1	30.96	1
		MIN	98.25	1	2129.25	1	-0.92	1	30.96	1
	26.67	MAX	93.38	1	1490.48	1	-0.92	1	24.83	1
		MIN	93.38	1	1490.48	1	-0.92	1	24.83	1
	33.33	MAX	88.52	1	884.12	1	-0.92	1	18.69	1
		MIN	88.52	1	884.12	1	-0.92	1	18.69	1
	40.00	MAX	83.66	1	310.16	1	-0.92	1	12.56	1
		MIN	83.66	1	310.16	1	-0.92	1	12.56	1
	46.67	MAX	78.80	1	-231.39	1	-0.92	1	6.42	1
		MIN	78.80	1	-231.39	1	-0.92	1	6.42	1
	53.33	MAX	73.94	1	-740.53	1	-0.92	1	0.29	1
		MIN	73.94	1	-740.53	1	-0.92	1	0.29	1
	60.00	MAX	69.08	1	-1217.27	1	-0.92	1	-5.85	1
		MIN	69.08	1	-1217.27	1	-0.92	1	-5.85	1
	66.67	MAX	64.22	1	-1661.60	1	-0.92	1	-11.99	1
		MIN	64.22	1	-1661.60	1	-0.92	1	-11.99	1
	73.33	MAX	59.36	1	-2073.52	1	-0.92	1	-18.12	1
		MIN	59.36	1	-2073.52	1	-0.92	1	-18.12	1
	80.00	MAX	54.50	1	-2453.04	1	-0.92	1	-24.26	1
		MIN	54.50	1	-2453.04	1	-0.92	1	-24.26	1
38	0.00	MAX	120.50	1	4727.37	1	0.00	1	0.00	1
		MIN	120.50	1	4727.37	1	0.00	1	0.00	1
	6.67	MAX	115.64	1	3940.25	1	0.00	1	0.00	1
		MIN	115.64	1	3940.25	1	0.00	1	0.00	1
	13.33	MAX	110.78	1	3185.53	1	0.00	1	0.00	1
		MIN	110.78	1	3185.53	1	0.00	1	0.00	1
	20.00	MAX	105.92	1	2463.22	1	0.00	1	0.00	1
		MIN	105.92	1	2463.22	1	0.00	1	0.00	1
	26.67	MAX	101.06	1	1773.31	1	0.00	1	0.00	1
		MIN	101.06	1	1773.31	1	0.00	1	0.00	1
	33.33	MAX	96.19	1	1115.81	1	0.00	1	0.00	1
		MIN	96.19	1	1115.81	1	0.00	1	0.00	1
	40.00	MAX	91.33	1	490.72	1	0.00	1	0.00	1
		MIN	91.33	1	490.72	1	0.00	1	0.00	1
	46.67	MAX	86.47	1	-101.97	1	0.00	1	0.00	1
		MIN	86.47	1	-101.97	1	0.00	1	0.00	1
	53.33	MAX	81.61	1	-662.25	1	0.00	1	0.00	1
		MIN	81.61	1	-662.25	1	0.00	1	0.00	1
	60.00	MAX	76.75	1	-1190.12	1	0.00	1	0.00	1
		MIN	76.75	1	-1190.12	1	0.00	1	0.00	1
	66.67	MAX	71.89	1	-1685.59	1	0.00	1	0.00	1
		MIN	71.89	1	-1685.59	1	0.00	1	0.00	1
	73.33	MAX	67.03	1	-2148.65	1	0.00	1	0.00	1
		MIN	67.03	1	-2148.65	1	0.00	1	0.00	1
	80.00	MAX	62.17	1	-2579.30	1	0.00	1	0.00	1
		MIN	62.17	1	-2579.30	1	0.00	1	0.00	1
39	0.00	MAX	112.83	1	4240.01	1	0.92	1	-49.37	1
		MIN	112.83	1	4240.01	1	0.92	1	-49.37	1
	6.67	MAX	107.97	1	3504.02	1	0.92	1	-43.24	1
		MIN	107.97	1	3504.02	1	0.92	1	-43.24	1
	13.33	MAX	103.11	1	2800.44	1	0.92	1	-37.10	1

		MIN	103.11	1	2800.44	1	0.92	1	-37.10	1
20.00		MAX	98.25	1	2129.27	1	0.92	1	-30.96	1
		MIN	98.25	1	2129.27	1	0.92	1	-30.96	1
26.67		MAX	93.38	1	1490.51	1	0.92	1	-24.83	1
		MIN	93.38	1	1490.51	1	0.92	1	-24.83	1
33.33		MAX	88.52	1	884.15	1	0.92	1	-18.69	1
		MIN	88.52	1	884.15	1	0.92	1	-18.69	1
40.00		MAX	83.66	1	310.20	1	0.92	1	-12.56	1
		MIN	83.66	1	310.20	1	0.92	1	-12.56	1
46.67		MAX	78.80	1	-231.35	1	0.92	1	-6.42	1
		MIN	78.80	1	-231.35	1	0.92	1	-6.42	1
53.33		MAX	73.94	1	-740.48	1	0.92	1	-0.29	1
		MIN	73.94	1	-740.48	1	0.92	1	-0.29	1
60.00		MAX	69.08	1	-1217.22	1	0.92	1	5.85	1
		MIN	69.08	1	-1217.22	1	0.92	1	5.85	1
66.67		MAX	64.22	1	-1661.54	1	0.92	1	11.98	1
		MIN	64.22	1	-1661.54	1	0.92	1	11.98	1
73.33		MAX	59.36	1	-2073.46	1	0.92	1	18.12	1
		MIN	59.36	1	-2073.46	1	0.92	1	18.12	1
80.00		MAX	54.50	1	-2452.97	1	0.92	1	24.26	1
		MIN	54.50	1	-2452.97	1	0.92	1	24.26	1
40	0.00	MAX	94.03	1	3101.59	1	-0.11	1	6.66	1
		MIN	94.03	1	3101.59	1	-0.11	1	6.66	1
	6.67	MAX	89.17	1	2490.95	1	-0.11	1	5.95	1
		MIN	89.17	1	2490.95	1	-0.11	1	5.95	1
	13.33	MAX	84.30	1	1912.72	1	-0.11	1	5.23	1
		MIN	84.30	1	1912.72	1	-0.11	1	5.23	1
	20.00	MAX	79.44	1	1366.89	1	-0.11	1	4.52	1
		MIN	79.44	1	1366.89	1	-0.11	1	4.52	1
	26.67	MAX	74.58	1	853.47	1	-0.11	1	3.80	1
		MIN	74.58	1	853.47	1	-0.11	1	3.80	1
	33.33	MAX	69.72	1	372.46	1	-0.11	1	3.09	1
		MIN	69.72	1	372.46	1	-0.11	1	3.09	1
	40.00	MAX	64.86	1	-76.15	1	-0.11	1	2.38	1
		MIN	64.86	1	-76.15	1	-0.11	1	2.38	1
	46.67	MAX	60.00	1	-492.35	1	-0.11	1	1.66	1
		MIN	60.00	1	-492.35	1	-0.11	1	1.66	1
	53.33	MAX	55.14	1	-876.15	1	-0.11	1	0.95	1
		MIN	55.14	1	-876.15	1	-0.11	1	0.95	1
	60.00	MAX	50.28	1	-1227.53	1	-0.11	1	0.23	1
		MIN	50.28	1	-1227.53	1	-0.11	1	0.23	1
	66.67	MAX	45.42	1	-1546.52	1	-0.11	1	-0.48	1
		MIN	45.42	1	-1546.52	1	-0.11	1	-0.48	1
	73.33	MAX	40.56	1	-1833.09	1	-0.11	1	-1.20	1
		MIN	40.56	1	-1833.09	1	-0.11	1	-1.20	1
	80.00	MAX	35.69	1	-2087.26	1	-0.11	1	-1.91	1
		MIN	35.69	1	-2087.26	1	-0.11	1	-1.91	1
41	0.00	MAX	82.81	1	2771.66	1	-1.51	1	82.91	1
		MIN	82.81	1	2771.66	1	-1.51	1	82.91	1
	6.67	MAX	77.95	1	2235.76	1	-1.51	1	72.84	1
		MIN	77.95	1	2235.76	1	-1.51	1	72.84	1
	13.33	MAX	73.09	1	1732.27	1	-1.51	1	62.76	1
		MIN	73.09	1	1732.27	1	-1.51	1	62.76	1
	20.00	MAX	68.23	1	1261.19	1	-1.51	1	52.69	1
		MIN	68.23	1	1261.19	1	-1.51	1	52.69	1
	26.67	MAX	63.37	1	822.51	1	-1.51	1	42.62	1
		MIN	63.37	1	822.51	1	-1.51	1	42.62	1
	33.33	MAX	58.51	1	416.25	1	-1.51	1	32.54	1
		MIN	58.51	1	416.25	1	-1.51	1	32.54	1
	40.00	MAX	53.65	1	42.38	1	-1.51	1	22.47	1
		MIN	53.65	1	42.38	1	-1.51	1	22.47	1

	46.67	MAX	48.79	1	-299.07	1	-1.51	1	12.40	1
		MIN	48.79	1	-299.07	1	-1.51	1	12.40	1
	53.33	MAX	43.93	1	-608.12	1	-1.51	1	2.32	1
		MIN	43.93	1	-608.12	1	-1.51	1	2.32	1
	60.00	MAX	39.07	1	-884.77	1	-1.51	1	-7.75	1
		MIN	39.07	1	-884.77	1	-1.51	1	-7.75	1
	66.67	MAX	34.20	1	-1129.00	1	-1.51	1	-17.82	1
		MIN	34.20	1	-1129.00	1	-1.51	1	-17.82	1
	73.33	MAX	29.34	1	-1340.83	1	-1.51	1	-27.90	1
		MIN	29.34	1	-1340.83	1	-1.51	1	-27.90	1
	80.00	MAX	24.48	1	-1520.26	1	-1.51	1	-37.97	1
		MIN	24.48	1	-1520.26	1	-1.51	1	-37.97	1
50	0.00	MAX	4238.64	1	47174.27	1	-545.56	1	5983.63	1
		MIN	4238.64	1	47174.27	1	-545.56	1	5983.63	1
	1.33	MAX	4238.64	1	41522.75	1	-545.56	1	5256.22	1
		MIN	4238.64	1	41522.75	1	-545.56	1	5256.22	1
	2.67	MAX	4238.64	1	35871.23	1	-545.56	1	4528.81	1
		MIN	4238.64	1	35871.23	1	-545.56	1	4528.81	1
	4.00	MAX	4238.64	1	30219.70	1	-545.56	1	3801.40	1
		MIN	4238.64	1	30219.70	1	-545.56	1	3801.40	1
	5.33	MAX	4238.64	1	24568.18	1	-545.56	1	3073.99	1
		MIN	4238.64	1	24568.18	1	-545.56	1	3073.99	1
	6.67	MAX	4238.64	1	18916.66	1	-545.56	1	2346.57	1
		MIN	4238.64	1	18916.66	1	-545.56	1	2346.57	1
	8.00	MAX	4238.64	1	13265.14	1	-545.56	1	1619.16	1
		MIN	4238.64	1	13265.14	1	-545.56	1	1619.16	1
	9.33	MAX	4238.64	1	7613.62	1	-545.56	1	891.75	1
		MIN	4238.64	1	7613.62	1	-545.56	1	891.75	1
	10.67	MAX	4238.64	1	1962.10	1	-545.56	1	164.34	1
		MIN	4238.64	1	1962.10	1	-545.56	1	164.34	1
	12.00	MAX	4238.64	1	-3689.42	1	-545.56	1	-563.07	1
		MIN	4238.64	1	-3689.42	1	-545.56	1	-563.07	1
	13.33	MAX	4238.64	1	-9340.94	1	-545.56	1	-1290.49	1
		MIN	4238.64	1	-9340.94	1	-545.56	1	-1290.49	1
	14.67	MAX	4238.64	1	-14992.46	1	-545.56	1	-2017.90	1
		MIN	4238.64	1	-14992.46	1	-545.56	1	-2017.90	1
	16.00	MAX	4238.64	1	-20643.98	1	-545.56	1	-2745.31	1
		MIN	4238.64	1	-20643.98	1	-545.56	1	-2745.31	1
51	0.00	MAX	4238.61	1	47173.89	1	545.56	1	-5983.64	1
		MIN	4238.61	1	47173.89	1	545.56	1	-5983.64	1
	1.33	MAX	4238.61	1	41522.41	1	545.56	1	-5256.23	1
		MIN	4238.61	1	41522.41	1	545.56	1	-5256.23	1
	2.67	MAX	4238.61	1	35870.94	1	545.56	1	-4528.82	1
		MIN	4238.61	1	35870.94	1	545.56	1	-4528.82	1
	4.00	MAX	4238.61	1	30219.46	1	545.56	1	-3801.40	1
		MIN	4238.61	1	30219.46	1	545.56	1	-3801.40	1
	5.33	MAX	4238.61	1	24567.98	1	545.56	1	-3073.99	1
		MIN	4238.61	1	24567.98	1	545.56	1	-3073.99	1
	6.67	MAX	4238.61	1	18916.51	1	545.56	1	-2346.58	1
		MIN	4238.61	1	18916.51	1	545.56	1	-2346.58	1
	8.00	MAX	4238.61	1	13265.03	1	545.56	1	-1619.17	1
		MIN	4238.61	1	13265.03	1	545.56	1	-1619.17	1
	9.33	MAX	4238.61	1	7613.55	1	545.56	1	-891.76	1
		MIN	4238.61	1	7613.55	1	545.56	1	-891.76	1
	10.67	MAX	4238.61	1	1962.07	1	545.56	1	-164.34	1
		MIN	4238.61	1	1962.07	1	545.56	1	-164.34	1
	12.00	MAX	4238.61	1	-3689.40	1	545.56	1	563.07	1
		MIN	4238.61	1	-3689.40	1	545.56	1	563.07	1
	13.33	MAX	4238.61	1	-9340.88	1	545.56	1	1290.48	1
		MIN	4238.61	1	-9340.88	1	545.56	1	1290.48	1
	14.67	MAX	4238.61	1	-14992.36	1	545.56	1	2017.89	1

	MIN	4238.61	1	-14992.36	1	545.56	1	2017.89	1
16.00	MAX	4238.61	1	-20643.84	1	545.56	1	2745.31	1
	MIN	4238.61	1	-20643.84	1	545.56	1	2745.31	1

F.5 Selected Output of Case 5 Blast Load

```

STAAD SPACE
START JOB INFORMATION
JOB NAME RESEARCH
JOB CLIENT FAMU-FSU COLLEGE OF ENGINEERING
JOB NO 1
JOB PART MODEL BRIDGE ANALYSIS
JOB REF LRFD
JOB COMMENT APPLY CASE 5 UNIFORM BLAST LOAD.
ENGINEER NAME ANWAR
ENGINEER DATE 07-FEB-05
END JOB INFORMATION
INPUT WIDTH 79
UNIT FEET KIP
JOINT COORDINATES
1 0 100 0; 2 0 100 3.5; 3 0 100 9.5; 4 0 100 15.5; 5 0 100 21.5; 6 0 100 27.5;
7 0 100 33.5; 8 0 100 39.5; 9 0 100 43; 10 80 100 0; 11 80 100 3.5;
12 80 100 9.5; 13 80 100 15.5; 14 80 100 21.5; 15 80 100 27.5; 16 80 100 33.5;
17 80 100 39.5; 18 80 100 43; 19 160 100 0; 20 160 100 3.5; 21 160 100 9.5;
22 160 100 15.5; 23 160 100 21.5; 24 160 100 27.5; 25 160 100 33.5;
26 160 100 39.5; 27 160 100 43; 28 0 84 3.5; 29 0 84 9.5; 30 0 84 15.5;
31 0 84 21.5; 32 0 84 27.5; 33 0 84 33.5; 34 0 84 39.5; 35 80 84 9.5;
36 80 84 33.5; 37 160 84 3.5; 38 160 84 9.5; 39 160 84 15.5; 40 160 84 21.5;
41 160 84 27.5; 42 160 84 33.5; 43 160 84 39.5; 44 0 100 0.01; 45 0 100 3.51;
46 0 100 9.51; 47 0 100 15.51; 48 0 100 21.51; 49 0 100 27.51;
50 0 100 33.51; 51 0 100 39.51; 52 0 100 42.99; 53 160 100 0.01;
54 160 100 3.51; 55 160 100 9.51; 56 160 100 15.51; 57 160 100 21.51;
58 160 100 27.51; 59 160 100 33.51; 60 160 100 39.51; 61 160 100 42.99;
MEMBER INCIDENCES
1 1 2; 2 2 3; 3 3 4; 4 4 5; 5 5 6; 6 6 7; 7 7 8; 8 8 9; 9 10 11; 10 11 12;
11 12 13; 12 13 14; 13 14 15; 14 15 16; 15 16 17; 16 17 18; 17 19 20; 18 20 21;
19 21 22; 20 22 23; 21 23 24; 22 24 25; 23 25 26; 24 26 27; 25 44 10; 26 45 11;
27 46 12; 28 47 13; 29 48 14; 30 49 15; 31 50 16; 32 51 17; 33 52 18; 34 10 53;
35 11 54; 36 12 55; 37 13 56; 38 14 57; 39 15 58; 40 16 59; 41 17 60; 42 18 61;
43 2 28; 44 3 29; 45 4 30; 46 5 31; 47 6 32; 48 7 33; 49 8 34; 50 12 35;
51 16 36; 52 20 37; 53 21 38; 54 22 39; 55 23 40; 56 24 41; 57 25 42; 58 26 43;
DEFINE MESH
A JOINT 44
B JOINT 45
C JOINT 51
D JOINT 52
E JOINT 61
F JOINT 60
G JOINT 54
H JOINT 53
GENERATE ELEMENT
MESH ABGH 1 16
MESH BCFG 6 16
MESH CDEF 1 16
ELEMENT PROPERTY
59 TO 186 TH 0.667
MEMBER PROPERTY
43 TO 49 52 TO 58 PRIS YD 1.5 ZD 1.5

```

```

1 TO 8 17 TO 24 PRIS YD 3 ZD 3
9 TO 16 PRIS YD 4 ZD 4
50 51 PRIS YD 3.5
26 TO 32 35 TO 41 PRIS YD 1.972 ZD 1.972
25 33 34 42 PRIS YD 2.67 ZD 1
DEFINE MATERIAL START
ISOTROPIC MATERIAL1
E 703803
POISSON 0.2
DENSITY 0.15
DAMP 2.8026e-044
ISOTROPIC MATERIAL2
E 647432
POISSON 0.2
DENSITY 0.15
DAMP 2.8026e-044
ISOTROPIC MATERIAL3
E 585625
POISSON 0.2
DENSITY 0.15
DAMP 2.8026e-044
END DEFINE MATERIAL
CONSTANTS
MATERIAL MATERIAL1 MEMB 26 TO 32 35 TO 41
MATERIAL MATERIAL2 MEMB 1 TO 24 43 TO 49 50 51 52 TO 58
MATERIAL MATERIAL3 MEMB 25 33 34 42 59 TO 186
SUPPORTS
28 TO 43 FIXED
45 TO 51 54 TO 60 PINNED
LOAD 1 CASE 5
MEMBER LOAD
51 UNI GX 540 6 14
13 TO 15 UNI GY 236.16
SELFWEIGHT Y -1.25
PERFORM ANALYSIS
PRINT MEMBER FORCES ALL
PRINT FORCE ENVELOPE ALL
PRINT JOINT DISPLACEMENTS ALL
PRINT SUPPORT REACTION ALL
FINISH

```

P R O B L E M S T A T I S T I C S

```

-----
NUMBER OF JOINTS/MEMBER+ELEMENTS/SUPPORTS = 196/ 186/ 30
ORIGINAL/FINAL BAND-WIDTH= 136/ 28/ 174 DOF
TOTAL PRIMARY LOAD CASES = 1, TOTAL DEGREES OF FREEDOM = 1080
SIZE OF STIFFNESS MATRIX = 188 DOUBLE KILO-WORDS
REQRD/AVAIL. DISK SPACE = 14.8/138997.9 MB, EXMEM = 792.7 MB

```

MEMBER END FORCES STRUCTURE TYPE = SPACE

ALL UNITS ARE -- KIP FEET

MEMBER	LOAD	JT	AXIAL	SHEAR-Y	SHEAR-Z	TORSION	MOM-Y	MOM-Z
9	1	10	0.01	-73.06	-8.92	-42.61	0.55	-76.17
		11	-0.01	83.56	8.92	42.61	30.67	-197.93
10	1	11	0.11	-198.22	-37.01	-83.50	-26.67	76.24
		12	-0.11	216.22	37.01	83.50	248.73	-1319.58

11	1	12	-164.97	-308.99	-11.38	-831.35	-256.37	-634.90
		13	164.97	326.99	11.38	831.35	324.63	-1273.06
12	1	13	-164.88	-458.49	-14.11	-910.83	-336.71	1249.19
		14	164.88	476.49	14.11	910.83	421.37	-4054.12
13	1	14	-164.80	-608.33	76.66	-1030.16	-447.82	4043.87
		15	164.80	-790.63	-76.66	1030.16	-12.11	-3496.96
14	1	15	-164.71	659.01	332.40	-1195.17	-22.84	3510.78
		16	164.71	-2057.97	-332.40	1195.17	-1971.55	4640.16
15	1	16	-0.09	-1200.51	-302.89	392.14	1976.14	-2909.98
		17	0.09	-198.45	302.89	-392.14	-158.80	-96.18
16	1	17	-0.01	83.77	-59.08	197.36	200.81	202.21
		18	0.01	-73.27	59.08	-197.36	5.96	72.60
50	1	12	36.00	62.71	165.17	-6.49	-1914.82	705.32
		35	-64.86	-62.71	-165.17	6.49	-727.93	298.10
51	1	16	-3129.62	-1039.97	-164.54	2.89	1701.47	-1806.61
		36	3100.76	-3280.03	164.54	-2.89	931.23	11087.06

***** END OF LATEST ANALYSIS RESULT *****

MEMBER FORCE ENVELOPE

MEMB	DISTANCE		FY	LD	MZ	LD	FZ	LD	MY	LD
26	0.00	MAX	1.24	1	-1118.73	1	0.09	1	-3.41	1
		MIN	1.24	1	-1118.73	1	0.09	1	-3.41	1
	6.67	MAX	-3.62	1	-1110.82	1	0.09	1	-2.79	1
		MIN	-3.62	1	-1110.82	1	0.09	1	-2.79	1
	13.33	MAX	-8.48	1	-1070.49	1	0.09	1	-2.16	1
		MIN	-8.48	1	-1070.49	1	0.09	1	-2.16	1
	20.00	MAX	-13.34	1	-997.77	1	0.09	1	-1.54	1
		MIN	-13.34	1	-997.77	1	0.09	1	-1.54	1
	26.67	MAX	-18.20	1	-892.63	1	0.09	1	-0.92	1
		MIN	-18.20	1	-892.63	1	0.09	1	-0.92	1
	33.33	MAX	-23.06	1	-755.09	1	0.09	1	-0.30	1
		MIN	-23.06	1	-755.09	1	0.09	1	-0.30	1
	40.00	MAX	-27.92	1	-585.14	1	0.09	1	0.32	1
		MIN	-27.92	1	-585.14	1	0.09	1	0.32	1
	46.67	MAX	-32.78	1	-382.79	1	0.09	1	0.94	1
		MIN	-32.78	1	-382.79	1	0.09	1	0.94	1
	53.33	MAX	-37.64	1	-148.03	1	0.09	1	1.57	1
		MIN	-37.64	1	-148.03	1	0.09	1	1.57	1
	60.00	MAX	-42.51	1	119.14	1	0.09	1	2.19	1
		MIN	-42.51	1	119.14	1	0.09	1	2.19	1
	66.67	MAX	-47.37	1	418.71	1	0.09	1	2.81	1
		MIN	-47.37	1	418.71	1	0.09	1	2.81	1
	73.33	MAX	-52.23	1	750.69	1	0.09	1	3.43	1
		MIN	-52.23	1	750.69	1	0.09	1	3.43	1
	80.00	MAX	-57.09	1	1115.08	1	0.09	1	4.05	1
		MIN	-57.09	1	1115.08	1	0.09	1	4.05	1
27	0.00	MAX	-5.82	1	-1493.17	1	0.05	1	-2.25	1
		MIN	-5.82	1	-1493.17	1	0.05	1	-2.25	1
		MAX	-10.68	1	-1438.14	1	0.05	1	-1.94	1

		MIN	-10.68	1	-1438.14	1	0.05	1	-1.94	1
13.33		MAX	-15.54	1	-1350.71	1	0.05	1	-1.63	1
		MIN	-15.54	1	-1350.71	1	0.05	1	-1.63	1
20.00		MAX	-20.41	1	-1230.88	1	0.05	1	-1.32	1
		MIN	-20.41	1	-1230.88	1	0.05	1	-1.32	1
26.67		MAX	-25.27	1	-1078.64	1	0.05	1	-1.00	1
		MIN	-25.27	1	-1078.64	1	0.05	1	-1.00	1
33.33		MAX	-30.13	1	-893.99	1	0.05	1	-0.69	1
		MIN	-30.13	1	-893.99	1	0.05	1	-0.69	1
40.00		MAX	-34.99	1	-676.93	1	0.05	1	-0.38	1
		MIN	-34.99	1	-676.93	1	0.05	1	-0.38	1
46.67		MAX	-39.85	1	-427.47	1	0.05	1	-0.07	1
		MIN	-39.85	1	-427.47	1	0.05	1	-0.07	1
53.33		MAX	-44.71	1	-145.60	1	0.05	1	0.24	1
		MIN	-44.71	1	-145.60	1	0.05	1	0.24	1
60.00		MAX	-49.57	1	168.67	1	0.05	1	0.55	1
		MIN	-49.57	1	168.67	1	0.05	1	0.55	1
66.67		MAX	-54.43	1	515.35	1	0.05	1	0.86	1
		MIN	-54.43	1	515.35	1	0.05	1	0.86	1
73.33		MAX	-59.29	1	894.44	1	0.05	1	1.17	1
		MIN	-59.29	1	894.44	1	0.05	1	1.17	1
80.00		MAX	-64.15	1	1305.93	1	0.05	1	1.49	1
		MIN	-64.15	1	1305.93	1	0.05	1	1.49	1
28	0.00	MAX	-6.92	1	-1559.59	1	-0.05	1	0.35	1
		MIN	-6.92	1	-1559.59	1	-0.05	1	0.35	1
	6.67	MAX	-11.78	1	-1497.26	1	-0.05	1	-0.02	1
		MIN	-11.78	1	-1497.26	1	-0.05	1	-0.02	1
13.33		MAX	-16.64	1	-1402.52	1	-0.05	1	-0.38	1
		MIN	-16.64	1	-1402.52	1	-0.05	1	-0.38	1
20.00		MAX	-21.50	1	-1275.37	1	-0.05	1	-0.75	1
		MIN	-21.50	1	-1275.37	1	-0.05	1	-0.75	1
26.67		MAX	-26.36	1	-1115.82	1	-0.05	1	-1.12	1
		MIN	-26.36	1	-1115.82	1	-0.05	1	-1.12	1
33.33		MAX	-31.22	1	-923.86	1	-0.05	1	-1.48	1
		MIN	-31.22	1	-923.86	1	-0.05	1	-1.48	1
40.00		MAX	-36.09	1	-699.49	1	-0.05	1	-1.85	1
		MIN	-36.09	1	-699.49	1	-0.05	1	-1.85	1
46.67		MAX	-40.95	1	-442.72	1	-0.05	1	-2.22	1
		MIN	-40.95	1	-442.72	1	-0.05	1	-2.22	1
53.33		MAX	-45.81	1	-153.54	1	-0.05	1	-2.58	1
		MIN	-45.81	1	-153.54	1	-0.05	1	-2.58	1
60.00		MAX	-50.67	1	168.04	1	-0.05	1	-2.95	1
		MIN	-50.67	1	168.04	1	-0.05	1	-2.95	1
66.67		MAX	-55.53	1	522.03	1	-0.05	1	-3.32	1
		MIN	-55.53	1	522.03	1	-0.05	1	-3.32	1
73.33		MAX	-60.39	1	908.43	1	-0.05	1	-3.68	1
		MIN	-60.39	1	908.43	1	-0.05	1	-3.68	1
80.00		MAX	-65.25	1	1327.24	1	-0.05	1	-4.05	1
		MIN	-65.25	1	1327.24	1	-0.05	1	-4.05	1
29	0.00	MAX	-6.81	1	-1563.80	1	-0.19	1	3.85	1
		MIN	-6.81	1	-1563.80	1	-0.19	1	3.85	1
	6.67	MAX	-11.67	1	-1502.18	1	-0.19	1	2.59	1
		MIN	-11.67	1	-1502.18	1	-0.19	1	2.59	1
13.33		MAX	-16.53	1	-1408.16	1	-0.19	1	1.32	1
		MIN	-16.53	1	-1408.16	1	-0.19	1	1.32	1
20.00		MAX	-21.39	1	-1281.73	1	-0.19	1	0.06	1
		MIN	-21.39	1	-1281.73	1	-0.19	1	0.06	1
26.67		MAX	-26.26	1	-1122.90	1	-0.19	1	-1.20	1
		MIN	-26.26	1	-1122.90	1	-0.19	1	-1.20	1
33.33		MAX	-31.12	1	-931.65	1	-0.19	1	-2.47	1
		MIN	-31.12	1	-931.65	1	-0.19	1	-2.47	1

	40.00	MAX	-35.98	1	-708.01	1	-0.19	1	-3.73	1
		MIN	-35.98	1	-708.01	1	-0.19	1	-3.73	1
	46.67	MAX	-40.84	1	-451.95	1	-0.19	1	-4.99	1
		MIN	-40.84	1	-451.95	1	-0.19	1	-4.99	1
	53.33	MAX	-45.70	1	-163.49	1	-0.19	1	-6.26	1
		MIN	-45.70	1	-163.49	1	-0.19	1	-6.26	1
	60.00	MAX	-50.56	1	157.38	1	-0.19	1	-7.52	1
		MIN	-50.56	1	157.38	1	-0.19	1	-7.52	1
	66.67	MAX	-55.42	1	510.65	1	-0.19	1	-8.78	1
		MIN	-55.42	1	510.65	1	-0.19	1	-8.78	1
	73.33	MAX	-60.28	1	896.33	1	-0.19	1	-10.05	1
		MIN	-60.28	1	896.33	1	-0.19	1	-10.05	1
	80.00	MAX	-65.14	1	1314.42	1	-0.19	1	-11.31	1
		MIN	-65.14	1	1314.42	1	-0.19	1	-11.31	1
30	0.00	MAX	-6.37	1	-1555.07	1	-0.27	1	6.13	1
		MIN	-6.37	1	-1555.07	1	-0.27	1	6.13	1
	6.67	MAX	-11.24	1	-1496.37	1	-0.27	1	4.31	1
		MIN	-11.24	1	-1496.37	1	-0.27	1	4.31	1
	13.33	MAX	-16.10	1	-1405.26	1	-0.27	1	2.50	1
		MIN	-16.10	1	-1405.26	1	-0.27	1	2.50	1
	20.00	MAX	-20.96	1	-1281.75	1	-0.27	1	0.69	1
		MIN	-20.96	1	-1281.75	1	-0.27	1	0.69	1
	26.67	MAX	-25.82	1	-1125.83	1	-0.27	1	-1.13	1
		MIN	-25.82	1	-1125.83	1	-0.27	1	-1.13	1
	33.33	MAX	-30.68	1	-937.50	1	-0.27	1	-2.94	1
		MIN	-30.68	1	-937.50	1	-0.27	1	-2.94	1
	40.00	MAX	-35.54	1	-716.77	1	-0.27	1	-4.75	1
		MIN	-35.54	1	-716.77	1	-0.27	1	-4.75	1
	46.67	MAX	-40.40	1	-463.63	1	-0.27	1	-6.57	1
		MIN	-40.40	1	-463.63	1	-0.27	1	-6.57	1
	53.33	MAX	-45.26	1	-178.09	1	-0.27	1	-8.38	1
		MIN	-45.26	1	-178.09	1	-0.27	1	-8.38	1
	60.00	MAX	-50.12	1	139.86	1	-0.27	1	-10.19	1
		MIN	-50.12	1	139.86	1	-0.27	1	-10.19	1
	66.67	MAX	-54.98	1	490.22	1	-0.27	1	-12.01	1
		MIN	-54.98	1	490.22	1	-0.27	1	-12.01	1
	73.33	MAX	-59.85	1	872.99	1	-0.27	1	-13.82	1
		MIN	-59.85	1	872.99	1	-0.27	1	-13.82	1
	80.00	MAX	-64.71	1	1288.16	1	-0.27	1	-15.63	1
		MIN	-64.71	1	1288.16	1	-0.27	1	-15.63	1
31	0.00	MAX	-4.59	1	-1479.15	1	0.06	1	-2.32	1
		MIN	-4.59	1	-1479.15	1	0.06	1	-2.32	1
	6.67	MAX	-9.45	1	-1432.38	1	0.06	1	-1.91	1
		MIN	-9.45	1	-1432.38	1	0.06	1	-1.91	1
	13.33	MAX	-14.31	1	-1353.20	1	0.06	1	-1.49	1
		MIN	-14.31	1	-1353.20	1	0.06	1	-1.49	1
	20.00	MAX	-19.17	1	-1241.62	1	0.06	1	-1.08	1
		MIN	-19.17	1	-1241.62	1	0.06	1	-1.08	1
	26.67	MAX	-24.03	1	-1097.63	1	0.06	1	-0.67	1
		MIN	-24.03	1	-1097.63	1	0.06	1	-0.67	1
	33.33	MAX	-28.89	1	-921.23	1	0.06	1	-0.26	1
		MIN	-28.89	1	-921.23	1	0.06	1	-0.26	1
	40.00	MAX	-33.75	1	-712.43	1	0.06	1	0.15	1
		MIN	-33.75	1	-712.43	1	0.06	1	0.15	1
	46.67	MAX	-38.61	1	-471.22	1	0.06	1	0.56	1
		MIN	-38.61	1	-471.22	1	0.06	1	0.56	1
	53.33	MAX	-43.47	1	-197.60	1	0.06	1	0.97	1
		MIN	-43.47	1	-197.60	1	0.06	1	0.97	1
	60.00	MAX	-48.33	1	108.42	1	0.06	1	1.38	1
		MIN	-48.33	1	108.42	1	0.06	1	1.38	1
	66.67	MAX	-53.19	1	446.85	1	0.06	1	1.79	1

		MIN	-53.19	1	446.85	1	0.06	1	1.79	1
	73.33	MAX	-58.06	1	817.69	1	0.06	1	2.20	1
		MIN	-58.06	1	817.69	1	0.06	1	2.20	1
	80.00	MAX	-62.92	1	1220.93	1	0.06	1	2.62	1
		MIN	-62.92	1	1220.93	1	0.06	1	2.62	1
32	0.00	MAX	2.24	1	-1111.13	1	0.43	1	-11.80	1
		MIN	2.24	1	-1111.13	1	0.43	1	-11.80	1
	6.67	MAX	-2.62	1	-1109.86	1	0.43	1	-8.92	1
		MIN	-2.62	1	-1109.86	1	0.43	1	-8.92	1
	13.33	MAX	-7.48	1	-1076.18	1	0.43	1	-6.04	1
		MIN	-7.48	1	-1076.18	1	0.43	1	-6.04	1
	20.00	MAX	-12.34	1	-1010.09	1	0.43	1	-3.16	1
		MIN	-12.34	1	-1010.09	1	0.43	1	-3.16	1
	26.67	MAX	-17.20	1	-911.60	1	0.43	1	-0.28	1
		MIN	-17.20	1	-911.60	1	0.43	1	-0.28	1
	33.33	MAX	-22.07	1	-780.70	1	0.43	1	2.60	1
		MIN	-22.07	1	-780.70	1	0.43	1	2.60	1
	40.00	MAX	-26.93	1	-617.40	1	0.43	1	5.48	1
		MIN	-26.93	1	-617.40	1	0.43	1	5.48	1
	46.67	MAX	-31.79	1	-421.69	1	0.43	1	8.36	1
		MIN	-31.79	1	-421.69	1	0.43	1	8.36	1
	53.33	MAX	-36.65	1	-193.57	1	0.43	1	11.25	1
		MIN	-36.65	1	-193.57	1	0.43	1	11.25	1
	60.00	MAX	-41.51	1	66.96	1	0.43	1	14.13	1
		MIN	-41.51	1	66.96	1	0.43	1	14.13	1
	66.67	MAX	-46.37	1	359.89	1	0.43	1	17.01	1
		MIN	-46.37	1	359.89	1	0.43	1	17.01	1
	73.33	MAX	-51.23	1	685.23	1	0.43	1	19.89	1
		MIN	-51.23	1	685.23	1	0.43	1	19.89	1
	80.00	MAX	-56.09	1	1042.97	1	0.43	1	22.77	1
		MIN	-56.09	1	1042.97	1	0.43	1	22.77	1
35	0.00	MAX	57.57	1	1155.97	1	0.00	1	0.05	1
		MIN	57.57	1	1155.97	1	0.00	1	0.05	1
	6.67	MAX	52.71	1	788.36	1	0.00	1	0.06	1
		MIN	52.71	1	788.36	1	0.00	1	0.06	1
	13.33	MAX	47.85	1	453.16	1	0.00	1	0.06	1
		MIN	47.85	1	453.16	1	0.00	1	0.06	1
	20.00	MAX	42.99	1	150.36	1	0.00	1	0.07	1
		MIN	42.99	1	150.36	1	0.00	1	0.07	1
	26.67	MAX	38.13	1	-120.03	1	0.00	1	0.07	1
		MIN	38.13	1	-120.03	1	0.00	1	0.07	1
	33.33	MAX	33.27	1	-358.01	1	0.00	1	0.08	1
		MIN	33.27	1	-358.01	1	0.00	1	0.08	1
	40.00	MAX	28.41	1	-563.59	1	0.00	1	0.08	1
		MIN	28.41	1	-563.59	1	0.00	1	0.08	1
	46.67	MAX	23.55	1	-736.76	1	0.00	1	0.09	1
		MIN	23.55	1	-736.76	1	0.00	1	0.09	1
	53.33	MAX	18.68	1	-877.52	1	0.00	1	0.10	1
		MIN	18.68	1	-877.52	1	0.00	1	0.10	1
	60.00	MAX	13.82	1	-985.88	1	0.00	1	0.10	1
		MIN	13.82	1	-985.88	1	0.00	1	0.10	1
	66.67	MAX	8.96	1	-1061.83	1	0.00	1	0.11	1
		MIN	8.96	1	-1061.83	1	0.00	1	0.11	1
	73.33	MAX	4.10	1	-1105.38	1	0.00	1	0.11	1
		MIN	4.10	1	-1105.38	1	0.00	1	0.11	1
	80.00	MAX	-0.76	1	-1116.51	1	0.00	1	0.12	1
		MIN	-0.76	1	-1116.51	1	0.00	1	0.12	1
36	0.00	MAX	64.61	1	1348.45	1	-0.05	1	2.64	1
		MIN	64.61	1	1348.45	1	-0.05	1	2.64	1
	6.67	MAX	59.75	1	933.90	1	-0.05	1	2.33	1
		MIN	59.75	1	933.90	1	-0.05	1	2.33	1

	13.33	MAX	54.89	1	551.75	1	-0.05	1	2.02	1
		MIN	54.89	1	551.75	1	-0.05	1	2.02	1
	20.00	MAX	50.03	1	202.01	1	-0.05	1	1.71	1
		MIN	50.03	1	202.01	1	-0.05	1	1.71	1
	26.67	MAX	45.17	1	-115.32	1	-0.05	1	1.40	1
		MIN	45.17	1	-115.32	1	-0.05	1	1.40	1
	33.33	MAX	40.31	1	-400.25	1	-0.05	1	1.09	1
		MIN	40.31	1	-400.25	1	-0.05	1	1.09	1
	40.00	MAX	35.45	1	-652.77	1	-0.05	1	0.78	1
		MIN	35.45	1	-652.77	1	-0.05	1	0.78	1
	46.67	MAX	30.59	1	-872.88	1	-0.05	1	0.47	1
		MIN	30.59	1	-872.88	1	-0.05	1	0.47	1
	53.33	MAX	25.73	1	-1060.59	1	-0.05	1	0.16	1
		MIN	25.73	1	-1060.59	1	-0.05	1	0.16	1
	60.00	MAX	20.86	1	-1215.89	1	-0.05	1	-0.15	1
		MIN	20.86	1	-1215.89	1	-0.05	1	-0.15	1
	66.67	MAX	16.00	1	-1338.79	1	-0.05	1	-0.46	1
		MIN	16.00	1	-1338.79	1	-0.05	1	-0.46	1
	73.33	MAX	11.14	1	-1429.27	1	-0.05	1	-0.77	1
		MIN	11.14	1	-1429.27	1	-0.05	1	-0.77	1
	80.00	MAX	6.28	1	-1487.36	1	-0.05	1	-1.08	1
		MIN	6.28	1	-1487.36	1	-0.05	1	-1.08	1
37	0.00	MAX	66.24	1	1406.72	1	-0.14	1	8.03	1
		MIN	66.24	1	1406.72	1	-0.14	1	8.03	1
	6.67	MAX	61.38	1	981.30	1	-0.14	1	7.06	1
		MIN	61.38	1	981.30	1	-0.14	1	7.06	1
	13.33	MAX	56.52	1	588.28	1	-0.14	1	6.10	1
		MIN	56.52	1	588.28	1	-0.14	1	6.10	1
	20.00	MAX	51.66	1	227.67	1	-0.14	1	5.13	1
		MIN	51.66	1	227.67	1	-0.14	1	5.13	1
	26.67	MAX	46.80	1	-100.53	1	-0.14	1	4.17	1
		MIN	46.80	1	-100.53	1	-0.14	1	4.17	1
	33.33	MAX	41.94	1	-396.32	1	-0.14	1	3.20	1
		MIN	41.94	1	-396.32	1	-0.14	1	3.20	1
	40.00	MAX	37.08	1	-659.71	1	-0.14	1	2.24	1
		MIN	37.08	1	-659.71	1	-0.14	1	2.24	1
	46.67	MAX	32.22	1	-890.70	1	-0.14	1	1.28	1
		MIN	32.22	1	-890.70	1	-0.14	1	1.28	1
	53.33	MAX	27.36	1	-1089.27	1	-0.14	1	0.31	1
		MIN	27.36	1	-1089.27	1	-0.14	1	0.31	1
	60.00	MAX	22.49	1	-1255.44	1	-0.14	1	-0.65	1
		MIN	22.49	1	-1255.44	1	-0.14	1	-0.65	1
	66.67	MAX	17.63	1	-1389.20	1	-0.14	1	-1.62	1
		MIN	17.63	1	-1389.20	1	-0.14	1	-1.62	1
	73.33	MAX	12.77	1	-1490.56	1	-0.14	1	-2.58	1
		MIN	12.77	1	-1490.56	1	-0.14	1	-2.58	1
	80.00	MAX	7.91	1	-1559.51	1	-0.14	1	-3.55	1
		MIN	7.91	1	-1559.51	1	-0.14	1	-3.55	1
38	0.00	MAX	66.70	1	1433.74	1	-0.28	1	15.14	1
		MIN	66.70	1	1433.74	1	-0.28	1	15.14	1
	6.67	MAX	61.84	1	1005.31	1	-0.28	1	13.30	1
		MIN	61.84	1	1005.31	1	-0.28	1	13.30	1
	13.33	MAX	56.97	1	609.28	1	-0.28	1	11.47	1
		MIN	56.97	1	609.28	1	-0.28	1	11.47	1
	20.00	MAX	52.11	1	245.65	1	-0.28	1	9.63	1
		MIN	52.11	1	245.65	1	-0.28	1	9.63	1
	26.67	MAX	47.25	1	-85.57	1	-0.28	1	7.79	1
		MIN	47.25	1	-85.57	1	-0.28	1	7.79	1
	33.33	MAX	42.39	1	-384.38	1	-0.28	1	5.95	1
		MIN	42.39	1	-384.38	1	-0.28	1	5.95	1
	40.00	MAX	37.53	1	-650.79	1	-0.28	1	4.11	1

		MIN	37.53	1	-650.79	1	-0.28	1	4.11	1
46.67		MAX	32.67	1	-884.79	1	-0.28	1	2.28	1
		MIN	32.67	1	-884.79	1	-0.28	1	2.28	1
53.33		MAX	27.81	1	-1086.38	1	-0.28	1	0.44	1
		MIN	27.81	1	-1086.38	1	-0.28	1	0.44	1
60.00		MAX	22.95	1	-1255.56	1	-0.28	1	-1.40	1
		MIN	22.95	1	-1255.56	1	-0.28	1	-1.40	1
66.67		MAX	18.09	1	-1392.34	1	-0.28	1	-3.24	1
		MIN	18.09	1	-1392.34	1	-0.28	1	-3.24	1
73.33		MAX	13.23	1	-1496.72	1	-0.28	1	-5.07	1
		MIN	13.23	1	-1496.72	1	-0.28	1	-5.07	1
80.00		MAX	8.36	1	-1568.68	1	-0.28	1	-6.91	1
		MIN	8.36	1	-1568.68	1	-0.28	1	-6.91	1
39	0.00	MAX	66.92	1	1453.17	1	-0.35	1	19.32	1
		MIN	66.92	1	1453.17	1	-0.35	1	19.32	1
	6.67	MAX	62.05	1	1023.27	1	-0.35	1	16.96	1
		MIN	62.05	1	1023.27	1	-0.35	1	16.96	1
	13.33	MAX	57.19	1	625.77	1	-0.35	1	14.59	1
		MIN	57.19	1	625.77	1	-0.35	1	14.59	1
	20.00	MAX	52.33	1	260.68	1	-0.35	1	12.23	1
		MIN	52.33	1	260.68	1	-0.35	1	12.23	1
	26.67	MAX	47.47	1	-72.00	1	-0.35	1	9.86	1
		MIN	47.47	1	-72.00	1	-0.35	1	9.86	1
	33.33	MAX	42.61	1	-372.28	1	-0.35	1	7.50	1
		MIN	42.61	1	-372.28	1	-0.35	1	7.50	1
	40.00	MAX	37.75	1	-640.15	1	-0.35	1	5.13	1
		MIN	37.75	1	-640.15	1	-0.35	1	5.13	1
	46.67	MAX	32.89	1	-875.61	1	-0.35	1	2.77	1
		MIN	32.89	1	-875.61	1	-0.35	1	2.77	1
	53.33	MAX	28.03	1	-1078.67	1	-0.35	1	0.40	1
		MIN	28.03	1	-1078.67	1	-0.35	1	0.40	1
	60.00	MAX	23.17	1	-1249.32	1	-0.35	1	-1.96	1
		MIN	23.17	1	-1249.32	1	-0.35	1	-1.96	1
	66.67	MAX	18.31	1	-1387.56	1	-0.35	1	-4.33	1
		MIN	18.31	1	-1387.56	1	-0.35	1	-4.33	1
	73.33	MAX	13.45	1	-1493.40	1	-0.35	1	-6.69	1
		MIN	13.45	1	-1493.40	1	-0.35	1	-6.69	1
	80.00	MAX	8.58	1	-1566.83	1	-0.35	1	-9.06	1
		MIN	8.58	1	-1566.83	1	-0.35	1	-9.06	1
40	0.00	MAX	65.94	1	1440.22	1	-0.02	1	0.92	1
		MIN	65.94	1	1440.22	1	-0.02	1	0.92	1
	6.67	MAX	61.08	1	1016.85	1	-0.02	1	0.80	1
		MIN	61.08	1	1016.85	1	-0.02	1	0.80	1
	13.33	MAX	56.21	1	625.88	1	-0.02	1	0.69	1
		MIN	56.21	1	625.88	1	-0.02	1	0.69	1
	20.00	MAX	51.35	1	267.32	1	-0.02	1	0.57	1
		MIN	51.35	1	267.32	1	-0.02	1	0.57	1
	26.67	MAX	46.49	1	-58.83	1	-0.02	1	0.46	1
		MIN	46.49	1	-58.83	1	-0.02	1	0.46	1
	33.33	MAX	41.63	1	-352.58	1	-0.02	1	0.34	1
		MIN	41.63	1	-352.58	1	-0.02	1	0.34	1
	40.00	MAX	36.77	1	-613.92	1	-0.02	1	0.22	1
		MIN	36.77	1	-613.92	1	-0.02	1	0.22	1
	46.67	MAX	31.91	1	-842.86	1	-0.02	1	0.11	1
		MIN	31.91	1	-842.86	1	-0.02	1	0.11	1
	53.33	MAX	27.05	1	-1039.39	1	-0.02	1	-0.01	1
		MIN	27.05	1	-1039.39	1	-0.02	1	-0.01	1
	60.00	MAX	22.19	1	-1203.51	1	-0.02	1	-0.12	1
		MIN	22.19	1	-1203.51	1	-0.02	1	-0.12	1
	66.67	MAX	17.33	1	-1335.22	1	-0.02	1	-0.24	1
		MIN	17.33	1	-1335.22	1	-0.02	1	-0.24	1

	73.33	MAX	12.47	1	-1434.53	1	-0.02	1	-0.35	1
		MIN	12.47	1	-1434.53	1	-0.02	1	-0.35	1
	80.00	MAX	7.60	1	-1501.44	1	-0.02	1	-0.47	1
		MIN	7.60	1	-1501.44	1	-0.02	1	-0.47	1
41	0.00	MAX	58.59	1	1237.75	1	0.35	1	-19.24	1
		MIN	58.59	1	1237.75	1	0.35	1	-19.24	1
	6.67	MAX	53.73	1	863.32	1	0.35	1	-16.89	1
		MIN	53.73	1	863.32	1	0.35	1	-16.89	1
	13.33	MAX	48.87	1	521.30	1	0.35	1	-14.53	1
		MIN	48.87	1	521.30	1	0.35	1	-14.53	1
	20.00	MAX	44.01	1	211.69	1	0.35	1	-12.17	1
		MIN	44.01	1	211.69	1	0.35	1	-12.17	1
	26.67	MAX	39.15	1	-65.51	1	0.35	1	-9.82	1
		MIN	39.15	1	-65.51	1	0.35	1	-9.82	1
	33.33	MAX	34.29	1	-310.31	1	0.35	1	-7.46	1
		MIN	34.29	1	-310.31	1	0.35	1	-7.46	1
	40.00	MAX	29.43	1	-522.71	1	0.35	1	-5.10	1
		MIN	29.43	1	-522.71	1	0.35	1	-5.10	1
	46.67	MAX	24.57	1	-702.69	1	0.35	1	-2.75	1
		MIN	24.57	1	-702.69	1	0.35	1	-2.75	1
	53.33	MAX	19.71	1	-850.27	1	0.35	1	-0.39	1
		MIN	19.71	1	-850.27	1	0.35	1	-0.39	1
	60.00	MAX	14.85	1	-965.45	1	0.35	1	1.96	1
		MIN	14.85	1	-965.45	1	0.35	1	1.96	1
	66.67	MAX	9.98	1	-1048.21	1	0.35	1	4.32	1
		MIN	9.98	1	-1048.21	1	0.35	1	4.32	1
	73.33	MAX	5.12	1	-1098.57	1	0.35	1	6.68	1
		MIN	5.12	1	-1098.57	1	0.35	1	6.68	1
	80.00	MAX	0.26	1	-1116.53	1	0.35	1	9.03	1
		MIN	0.26	1	-1116.53	1	0.35	1	9.03	1
50	0.00	MAX	62.71	1	705.32	1	165.17	1	-1914.82	1
		MIN	62.71	1	705.32	1	165.17	1	-1914.82	1
	1.33	MAX	62.71	1	621.71	1	165.17	1	-1694.59	1
		MIN	62.71	1	621.71	1	165.17	1	-1694.59	1
	2.67	MAX	62.71	1	538.09	1	165.17	1	-1474.36	1
		MIN	62.71	1	538.09	1	165.17	1	-1474.36	1
	4.00	MAX	62.71	1	454.47	1	165.17	1	-1254.13	1
		MIN	62.71	1	454.47	1	165.17	1	-1254.13	1
	5.33	MAX	62.71	1	370.85	1	165.17	1	-1033.90	1
		MIN	62.71	1	370.85	1	165.17	1	-1033.90	1
	6.67	MAX	62.71	1	287.23	1	165.17	1	-813.67	1
		MIN	62.71	1	287.23	1	165.17	1	-813.67	1
	8.00	MAX	62.71	1	203.61	1	165.17	1	-593.44	1
		MIN	62.71	1	203.61	1	165.17	1	-593.44	1
	9.33	MAX	62.71	1	119.99	1	165.17	1	-373.21	1
		MIN	62.71	1	119.99	1	165.17	1	-373.21	1
	10.67	MAX	62.71	1	36.38	1	165.17	1	-152.99	1
		MIN	62.71	1	36.38	1	165.17	1	-152.99	1
	12.00	MAX	62.71	1	-47.24	1	165.17	1	67.24	1
		MIN	62.71	1	-47.24	1	165.17	1	67.24	1
	13.33	MAX	62.71	1	-130.86	1	165.17	1	287.47	1
		MIN	62.71	1	-130.86	1	165.17	1	287.47	1
	14.67	MAX	62.71	1	-214.48	1	165.17	1	507.70	1
		MIN	62.71	1	-214.48	1	165.17	1	507.70	1
	16.00	MAX	62.71	1	-298.10	1	165.17	1	727.93	1
		MIN	62.71	1	-298.10	1	165.17	1	727.93	1
51	0.00	MAX	-1039.97	1	-1806.61	1	-164.54	1	1701.47	1
		MIN	-1039.97	1	-1806.61	1	-164.54	1	1701.47	1
	1.33	MAX	-1039.97	1	-419.98	1	-164.54	1	1482.08	1
		MIN	-1039.97	1	-419.98	1	-164.54	1	1482.08	1

2.67	MAX	-1039.97	1	966.65	1	-164.54	1	1262.68	1
	MIN	-1039.97	1	966.65	1	-164.54	1	1262.68	1
4.00	MAX	-1039.97	1	2353.28	1	-164.54	1	1043.29	1
	MIN	-1039.97	1	2353.28	1	-164.54	1	1043.29	1
5.33	MAX	-1039.97	1	3739.91	1	-164.54	1	823.90	1
	MIN	-1039.97	1	3739.91	1	-164.54	1	823.90	1
6.67	MAX	-679.97	1	5006.54	1	-164.54	1	604.51	1
	MIN	-679.97	1	5006.54	1	-164.54	1	604.51	1
8.00	MAX	40.03	1	5433.17	1	-164.54	1	385.12	1
	MIN	40.03	1	5433.17	1	-164.54	1	385.12	1
9.33	MAX	760.03	1	4899.79	1	-164.54	1	165.73	1
	MIN	760.03	1	4899.79	1	-164.54	1	165.73	1
10.67	MAX	1480.03	1	3406.42	1	-164.54	1	-53.67	1
	MIN	1480.03	1	3406.42	1	-164.54	1	-53.67	1
12.00	MAX	2200.03	1	953.05	1	-164.54	1	-273.06	1
	MIN	2200.03	1	953.05	1	-164.54	1	-273.06	1
13.33	MAX	2920.03	1	-2460.32	1	-164.54	1	-492.45	1
	MIN	2920.03	1	-2460.32	1	-164.54	1	-492.45	1
14.67	MAX	3280.03	1	-6713.69	1	-164.54	1	-711.84	1
	MIN	3280.03	1	-6713.69	1	-164.54	1	-711.84	1
16.00	MAX	3280.03	1	-11087.06	1	-164.54	1	-931.23	1
	MIN	3280.03	1	-11087.06	1	-164.54	1	-931.23	1

REFERENCES

1. National Bridge Inventory (NBI), Federal Highway Administration (FHWA), December 2003.
2. National Cooperative Highway Research Program (NCHRP), Project No. 12-72, FY 2005.
3. Load and Resistant Factor Design, Bridge Design Specifications, American Association of State Highway and Officials (AASHTO), 2003.
4. Structures Design Guidelines, Florida Department of Transportation, 2004.
5. TM 5-1300, Structures to Resist the Effects of Accidental Explosions, US Department of Defense, December 1990.
6. Research Engineers International, USA, STAAD.Pro 2004.
7. Florida Department of Transportation, LRFD Prestressed Beam Program, English v1.85, February 2001.
8. Florida Department of Transportation, Biaxial Column Program, v2.3, November 2001.
9. ATBlast Software, Developed by Applied Research Associates (ARA), Inc.
10. Design of Blast Resistant Buildings in Petrochemical Facilities, ASCE Task Committee on Blast Resistant Design, 1997.
11. Process Safety Management of Highly Hazardous Chemicals, OSHA, May 1992.
12. Explosion Effects and Structural Design for Blast, A Two-Day Training Course, National Center for Explosion Resistant Design (NCERD), Department of Civil and Environmental Engineering, University of Missouri-Columbia.
13. Uniform Building Code (UBC), International Conference of Building Officials, 1997.

14. Recommendation for Bridge and Tunnel Security, AASHTO Blue Ribbon Panel on Bridge and Tunnel Security, September 2003.
15. Analysis of Blast Load on Bridge Substructures, K. Marchand, E.B. Williamson & D.G. Winget, Structures Under Shock and Impact VIII, Wessex Institute of Technology Press (WIT Press), 2004.
16. Connecticut Post, Bridgeport, Connecticut, March 26, 2004.
17. Highway-Marine Accident Report, National Transportation Safety Board, Report No. HAR-94/03, June 1994.
18. Highway Accident Report, National Transportation Safety Board, Report No. HAR-94/02, April 1994.
19. Highway Accident Report, National Transportation Safety Board, Report No. HAR-76/03, April 1976.
20. Robert Pekelnicky, An Assessment of the Blast Resistance Gained from Seismic Detailing, ACI Fall 2003 Convention, September 28, 2003.
21. Jack Hayes, US Army Corps of Engineers, Could Seismic Strengthening have Improved the Blast Resistance of the Murrah Federal Building?, ACI Fall 2003 Convention, September 2003.
22. Report on “Application of Seismic Rehabilitation”, National Institute of Standards and Technology (NIST), September 2001.
23. Increasing Blast and Fire Resistance in Buildings: Design Techniques for Combined Nuclear Weapon Effects, Department of Defense (DOD), Defense Civil Preparedness Agency, TR-62, May 1976.
24. Dr. Alex Remennikov, Evaluation of Blast Loads on Commercial Buildings: From Hand Calculations to GIS-Based Numerical Simulations, Second National Engineering & Security Research Forum, Melbourne, Australia, February 10, 2004.
25. Justin T. Domire, Silver Spring District Courthouse, Architectural Engineering Senior Thesis, Pennsylvania State University, Spring 2003.
26. Standard Specifications for Roads and Bridges Construction, Florida Department of Transportation, 2004.

BIOGRAPHICAL SKETCH

- Date of Birth:** July 1, 1968, Munshigonj, Bangladesh.
- Education:** B.Sc. Engineering (Civil), First Class, Bangladesh University of Engineering & Technology, 1992. Thesis Title: “Computer Aided Design of a Guyed Tower.”
- M.S. (Civil Engineering), GPA: 4.0, Florida State University, Tallahassee, Florida, 2000. Thesis Title: “Post-Storm Model for the Reconstruction of Habitable Coastal Structures.”
- Ph.D. (Structural Engineering), GPA: 4.0, Florida State University, 2005. Dissertation Title: “Performance of AASHTO Girder Bridge under Blast Loading.”
- Experience:** Senior Design Engineer, December 2004 – Present, Leon County Public Works, Tallahassee, Florida.
- Senior Structural Engineer, September 2000 – December 2004, PBS&J, Tallahassee, Florida.
- Research Assistant, May 1999 – Present, Florida State University, Tallahassee, Florida.
- Structural Engineer, June 1997 – December 1998, Public Works Department, Singapore.
- Structural Engineer, May 1995 – May 1997, Hyundai Engineering & Co., Jamuna Multipurpose Bridge Project, Bangladesh.
- Structural Engineer, October 1994 – April 2005, Housing & Development Board, Singapore.
- Project Engineer, October 1992 – September 1994, Aqua Consultants & Associates, Bangladesh.

Interests: Contemporary Eastern and Western Literature, Music, Arts, Chess and Guitar.

Awards: Obtained Bangladesh Government scholarships in Elementary, Middle and High School, and University.

US Federal Government Scholarship in Lamar University, Beaumont, Texas.

Placed as one of the Finalists in the “International Open Poetry Competition, 1999,” organized by International Library of Poetry, Maryland, USA.

Research Assistantship, May 1999 – December 2000, Florida Sea Grant College Program.

Publication & Presentation:

"Post-Storm Model for the Reconstruction of Habitable Coastal Structures", ASCE Journal of Performance of Constructed Facilities, August 2002, Volume 16, Number 3.

"Post-Storm Model for the Reconstruction of Habitable Coastal Structures", Presented in Conference on Coastal Engineering, Singapore, December 19-21, 2001.

“Jamuna Bridge: A Signature Bridge in Bangladesh”, Presented in the ASCE Tallahassee Section, November 2003.

Performance of AASHTO Girder Superstructure under Blast Loading (in preparation).

Performance of Bridge Substructure under Blast Loading (in preparation).

Family: Married with Tamanna E-Kabir Chowdhury, October 15, 1992.

Two sons, Bisshoy Anwar (February 7, 1997), Ikra Anwar (August 5, 2000).